Chapter 7: Clouds and Aerosols

Coordinating Lead Authors: Olivier Boucher (France), David Randall (USA)

Lead Authors: Paulo Artaxo (Brazil), Christopher Bretherton (USA), Graham Feingold (USA), Piers Forster (UK), Veli-Matti Kerminen (Finland), Yutaka Kondo (Japan), Hong Liao (China), Ulrike Lohmann (Switzerland), Philip Rasch (USA), S. K. Satheesh (India), Steven Sherwood (Australia), Bjorn Stevens (Germany), Xiao-Ye Zhang (China)

Contributing Authors: Govindswamy Bala (India), Nicolas Bellouin (UK), Angela Benedetti (UK), Sandrine Bony (France), Ken Caldeira (USA), Antony Del Genio (USA), Maria Cristina Facchini (Italy), Mark Flanner (USA), Steven Ghan (USA), Claire Granier (France), Corinna Hoose (Germany), Andy Jones (UK), Makoto Koike (Japan), Ben Kravitz (USA), Ben Laken (Spain), Matthew Lebsock (USA), Natalie Mahowald (USA), Gunnar Myhre (Norway), Colin O'Dowd (Ireland), Alan Robock (USA), Bjørn Samset (Norway), Hauke Schmidt (Germany), Michael Schulz (Norway), Graeme Stephens (USA), Trude Storelvmo (USA), Dave Winker (USA), Matthew Wyant (USA)

Review Editors: Sandro Fuzzi (Italy), Joyce Penner (USA), Venkatachalam Ramaswamy (USA), Claudia Stubenrauch (France)

Date of Draft: 5 October 2012

Notes: TSU Compiled Version

Table of Contents

Executive Summary

A new framework is used, which separates forcing (instantaneous change in the radiative budget) and rapid adjustments (which modify the radiative budget indirectly through fast atmospheric and surface changes) from feedbacks (which operate through changes in climate variables that are mediated by a change in surface temperature). This framework offers a clear distinction between the traditional concept of radiative forcing (RF) and the relatively new concept of adjusted forcing (AF). For aerosols one can further distinguish forcing processes arising from aerosol-radiation interactions (ari) and aerosol-cloud interactions (aci). [7.1, Figures 7.1 and 7.2]

Clouds exert an average cooling influence on Earth, of about −17 W m^{-2}. This is the net result of a greenhouse (infrared) warming due mainly to high clouds (about +30 W m^{-2}) and a cooling effect from reflecting solar radiation contributed by all cloud types (about −47 W m^{-2}). This result is not new since AR4, but the important role of clouds in redistributing radiative fluxes vertically within the atmosphere is now better quantified. [7.2.1, 7.2.2, Figure 7.6]

The net "clear-sky" feedback from water vapour and lapse rate changes together is *very likely* positive, that is, amplifies global climate changes. We estimate a *very likely* (90%) range[1] for this feedback parameter, as traditionally defined, of 1.09 (0.91 to 1.27) W m^{-2} K^{-1}. The mean value and spread in climate models are essentially unchanged from AR4, but are now supported by stronger observational evidence and better process understanding of what determines relative humidity distributions. However the traditional view of a weak inherent climate sensitivity boosted by strong positive feedback from water vapour depends on the analysis framework; a valid alternative yields stronger intrinsic sensitivity, with a weak net clear-sky feedback. [7.2.4, Figure 7.8]

The net radiative feedback due to all cloud types is *likely* (>66% chance) positive, although a negative feedback (damping global climate changes) is still possible. We assign a *very likely* range of −0.2 to 1.4 W m^{-2} K^{-1} for the cloud feedback parameter. This conclusion is reached by considering a plausible range for unknown contributions by processes yet to be accounted for, in addition to those occurring in current climate models. The cloud feedback remains the most uncertain radiative feedback in climate models. Observations alone do not currently provide a robust, direct constraint, but multiple lines of evidence now indicate positive feedback contributions from changes in both the height of high clouds and the horizontal distribution of clouds. Additional feedback from low cloud amount is also positive in most climate models, but that result is not well understood, nor effectively constrained by observations, so confidence in it is low. [7.2.4, Figures 7.9-7.10]

Persistent contrails from aviation contribute a RF of +0.02 (+0.01 to +0.03) W m^{-2} for year 2010, and the combined contrail and contrail-cirrus AF from aviation is assessed to be +0.05 (+0.02 to +0.15) W m^{-2}. This forcing can be much larger regionally but is very unlikely to produce observable regional effects on either the mean or diurnal range of surface temperature. [7.2.5]

Climate-relevant aerosol properties result from aerosol sources and a number of atmospheric processes, which are considerably better understood than at time of the last IPCC assessment, but the representation of these processes varies greatly in global models. For instance, the importance of new particle formation, the role of organics, and how mixing increases aerosol mass absorption efficiency are better appreciated. However, it remains unclear what level of sophistication in global aerosol and climate models is required to estimate aerosol-radiation and aerosol-cloud interactions to a sufficient accuracy. [7.3.1, 7.3.2, 7.3.3, Figures 7.11-7.14]

Aerosol-radiation interactions result in rapid adjustments, which affect the stability of the atmosphere and cause changes in cloud dynamics that are distinct from any aerosol-cloud interaction. Observations and detailed large eddy simulations show cloud cover decreases with absorbing aerosol embedded in the cloud layer, and increases when aerosols are above cloud. There is however limited evidence to gauge the relative importance of these two effects at the global scale. [7.3.4]

[1] Unless specified otherwise, all ranges for forcing and feedback parameters are 5 to 95% uncertainty intervals.

Aerosol-climate feedbacks occur mainly through changes in the source strength of natural aerosols or changes in the sink efficiency of natural and anthropogenic aerosols; a limited number of modelling studies have bracketed the feedback parameter within ±0.2 W m^{-2} K^{-1} with a low level of confidence. There is medium confidence for a weak DMS-CCN-cloud albedo feedback due to a weak sensitivity of CCN population to changes in DMS emissions. Although the limited evidence is for a rather weak aerosol-climate feedback at the global scale during the 21st century, regional effects on the aerosol may be important. [7.3.5]

Research continues to provide evidence for an aerosol influence on the microphysical properties of clouds. There is emerging evidence from observations and large eddy simulations that some of these influences may compensate and thus yield smaller net effects. However there is also evidence for strong aerosol influences that can play an important role in determining the cloud fraction and associated adjusted forcing. These two types of responses are evident in both liquid-only and mixed-phase stratiform clouds. We do not have a good understanding of the prevalence of these two responses. [7.4.2, 7.4.3, 7.4.4]

Research now emphasises the importance of considering the aerosol-cloud-precipitation *system*, as opposed to aerosol influences in individual clouds. This replaces earlier thinking that correctly identified aerosol-cloud microphysical processes but did not adequately address the multiple feedbacks that can occur within an evolving system. This new paradigm allows for a broader spectrum of responses in climate models and is preferable to earlier approaches that constrained climate model responses to be monotonic and relatively strong. [7.4.3, Figure 7.16]

The representation of aerosol-cloud processes in climate models continues to be a challenge. Aerosol and cloud variability at scales significantly smaller than those resolved in climate models, and the subtle responses of clouds to aerosol at these scales, mean that for the foreseeable future, climate models will continue to rely on parameterisations of aerosol-cloud interactions or other methods that represent subgrid variability. This implies large uncertainties for estimates of the forcings associated with aerosol-cloud interactions. [7.4, 7.5.2]

Cosmic rays enhance aerosol nucleation and cloud condensation nuclei production in the free troposphere, but the effect is too weak to have any climatic influence during a solar cycle or over the last century (*medium evidence, high agreement*). Changes in solar activity affect the flux of galactic cosmic rays impinging upon the Earth's atmosphere, which has been hypothesized to affect climate through changes in cloudiness. Based on available information, no robust association between changes in cosmic rays and cloudiness have been identified. In the event that such an association exists, it is very unlikely to be due to cosmic ray-induced nucleation of new aerosol particles. [7.3, 7.4.5]

The radiative forcing due to aerosol-radiation interactions (RFari) is assessed to be –0.4 (–0.7 to –0.1) W m^{-2}.This assessment is less negative than reported in AR4 because of a re-evaluation of aerosol absorption. The uncertainty estimate is also more robust and based on multiple lines of evidence from models, remotely sensed data, and ground based measurements. [7.5.1, Figure 7.17]

The RFari of different aerosol species (see Table 7.1) shows that aerosols have both negative and positive forcings. These estimates are not as robust as the total RFari as there is not as much supporting observational evidence. The dust RFari could be largely from natural and/or climate feedback effects and should not be considered solely as an anthropogenic forcing agent. [7.3.6, 7.5.1, Figure 7.18]

Table 7.1: The RFari of different aerosol species.

Species	RFari (W m^{-2})
Sulphate	–0.4 (–0.6 to –0.2)
Black carbon from fossil fuel and biofuel	+0.3 (+0.1 to +0.5)
Nitrate	–0.13 (–0.23 to –0.03)
Biomass burning aerosol	+0.0 (–0.1 to +0.1)
Secondary organic aerosol	–0.08 (–0.28 to +0.12)
Primary organic matter	–0.05 (–0.09 to –0.01)
Dust (not necessarily anthropogenic)	–0.1 (–0.3 to +0.1)

The adjusted forcing due to aerosol-radiation interactions (AFari) is assessed to be –0.5 (–0.9 to –0.1) W m^{-2}. The AF includes a rapid adjustment of cloud of –0.1 (–0.3 to +0.1) W m^{-2}. While there is robust evidence for the existence of rapid adjustment of clouds in response to absorbing aerosols, these effects are multiple and poorly represented in climate models, leading to a rather large uncertainty. There is the potential of an additional positive contribution to AFari from cloud drop inclusions that is currently not included in this assessment because of the low agreement among the few available studies. [7.3.4, 7.5.2]

The RF from absorbing aerosol on snow and ice is assessed to be +0.04 (+0.02 to +0.09) W m^{-2}. Unlike in the last IPCC assessment, this estimate includes the effects on sea-ice, accounts for more physical processes, and incorporates evidence from both models and observations. This RF has a 2-4 times larger global mean surface temperature change per unit forcing and represents a significant forcing mechanism in the Arctic and over Tibet. [7.3.4, 7.5.1]

The total adjusted forcing due to aerosols (AFari+aci, excluding the effect of absorbing aerosol on snow and ice) is assessed to be –0.9 (–1.5 to –0.3) W m^{-2}. The AFari+aci estimate includes rapid adjustments, such as changes to the cloud lifetime and aerosol microphysical effects on mixed-phase, ice and convective clouds. This range was obtained by giving equal weight to satellite-based studies and estimates from climate models and inverse studies grouped together, and includes a small correction term to be in line with a 1750 reference period. It is consistent with multiple lines of evidence suggesting less negative estimates for aerosol-cloud interactions than in AR4. [7.4, 7.5.2, 7.5.3, Figure 7.19]

The radiative and adjusted forcings due to aerosol-cloud interactions (RFaci and AFaci) are assessed to be –0.3 (–0.7 to 0) W m^{-2} and –0.4 (–0.9 to 0) W m^{-2}. The AFaci is estimated as the residual between AFari+aci and AFari. These ranges reflect our understanding of aerosol-cloud interactions in liquid and ice clouds, in particular from observations and large-eddy simulations, which reveal some compensating effects. However they remain somewhat inconsistent with available estimates from climate models, which do not capture all of the relevant processes and tend to simulate more negative forcings. [7.5.2, 7.5.3, Figure 7.19]

Multiple lines of evidence suggest that global mean precipitation increases in a warming climate, but at a rate that is limited by the increase of radiant energy absorbed by the surface rather than by the more rapid increase in atmospheric water vapour. [7.6.2, 7.6.3]

Regional precipitation changes will vary and are hard to predict, but a physical basis exists for predicting some systematic aspects of the changes. First, there is high confidence (high agreement, medium evidence) that as climate warms wet regions will become wetter on average and dry regions drier, although circulation changes will alter results in specific regions. Second, there is also high confidence (high agreement, medium evidence) that short-duration (a few days or less) precipitation extremes as a whole will increase more strongly with temperature than will the globally-averaged precipitation, but this will vary by region according to local shifts in mean precipitation. Lack of understanding of soil moisture, clouds and precipitation interactions, as well as controls on local circulations, limits confidence in projections of precipitation changes on the scale of even the largest catchments. [7.6.2, 7.6.3, 7.6.5]

There is a variety of evidence that rapid responses related to aerosol-cloud interactions impact the spatial and temporal distribution of precipitation, but these effects are situation dependent and not systematic. There is very little evidence that aerosol-cloud interactions have a marked impact on the total amount of precipitation, except in so far as they modify globally averaged surface temperatures. [7.6.4]

Theory, model studies and observations suggest that some Solar Radiation Management (SRM) methods, if realisable, could substantially offset a global temperature rise and some of its effects. There is medium confidence (*medium evidence, medium agreement*) that stratospheric aerosol SRM is scalable to counter the RF and some of the climate effects expected from a twofold increase in CO_2 concentration. Models cited in this assessment explored various source injection strategies and treated aerosol microphysics differently; these variations produce significantly different estimates for the injection rate of chemicals needed to generate the required RF. There is no consensus on whether a similarly large RF could be achieved from cloud brightening SRM due to insufficient understanding of aerosol-cloud interactions. It does not

appear that land albedo change SRM can produce a large RF. Limited literature on other SRM methods precludes their assessment. [7.4.3, 7.7.2, 7.7.3, 7.7.4]

SRM would produce an inexact compensation for the RF by greenhouse gases. There is very high confidence that there would be residual regional differences in climate (e.g., temperature and rainfall) in comparison to an unperturbed climate, however models consistently suggest that SRM would generally reduce climate differences compared to a world with the same elevated greenhouse gas concentrations and no SRM. [7.7.3, Figures 7.22-7.23]

Numerous side effects and risks from SRM have been identified. For example, there is high confidence that SRM by stratospheric sulfate aerosols would increase polar stratospheric ozone depletion. Moreover, if SRM were used to counter a large RF by greenhouse gases and then terminated, most of the warming that had been offset would become evident within a few decades, and the rate of climate change would exceed the rate that would have occurred in the absence of SRM. Other side effects have been identified, and there would be other unanticipated or unexplored impacts. SRM will not compensate for ocean acidification from increasing CO_2. [7.7.2, 7.7.3, 7.7.4, Figure 7.24]

7.1 Introduction

The atmosphere is mostly composed of gases, but also contains liquid and solid matter in the form of particles. It is usual to distinguish these particles according to their size, chemical composition, water content and sedimentation velocity into atmospheric aerosol particles, cloud particles and falling hydrometeors. Despite their small mass or volume fraction, particles in the atmosphere strongly influence the transfer of radiant energy and the spatial distribution of latent heating through the atmosphere, thereby influencing the weather and climate.

Clouds usually form in rising air, which expands adiabatically and cools until cloud formation occurs, usually through the nucleation or freezing of aerosol particles. Cloud particles are generally larger than aerosol particles and mostly composed of liquid water or ice. The evolution of a cloud is governed by the balance between a number of dynamical, radiative and microphysical processes. Cloud particles of sufficient size become falling hydrometeors, which are categorised as drizzle drops, raindrops, snow crystals, graupel and hailstones. Precipitation is an important, but difficult to comprehend, climate variable which is influenced by the distribution of moisture and cloudiness, and to a lesser extent by the concentrations and properties of aerosol particles.

Atmospheric aerosols are small solid and liquid particles suspended in the air that can be of natural or anthropogenic origin. They interact with solar radiation, through absorption and scattering, and to a lesser extent with terrestrial radiation, through absorption, scattering and emission. Aerosols can serve as cloud condensation nuclei (CCN) and ice nuclei (IN) upon which cloud droplets and ice crystals form. They also play a wider role in biogeochemical cycles in the Earth system, for instance by carrying nutrients to ocean ecosystems.

Cloud and aerosol amounts and properties are extremely variable in space and time. The short lifetime of cloud particles in subsaturated air creates relatively sharp cloud edges and fine-scale variations in cloud properties, which is much less typical of aerosol layers. While the distinction between aerosols and clouds is generally appropriate and useful, it is not always unambiguous, which can cause interpretational difficulties (e.g., Charlson et al., 2007; Koren et al., 2007).

Clouds respond to climate forcing mechanisms in multiple ways, and can alter both the net response of the system, for instance the globally-averaged surface temperature, but also modify the potency of the initial forcing. The representation of cloud processes in climate models has been recognised for decades as a continuing source of much of the uncertainty associated with our understanding of changes in the climate system (e.g., Arakawa, 1975; Arakawa, 2004; Bony et al., 2006; Cess et al., 1989; Charney, 1979; Randall et al., 2003), but cloud processes have never been systematically assessed by the IPCC before. Key issues include the representation of cumulus convection, cloud formation and dissipation processes. Inter-model differences in cloud feedbacks constitute by far the primary source of spread of both equilibrium and transient climate responses simulated by the CMIP3 climate models (Dufresne and Bony, 2008) despite the fact that most models simulate a near-neutral or positive cloud feedback (Randall et al., 2007 ; and later in this chapter).

Anthropogenic aerosols are responsible for a radiative forcing of climate change through their interaction with radiation and as a result of their interaction with clouds. Quantification of these effects is fraught with uncertainties (Haywood and Boucher, 2000; Lohmann and Feichter, 2005). While previous attempts to quantify the net anthropogenic radiative forcing from first principles have found that it is very likely or virtually certain to be negative, they could not rule out the possibility of positive values (Forster et al., 2007; Haywood and Schulz, 2007). Our inability to better quantify non-greenhouse-gas radiative forcings, and primarily those that result from aerosol-cloud interactions, underlie difficulties in constraining climate sensitivity from observations, even if we had a perfect knowledge of the temperature record (Stevens and Schwartz, 2012).

How clouds and aerosols contribute to climate change is conceptualized with the help of Figure 7.1, which also provides an overview of important terminological distinctions. *Forcings* associated with forcing agents such as greenhouse gases and aerosols act on global mean surface temperature through the global radiative (energy) budget. *Rapid forcing adjustments* (sometimes called rapid responses) arise when forcing agents, by

altering flows of energy internal to the system, affect cloud cover or other components of the climate system and thereby alter the global budget indirectly. Because these adjustments do not operate through changes in the global mean surface temperature, which are slowed by the massive heat capacity of the oceans, they are generally rapid and most are thought to occur within a few weeks. *Feedbacks* are associated with changes in climate variables that are mediated by a change in temperature; they contribute to amplify or damp the changes to the global mean surface temperature via their impact on the radiative budget. Such a framework offers a clear distinction between the traditional concept of radiative forcing (RF, defined as the instantaneous radiative forcing with stratospheric adjustment only) and the relatively new concept of adjusted forcing (AF, which includes other atmospheric and surface rapid adjustments) as introduced in Chapter 1 and further discussed in Section 8.1. Figure 7.2 links the former terminology of aerosol direct, semi-direct and indirect effects with the new terminology used in this Chapter and in Chapter 8.

[INSERT FIGURE 7.1 HERE]

Figure 7.1: Overview of feedback and forcing pathways involving clouds and aerosols. Forcing mechanisms are represented by black arrows; forcing agents are boxes with grey shadows, rapid forcing adjustments (also called rapid responses) are shown with brown arrows and feedbacks are other-coloured arrows. See text for further discussion.

[INSERT FIGURE 7.2 HERE]

Figure 7.2: Schematic of the new terminology used in this assessment report for aerosol-radiation and aerosol-cloud interactions and how they relate to the terminology used in AR4. The radiative forcing from aerosol-radiation interactions (abbreviated RFari) encompasses radiative effects from anthropogenic aerosols before any adjustment takes place, and corresponds to what is usually referred to as the aerosol direct effect. Rapid adjustments induced by aerosol radiative effects on the surface energy budget, the atmospheric profile and cloudiness contribute to the adjusted forcing from aerosol-radiation interactions (abbreviated AFari). They include what has earlier been referred to as the semi-direct effect. The radiative forcing from aerosol-cloud interactions (abbreviated RFaci) refers to the instantaneous effect on cloud albedo due to changing concentrations of cloud condensation and ice nuclei. All subsequent changes to the cloud lifetime and thermodynamics are rapid adjustments, which contribute to the adjusted forcing from aerosol-cloud interactions (abbreviated AFaci).

For the first time in the IPCC WGI assessment reports, clouds and aerosols are discussed together in a single chapter. Doing so allows us to assess, and place in context, recent developments in a large and growing area of climate change research. In addition to assessing cloud feedbacks and aerosol forcings, which were covered in previous assessment reports in a less unified manner, it becomes possible to assess understanding of the multiple interactions among aerosols, clouds and precipitation and their relevance for climate and climate change. Section 7.2 describes understanding of the role of clouds in climate change, and Section 7.3 discusses aerosol processes and properties. Section 7.4 covers aerosol-cloud interactions. Estimates of the aerosol RF and AF due to aerosol-radiation and aerosol-cloud interactions are synthesised in Section 7.5. Section 7.6 is devoted to precipitation processes. Finally Section 7.7 assesses solar radiation management techniques aimed at cooling the planet as a number of these techniques rely on the modification of aerosols and clouds.

7.2 Clouds

This section summarises our understanding of clouds in the current climate from observations and process models; advances in the representation of cloud processes in climate models since AR4; assessment of cloud, water vapour and lapse rate feedbacks; and the radiative forcing due to clouds induced by moisture released by two anthropogenic processes (air traffic and irrigation). Aerosol-cloud interactions are assessed in Section 7.4. The fidelity of climate model simulations of clouds in the current climate is assessed in Chapter 9.

7.2.1 Clouds in the Present-Day Climate System

7.2.1.1 Cloud Formation, Cloud Types, and Cloud Climatology

To form a cloud, air must cool or moisten until it is sufficiently supersaturated to nucleate some of the available condensation or freezing nuclei. Clouds may be composed of liquid water (possibly supercooled), ice, or both (mixed phase). The nucleated cloud particles are initially very small, but grow by vapour deposition. Other microphysical mechanisms dependent on the cloud phase (e.g., droplet collision and coalescence for liquid clouds, riming and Wegener-Bergeron-Findeisen processes for mixed-phase clouds,

and snow formation for ice clouds) can produce a broader spectrum of particle sizes and types; turbulent mixing produces further variations in cloud properties on scales from kilometres to less than a centimetre (Brenguier, 1993). If and when some of the droplets or ice particles become large enough, these will fall out of the cloud as precipitation.

Clouds form in diverse ways, including large-scale or orographically-driven ascent, convection in unstable atmospheric layers, radiative or evaporative cooling, or turbulent mixing of a moist layer. Air circulations often organise convection and associated clouds into coherent systems having scales from tens to thousands of kilometres, such as cyclones or frontal systems. These represent a significant modelling and theoretical challenge, since they are usually too large to represent in explicit cloud models (Section 7.2.2.1.1), but are also not well resolved nor parameterised by most climate models; this gap however is beginning to close (Section 7.2.2.1.2). Finally, clouds and cloud systems are organized by larger-scale circulations into different regimes such as deep convection near the equator, subtropical marine stratocumulus, or midlatitude storm tracks guided by the tropospheric westerly jets. Figure 7.3 shows a selection of widely occurring cloud regimes schematically and as they might appear in a typical geostationary satellite image.

[INSERT FIGURE 7.3 HERE]

Figure 7.3: Diverse cloud regimes reflect diverse meteorology. (a) A visible-wavelength geostationary satellite image shows (from top to bottom) expanses and long arcs of cloud associated with extratropical cyclones, subtropical coastal stratocumulus near Baja California breaking up into shallow cumulus clouds in the central Pacific, and mesoscale convective systems outlining the Pacific intertropical convergence zone or ITCZ. (b) A schematic section through a typical warm front of an extratropical cyclone (see orange dots in panel (a)) showing multiple layers of upper-tropospheric ice (cirrus) and mid-tropospheric water (altostratus) cloud upwind of the frontal zone, an extensive region of nimbostratus associated with frontal uplift and turbulence-driven boundary layer cloud in the warm sector. (c) A schematic section along the low-level trade wind flow from a subtropical west coast of a continent to the ITCZ (see red dots in panel (a)), showing typical low-latitude cloud types, shallow stratocumulus above the cool waters of the oceanic upwelling zone near the coast and trapped under a strong subsidence inversion, and shallow cumulus over warmer waters further offshore transitioning to precipitating cumulonimbus cloud systems with extensive cirrus anvils associated with rising air motions in the ITCZ.

Clouds cover about two thirds of the globe (Figure 7.4a,c). The midlatitude oceanic storm tracks and tropical precipitation belts are particularly cloudy, while continental desert regions and the central subtropical oceans are relatively cloud-free. Clouds are composed of liquid at temperatures above 0°C, ice below –38°C, and either phase at intermediate temperatures (Figure 7.4b). While temperatures at any given altitude are warmer in the tropics, clouds also extend higher there, such that ice cloud amounts are comparable to those at high latitudes. Approximately 40% of the liquid clouds are at least lightly precipitating (Figure 7.4d), but this fraction is much smaller for ice clouds. These fractions are sensitive to the criterion for defining precipitation, especially for ice clouds.

In this chapter clouds above the 440 hPa pressure level are considered “high,” those below 680 hPa “low,” and those in-between are considered mid-level, following Rossow and Schiffer (1991). Most high clouds (mainly cirrus and deep cumulus outflows) occur near the equator and over tropical continents, but can also be seen in the midlatitude storm track regions and over midlatitude continents in summer (Figure 7.5a,e); they are produced by the storms generating most of the global rainfall in regions where tropospheric air motion is upward, such that dynamical, rainfall and high-cloud fields closely resemble one another (Figure 7.5d, h). Mid-level clouds (Figure 7.5b,f), comprising a variety of types, are seen mainly in the storm tracks. Low clouds (Figure 7.5c,g), including shallow cumulus and stratiform clouds, occur over essentially all oceans but are most prevalent over cooler subtropical oceans where tropospheric air motion is downward. They are less common over land, except at night and in winter.

[INSERT FIGURE 7.4 HERE]

Figure 7.4: (a) Annual mean cloud fractional occurrence (CloudSat/CALIPSO 2B-GEOPROF-LIDAR dataset for 2006–2011); (b) annual zonal mean liquid water path (blue shading, ocean only, O’Dell et al. (2008) microwave radiometer dataset for 1988–2005; the 90% uncertainty range, assessed to be 70–150% of the plotted value, is schematically indicated by the white error bar) and ice water path (grey shading, from CloudSat 2C-ICE dataset for 2006–2011; the 90% uncertainty range, assessed to be 50–200% of the plotted value, is schematically indicated by the black error bar). (c-d) latitude-height sections of annual zonal mean cloud (including precipitation falling from cloud) occurrence and precipitation (attenuation-corrected radar reflectivity >0 dBZ) occurrence; the latter has been doubled to

make use of a common colour scale (2B-GEOPROF-LIDAR dataset). The dashed curves show the annual-mean 0°C and −38°C isotherms.

[INSERT FIGURE 7.5 HERE]

Figure 7.5: (a-d) DJF mean high, middle and low cloud cover from CloudSat/CALIPSO GEOPROF dataset (2006–2011), and 500 hPa vertical pressure velocity (colours) and GPCP precipitation (magenta contours at 3 mm day^{-1} in dash and 7 mm day^{-1} in solid); (e-h) same as (a-d), except for JJA. For low clouds, the CALIPSO-only GOCCP dataset is used at locations where it indicates as larger fractional cloud cover, because the GEOPROF dataset removes some clouds with tops at altitudes below 750 m. Low cloud amounts are likely underrepresented in regions of high cloud (Chepfer et al., 2008), although not as severely as with earlier satellite technologies.

7.2.1.2 Effects of Clouds on Earth's Radiation Budget

The effect of clouds on Earth's present-day top-of-atmosphere (TOA) radiation budget, or cloud radiative effect (CRE), can be inferred from satellite data by comparing upwelling radiation in cloudy and non-cloudy conditions. Loeb et al. (2009) estimate that by enhancing the planetary albedo, clouds exert a global and annual shortwave cloud radiative effect (SWCRE) of –47 W m^{-2} and, by contributing to the greenhouse effect, exert a mean longwave effect (LWCRE) of +30 W m^{-2}. Other published satellite estimates differ from these by 10% or less (Loeb et al., 2009). The net global mean CRE of –17 W m^{-2} implies a net cooling effect of clouds on climate. Each of the individual longwave and shortwave CREs is large compared to the ~4 W m^{-2} radiative forcing of doubling CO_2. Thus clouds have the potential to cause significant climate feedback, depending on how climate-sensitive are the properties governing these two effects (Section 7.2.4). Clouds also exert a CRE at the surface, thus affecting the hydrological cycle (Section 7.6), though this aspect of CRE has received less attention (see Section 7.2.2.2).

[INSERT FIGURE 7.6 HERE]

Figure 7.6: Distribution of annual-mean top of atmosphere (a) SWCRE, (b) LWCRE, (c) net CRE (2001–2010 average from CERES-EBAF) and (d) precipitation (1981–2000 average from GPCP).

The regional patterns of annual-mean TOA CRE (Figure 7.6a-b) reflect those of the altitude-dependent cloud distributions. High clouds, which are cold compared to the underlying surface, dominate patterns of LWCRE, while the SWCRE is sensitive to optically thick clouds at all altitudes. Regions of deep, thick cloud with large LWCRE and large negative SWCRE tend to accompany precipitation (Figure 7.6d), showing their intimate connection with the hydrological cycle. The net CRE is negative over most of the globe and most negative in regions of very extensive low-lying reflective stratus and stratocumulus cloud such as the midlatitude and eastern subtropical oceans, where SWCRE is strong but LWCRE is weak. In these regions, the spatial distribution of net CRE on seasonal timescales is strongly correlated with measures of low-level stability or inversion strength (Klein and Hartmann, 1993; Williams et al., 2006; Wood and Bretherton, 2006; Zhang et al., 2010). However, models with comparably good simulations of this behaviour in the current climate can produce a broad range of cloud responses to climate perturbations (Wyant et al., 2006).

7.2.2 Cloud Processes

7.2.2.1 Modelling of Cloud Processes

Cloud formation processes span scales from the submicron scale of cloud condensation nuclei to cloud system scales of up to thousands of kilometres. This range of scales is impossible to resolve with numerical simulations on computers, and is unlikely to become so for decades if ever. Nonetheless progress has been made through a variety of modelling strategies.

7.2.2.1.1 Explicit simulations in small domains

High-resolution models in small domains have been widely used to simulate interactions of turbulence with various types of cloud, e.g., cumulus, stratocumulus and cirrus. The grid spacing is chosen to be small enough to resolve explicitly the dominant turbulent eddies that drive cloud heterogeneity, with the effects of smaller-scale phenomena parameterized. This strategy is typically called large-eddy simulation (LES) when boundary-layer eddies are resolved, and cloud-resolving modelling (CRM) when only deep cumulus motions are well resolved. It is useful not only in simulating cloud and precipitation characteristics, but also in understanding how turbulent circulations within clouds transport and process aerosols and chemical

constituents. Cloud microphysics, precipitation and aerosol interactions are treated with varying levels of sophistication. Such models can be run in idealised settings, or with boundary conditions for specific observed cases.

Such models have come to play several key scientific roles. First, they can be directly compared to in-situ and high-resolution remote sensing observations (e.g., Blossey et al., 2007; Fridlind et al., 2007; Stevens et al., 2005a). Second, they have revealed important influences of small-scale interactions, turbulence, entrainment and precipitation on cloud dynamics that must eventually be accounted for in parameterizations (e.g., Ackerman et al., 2009; Derbyshire et al., 2004; Krueger et al., 1995; Kuang and Bretherton, 2006). Third, they can be used to predict how cloud ensemble properties (such as cloud cover, depth, or radiative effect) may respond to climate changes (e.g., Ackerman et al., 2003; Tompkins and Craig, 1998). Fourth, they have become an important tool in testing and improving parameterizations of cloud-controlling processes such as cumulus convection, turbulent mixing, small-scale horizontal cloud variability, and aerosol-cloud interactions (Fletcher and Bretherton, 2010; Lock, 2009; Randall et al., 2003; Rio and Hourdin, 2008; Stevens and Seifert, 2008), as well as the interplay between convection and large-scale circulations (Kuang, 2008).

CRMs of deep convective cloud systems with horizontal resolutions of 2 km or finer (Bryan et al., 2003) can reasonably characterise observed statistical properties of the cloud ensemble, including fractional area coverage of cloud (Xu et al., 2002), vertical thermodynamic structure (Blossey et al., 2007), the distribution of updraughts and downdraughts (Khairoutdinov et al., 2009), and organisation into mesoscale convective systems (Grabowski et al., 1998). Finer grids (down to hundreds of meters) often give significantly better or different results for individual storm characteristics such as vertical velocity or tracer transport, however. Some cloud ensemble properties remain sensitive to CRM microphysical parameterization assumptions regardless of resolution, particularly the vertical distribution and optical depth of clouds containing ice.

It is computationally demanding to run a CRM in a domain large enough to capture convective organisation or perform regional forecasts. Some studies have created smaller regions of CRM-like resolution within realistically forced regional-scale models (e.g., Boutle and Abel, 2012; Zhu et al., 2010; Zhu et al., 2012), a special case of the common "nesting" approach for regional downscaling (see Section 9.6). One application has been to orographic precipitation, both associated with extratropical cyclones (e.g., Garvert et al., 2005) and with explicitly simulated cumulus convection (e.g., Hohenegger et al., 2008); better resolution of the orography improves the simulation of precipitation initiation and wind drift of falling rain and snow between watersheds.

LES of shallow cumulus cloud fields with horizontal grid spacing of about 100 m and vertical grid spacing of about 40 m produces vertical profiles of cloud fraction, temperature, moisture and turbulent fluxes that agree well with available observations (Siebesma et al., 2003), though the simulated precipitation efficiency still shows some sensitivity to microphysical parameterizations (vanZanten et al., 2011). LES of stratocumulus-topped boundary layers reproduces the turbulence statistics and vertical thermodynamic structure well (e.g., Ackerman et al., 2009; Stevens et al., 2005a), and has been used to study the sensitivity of stratocumulus properties to aerosols (e.g., Savic-Jovcic and Stevens, 2008; Xue et al., 2008) and meteorological conditions. However, the simulated entrainment rate and cloud liquid water path are sensitive to the underlying numerical algorithms, even with vertical grid spacings as small as 5 m, due to poor resolution of the sharp capping inversion (Stevens et al., 2005b). On the other hand, using modern high-order turbulence closure schemes, the statistics of boundary-layer cloud distributions can be reasonably simulated even at CRM-like horizontal resolution of 1 km or larger (Cheng and Xu, 2008; Cheng and Xu, 2006).

7.2.2.1.2 Cloud-resolving global models

Since AR4, increasing computer power has led to three types of developments in global atmospheric models. First, models have been run with resolution that is higher than in the past, but not sufficiently high that cumulus clouds can be resolved. Second, models have been run with resolution high enough to resolve (or "permit") large individual cumulus clouds over the entire globe. In a third approach, the parameterizations of global models have been replaced by embedded CRMs. The first approach is assessed in Chapter 9. The other two approaches are discussed below.

Global cloud-resolving models (GCRMs) have been run with grid spacings as small as 3.5 km (Putman and Suarez, 2011; Tomita et al., 2005). At present GCRMs can only be used for relatively short simulations of a few simulated months to a year or two on the fastest supercomputers, but in the not-too distant future they may provide climate projections. GCRMs provide a consistent way to couple convective circulations to large-scale dynamics, but must still parameterize the effects of individual clouds, microphysics, and boundary-layer circulations.

Because they avoid many of the biases associated with uncertain aspects of cumulus parameterization, GCRMs better simulate many properties of convective circulations that are very challenging for conventional GCMs, including the diurnal cycles of precipitation (Sato et al., 2009) and the Asian summer monsoon (Oouchi et al., 2009). Inoue et al. (2010) showed that the cloudiness simulated by NICAM is in good agreement with observations from CloudSat and CALIPSO, but the results are sensitive to the parameterizations of turbulence and cloud microphysics (Iga et al., 2011; Inoue et al., 2010).

Heterogeneous multiscale methods, in which cloud-resolving models are embedded in each grid cell of a larger scale model (Grabowski and Smolarkiewicz, 1999), have also been further developed as a way to realise some of the advantages of GCRMs but at less cost. This approach has come to be known as superparameterization, because the CRM effectively replaces some of the existing GCM parameterizations (e.g., Khairoutdinov and Randall, 2001; Tao et al., 2009). Super-parameterized models occupy a middle ground between “process models” and “climate models” (see Figure 7.7) in terms of both advantages and cost.

Like GCRMs, super-parameterized models give more realistic simulations of the diurnal cycle of precipitation (Khairoutdinov et al., 2005; Pritchard and Somerville, 2010) and the MJO (Benedict and Randall, 2009) than most standard GCMs; they can also improve aspects of the Asian monsoon and the El Niño-Southern Oscillation (DeMott et al., 2011; Stan et al., 2010). Moreover, because they also begin to resolve cloud-scale circulations, both strategies provide a framework for studying aerosol-cloud interactions that standard GCMs lack (Wang et al., 2011b).

[INSERT FIGURE 7.7 HERE]

Figure 7.7: Model and simulation strategy for representing the climate system and climate processes at different space and time scales. Models are usually defined based on the range of spatial scales they represent, shown by square brackets. The temporal scales that can be represented for a given model class can vary; for instance climate models can be run for a few time steps, or can simulate millennia. The figure indicates the typical timescales for which a given model is used. Computational power prevents one model from covering all time and space scales. Since the AR4 the development of global cloud resolving models, and hybrid approaches such as the multi-scale modelling framework, have helped fill the gap between climate system and climate process models.

7.2.2.2 Recent Observational Advances

New observations, and continuing support for existing observational networks have also led to advances in understanding cloud processes since AR4. Observational constraints on long-term cloudiness changes or on cloud feedbacks are discussed respectively in Sections 2.3.8 and 7.2.4.

In 2006, two new coordinated, downward-pointing active sensors, the cloud profiling radar (CPR) on the CloudSat satellite and the CALIOP lidar on board the CALIPSO satellite were placed in orbit. These sensors have significantly improved our ability to quantify cloud amounts, water content and precipitation globally (see Figures 7.4 and 7.5), and complement the detection capabilities of passive multispectral sensors (e.g., Chan and Comiso, 2011). An international network of surface-based active cloud sensors now deployed at several well-instrumented sites sampling a variety of climate regimes are being systematically compared with climate models (Illingworth et al., 2007) and their parameterizations (Hogan et al., 2009; Neggers et al., 2012). Finally, field programs continue to give insights into cloud processes such as tropical cumulus convection over land (Lebel et al., 2010), cirrus formation (May et al., 2008) and aerosol-cloud-precipitation interactions associated with low-lying, liquid water clouds (Rauber et al., 2007; Wood et al., 2011b).

The net downward flux of radiation at the surface, which is a key driver of the global hydrological cycle, is sensitive to the vertical distribution of clouds. Through radiation budget measurements and cloud profiling it has been estimated more accurately (Kato et al., 2011). Based on these observations, the global mean surface

longwave flux is about 10 W m^{-2} larger than the average in climate models, likely due to insufficient model-simulated cloud cover or lower tropospheric moisture (Stephens et al., 2012).

Satellite cloud-observing capacities are reviewed by Stubenrauch et al. (2012). New sensors show more clearly that low clouds are prevalent in nearly all types of convective system, to an extent not always captured in models (Chepfer et al., 2008; Haynes et al., 2011; Naud et al., 2010). Cloud layers at different levels overlap less often than often assumed in GCMs, especially over high-latitude continents (Mace et al., 2009; Naud et al., 2008), and the common assumption that the radiative effects of precipitating ice can be neglected is not necessarily warranted (Waliser et al., 2011). New observations have led to revised treatments of overlap in some models, which significantly affects cloud radiative effects (Pincus et al., 2006). Active sensors have also been useful in detecting low-lying Arctic clouds over sea ice (Kay et al., 2008), improving our ability to test climate model simulations of the interaction between sea ice loss and cloud cover (Kay et al., 2011).

Recent studies have confirmed that aircraft observations of unexpectedly numerous small ice crystals are largely an artefact of crystal shattering (Korolev et al., 2011), helping to reconcile in-situ and satellite observations. Satellite observations of ice water content have enabled model microphysical schemes to be tested globally, revealing for example that the rate of conversion of cloud ice to precipitation varies geographically in ways not consistent with current assumptions (Ma et al., 2012a) and that liquid water clouds in CRMs generally begin to rain too early (Suzuki et al., 2011). Global datasets of low-lying liquid cloud droplet number concentration based on passive observations at multiple wavelengths are being improved (Bennartz, 2007; Quaas et al., 2006) and are gaining popularity as a metric for climate model simulation of aerosol-cloud interactions (Wang et al., 2011b).

7.2.3 Parameterization of Clouds in Climate Models

7.2.3.1 Challenges of Parameterization

Cloud droplets or ice crystals form from vapour, evolve, collide, may grow to form precipitation, and ultimately evaporate or fall out of the atmosphere. The representation of these processes in climate models is particularly challenging, in part because some of the fundamental details of these microphysical processes are poorly understood (particularly for ice- and mixed-phase clouds), and because the spatial heterogeneity of the clouds and their turbulent properties occurs at scales significantly smaller than a GCM grid box.

Most CMIP5 climate model simulations use horizontal resolutions of 100–200 km in the atmosphere, with vertical layers varying between 100 m near the surface to more than 1000 m aloft. Within regions of this size in the real world, there is usually enormous subgrid-scale variability in cloud properties, associated with variability in humidity, temperature and vertical motion (Figure 7.16). This variability must be accounted for to accurately simulate cloud-radiation interaction, condensation, evaporation and precipitation, and other cloud processes that crucially depend on how cloud condensate is distributed across each grid box (Cahalan et al., 1994; Larson et al., 2001; Pincus and Klein, 2000).

The simulation of clouds in modern climate models involves several parameterizations that must closely work together as a system. These include parameterization of turbulence and cumulus convection, cloud fraction and microphysical processes (including their vertical overlap between different grid levels), and aerosol and chemical transport. The system of parameterizations must balance simplicity, realism, computational stability and efficiency. Each parameterization makes simplifying mathematical assumptions about the subgrid variability within each grid cell; these assumptions vary significantly from model to model and for pragmatic and historical reasons may not even be fully consistent across the parameterizations used in one model. For example, clouds in a grid column may be assumed to be vertically stacked for the radiation calculation, but not for calculating evaporation of precipitation. In summary, realistic simulation of clouds and their response to climate change forms one of the greatest challenges of climate modelling.

Cloud process parameterization is important for specialized chemical-aerosol-climate models (see review by Zhang, 2008) and for regional climate models as well as for CMIP5-class global models. A few of the former models have added complexity in representing subgrid cloud variability and the cloud particle size distribution (e.g., Jacobson, 2003).

7.2.3.2 Recent Advances in Representing Cloud Microphysical Processes

7.2.3.2.1 Liquid clouds

Recent development efforts have been focused on the introduction of more complex representations of microphysical processes, with the dual goals of coupling them better to atmospheric aerosols and linking them more consistently to the sub-grid variability assumed by the model for other calculations. For example, most AR4-era climate models used a single moment formulation for stratiform cloud water, predicting only the average cloud and rain water mass in each grid cell at a given time, diagnosing the droplet concentration using empirical relationships based on aerosol mass (e.g., Boucher and Lohmann, 1995; Menon et al., 2002), or altitude and proximity to land. Many were forced to employ an arbitrary lower bound on droplet concentration to reduce the aerosol radiative forcing (Hoose et al., 2009). Such formulations oversimplify microphysically-mediated cloud variations.

By contrast, more models participating in CMIP5 use two-moment schemes for liquid stratiform cloud. Some diagnose rain and snow number concentrations and mixing ratios (Morrison and Gettelman, 2008; Salzmann et al., 2010), allowing treatment of aerosol scavenging and the radiative effect of snow. Some models explicitly treat subgrid cloud water variability for calculating microphysical process rates (Morrison and Gettelman, 2008). Cloud droplet activation schemes now account more realistically for subadiabaticity, particle composition, and particle size (Abdul-Razzak and Ghan, 2000; Ghan et al., 2011; Liu et al., 2012). Despite such advances in internal consistency, a continuing weakness in traditional GCMs (and even in GCRMs and superparameterized models, albeit to a much lesser extent) is their inability to (fully) resolve cloud-scale vertical motions, to which microphysical processes are highly sensitive.

7.2.3.2.2 Mixed-phase and ice clouds

Ice treatments are following a similar path to those for liquid water, and face similar challenges but amplified by the greater complexity of ice processes. Many AR4 models predicted the condensed water amount in just two categories – cloud and precipitation – with a temperature-dependent partitioning between liquid and ice within either category. Although supersaturation with respect to ice is commonly observed at low temperatures, only one CMIP3 GCM (ECHAM) allowed ice supersaturation (Lohmann and Kärcher, 2002). Many climate models now include separate, physically-based equations for cloud liquid versus cloud ice, and for rain versus snow, allowing a more realistic treatment of mixed-phase processes and ice supersaturation (Gettelman et al., 2010; Liu et al., 2007; Salzmann et al., 2010; Tompkins et al., 2007; see also Section 7.4.4). These new schemes are tested in a single-column model against cases observed in field campaigns (e.g., Klein et al., 2009) or against satellite observations (e.g., Kay et al., 2012), and provide superior simulations of cloud structure than typical AR4-class parameterizations (Kay et al., 2012). New representations of the Wegener-Bergeron-Findeisen process in mixed-phase clouds (Lohmann and Hoose, 2009; Storelvmo et al., 2008b) compare the rate at which the pre-existing ice crystals deplete the water vapour (Korolev, 2007) with the condensation rate for liquid water driven by vertical updraught speed; these are not yet included in CMIP5 models. Climate models are increasingly representing detailed microphysics, including mixed-phase processes, inside convective clouds (Fowler and Randall, 2002; Lohmann, 2008; Song and Zhang, 2011). Such processes can influence storm characteristics like strength and electrification. We reiterate that microphysical detail may not translate to improved simulation if the dynamics is not commensurately well resolved.

7.2.3.3 Recent Advances in Parameterizing Moist Turbulence and Convection

Both the mean state and variability in climate models are sensitive to the parameterization of cumulus convection. Since AR4, the development of convective parameterization has been driven largely by rapidly growing use of process models, in particular LES and CRMs, to inform parameterization development (see Hourdin et al., 2012).

Accounting for greater or more state-dependent entrainment of air into deep cumulus updraughts has improved simulations of the Madden-Julian Oscillation (MJO), tropical convectively-coupled waves, and mean rainfall patterns in some models (Bechtold et al., 2008; Chikira and Sugiyama, 2010; Del Genio et al., 2012; Del Genio et al., 2007; Hohenegger and Bretherton, 2011; Kim et al., 2012; Mapes and Neale, 2011; Song and Zhang, 2009) but usually at the expense of other aspects of the simulation. Improved activation

criteria and parameterizations of cumulus momentum fluxes in another model improved ENSO and tropical vertical temperature profiles (Neale et al., 2008; Richter and Rasch, 2008). Since AR4, more climate models have adopted cumulus parameterizations that diagnose the expected vertical velocity in cumulus updraughts (e.g., Chikira and Sugiyama, 2010; Donner et al., 2011; Park and Bretherton, 2009), in principle allowing more complete representations of aerosol activation, cloud microphysical evolution, and gravity wave generation by the convection.

Several global models now couple shallow cumulus convection more closely to moist boundary layer turbulence (Couvreux et al., 2010; Neggers, 2009; Neggers et al., 2009; Siebesma et al., 2007) including cold pools generated by nearby deep convection (Grandpeix and Lafore, 2010). Many of these efforts have led to more accurate simulations of boundary-layer cloud radiative properties and vertical structure (e.g., Köhler et al., 2011; Park and Bretherton, 2009), and have ameliorated the common problem of premature deep convective initiation over land in one CMIP5 GCM (Rio et al., 2009).

7.2.3.4 Recent Advances in Parameterizing Cloud Radiative Effects

Some models have improved representation of subgrid cloud variability, which has important effects on grid-mean radiative fluxes and precipitation fluxes, for example based on the use of probability density functions of thermodynamic variables (Watanabe et al., 2009). Stochastic approaches for radiative transfer can account for this variability in a computationally efficient way (Barker et al., 2008). New treatments of cloud overlap have been motivated by new observations (Section 7.2.2.2).

7.2.4 Cloud, Water-Vapour and Lapse Rate Feedbacks

Climate feedbacks are a central concern for projecting the magnitude of climate change, because they determine the sensitivity of global surface temperature to external forcing agents (see Chapter 9). Water vapour, lapse rate and cloud feedbacks each involve moist atmospheric processes closely linked to clouds, and in combination, produce most of the simulated climate feedback and most of its inter-model spread. The strength of a radiative feedback can be expressed as its impact on the top-of-atmosphere net downward radiative flux per degree of global surface temperature increase (or feedback parameter) and may be compared with the basic "black-body" response of -3.4 W m^{-2} K^{-1}.

7.2.4.1 Water-Vapour Response and Feedback

As pointed out in previous reports (Randall et al., 2007, Section 8.6.3.1), physical arguments and models of all types suggest global water vapour amounts increase in a warmer climate, leading to a positive feedback via its enhanced greenhouse effect. The saturated water vapour mixing ratio (WVMR) increases nearly exponentially and very rapidly with temperature, at 6–10% per degree near the surface, and even more steeply aloft (up to 17% per degree) where air is colder. Mounting evidence continues to indicate that changes in relative humidity in warmer climates will be nowhere near this rapid, at least in a global and statistical sense, although new work highlights some robust changes that vary by region. Hence the WVMR is expected to increase, on average, at a rate similar to the saturated WVMR.

Because global temperatures have been rising, the above arguments imply WVMR should be rising accordingly, and multiple observing systems indeed show this (Section 2.3.6). One exception is that meteorological station data suggest a plateauing of WVMR near the land surface over the last decade or so, but humidity at this level exerts little greenhouse effect (Soden and Held, 2006) and is governed by mechanisms different from those operating at upper levels (Joshi et al., 2008). A study challenging the water vapour increase (Paltridge et al., 2009) used an older reanalysis product, whose trends are contradicted by newer ones (Dessler and Davis, 2010) and by direct global observations which are considered more reliable for trends (see Box 2.3). The study also reported decreasing relative humidity in data from Australian radiosondes, but more complete studies show that region to be anomalous in this respect (Dai et al., 2011). Thus reliable, large-scale, multi-decade trend data remain consistent with the expected global feedback.

Some studies have proposed that the response of upper-level humidity to natural fluctuations in the global mean surface temperature is informative about the feedback. However, small changes to the global mean (primarily from ENSO) involve geographically heterogeneous temperature change patterns, the responses to

which may be a poor analogue for global warming (Hurley and Galewsky, 2010b). Most climate models reproduce these natural responses reasonably well (Dessler and Wong, 2009; Gettelman and Fu, 2008), providing additional evidence that they at least represent the key processes.

The "last-saturation" concept approximates the WVMR of air by its saturation value when it was last in a cloud (see Sherwood et al., 2010b for a review), which can be inferred from trajectory analysis. Studies since the AR4 using a variety of models and observations (including concentrations of isotopically substituted water vapour molecules) support this concept (Galewsky and Hurley, 2010; Sherwood and Meyer, 2006). The concept has clarified what determines relative humidity in the subtropical upper troposphere and placed the water-vapour feedback on firmer theoretical footing by directly linking actual and saturation WVMR values (Hurley and Galewsky, 2010a).

In a warmer climate, an upward shift of the tropopause and poleward shift of the jets and associated climate zones is expected (Sections 2.6.4 and 2.6.5) and simulated by most GCMs (Section 10.3.3.1). These changes account, at least qualitatively, for robust regional changes in the relative humidity simulated in warmer climate by GCMs, including decreases in the subtropical troposphere and tropical uppermost troposphere, and increases near the extratropical tropopause and high latitudes (Sherwood et al., 2010a). This pattern may be amplified however by non-uniform atmospheric temperature or wind changes (Hurley and Galewsky, 2010b). It is also the likely cause of most model-predicted changes in mid- and upper-level cloudiness patterns (Sherwood et al., 2010a; Wetherald and Manabe, 1980; see also Section 7.2.4.3.3). Idealised CRM simulations of warming climates also show upward shifts, with otherwise little change in mean relative humidity (e.g., Kuang and Hartmann, 2007; Romps, 2011).

It remains unclear whether stratospheric water vapour contributes significantly to climate feedback. Observations have shown decadal variations in stratospheric water vapour, which may have affected the planetary radiation budget somewhat (Solomon et al., 2010) but do not have a clear relation to global warming (Trenberth et al., 2007, Section 3.4.2.4). GCMs can simulate strong positive feedbacks from stratospheric water vapour (Joshi et al., 2010), but with parameter settings producing unrealistic behaviour in the present climate.

7.2.4.2 Relationship Between Water Vapour and Lapse-Rate Feedbacks

Lapse rates in the tropics should change roughly as predicted by a moist adiabat, due to the strong restoring influence of convective heating. This restoring influence has now been directly inferred from satellite data (Lebsock et al., 2010), and the near-constancy of tropical atmospheric stability and deep-convective thresholds over recent decades is also now observable in sea surface temperature (SST) and deep convective data (Johnson and Xie, 2010). The stronger warming of the atmosphere relative to the surface produces a negative feedback on global temperature because the warmed system radiates more thermal emission to space for a given increase in surface temperature than in the reference case where the lapse rate is fixed. This feedback is not equally strong in all models, because lapse rates in middle and high latitudes change differently (Dessler and Wong, 2009).

[INSERT FIGURE 7.8 HERE]

Figure 7.8: Clear-sky feedback parameters as predicted by [CMIP3] GCMs. Black points in the centre show the total radiative response including the Planck response, with the Planck response and individual feedbacks from water vapour and lapse rate shown to the right in red. On the left are the equivalent three parameters calculated in an alternative, relative humidity-based framework. In this framework the Planck stabilization and each of the two feedbacks are all weaker and more consistent among the models. [PLACEHOLDER FOR FINAL DRAFT: Current working draft of figure taken from Held and Shell (2012); additional data from CMIP5 TBA].

As shown by Cess (1975) and discussed in the AR4 (Randall et al., 2007), models with a more negative lapse-rate feedback tend to have a more positive water-vapour feedback. Cancellation between these is close enough that their sum, or "clear-sky feedback," has a 90% range in CMIP3 models of only +0.96 to +1.22 W m^{-2} K^{-1} (based on a Gaussian fit to the data of Held and Shell (2012), see Figure 7.8). The physical reason for this cancellation is that as long as water vapour infrared absorption bands are nearly saturated, outgoing longwave radiation is determined by relative humidity (Ingram, 2010) which exhibits little systematic change in any model (Section 7.2.4.1). In fact, Held and Shell (2012) and Ingram (2012a) argue that it makes more sense physically to consider a reference climate perturbation in which relative humidity is held fixed, rather

than specific humidity as per the usual convention. In that framework, the climate is fundamentally less stable but the water-vapour and lapse-rate feedbacks are each small; the large and partially compensating conventional feedbacks are seen to have arisen from unphysical choices made in first setting out the traditional framework.

There is some observational evidence suggesting significant departures from the adiabatic lapse rate in the tropical upper troposphere (Section 2.2.4), which would be larger than simulated by models (Section 9.4.1). Since the combined clear-sky feedback depends on relative humidity change, however, the imputed lapse-rate variations would have little influence on the total feedback and might even slightly increase it (Ingram, 2012b). In summary, all sound evidence continues to support a strong, positive feedback (measured in the traditional framework) from the combination of water-vapour and lapse-rate changes.

7.2.4.3 Cloud Feedbacks

The dominant source of spread among GCM climate sensitivities in AR4 was due to diverging cloud feedbacks, particularly due to low clouds, and this continues to be true (Chapter 9). The net cloud feedback also continues to be nearly zero or positive in all global models. Progress has been made since the AR4 in understanding which simulated cloud changes underlie the positive feedbacks, and providing a stronger theoretical and observational basis for key positive cloud feedbacks. There has also been progress in quantifying cloud feedbacks, including separating the effects of different cloud types, using radiative-kernel residual methods (Soden et al., 2008) and satellite simulators (see Section 9.2.2.3) (Zelinka et al., 2012a).

Until very recently cloud feedbacks have been diagnosed in models by differencing cloud radiative effects in doubled CO_2 and control climates, normalized by the change in global mean surface temperature. Different diagnosis methods do not always agree, and some simple methods can make positive cloud feedbacks look negative (Soden and Held, 2006). Moreover, it is now recognised that some of the cloud changes are induced directly by the atmospheric radiative effects of CO_2 independently of surface warming, and are therefore rapid adjustments rather than feedbacks. Most of the published studies available for this assessment did not separate these effects, but we do so where possible. It appears that these adjustments are sufficiently small in most models (see Section 7.2.4.3.6) that general conclusions regarding feedbacks are not significantly affected.

Four aspects of the global cloud response to greenhouse gas-induced climate change are distinguished here: altitude increases of high-level clouds, effects of hydrological cycle and storm track changes on middle and high clouds, changes in low-level cloud cover, and changes in high-latitude clouds. Finally, recent research on the rapid cloud adjustments to CO_2 is assessed. Cloud changes cause both longwave (greenhouse warming) and shortwave (reflective cooling) effects, which combine to give the overall cloud feedback or forcing adjustment for global climate.

7.2.4.3.1 Cloud altitude feedback mechanisms involving high-level clouds

High clouds at low and middle latitudes exert little net top-of-atmosphere radiative effect in the current climate due to near-compensation between their longwave and shortwave cloud radiative effects (Kiehl, 1994). Nonetheless, systematic changes in their height or optical thickness could produce a significant radiative feedback by altering this balance.

The dominant driver of net longwave cloud feedback in models, and a dominant contributor to net positive cloud feedback overall, appears to be a robust consequence of global warming: an increase in the height of the tropopause and the main level at which the deepest convective clouds stop rising and cloudy air flows outward, tentatively attributed in AR4 to the so-called “fixed anvil-temperature” mechanism (Hartmann and Larson, 2002). According to this mechanism, the outflow level from tropical deep convective systems is determined ultimately by the highest point at which water vapour emits significant infrared radiation; this point is governed by the water vapour partial pressure, therefore occurring at a similar temperature (higher altitude) in a warmer climate. A positive cloud altitude feedback results because the temperature difference between the cloud and the surface increases, increasing the cloud’s greenhouse effect without necessarily affecting its albedo. This occurs at all latitudes and has long been noted in model simulations (Cess et al., 1990; Hansen et al., 1984). New studies confirm that this mechanism operates in GCMs, with a small modification to account for lapse-rate changes, and accounts for most of the total longwave cloud feedback

in CMIP3 GCMs (Soden and Vecchi, 2011; Zelinka and Hartmann, 2010; Zelinka et al., 2012a). In some GCMs the overall contributions from high cloud and from cloud height changes can be isolated (Figure 7.9) with net (LW+SW) estimates for the feedback parameter of +0.14 (0.0 to +0.30) W m^{-2} K^{-1} and +0.34 (+0.05 to +0.62) W m^{-2} K^{-1}, respectively. The increase in cloud height also occurs consistently in cloud-resolving models (Kuang and Hartmann, 2007; Kubar et al., 2007).

[INSERT FIGURE 7.9 HERE]

Figure 7.9: Cloud feedback parameters as predicted by GCMs. Total feedback shown at left by black symbols, broken out into infrared and visible components in red and blue, respectively (Zelinka et al., 2012a; Zelinka et al., 2012b). Centre panel shows components attributable to clouds in different height ranges (see text); values reported by Soden and Vecchi (2011) do not conform exactly to this definition but are shown for comparison, with their "mixed" category assigned "medium". Right panel shows components attributable to different cloud property changes (not available from all studies).

The observational record allows us to verify various elements of the above mechanism. First, the global tropopause is rising as expected (Chapter 2). Second, cloud heights change as predicted with regional, seasonal and interannual changes in near-tropopause temperature structure (Eitzen et al., 2009; Xu et al., 2007; Zelinka and Hartmann, 2010), although the response may be affected by changes in stratospheric circulation (Chae and Sherwood, 2010; Eitzen et al., 2009). Third, Norris et al. (2012) report that two satellite datasets show a rising trend in high clouds since 1979 roughly consistent with the mechanism. Davies and Molloy (2012) report a downward height trend among all clouds in a shorter record from a satellite that measures heights more directly, but this is likely an artefact of instrument problems early in that record (Evan and Norris, 2012).

7.2.4.3.2 Feedback mechanisms involving the amount of middle and high cloud

Nearly all GCMs simulate a reduced middle and high cloud amount in warmer climates in low- and mid-latitudes, especially in the subtropics (Trenberth and Fasullo, 2009; Zelinka and Hartmann, 2010). In global average, these cloudiness reductions cause a positive shortwave and negative longwave feedback; the latter almost completely cancels the altitude response (Figure 7.9), which may explain why the important role of cloud altitude feedbacks was not fully appreciated until recently. The net effect of changes in amount of all cloud types is a positive feedback, but this comes mainly from the changes low clouds (see the following section), implying a near-cancellation of LW and SW effects for the mid- and high-level amount changes.

Changes in predicted cloud cover are geographically correlated with simulated subtropical drying (Meehl et al., 2007), suggesting that they are partly tied to large-scale circulation changes including the poleward shifts found in most models (Sherwood et al., 2010a; Wetherald and Manabe, 1980). Bender et al. (2012) and Norris et al. (2012) also report latitudinal variations in observed cloudiness trends since 1979 consistent with the poleward shift of the circulation indicated in several other observables (see Chapter 2) and simulated (albeit with weaker amplitude) by most GCMs (Yin, 2005). This shifts clouds to latitudes of weaker sunlight, decreasing the planetary albedo. The impact of the observed shift appears to be significant and would imply a strong positive feedback if it were due to global warming (Bender et al., 2012). Recent studies call into question how much of the observed shifts are temperature- or ozone-driven however (Chapter 10.3), so the true amount of positive feedback coming from poleward shifts remains highly uncertain but could be underestimated by GCMs.

Tselioudis and Rossow (2006) predict reduced cloud cover in the storm-track itself in warmer climates based on observed present-day relationships with meteorological variables combined with model-simulated changes to those driving variables. In agreement with the above analysis, they found that this reduction contributed little to net cloud feedback. The upward mass flux in deep clouds should decrease in a warmer climate (Section 7.6) which might contribute to cloudiness decreases in convective regions (e.g., the ITCZ). Most CMIP3 GCMs produce too little storm-track cloud in the southern hemisphere compared to nearly-overcast conditions in reality. This bias could also imply that positive feedback from poleward shifts is greater than in GCMs, or that the negative feedback many GCMs simulate in these regions from increasing cloud amount may be unrealistic (Trenberth and Fasullo, 2010).

Changing coverage of thin cirrus clouds could in principle exert a significant feedback due to the net warming effect of these clouds (e.g., Rondanelli and Lindzen, 2010), but no mechanistic argument for a

particular change one way or the other has been advanced, and responses in GCMs so far are small (Zelinka et al., 2012b).

7.2.4.3.3 Feedback mechanisms involving low clouds

Differences in the response of low clouds to a warming are responsible for most of the spread in model-based estimates of equilibrium climate sensitivity (Bony and Dufresne, 2005). Since the AR4 this finding has withstood further scrutiny (e.g., Soden and Vecchi, 2011; Webb et al., 2012), holds in CMIP5 models (Vial et al., 2012), and has been shown to apply also to the transient climate response (e.g., Dufresne and Bony, 2008). This 'low-cloud problem' is most potent over tropical and sub-tropical oceans (Williams and Tselioudis, 2007; Williams and Webb, 2009; Xu et al., 2010), although not exclusively so (Trenberth and Fasullo, 2010), and is usually associated with the representation of shallow cumulus or stratocumulus clouds (Williams and Tselioudis, 2007; Williams and Webb, 2009; Xu et al., 2010). Because the low-cloud problem emerges in a variety of idealized model formulations (Medeiros et al., 2008; Zhang and Bretherton, 2008), or conditioned on a particular dynamical state (Bony et al., 2004), it appears to be attributable to how cloud, convective and boundary layer processes are parameterized in GCMs.

The modelled response of low clouds does not appear to be dominated by a single feedback mechanism, but rather the net effect of several potentially competing mechanisms as elucidated in LES and GCM sensitivity studies (e.g., Bretherton et al., 2012; Zhang et al., 2012a; Zhang and Bretherton, 2008). Starting with some proposed negative feedback mechanisms, it has been argued that in a warmer climate, low clouds will be: (i) horizontally more extensive, because changes in the lapse rate of temperature also modify the lower-tropospheric stability (Miller, 1997); (ii) optically thicker, because adiabatic ascent is accompanied by a larger condensation rate (Somerville and Remer, 1984); and (iii) vertically more extensive, in response to a weakening of the tropical overturning circulation (Caldwell and Bretherton, 2009). While these mechanisms may play some role in subtropical low cloud feedbacks, none of them appears dominant. Regarding the first mechanism, model fidelity to relationships observed to hold for the present climate fails to constrain the response of models to climate change (Section 7.2.1.2; see also Webb and Lock, 2012). The second mechanism, discussed briefly in the next section, appears to be a small effect. The third mechanism cannot yet be ruled out, but does not appear to be the dominant factor in determining subtropical cloud changes in GCMs (Bony and Dufresne, 2005; Zhang and Bretherton, 2008).

Since the AR4, several new positive feedback mechanisms have been proposed, most associated with the marine boundary layer clouds thought to be at the core of the 'cloud problem.' These include the ideas that: warming-induced changes in the absolute humidity lapse rate change the energetics of mixing in ways that demand a reduction in cloud amount or thickness (Bretherton et al., 2012; Brient and Bony, 2012; Lock, 2009); energetic constraints prevent the surface evaporation from increasing with warming at a rate sufficient to balance expected changes in dry air entrainment thereby reducing the supply of moisture to form clouds (Rieck et al., 2012; Webb and Lock, 2012); and that increased concentrations of greenhouse gases reduce the radiative cooling that drives stratiform cloud layers and thereby the cloud amount (Bretherton et al., 2012; Caldwell and Bretherton, 2009; Stevens and Brenguier, 2009). These mechanisms could explain why models consistently produce positive low-cloud feedbacks. Among CFMIP GCMs, the feedback parameter ranges from +0.09 to +0.63 W m^{-2} K^{-1}, and is largely associated with a reduction in low-cloud amount, albeit with considerable variability in the spatial structure of these changes (Webb et al., 2012). One "superparameterized" GCM (Section 7.2.2.1) simulates a negative low-cloud feedback (Wyant et al., 2006; Wyant et al., 2009), but that model's representation of low clouds was worse than some conventional GCMs.

The tendency of both GCMs and process models to produce these positive feedback effects suggests that the feedback contribution from changes in low clouds is positive. However, the well-known deficiencies in model representation of low clouds globally, the diversity of model results, the lack of reliable observational constraints, and the tentative nature of the suggested mechanisms leaves us with low overall confidence in the sign of the low-cloud feedback contribution.

7.2.4.3.4 Feedbacks involving changes in cloud optical depth

It has long been suggested that cloud water content could increase in a warmer climate simply due to the availability of more vapour for condensation in a warmer atmosphere, yielding a negative feedback (Paltridge, 1980; Somerville and Remer, 1984), but this argument ignores the physics of crucial cloud-

regulating processes like precipitation formation and turbulence. Observational evidence discounting a large effect of this kind was reported in AR4 (Randall et al., 2007).

The global-mean net feedback from cloud optical depth changes in CFMIP models (Figure 7.9) scatters around zero but is slightly positive on average. Optical depths tend to reduce slightly at low and middle latitudes, but increase consistently at latitudes poleward of 50°, yielding a positive longwave feedback that slightly outweighs the negative shortwave feedback. These latitude-dependent optical depth changes may be attributed to phase changes at high latitudes and greater poleward moisture transport (Vavrus et al., 2009), and possible to poleward shifts of the circulation.

The phase change contribution arises because at mixed-phase temperatures of –40°C–0°C, cloud ice particles are typically several-fold larger than cloud water drops (e.g., Mitchell et al., 2010), so a given mass of cloud ice reflects less sunlight than the same mass of cloud water droplets. As climate warms, the shift from ice to liquid clouds would raise albedos for a given water mass, and the slower fall speeds of liquid could increase the water mass. The resulting negative cloud feedback appears in GCMs (Senior and Mitchell, 1993), with a magnitude that correlates with the simulated amount of cloud ice in mixed-phase clouds (Tsushima et al., 2006). The key physics is however not adequately represented in climate models, so this particular feedback mechanism is highly uncertain.

7.2.4.3.5 Feedback from Arctic cloud interactions with sea ice

Arctic clouds, despite their low altitude, have a net warming effect at the surface in the present climate because their downward emission of infrared radiation over the year outweighs their reflection of sunlight during the short summer season. They also cool the atmosphere, however, so their effect on the energy balance of the whole system is ambiguous and depends on the details of the vertical cloud distribution and the impact of cloud radiative interactions on ice cover (Palm et al., 2010).

Low cloud amount over the Arctic oceans varies inversely with sea ice amount (open water producing more cloud) as now confirmed since AR4 by visual cloud reports (Eastman and Warren, 2010) and lidar and radar observations (Kay and Gettelman, 2009; Palm et al., 2010). The observed effect is weak in boreal summer, when the melting sea-ice is at a similar temperature to open water and stable boundary layers with extensive low cloud are common over both surfaces, and strongest in boreal autumn when cold air flowing over regions of open water stimulates cloud formation by boundary-layer convection (Kay and Gettelman, 2009; Vavrus et al., 2011). Kay et al. (2011) show that a GCM can represent this seasonal sensitivity of low cloud to open water, but doing so depends on the details of how boundary-layer clouds are parameterized. Vavrus et al. (2009) show that in a global warming scenario, GCMs simulate more Arctic low-level cloud in all seasons, but especially during autumn and winter when open water and very thin sea ice increase considerably, increasing upward moisture transport to the clouds.

A negative Arctic cloud feedback was suggested by Liu et al. (2008) on the basis that recent observed surface warming has been greater in less cloudy areas, but this argument was not tested in a climate model and does not control for the large correlated effects of weather on both clouds and surface temperature. Gagen et al. (2011) present tree-ring evidence that summertime Arctic cloud cover was negatively correlated with Arctic temperatures over the last millennium, which is consistent with the conclusions of the above studies assuming there was less ice during warmer periods. Gagen et al. (2011) presented this as evidence of a negative shortwave cloud feedback, but the year-round longwave feedback would likely offset this as noted above. Note that there are pitfalls to using natural climate variations to infer cloud feedbacks in any case (see Section 7.2.4.3.7).

7.2.4.3.6 Rapid adjustment of clouds to a CO_2 change

Gregory and Webb (2008) partitioned the response of top-of-atmosphere radiation in GCMs to an instantaneous doubling of CO_2 into a 'rapid' (sub-seasonal) adjustment in which the land surface, atmospheric circulations and clouds respond to the radiative effect of the CO_2 increase, and an 'SST-mediated' response that develops more slowly as the oceans warm. This distinction is important not only to help understand what is going on in the models, but because the presence rapid adjustments would cause clouds to respond slightly differently to a transient climate change (in which SST changes have not caught up to CO_2 changes) or to a climate change caused by other forcings, than they would to the same warming at

equilibrium driven by CO_2. There is also a rapid adjustment of the precipitation field, discussed in Section 7.6.3.

Gregory and Webb (2008) found that in some climate models, rapid adjustment of clouds can have comparable top-of-atmosphere radiative effects to the ensuing SST-mediated cloud changes. Andrews and Forster (2008) found that this behaviour was exceptional, and that on average, rapid cloud adjustments in a suite of climate models causes less than 20% of their equilibrium radiative feedback; most of these come from low cloud (Colman and McAvaney, 2011). Webb et al. (2012) and Andrews et al. (2012), however, each showed using different model ensembles that adjustments contribute half the uncertainty that feedbacks do, for example 2.2 K uncertainty from feedbacks as compared to 1.08 K from adjustments in the latter study. Thus a better understanding of rapid adjustments could narrow the uncertainty in climate projections.

7.2.4.3.7 Observational constraints on global cloud feedback

A number of studies since AR4 have attempted to constrain cloud feedback (or total climate sensitivity) from observations; here we discuss those using modern cloud, radiation or other measurements. Section 12.5 discusses those based on past temperature data and forcing proxies.

One approach is to seek observable aspects of present-day cloud behaviour that reveal cloud feedback. Varying parameters in a GCM sometimes produces changes in cloud feedback that correlate with the properties of cloud simulated for the present day, but this depends on the GCM (Yokohata et al., 2010), and the resulting relationships do not hold across multiple models such as those from CMIP3 (Collins et al., 2011; Gettelman et al., 2012a). Among the AR4 models, net cloud feedback is strongly correlated with mid-latitude relative humidity (Volodin, 2008) and with characteristics of the southern-hemisphere storm track (Trenberth and Fasullo, 2010); if valid either regression relation would imply a relatively strong positive cloud feedback in reality, but no mechanism has been proposed to explain or validate these empirical relationships and such apparent skill can easily arise fortuitously (Klocke et al., 2011). Likewise, Clement et al. (2009) found realistic decadal variations of low cloud over the North Pacific in only one model (HadGEM1) and argued that the relatively strong cloud feedback in this model should therefore be regarded as more likely, but provided no evidence for such a link. Chang and Coakley (2007) examined midlatitude maritime clouds and found cloud thinning with increasing temperature, consistent with a positive feedback, while Gordon and Norris (2010) found the opposite result following a methodology that tried to isolate thermal and advective effects. In summary, there is no evidence of a robust link between any of the noted observables and the global feedback, though some apparent connections are tantalising and are being further studied.

Several studies have attempted to derive global climate sensitivity from interannual relationships between global-mean observations of top-of-atmosphere radiation and surface temperature. One problem with this is the different spatial character of interannual and long-term warming; another is that the methodology can be confounded by cloud variations not caused by those of surface temperature (Spencer and Braswell, 2008). A range of climate sensitivities has been inferred based on such analyses (Forster and Gregory, 2006; Lindzen and Choi, 2011). Crucially, however, among different GCMs there is no correlation between the interannual and long-term cloud-temperature relationships (Dessler, 2010), contradicting the basic assumption of these methods. Many but not all AOGCMs predict relationships that are consistent with observations (Dessler, 2010). More recently there is interest in relating the time-lagged correlations of cloud and temperature to feedback processes (Spencer and Braswell, 2010) but again these relationships appear to reveal only a model's ability to simulate ENSO or other modes of interannual variability properly, which are not obviously informative about the cloud feedback on long-term global warming (Dessler, 2011).

While a number of studies have proposed methods to infer the long-term cloud feedback from observed variability, for a method to be accepted it should have a sound physical basis and be shown to work consistently when applied to different climate models. No method yet proposed passes both tests. Moreover, some model studies show that the response of global cloud radiative effect to a global warming is sensitive to relatively subtle details in the geographic warming pattern, such as the slight hemispheric asymmetry due to the lag of southern ocean warming relative to northern latitudes (Senior and Mitchell, 2000; Yokohata et al., 2008). Cloud responses to specified uniform ocean warming without CO_2 increases are not the same as those to CO_2-induced global warming simulated with more realistic oceans (Ringer et al., 2006), partly because of rapid adjustments (Section 7.2.4.3.6) and because low clouds also feed back tightly to the underlying surface

(Caldwell and Bretherton, 2009). Simulated cloud feedbacks also differ significantly between colder and warmer climates in some models (Crucifix, 2006; Yoshimori et al., 2009). These sensitivities highlight the challenges facing any attempt to infer long-term cloud feedbacks from simple data analyses.

7.2.4.4 Feedback Synthesis

Together, the water-vapour, lapse-rate and cloud feedbacks are the principal determinants of climate sensitivity. The water-vapour and lapse-rate feedbacks should be thought of as a single phenomenon rather than in isolation. To estimate a 90% probability range for that feedback, we double the variance of GCM results about the mean to account for possible common errors among models, to arrive at +1.09 (+0.91 to +1.27) W m^{-2} K^{-1}, similar to AR4. Values in this range are supported by a steadily growing body of observational evidence, model tests, and physical reasoning. Key aspects of the responses of water vapour and clouds to climate warming now appear to be constrained by large-scale dynamical mechanisms that are not sensitive to poorly-represented small-scale processes, and as such, are more credible.

Several cloud feedback mechanisms now appear consistently in GCMs, summarised in Figure 7.10, most supported by other lines of evidence. They nearly all act in a positive direction. First, high clouds are expected to rise in altitude and thereby exert a stronger greenhouse effect in warmer climates. This altitude feedback mechanism is well understood, has theoretical and observational support, occurs consistently in GCMs and CRMs, and explains about half of the mean positive cloud feedback in GCMs. Second, middle and high-level cloud cover tends to decrease in warmer climates even within the ITCZ, decreasing the albedo more than it increases the greenhouse effect thus adding positive feedback. This cannot be tested observationally but is consistent with anticipated changes to atmospheric water transport. Third, observations and most models suggest storm tracks shift poleward in a warmer climate, drying the subtropics and moistening the high latitudes, which causes further positive feedback via a net shift of cloud cover to latitudes that receive less sunshine. Finally, most GCMs also predict that low cloud amount decreases, especially in the subtropics, another source of positive feedback though one that differs significantly among models and lacks a well-accepted theoretical basis. Over middle and high latitudes, GCMs suggest warming-induced transitions from ice to water clouds may cause clouds to become more opaque, but this appears to have a small net radiative effect.

[INSERT FIGURE 7.10 HERE]

Figure 7.10: Robust cloud responses to greenhouse warming (those simulated by most models and possessing some kind of independent support or understanding). Key climatological features (tropopause, freezing level, circulations) are shown in grey. Changes anticipated in a warmer climate are shown in red (if contributing positive feedback) or brown (if contributing little or ambiguously to feedback); no robust mechanisms contribute negative feedback. Changes include rising high cloud tops and melting level, and increased polar cloud cover and/or optical thickness (high confidence); broadening of the Hadley Cell and/or poleward migration of storm tracks, and narrowing of the ITCZ (medium confidence); and reduced low-cloud amount and/or optical thickness (low confidence). Confidence assessments are based on degree of GCM consensus, strength of independent lines of evidence from observations or process models, and degree of basic understanding.

Currently, neither cloud process models (CRMs and LES) nor observations provide clear evidence to contradict or confirm any of the above mechanisms, except as noted. In some cases these models show stronger low-cloud feedbacks than GCMs, but each model type has limitations, and some GCM biases suggest positive feedbacks are underestimated. For low clouds, cloud process models suggest a variety of potentially opposing response mechanisms that may account for the current spread of GCM feedbacks. In summary we find no evidence to contradict either the cloud or water-vapour-lapse-rate feedback ranges shown by current GCMs, although the many uncertainties mean that true feedback could still lie outside these ranges.

Based on the above synthesis of cloud behaviour, the net radiative feedback due to all cloud types is judged *likely* (>66% chance) to be positive. This is reasoned probabilistically as follows. First, since evidence from observations and process models is mixed as to whether GCM cloud feedback is too strong or too weak overall, and since the positive feedback found in GCMs comes mostly from mechanisms now supported by other lines of evidence, the central (most likely) estimate of the total cloud feedback is taken as the mean from GCMs (+0.8 W m^{-2} K^{-1}). Second, since there is no accepted basis to discredit individual GCMs, the probability distribution of the true feedback must be at least as broad as the distribution of GCM results.

Third, since feedback mechanisms are probably missing from GCMs (particularly involving thin high clouds or low clouds) and some CRMs suggest feedbacks outside the range in GCMs, the probable range of the feedback must be broader than its spread in GCMs. We estimate the likely range of this feedback by doubling the spread (quadrupling the variance) about the mean of the data in Figure 7.9, that is assuming an uncertainty 170% as large as that encapsulated in the GCM range added to it in quadrature, and assuming Gaussian errors. This yields a 90% (very likely) range of −0.2 to 1.4 W m^{-2} K^{-1}, with a 16% probability of a negative feedback.

Note that the assessment of feedbacks in this chapter is independent of constraints on climate sensitivity from observed trends or palaeoclimate information discussed in Section 12.4.

7.2.5 Anthropogenic Sources of Moisture and Cloudiness

Human activity can be a source of additional cloudiness through specific processes involving a source of water vapour in the atmosphere. We discuss here the impact of aviation and irrigation on water vapour and cloudiness. The impact of water vapour sources from combustion at the Earth's surface is thought to be negligible. Changes to the hydrological cycle because of land use change are not discussed.

7.2.5.1 Contrails and Contrail-Induced Cirrus

Aviation jet engines emit hot moist air, which can form line shaped persistent condensation trails (contrails) in environments that are supersaturated with respect to ice and colder than –40°C. The contrails are composed of ice crystals that are typically smaller than those of background cirrus (Frömming et al., 2011; Heymsfield et al., 2010). Their effect on longwave radiation dominates over their shortwave effect (Burkhardt and Kärcher, 2011; Rap et al., 2010a; Stuber and Forster, 2007) but models disagree on the relative importance of the two effects. Contrails have been observed to spread into large cirrus sheets which may persist for several hours, and observational studies confirm their overall positive net RF impact (Haywood et al., 2009). Aerosol emitted within the aircraft exhaust may also affect high-level cloudiness. This last effect is classified as an aerosol-cloud interaction and is discussed in Section 7.4.4. Rap et al. (2010b) confirmed the assessment that aviation contrails are very unlikely, at current levels of coverage, to have an observable effect on surface temperature or diurnal temperature range.

Forster et al. (2007) estimated the 2005 RF from contrails as +0.01 (–0.007 to +0.02) W m^{-2} ,and quoted Sausen et al. (2005) to update the 2000 forcing for aviation-induced cirrus (including linear contrails) to +0.03 (+0.01 to +0.08) W m^{-2} . Lee et al. (2009) scaled these estimates upward 18% to account for revised fuel use estimates, propulsive efficiency and flight routes for year 2005. Kärcher et al. (2010) obtain a range of +0.008 to +0.020 W m^{-2} for contrails in the year 2000. Traffic distance has further increased by 22% between 2005 and 2010, so that overall we adopt a RF estimate of +0.02 (+0.01 to +0.03) W m^{-2} for persistent (linear) contrails for 2010.

Satellite estimates of contrail-induced cirrus forcing estimates (e.g., Boucher, 1999) may unintentionally include cirrus changes not directly caused by aviation. Schumann and Graf (2012) constrained their model with observations of the diurnal cycle of contrails and cirrus in a region with high air traffic relative to a region with little air traffic, and estimated an AF of +0.045 to +0.075 W m^{-2} for contrails and contrail-induced cirrus in 2006, but their model has a large SW contribution, suggesting larger estimates are possible. An alternative approach was taken by Burkhardt and Kärcher (2011), who estimated for year 2002 a global RF of +0.03 W m^{-2} from contrails and contrail cirrus within a climate model (Burkhardt and Kärcher, 2009), after compensating for reduced background cirrus cloudiness in the main traffic areas. Combining these estimates with uncertainties on spreading rate, optical depth, ice particle shape and radiative transfer (Markowicz and Witek, 2011) and accounting for the ongoing increase in air traffic, we assess a combined contrail and contrail-induced cirrus AF for year 2010 to be +0.05 (+0.02 to +0.15) W m^{-2}.

7.2.5.2 Irrigation-Induced Cloudiness

Boucher et al. (2004) estimated a global AF due to water vapour from irrigation in the range of +0.03 to +0.10 W m^{-2} but the net climate effect was dominated by the evaporative cooling at the surface and by atmospheric thermal responses to low-level humidification. Regional surface cooling was confirmed by a

number of more recent regional and global studies (Kueppers et al., 2007; Lobell et al., 2009). The resulting increase in water vapour may induce a small enhancement in precipitation downwind of the major irrigation areas (Puma and Cook, 2010), as well as some regional circulation patterns (Kueppers et al., 2007). Sacks et al. (2009) reported a 0.001 increase in cloud fraction over land (0.002 over irrigated land). This suggests an AF no more negative than –0.1 W m^{-2} with very low confidence.

7.3 Aerosols

The section assesses the role of aerosol particles (aerosols) in the climate system, focusing on aerosol processes and properties, as well as other factors, that influence aerosol-radiation and aerosol-cloud interactions. Processes directly relevant to aerosol-cloud interactions are discussed in Section 7.4, and estimates of aerosol radiative and adjusted forcings are assessed in Section 7.5. The time evolution of aerosols and their forcing are discussed in Chapters 2 and 8, with Chapter 8 also covering changes in natural volcanic aerosols.

7.3.1 Aerosols in the Present-Day Climate System

7.3.1.1 Aerosol Formation and Aerosol Types

Atmospheric aerosols, whether natural or anthropogenic, originate from two different pathways: emissions of primary particulate matter and formation of secondary particulate matter from gaseous precursors (Figure 7.11). The main constituents of the atmospheric aerosol are inorganic species (such as sulphate, nitrate, sea salt), organic species (also termed organic carbon or organic aerosol), black carbon (BC, a distinct type of carbonaceous material formed from the incomplete combustion of fossil and biomass based fuels), and mineral species (mostly desert dust). Dust, sea spray and BC are introduced into the atmosphere as primary particles, whereas non-sea-salt sulphate and nitrate are predominantly from secondary aerosol formation processes. Organic aerosol (OA) has both significant primary and secondary sources. In the present-day atmosphere, the majority of BC, sulphate and nitrate come from anthropogenic sources, whereas sea spray and most mineral aerosol is of natural origin. Atmospheric OA is influenced by both natural and anthropogenic sources of volatile organic compounds. Emission rates of aerosols and aerosol precursors are summarized in Table 7.2. The characteristics and role of the main aerosol species are listed in Table 7.2.

[INSERT FIGURE 7.11 HERE]
Figure 7.11: Overview of atmospheric aerosol processes and environmental variables influencing aerosol-radiation and aerosol-cloud interactions. Gas-phase processes and variables are highlighted in red while particulate-phase processes and variables appear in green. Although this figure shows a linear chain of processes from aerosols to forcings, it is increasingly recognized that aerosols and clouds form a coupled system with two-way interactions.

[INSERT TABLE 7.2 HERE]
Table 7.2: Global and regional anthropogenic and natural emissions important for atmospheric aerosols. For the anthropogenic components the maximum and minimum values from available inventories are presented according to Granier et al. (2011). Units are Tg yr^{-1} except for BVOCs in TgC yr^{-1} and DMS in TgS yr^{-1}. Dust and sea-spray estimates span the range in the historical CMIP5 simulations. SOA range is taken from Spracklen et al. (2011). BVOC range from Arneth et al. (2008).

[INSERT TABLE 7.3 HERE]
Table 7.3: Key aerosol properties of the main aerosol species in the troposphere. Brown carbon is a particular type of OA but is treated here as an additional component because it is light absorbing. The estimate of aerosol burdens and lifetimes in the troposphere are based on the AeroCom models, except for primary biological aerosol particles (PBAP), which are treated by analogy to other coarse mode aerosol types.

7.3.1.2 Aerosol Climatology

Since the AR4, new and improved observational aerosol datasets have emerged. A number of field experiments have taken place such as the Intercontinental Chemical Transport Experiment (INTEX, Bergstrom et al., 2010; Logan et al., 2010), African Monsoon Multidisciplinary Analysis (AMMA, Hansell et al., 2010; Jeong et al., 2008), Integrated Campaign for Aerosols, gases and Radiation Budget (ICARB, 2008 and references therein), Megacity Impact on Regional and Global Environments field experiment

(MILAGRO, Paredes-Miranda et al., 2009), Geostationary Earth Radiation Budget Inter-comparisons of Longwave and Shortwave (GERBILS, Christopher et al., 2009), Research of the Composition of the Troposphere from Aircraft and Satellites (ARCTAS, Lyapustin et al., 2010), the Amazonian Aerosol Characterization Experiment 2008 (AMAZA-08, Martin et al., 2010a) and Atmospheric Brown Clouds (ABC, Engling and Gelencsér, 2010; Nakajima et al., 2007), which have improved our understanding of regional aerosol properties.

Long-term aerosol mass concentrations are also measured more systematically at the surface by global and regional networks (see Chapter 2), and there are institutional efforts to improve the coordination and quality assurance of the measurements. A survey of the main aerosol types can be constructed from such measurements (e.g., Jimenez et al., 2009; Figure 7.12). Such analyses show a wide spatial variability in aerosol concentrations, dominant aerosol type, and aerosol composition worldwide. Mineral dust dominates the aerosol mass over some continental regions with relatively higher concentrations in urban S. Asia, accounting for about 35% of the total aerosol mass with diameter smaller than 10 μm. In the rural U.S. and South America, OC contributes the largest fraction to the atmospheric aerosol (i.e., 20% or more), while in other areas of the world the OC fraction ranks second or third with a mean of about16%. Sulfate normally accounts for about 10–30% by mass, except for the areas in rural Africa, urban Oceania and South America with less than about 10%. The mass fractions of nitrate and ammonium are only around 6% and 4% on average, respectively. In most areas, BC fractions are less than 5% of the aerosol mass, although this percentage may be larger (about 12%) in South America, urban Africa, urban Europe, South-East and East Asia and urban Oceania due to the larger impact of combustion sources. Sea-salt aerosols can be dominant at oceanic remote sites with 50-70% of aerosol mass.

[INSERT FIGURE 7.12 HERE]

Figure 7.12: Bar chart plots summarizing the annual, seasonal or monthly mean mass surface concentration (μg m^{-3}) of seven major aerosol components for particles with diameter smaller than 10 μm, from various rural and urban sites in six continental areas of the world with at least an entire year of data, and two marine sites. For each location, the panels represent the median, the 25–75 percentiles (box), and the 10–90 percentiles (whiskers) for each aerosol component. These include: 1) urban North America. (Chow et al., 1993; Ito et al., 2004; Kim et al., 2000; Liu et al., 2005; Malm and Schichtel, 2004; Sawant et al., 2004); rural North America (Chow et al., 1993; Liu et al., 2005; Malm and Schichtel, 2004; Malm et al., 1994); 2) marine northern hemisphere Atlantic Ocean (Ovadnevaite et al., 2011; Rinaldi et al., 2009); 3) urban Europe (Hueglin et al., 2005; Lenschow et al., 2001; Lodhi et al., 2009; Lonati et al., 2005; Perez et al., 2008; Putaud et al., 2004; Querol et al., 2006; Querol et al., 2008; Querol et al., 2001; Querol et al., 2004; Rodriguez et al., 2002; Rodrıguez et al., 2004; Roosli et al., 2001; Viana et al., 2006; Viana et al., 2007; Yin and Harrison, 2008); rural Europe (Gullu et al., 2000; Hueglin et al., 2005; Kocak et al., 2007; Putaud et al., 2004; Puxbaum et al., 2004; Querol et al., 2009; Querol et al., 2001; Querol et al., 2004; Rodriguez et al., 2002; Rodrıguez et al., 2004; Salvador et al., 2007; Theodosi et al., 2010; Viana et al., 2008; Yin and Harrison, 2008; Yttri, 2007); 4) high Asia, with altitude larger than 1680 m. (Carrico et al., 2003; Decesari et al., 2010; Ming et al., 2007a; Qu et al., 2008; Ram et al., 2010; Rastogi and Sarin, 2005; Rengarajan et al., 2007; Shresth et al., 2000; Zhang et al., 2001; Zhang et al., 2012c; Zhang et al., 2008); urban South Asia (Chakraborty and Gupta, 2010; Khare and Baruah, 2010; Kumar et al., 2007; Lodhi et al., 2009; Raman et al., 2010; Rastogi and Sarin, 2005; Safai et al., 2010; Stone et al., 2010); urban China (Cheng et al., 2000; Hagler et al., 2006; Oanh et al., 2006; Wang et al., 2003; Wang et al., 2005b; Wang et al., 2006; Xiao and Liu, 2004; Yao et al., 2002; Ye et al., 2003; Zhang et al., 2002; Zhang et al., 2012c; Zhang et al., 2011); rural China (Hagler et al., 2006; Hu et al., 2002; Zhang et al., 2012c) [PANEL MISSING]; urban China (Cheng et al., 2000; Hagler et al., 2006; Oanh et al., 2006; Wang et al., 2003; Wang et al., 2005b; Wang et al., 2006; Xiao and Liu, 2004; Yao et al., 2002; Ye et al., 2003; Zhang et al., 2002; Zhang et al., 2012c; Zhang et al., 2011); South-East and East Asia (Han et al., 2008; Khan et al., 2010; Kim et al., 2007; Lee and Kang, 2001; Oanh et al., 2006); 5) South America (Artaxo et al., 1998; Artaxo et al., 2002; Bourotte et al., 2007; Celis et al., 2004; Fuzzi et al., 2007; Gioda et al., 2011; Mariani and Mello, 2007; Martin et al., 2010b; Morales et al., 1998; Souza et al., 2010); 6) urban Africa (Favez et al., 2008; Mkoma, 2008; Mkoma et al., 2009b); rural Africa (Maenhaut et al., 1996; Mkoma, 2008; Mkoma et al., 2009a; Mkoma et al., 2009b; Nyanganyura et al., 2007; Weinstein et al., 2010); 7) marine southern hemisphere Indian Ocean (Rinaldi et al., 2011; Sciare et al., 2009); 8) urban Oceania (Chan et al., 1997; Maenhaut et al., 2000; Radhi et al., 2010; Wang et al., 2005a; Wang and Shooter, 2001).

Aerosol optical depth (AOD), which is related to the column-integrated aerosol amount, is measured by the Aerosol Robotic Network (AERONET, Holben et al., 1998; Holben et al., 2001), other ground-based networks, and a number of satellite-based sensors. Retrievals from aerosol-dedicated instruments such as MODIS (Kleidman et al., 2012; Levy et al., 2010; Remer et al., 2005), MISR (Kahn et al., 2005; Kahn et al., 2007) and POLDER/PARASOL (Tanré et al., 2011) are used preferentially to less specialised instrumentation such as AVHRR (Geogdzhayev et al., 2002; Jeong and Li, 2005), TOMS (Torres et al.,

1998; Torres et al., 2002) and ATSR/AATSR although the latter are useful because of their longer measurement records (see Chapter 2). While each AOD retrieval shows some skill against more accurate AERONET measurements, there are still large differences in regional and seasonal patterns because of differences in sampling, cloud screening and treatment of the surface reflectivity (Kokhanovsky et al., 2010). The global but incomplete satellite measurements can be combined with information from global aerosol models through data assimilation techniques (e.g., Benedetti et al., 2009; Figure 7.13a). Due to the heterogeneity in their sources, their short lifetime and the dependence of sinks on the meteorology, aerosol distributions show large variations on daily, seasonal and interannual scales.

[INSERT FIGURE 7.13 HERE]

Figure 7.13: a) spatial distribution of the AOD (unitless) from the MACC model with assimilation of MODIS AOD (Benedetti et al., 2009; Morcrette et al., 2009) for the year 2010; b) to e) latitudinal vertical cross-sections of the aerosol extinction coefficient (km^{-1}) for four longitudinal bands (180°W to 120°W, 120°W to 60°W, 20°W to 40°E, and 60°E to 120°E) from the CALIOP instrument (Winker et al., 2009). The black circles show the extinction scale height for 90% (top) and 63% (bottom) of the average AOD.

Spaceborne lidars, such as on the CALIPSO mission (Winker et al., 2009), now provide a climatology of the aerosol extinction coefficient (Figure 7.13b-d), highlighting that over most regions the majority of the optically-active aerosol resides in the lowest 1–2 km. There is less information available on the vertical profile of aerosol number and mass concentrations, although a number of field experiments involving research aircraft have measured aerosol concentrations. In particular BC mixing ratios have been measured during the ARCTAS (Jacob et al., 2010), ARCPAC (Warneke et al., 2010), A-FORCE and HIPPO1 (Schwarz et al., 2006; Schwarz et al., 2010) campaigns (Figure 7.14). Commercial aircraft also report total aerosol number concentrations (Brenninkmeijer et al., 2007).

[INSERT FIGURE 7.14 HERE]

Figure 7.14: Comparison of profiles of BC mass mixing ratios (ng kg^{-1}) as measured by airborne SP2 instruments during the ARCTAS (Jacob et al., 2010), HIPPO1 (Schwarz et al., 2006; Schwarz et al., 2010) and A-FORCE (Oshima et al., 2012) campaigns and as simulated by a range of AeroCom models. The model values are averages for the month corresponding to each field campaign.

7.3.2 Aerosol Sources and Processes

7.3.2.1 Aerosol Sources

Sea spray particles comprise sea salt and primary marine matter, and are produced at the sea surface by bubble bursting induced mostly by breaking waves. The effective emission flux of sea spray particles to the atmosphere depends on the surface wind speed and atmospheric stability, and to a lesser extent on the temperature and composition of the sea water. Our understanding of sea spray emissions has increased substantially since AR4; however, process-based estimates of the total mass, number size distribution and chemical composition of emitted sea spray particles continue to have large uncertainties (de Leeuw et al., 2011; Table 7.2). It has been shown that sea spray can contain primary organic matter, preferentially in the submicronic size range, the amount of which depends on biological activity in ocean waters (Facchini et al., 2008). Uncertainty in the source translates into a large uncertainty in the natural level of aerosol number concentration in the marine atmosphere which, unlike the aerosol optical depth and sea spray mass concentrations, is more difficult to constrain from space observations (Jaeglé et al., 2011).

Dust particles are produced mainly by disintegration of aggregates following creeping and saltation of larger soil particles over desert and other arid surfaces (Kok, 2011; Zhao et al., 2006). The magnitude of dust emissions to the atmosphere depends on the surface wind speed and many soil-related factors such as its texture, moisture and vegetation cover. The range of estimates for the global dust emissions spans a factor of about 5 (Huneeus et al., 2011; Table 7.2). The fraction of dust coming from anthropogenic sources remain ill quantified although some recent satellite observations suggest it could be 20 to 25% (Ginoux et al., 2012a; Ginoux et al., 2012b).

Primary biological aerosol particles (PBAP) include bacteria, pollen, fungal spores, lichen, viruses and fragments of animals and plants (Després et al., 2012). Most of these particles are emitted in the coarse mode (Pöschl et al., 2010) and the contribution to the accumulation mode is likely to be very small. There are only

a few estimates of the global flux of PBAP and these are poorly constrained (Burrows et al., 2009; Heald and Spracklen, 2009; see Table 7.2).

The main natural aerosol precursors are dimethylsulfide (DMS) emitted by the oceans and biogenic volatile organic compounds (BVOC) emitted mainly by the terrestrial biosphere. BVOC emissions depend on the amount and type of vegetation, temperature, radiation and several environmental factors such as the ambient CO_2 concentration (Grote and Niinemets, 2008; Pacifico et al., 2009). While speciated BVOC emission inventories have been derived for some continental regions, global emission inventories or schemes are available only for isoprene and some monoterpenes (Guenther et al., 2006; Muller et al., 2008). The total global BVOC emissions have large uncertainties, despite the apparent convergence in different model-based estimates (Arneth et al., 2008).

The contribution of secondary organic aerosol (SOA) to the total organic aerosol is larger than previously thought, but the split between primary organic aerosol (POA) and SOA has remained somewhat ambiguous due to atmospheric transformation processes affecting both these components (Jimenez et al., 2009; Robinson et al., 2007). Globally, most of atmospheric SOA is expected to originate from biogenic sources, even though anthropogenic sources could be equally important at northern midlatitudes (De Gouw and Jimenez, 2009; Lin et al., 2012). Recent studies suggest that the SOA formation from BVOCs may be enhanced substantially by anthropogenic pollution due to i) high nitrogen oxide concentrations enhancing BVOC oxidation, and ii) high anthropogenic POA concentrations that facilitate transformation of VOCs to the particle phase (Carlton et al., 2010; Heald et al., 2011; Spracklen et al., 2011). The uncertainty range of atmospheric SOA formation has decreased since AR4 but is still larger than a factor of 5 (Farina et al., 2010; Hallquist et al., 2009; Heald et al., 2010; Spracklen et al., 2011; Table 7.2).

Anthropogenic sources of aerosols (BC, POA) and aerosol precursors (sulphur dioxide, ammonia, nitric acid and VOCs) are known from emission inventories (Table 7.2). They are generally better constrained than natural sources, exceptions being anthropogenic sources of BC, which are likely to be underestimated (Bond et al., 2012), and anthropogenic emissions of some VOCs, fly-ash and dust which are still poorly known. Since AR4, remote sensing by satellites has been increasingly used to constrain natural and anthropogenic aerosol and aerosol precursor emissions (e.g., Dubovik et al., 2008; Huneeus et al., 2012; Jaeglé et al., 2011).

7.3.2.2 Aerosol Processes

New particle formation is the process by which low-volatility vapors nucleate into stable embryos, which under certain condensable vapor regimes, can grow rapidly to produce nanometre-sized aerosol particles. Since AR4, substantial progress in our understanding of atmospheric nucleation and new particle formation has been made (Zhang et al., 2012b). Multiple lines of evidence indicate that while sulfuric acid is the main driver of nucleation (Kerminen et al., 2010; Sipila et al., 2010), the nucleation rate is affected by ammonia and amines (Kirkby et al., 2011; Kurten et al., 2008; Smith et al., 2010; Yu et al., 2012) as well as low-volatile organic vapors (Metzger et al., 2010; Paasonen et al., 2010; Wang et al., 2010a). Neutral nucleation pathways are very likely to dominate over ion-induced nucleation in continental boundary layers, but the situation might be different higher up in the atmosphere (Hirsikko et al., 2011; Kazil et al., 2010).

Condensation is the main process transferring low-volatile vapors between the gas phase and aerosol particles, and also the dominant process for growth to larger sizes. The growth of the smallest particles depends crucially on the condensation of organic vapors (Riipinen et al., 2011), and is therefore tied strongly with atmospheric SOA formation discussed in Section 7.3.3.1. The treatment of condensation of semi-volatile compounds, such as ammonium nitrate and most organic vapors, remains a challenge in climate modeling.

Small aerosol particles collide with one other and stick together. This process, termed Brownian coagulation, affects the aerosol mixing state and is the main sink for the smallest aerosol particles. In locations where aerosol lifetimes are long and amounts of condensable vapors are low, such as in the stratosphere and large parts of the free troposphere, coagulation can contribute significantly to aerosol growth.

Since AR4, observations of atmospheric nucleation and subsequent growth of nucleated particles to larger sizes have been increasingly reported in different atmospheric environments (Kulmala and Kerminen, 2008;

Manninen et al., 2010; O'Dowd et al., 2010). Global model studies suggest that after their growth in the atmosphere, nucleated particles have a large impact on the cloud condensation nuclei (CCN) concentrations (Merikanto et al., 2009; Pierce and Adams, 2009b; Spracklen et al., 2008; Yu and Luo, 2009) and potentially also on cloud droplet number concentrations and aerosol-cloud interactions (Kazil et al., 2010; Makkonen et al., 2012; Wang and Penner, 2009). Quantifying the climatic effects caused by atmospheric nucleation remain, however, very difficult because these effects depend in a non-linear way on the nucleation rate, the survival probability of nucleated particles against coagulation, the growth of these particles to larger sizes, and the number concentration and size distribution of primary particle emissions (Chang et al., 2009; Reddington et al., 2011; Spracklen et al., 2010).

Cloud processing affects the number concentration, composition, size and mixing state of atmospheric aerosol particles via aqueous-phase chemistry taking place inside clouds, via altering aerosol precursor chemistry around and below clouds, and via different aerosol-cloud hydrometeor interactions. A more detailed discussion on aerosol-cloud interactions will be presented in Section 7.4.

The understanding and modelling of aerosol sinks has seen less progress since AR4. Improved dry deposition models, which depend on the particle size as well as the roughness properties of the surface, have been developed and are increasingly being used in global aerosol models (Feng, 2008; Kerkweg et al., 2006; Petroff and Zhang, 2010). For the largest particles in the coarse mode, it is important to consider sedimentation throughout the atmosphere and its role in dry deposition at the surface. The uncertainty in the estimate of wet deposition (in-cloud and below-cloud scavenging) is controlled by the uncertainties in the prediction of the amount of precipitation, the size and to some extent the chemical composition of particles. For insoluble primary particles like BC and dust, wet deposition also depends strongly on their degree of mixing with soluble compounds. Parameterization of wet deposition of aerosols remains a key source of uncertainty in aerosol models, which affects the vertical distribution and long-range transport of aerosols (Lee et al., 2011; Vignati et al., 2010), with further impact on model estimates of aerosol forcings. It should be noted however that, when the aerosol source term is known, aerosol sinks can be adjusted in global aerosol models by constraining aerosol concentrations against observations, which helps to limit the impact of the very large uncertainties on aerosol sources and sink processes.

7.3.3 Progresses and Gaps in Understanding Climate Relevant Aerosol Properties

The climate effects of atmospheric aerosol particles depend on their atmospheric distribution, along with their hygroscopicity, optical properties and ability to act as CCN and ice nuclei (IN). Key quantities for aerosol optical and cloud forming properties are the particle number size distribution, chemical composition, mixing state and shape. These properties are determined by a complex interplay between their sources, atmospheric transformation processes and their removal from the atmosphere (Section 7.3.2 and Figure 7.11). Since AR4, measurement of some of the key aerosols properties has been greatly improved in laboratory and field experiments using advanced instrumentation, which allows for instance the analysis of individual particles. These experimental studies have in turn stimulated improvement in the model representations of the aerosol physical, chemical and optical properties. We focus our assessment on some of the key issues where there has been progress since AR4.

7.3.3.1 Chemical Composition and Mixing State

Research on the climate impacts of aerosols has moved further away from the simple paradigm of externally-mixed sulphate, BC and biomass burning aerosols. Although the role of inorganic aerosols as an important anthropogenic contributor to aerosol-radiation and aerosol-cloud interactions has not been questioned, BC and organics have received increasing attention.

The physical properties of BC (strongly light-absorbing, refractory with a vaporization temperature near 400 K, aggregate in morphology, insoluble in most organic solvents) allow a strict definition at least in principle (Bond et al., 2012). Direct measurement of individual BC-containing particles is possible with a laser-induced incandescence (also called SP2, Gao et al., 2007; Moteki and Kondo, 2010; Schwarz et al., 2008b), which has enabled accurate measurements of the size of BC cores, as well as total BC mass concentrations. Condensation of gas-phase compounds on BC and coagulation with other particles alter the mixing state of BC (e.g., Adachi et al., 2010; Li et al., 2003; Pósfai et al., 2003), which can make internally mixed BC in

polluted urban air on a timescale of about 12 h (McMeeking et al., 2010; Moteki et al., 2007). The resulting BC-containing particles could become hygroscopic, which can lead to reduced lifetime and atmospheric loading (Stier et al., 2006). Koch et al. (2009b) and Schwarz et al. (2010) used airborne measurements to evaluate AeroCom model simulations of the vertical distribution of BC aerosol in many regions, and found that most models simulate too much BC in the upper troposphere (Schwarz et al., 2010, see Figure 7.14).

Formation processes of OA remain highly uncertain, which is a major weakness in the present understanding and model representation of atmospheric aerosols (Hallquist et al., 2009; Kanakidou et al., 2005). Measurements by aerosol mass spectrometers have provided some insights into sources and atmospheric processing of OA (Lanz et al., 2007; Ulbrich et al., 2009; Zhang et al., 2005a). Measurements at continental midlatitudes including urban and rural/remote air suggest that the majority of SOA is likely to be oxygenated OA (Zhang et al., 2007a; Zhang et al., 2005b). Measurements within and downstream of urban air indicate that under most circumstances SOA substantially contributes to the total OA mass (de Gouw et al., 2005; Volkamer et al., 2006; Zhang et al., 2007a). Some of the OA is light absorbing and can be referred to as brown carbon (BrC, Andreae and Gelencser, 2006). The absorption properties of BrC can be attributed to water soluble organic compounds and humic-like substances (Graber and Rudich, 2006; Kirchstetter et al., 2004), although they are poorly quantified (Alexander et al., 2008; Flowers et al., 2010).

There is a large range in the complexity with which OA is represented in global aerosol models. Some complex, yet still parameterized, chemical schemes have been developed recently which account for multigenerational oxidation (Donahue et al., 2011; Jimenez et al., 2009; Robinson et al., 2007). Some regional and global models use semi-empirical schemes, where semi- or non-volatile organic compounds (SVOC) are produced from parent VOCs by oxidation processes and partitioned between the aerosol and gas phases (Fan et al., 2005; Heald et al., 2005; Russell and Allen, 2005; Tsigaridis and Kanakidou, 2003). The representation of SOA in many of the models used in CMIP5 is still very crude in that the source terms are prescribed and/or the models ignore the complex chemical and aging processes (Hennigan et al., 2009), but the impact of these simplifications on aerosol forcing estimates is unclear.

There are multiple observations that show co-existence of external and internal mixtures relatively soon after emission (Hara et al., 2003; Schwarz et al., 2008a; Twohy and Anderson, 2008). Generally, in biomass burning aerosol, organic compounds and black carbon were frequently found to be internally mixed with ammonium, nitrate, and sulphate (Deboudt et al., 2010; Pratt and Prather, 2010). Studies over urban locations revealed that as much as 90% of the particles are internally mixed with secondary inorganic species (Bi et al., 2011). Likewise there is evidence of internal mixing between dust and biomass burning aerosols when these aerosol types age together (Hand et al., 2010). In sea-spray the primary organic matter is mixed with the sea salt with increasing percentage mass contribution in submicron sizes with decreasing particle size. Studies have shown that the state of mixing can alter particle hygroscopicity and hence their ability to act as CCN (Wex et al., 2010).

7.3.3.2 Size Distribution and Optical Properties

Aerosol size distribution is one of a key parameter determining both the aerosol spectral optical and CCN properties. Since AR4 much effort has been put on measuring and simulating the aerosol number rather than volume size distribution. For instance, number size distributions in the submicron range (30-500 nm) were measured at 24 sites in Europe for two years (Asmi et al., 2011), although systematic measurements of this parameter are still limited in other regions. Validation studies show agreement between column-averaged volume size distribution from sun photometer measurements (Dubovik et al., 2006) and direct in situ (surface as well as aircraft-based) measurements (Gerasopoulos et al., 2007; Haywood et al., 2011; Radhi et al., 2010; Smirnov et al., 2011), but these inversion products have not been comprehensively validated.

The aerosol extinction coefficient depends on aerosol size distribution, aerosol refractive index and mixing state. Humidification of internally-mixed aerosols as the RH increases, further influences their light scattering and absorption properties through changes in particle shape, size, and refractive index (Freney et al., 2010). Lidars provide further measurements of the vertical profile of aerosol extinction coefficient. Yu et al. (2010) and Koffi et al. (2012) found that global aerosol models tend to have a positive bias on the aerosol extinction scale height in some (but not all) regions, resulting in an overestimate of aerosol concentrations above 6 km. The vertical integral of the extinction ceofficient is the aerosol optical depth or AOD. It is a key

ingredient to estimate aerosol radiative effects (see Section 7.3.4) and can be measured to a good accuracy at particular locations from sunphotometry. Satellite retrievals of AOD are more uncertain. While error estimates exist for individual measurements (Kleidman et al., 2012; Remer et al., 2005), the uncertainty on the global-mean AOD can only be obtained from the spread between different satellite retrievals (see Section 7.3.1.2) or model simulations. This remains a source of uncertainty when estimating aerosol-radiation interactions, more so for the anthropogenic AOD which is more difficult to constrain from observations (Su et al., 2012).

Aerosol absorption is another key climate-relevant aerosol property. Earlier in-situ methods to measure absorption suffered from important uncertainties (Moosmüller et al., 2009). Recent measurements using photo-acoustic methods and laser-induced incandescence methods are more accurate but remain sparse. Coating of soluble material over a primary aerosol such as a BC or dust core enhance the BC mass absorption efficiency by up to a factor of 2 (Bond and Bergstrom, 2006; Cross et al., 2010), with typical values of about 8–20 $m^2 g^{-1}$ at a wavelength of 532 nm. Absorption AOD can be retrieved from sunphotometer measurements in situations where AOD is larger than 0.2. Koch et al. (2009b) used AERONET retrievals of aerosol AOD to show that most AeroCom models underestimate absorption in many regions, but there remain representativeness issues when comparing point observations to a model climatology.

7.3.3.3 CCN Properties of Atmospheric Aerosols

A subset of aerosol particles acts as CCN. The ability of an aerosol particle to take up water and subsequently activate is determined by its size and composition. Whether these particles eventually become cloud droplets or not, understanding the water vapour uptake of aerosol is an important step in assessing RFari. Common CCN in the atmosphere are composed of sea salt, sulphates and sulphuric acid, nitrate and some organics (Table 7.3). CCN activity of inorganic aerosols is relatively well understood. Lately most attention has been paid to the CCN activity of mixed organic/inorganic aerosols (e.g., King et al., 2010; Prisle et al., 2010). Uncertainties in our current understanding of CCN properties are associated with SOA (Good et al., 2010), mainly because OA is still poorly characterized (Jimenez et al., 2009). For SOA it is not clear how important surface tension effects and bulk-to-surface partitioning are, and if the water activity coefficient changes significantly as a function of the solute concentration (Good et al., 2010; Prisle et al., 2008). The size of the CCN has been found to be more important than their chemical composition at two continental locations as larger particles are more readily activated than smaller particles because they require a lower critical supersaturation (Dusek et al., 2006; Ervens et al., 2007). However, the chemical composition may be important in other locations such as the marine environment, where primary organic particles (hydrogels) have been shown to be exceptionally good CCN (Ovadnevaite et al., 2011).

The bulk hygroscopicity parameter κ (Petters and Kreidenweis, 2007), has been introduced to provide a concise way to describe how effectively an aerosol particle functions as a CCN. It can be measured experimentally and is increasingly being used as a way to characterize aerosol properties. Pringle et al. (2010) used surface and aircraft measurements to evaluate the values of the hygroscopicity parameter simulated by a global aerosol model, and found generally good agreement. When the aerosol is dominated by organics, discrepancies between values of κ obtained directly from both CCN activity measurements and sub-saturated particle water uptake measurements have been observed in some instances (e.g., Irwin et al., 2010; Prenni et al., 2007; Roberts et al., 2010), whereas in other studies closure has been obtained (e.g., Duplissy et al., 2008; Rose et al., 2011). Adsorption theory (Kumar et al., 2011) replaces κ-theory for CCN activation for insoluble particles (e.g., dust) while alternative theories are still required for explanation of primary marine organics that seem to have peculiar gel-like properties (Ovadnevaite et al., 2011).

7.3.3.4 IN Properties of Aerosols

Aerosols that act as IN are solid substances at atmospheric temperatures and supersaturations. Mineral dust and primary bioaerosols such as bacteria, fungal spores and pollen, are typically known as good IN. Conflicting evidence has been presented for the ability of BC, organic and biomass burning particles to act as IN. Four heterogeneous ice nucleation modes are distinguished in the literature. Immersion freezing refers to freezing that is initiated from within a cloud droplet, condensation freezing refers to freezing during droplet formation, and contact freezing is initiated when an IN collides with a supercooled cloud droplet. Deposition

nucleation refers to the direct deposition of vapour onto IN. Lidar observations revealed that liquid cloud droplets are present before ice crystals form via heterogeneous freezing mechanisms (Ansmann et al., 2008; de Boer et al., 2011) indicating that deposition nucleation does not seem to be important for mixed-phase clouds.

Laboratory measurements of the ice activity of various aerosols is summarized in terms of their ice onset temperatures versus relative humidities, for both deposition/condensation nucleation and immersion freezing, in Figure 7.15. The reported nucleation onset points refer to different fractions of ice nucleating particles due to different detection thresholds of measurement methods. Bioaerosols initiate immersion freezing at the highest temperatures and are considered as very efficient IN, but their concentration in the upper troposphere is relatively low (Hoose et al., 2010a). Remote sensing observations confirm that ice clouds in air containing dust can be found at significantly warmer temperatures than in dust-free conditions (Choi et al., 2010; Sassen et al., 2003; Seifert et al., 2010). Laboratory results indicate that, in comparison with natural IN such as mineral dust and biological particles, soot initiates ice only at the coldest temperatures (Hoose and Möhler, 2012). As in-situ observations indicate an enrichment of BC in atmospheric ice particle residuals in tropospheric mixed phase clouds (Cozic et al., 2008; Targino et al., 2009; Twohy et al., 2010), there must be some mechanism for BC to enter ice clouds, but that does not necessarily mean that BC acted as IN. Since BC has anthropogenic sources its increase since pre-industrial times may have caused changes to the lifetime of mixed-phase clouds, as discussed in Section 7.4, and thus to AFaci as summarized in Section 7.5.

IN can either be bare or mixed with other substances. As bare particles age in the atmosphere, they acquire liquid surface coatings by condensing soluble species and water vapour or by scavenging soluble particles, which may transform IN from deposition or contact nuclei into possible immersion nuclei. A change from contact to immersion freezing implies an activation at colder temperatures with consequences for the lifetime of mixed-phase clouds and AFaci (Section 7.5).

[INSERT FIGURE 7.15 HERE]

Figure 7.15: The onset temperatures and relative humidities for deposition/condensation freezing and immersion freezing for **bioaerosols** (Ahern et al., 2007; Diehl et al., 2001; Iannone et al., 2011; Kanji et al., 2011; Mohler et al., 2008; Mortazavi et al., 2008; von Blohn et al., 2005; Yankofsky et al., 1981), **mineral dusts** (Archuleta et al., 2005; Bundke et al., 2008; Connolly et al., 2009; Cziczo et al., 2009a; Field et al., 2006; Kanji and Abbatt, 2006; Kanji et al., 2011; Knopf and Koop, 2006; Koehler et al., 2010; Kulkarni and Dobbie, 2010; Lüönd et al., 2010; Mohler et al., 2006; Murray et al., 2011; Niedermeier et al., 2010; Niemand et al., 2012; Roberts and Hallett, 1968; Salam et al., 2006; Schaller and Fukuta, 1979; Welti et al., 2009; Zimmermann et al., 2008), **organics** (Baustian et al., 2010; Kanji et al., 2008; Petters et al., 2009; Prenni et al., 2007; Shilling et al., 2006; Wagner et al., 2010; 2011; Wang and Knopf, 2011; Zobrist et al., 2007), **solid ammonium sulphate** (Abbatt et al., 2006; Baustian et al., 2010; Mangold et al., 2005; Shilling et al., 2006; Wise et al., 2009; 2010) and **BC (soot)** (Crawford et al., 2011; DeMott, 1990; DeMott et al., 1999; Diehl and Mitra, 1998; Dymarska et al., 2006; Fornea et al., 2009; Gorbunov et al., 2001; Kanji et al., 2011; Mohler et al., 2005), from a compilation of experimental data of sub- and super-micron aerosol particles in the literature (for references see supplementary material). The large range of observed ice nucleation onset conditions is due to different experimental setups, particle sizes, activated fractions and chemical composition. Only those IN species for which at least three papers exists are shown. The solid line refers to saturation with respect to liquid water and the dashed line refers to the homogeneous freezing of solution droplets after Koop et al. (2000). Adapted from Hoose and Möhler (2012).

7.3.4 Aerosol-Radiation Interactions (ARI)

7.3.4.1 Aerosol-Radiation Interactions

Direct radiative effect (DRE) is the change in radiative flux caused by the combined direct effect of anthropogenic and natural aerosols. The DRE results from well-understood physics and is close to being an observable quantity, yet our knowledge of aerosol and environmental characteristics needed to quantify the DRE at the global scale remains incomplete (Anderson et al., 2005; Jaeglé et al., 2011; Satheesh and Moorthy, 2005). The DRE requires knowledge of the spectrally-varying aerosol extinction coefficient, single scattering albedo and phase function, which can in principle be estimated from the aerosol size distribution, shape, chemical composition, hygroscopicity, and mixing state (Figure 7.11). Radiative properties of the surface, atmospheric molecules and clouds also influence the DRE. In the solar spectrum and cloud-free conditions, the DRE is typically negative at the top-of-atmosphere but gets weaker, and can become positive with increasing aerosol absorption, decreasing upscatter fraction, or increasing albedo of the underlying

surface. DRE is weaker in cloudy conditions, except where the cloud layer is thin or where aerosols are located above or between clouds (e.g., Chand et al., 2009). The DRE at the surface is negative and can be much stronger than the DRE at the top-of-atmosphere over regions where aerosols are absorbing (Li et al., 2010). In the longwave spectrum, top-of-atmosphere DRE is generally positive and mainly exerted by coarse-mode aerosols such as desert dust (Reddy et al., 2005), and stratospheric aerosols (Jacobson, 2001).

There have been many measurement-based estimates of the DRE (Bauer et al., 2011; Bergamo et al., 2008; Di Biagio et al., 2010; Yu et al., 2006) although some studies involve some degree of modelling. Observed and calculated shortwave radiative fluxes agree within measurement uncertainty when aerosol properties are known (e.g., Osborne et al., 2011). Global observational estimates of the DRE rely on satellite remote sensing of aerosol properties and/or measurements of the Earth's radiative budget (Chen et al., 2011; Kahn, 2012). Estimates of shortwave cloud-free top-of-atmosphere DRE over the ocean range from –4 to –6 W m^{-2} on a global, annual average, mainly contributed by sea spray (Bellouin et al., 2005; Loeb and Manalo-Smith, 2005; Myhre et al., 2007; Yu et al., 2006). However, DRE can reach tens of W m^{-2} locally. Estimates over land are more difficult as the surface is less well characterised (Chen et al., 2009; Jethva et al., 2009) despite recent progress in aerosol inversion algorithms (e.g., Dubovik et al., 2011). Attempts to estimate the DRE in cloudy-sky remain elusive (e.g., Peters et al., 2011a) although passive and active remote sensing of aerosols over clouds is now possible (de Graaf et al., 2012; Omar et al., 2009; Torres et al., 2007; Waquet et al., 2009). Notable areas of positive top-of-atmosphere DRE exerted by absorbing aerosols include the Arctic over ice surfaces (Stone et al., 2008) and seasonally off the shore of Namibia over stratocumulus clouds. While AOD and aerosol size are relatively well constrained, uncertainties in the aerosol single-scattering albedo (Loeb and Su, 2010) and vertical profile (e.g., Zarzycki and Bond, 2010) contribute significantly to the overall uncertainties in DRE.

7.3.4.2 Rapid Adjustments to ARI

Aerosol-radiation interactions give rise to rapid adjustments, which are particularly pronounced for absorbing aerosols, where the associated cloud changes are often referred to as the semi-direct effect (see Figure 7.2). The adjusted forcing (AF) from aerosol-radiation interactions is quantified in Section 7.5; only the corresponding processes governing rapid adjustments are discussed here. Impacts on precipitation are discussed in Section 7.6.

Since AR4, additional studies have found correlations between cloud cover and absorbing aerosols (e.g., Brioude et al., 2009; Wilcox, 2010), and eddy-resolving, regional and global scale modelling studies have helped confirm a causal link. Relationships between cloud and aerosol reveal a more complicated picture than initially anticipated (e.g., Ghan et al., 2012; Hill and Dobbie, 2008; Koch and Del Genio, 2010; Sakaeda et al., 2011; Zhuang et al., 2010).

Absorbing aerosols modify atmospheric stability. The effect of this on cloud cover depends on the height of the aerosol relative to the cloud and the type of cloud (Allen and Sherwood, 2010; Koch and Del Genio, 2010; Yoshimori and Broccoli, 2008). Aerosol also reduces the downwelling solar radiation at the surface. Together the changes in atmospheric stability and reduction in surface fluxes provide a means for aerosols to significantly modify the fraction of surface-forced clouds (Feingold et al., 2005; Sakaeda et al., 2011). These changes may also affect precipitation as discussed in Section 7.6.2.

Cloud cover is expected to decrease if absorbing aerosol is embedded in the cloud layer. This has been observed (Koren et al., 2004) and simulated (e.g., Feingold et al., 2005) for clouds over the Amazon forest in the presence of smoke aerosols. In the stratocumulus regime, absorbing aerosol above cloud-top strengthens the temperature inversion, reduces entrainment and tends to enhance cloudiness. Satellite observations (Wilcox, 2010) and modelling (Johnson et al., 2004) of marine stratocumulus show a thickening of the cloud layer beneath layers of absorbing smoke aerosol, which induces a local negative forcing. The responses of other cloud types, such as those associated with deep convection, are not well determined.

Absorbing aerosols embedded in cloud drops enhances their absorption, which can affect the dissipation of cloud. The contribution to RFari is small (Ghan et al., 2012; Stier et al., 2007), and there is contradictory evidence regarding the magnitude of the cloud dissipation effect influencing AFari (Bond et al., 2012; Feingold et al., 2005; Ghan et al., 2012; Jacobson, 2012).

Global forcing estimates are necessarily based on global models (see Section 7.5.2), although the accuracy of GCMs in this regard is limited by their ability to represent low cloud controlling processes with fidelity. This is an area of concern as discussed in Section 7.2, and limits confidence in these estimates.

7.3.5 Aerosol Responses to Climate Change and Feedback

The climate drivers of changes in aerosols can be split into physical changes (temperature, humidity, precipitation, soil moisture, solar radiation, wind speed, sea ice extent, etc), chemical changes (availability of oxidants) and biological changes (vegetation cover and properties, plankton abundance and speciation, etc). The response of aerosols to climate change may constitute a feedback loop whereby climate processes amplify or dampen the initial perturbation (Carslaw et al., 2010; Raes et al., 2010). We assess here the relevance and strength of aerosol-climate feedbacks in the context of future climate change scenarios.

7.3.5.1 Changes in Sea Spray and Mineral Dust

Concentrations in sea spray will respond to changes in surface wind speed, precipitation and to the expected decrease in sea ice cover (Struthers et al., 2011). There is no agreement among climate models about the balance of effects, with estimates ranging from an overall 19% reduction in global sea salt burden from the present-day to year 2100 (Liao et al., 2006), to little sensitivity (Mahowald et al., 2006a), or a sizeable increase (Bellouin et al., 2011; Jones et al., 2007). In particular there is little understanding of how surface wind speed may change over the ocean in a warmer climate, and observed recent changes (e.g., Young et al., 2011; Chapter 2) may not be indicative of future changes. Given that sea spray particles comprise a significant fraction of CCN concentrations over the oceans, such large changes will feed back on climate through changes in cloud droplet number (Korhonen et al., 2010a).

Studies of the effects of climate change on dust loadings give a wide range of results. Woodward et al. (2005) found a factor of 3 increase in dust burden in 2100 relative to present-day because of a large increase in bare soil fraction. A few studies reported moderate (−10 to −20%) increases or decreases (e.g., Jacobson and Streets, 2009; Liao et al., 2009; Tegen et al., 2004). Mahowald et al. (2006b) found a 60% decrease under double CO_2 concentration. The large range reflects different responses of the atmosphere and vegetation cover to climate change forcings and results in low confidence in these predictions.

7.3.5.2 Changes in Sulfate, Ammonium and Nitrate Aerosols

The DMS-sulfate-cloud-climate feedback loop could operate in numerous ways through changes in temperature, absorbed solar radiation, mixed layer depth and nutrient recycling, sea-ice extent, wind speed, shift in marine ecosystems due to ocean acidification and climate change, atmospheric processing of DMS into CCN, and no study has included all the relevant effects. However two decades of research have yielded important insights into this complex, coupled system (Ayers and Cainey, 2007; Carslaw et al., 2010). There is now medium agreement between observations and Earth System model simulations for a weak feedback due to a weak sensitivity of the CCN population to changes in DMS emissions (Carslaw et al., 2010; Quinn and Bates, 2011; Woodhouse et al., 2010). Parameterisations of oceanic DMS production lack robust mechanistic justification (Halloran et al., 2010) and as a result the sensitivity to ocean acidification and climate change remains uncertain (Bopp et al., 2004; Cameron-Smith et al., 2011; Kim et al., 2010).

In the atmosphere chemical production of sulfate increases with temperature (Aw and Kleeman, 2003; Dawson et al., 2007; Kleeman, 2008), but most studies to date predict a small (0 to 9%) reduction in global sulfate burden, mainly because of future increases in precipitation (Liao et al., 2006; Pye et al., 2009; Racherla and Adams, 2006; Unger et al., 2006). However Rae et al. (2007) found a small increase in global sulfate burden from 2000–2100 because the simulated future precipitation was reduced in regions of high sulphate abundance.

Changes in temperature have a large impact on nitrate aerosol formation through the Clausius-Clapeyron relation for HNO_3. There is some agreement among global aerosol models that climate change alone will contribute to a decrease in the nitrate concentrations (Bellouin et al., 2011; Liao et al., 2006; Pye et al., 2009; Racherla and Adams, 2006) with the exception of Bauer et al. (2007) who found little change in nitrate for

year 2030. It should be noted however that changes in precursor emissions are likely to increase nitrate concentrations in the future (Bellouin et al., 2011). Besides the changes in meteorological parameters, climate change can also influence ammonium formation by changing concentrations of sulfate and nitrate, but the effect of climate change alone was found to be small (Pye et al., 2009).

7.3.5.3 Changes in Carbonaceous Aerosols

There is evidence that future climate change could lead to increases in the occurrence of wildfires because of changes in fuel availability, readiness of the fuel to burn and ignition sources (Kloster et al., 2010; Marlon et al., 2008; Mouillot et al., 2006; Pechony and Shindell, 2010). However vegetation dynamics may also play a role that is not well understood. Increased fire occurrence would increase aerosol emissions, but decrease BVOC emissions. This could lead to a small positive or negative net radiative effect and feedback (Carslaw et al., 2010).

A large fraction of secondary organic carbon aerosol forms from the oxidation of isoprene, sesquiterpenes and monoterpenes from biogenic sources. Emissions from vegetation can increase in a warmer atmosphere, everything else being constant (Guenther et al., 2006). Global aerosol models simulate an increase in isoprene emissions of 22 to 55% by 2100 in response to temperature change (Heald et al., 2008; Liao et al., 2006; Sanderson et al., 2003) and a change in global SOA burden of −6% to +11% through the climate-induced changes in aerosol processes and removal rates (Heald et al., 2008; Liao et al., 2006; Tsigaridis and Kanakidou, 2007). Increasing CO_2 concentrations are believed to inhibit BVOC emissions (Arneth et al., 2007) which could offset the temperature effect and adds significant uncertainty to future emissions. Future changes in vegetation cover, whether they are natural or anthropogenic, also introduce large uncertainty in emissions (Lathière et al., 2010). There is little understanding on how the marine source of organic aerosol may change with climate, notwithstanding the large range of emission estimates for the present day (Carslaw et al., 2010).

7.3.5.4 Synthesis

The emissions, properties and concentrations of aerosols or aerosol precursors could respond significantly to climate change, but there is little consistency across studies in the magnitude or sign of this response. The lack of consistency arises mostly from our limited understanding of processes governing the source of natural aerosols and the complex interplay of aerosols with the hydrological cycle. The feedback parameter as a result of the future changes in emissions of natural aerosols is mostly bracketed within ±0.1 W m^{-2} K^{-1} (Carslaw et al., 2010). With respect to anthropogenic aerosols, Liao et al. (2009) showed a significant positive feedback (feedback parameter of +0.04 to +0.15 W m^{-2} K^{-1} on a global mean basis) while Bellouin et al. (2011) simulated a smaller feedback of −0.02 to −0.08 W m^{-2} K^{-1}. Overall we assess that models simulate relatively small feedback parameters (i.e., within ±0.2 W m^{-2} K^{-1}) with very low confidence, however regional effects on the aerosol may be important.

7.4 Aerosol-Cloud Interactions

7.4.1 Introduction

This section assesses our understanding of aerosol-cloud-precipitation interactions, emphasizing the ways in which anthropogenic aerosols may be affecting the distribution and radiative properties of clouds and precipitation. The idea that anthropogenic aerosols are changing cloudiness, thus contributing a substantial forcing to the climate system, has been addressed to varying degrees in all of the previous IPCC assessment reports.

Since AR4, research has continued to articulate new pathways through which the aerosol may affect the radiative properties of clouds, as well as the intensity and spatial patterns of precipitation (e.g., Rosenfeld et al., 2008). Progress can be identified on four fronts: (i) global-scale modelling has advanced in its ability to represent a greater diversity of aerosol-cloud interactions, and with greater internal consistency; (ii) observational studies continue to document strong local correlations between CCN proxies and clouds or precipitation, but have become more quantitative and are increasingly identifying the methodological challenges associated with such correlations; (iii) regional-scale modelling is increasingly being used to

assess regional influences of aerosol on cloud field properties and precipitation; (iv) fine-scale modelling studies have begun to be used more widely, and among other things have shown how turbulent mixing, cloud and regional-scale circulations may buffer the effects of aerosol perturbations.

This section focuses on the microphysics of aerosol-cloud interactions in liquid and mixed-phase clouds. Their radiative implications are quantified in Section 7.5. This section also includes discussion of aerosol influences on light precipitation in shallow clouds but defers discussion of aerosol effects on precipitation from mixed-phase clouds to Section 7.6.

7.4.1.1 Overview and Classification of Hypothesized Aerosol-Cloud Interactions

Denman et al. (2007) catalogued several possible pathways via which the aerosol might affect clouds. Given the number of possible aerosol-cloud interactions, and the difficulty of isolating them individually, we see little value in attempting to assess each effect in isolation, especially since modelling studies suggest that the effects may interact and compensate (Morrison and Grabowski, 2011; Stevens and Feingold, 2009). Instead, we group all radiative consequences of aerosol-cloud interactions into two broad categories: the immediate impact in the absence of macrophysical changes to clouds, denoted "radiative forcing due to aerosol-cloud interactions" or RFaci, and the final result including follow-on impacts of macrophysical responses to the initial change, denoted "adjusted forcing due to aerosol-cloud interactions", or AFaci (Figure 7.2). RFaci represents the classical "Twomey (1977)" or cloud albedo effect whereby greater CCN numbers increase the droplet surface area, but is extended to include changes in the breadth of the size distribution (Section 7.4.2). AFaci additionally accounts for any secondary effects that result as clouds adjust to the rapid changes in their environment accompanying an aerosol perturbation (Figure 7.1), such as lifetime effects, wherein cloud macrostructure adjusts to changes in cloud microstructure (Albrecht, 1989; Liou and Ou, 1989; Pincus and Baker, 1994). AFaci does not, however, include adjustments associated with aerosol-radiation interactions. Although AFaci subsumes RFaci, we retain an estimate of RFaci in Section 7.5 for continuity with prior assessments, and because it is better understood than the model-dependent effects determining AFaci. Possible contributions to the AFaci from liquid clouds are discussed in Section 7.4.3, separately from those associated with adjustments by ice or mixed phase clouds (Section 7.4.4). Figure 7.16 shows a schematic of many of the processes to be discussed in Sections 7.4, 7.5, and 7.6.

[INSERT FIGURE 7.16 HERE]

Figure 7.16: Schematic depicting the myriad aerosol-cloud-precipitation related processes occurring within a typical GCM grid box. The schematic conveys the importance of considering aerosol-cloud-precipitation processes as part of an interactive system encompassing a large range of spatiotemporal scales. Cloud types include low-level stratocumulus and cumulus where research focuses on droplet activation, mixing, cloud scavenging, and new particle formation; ice-phase cirrus clouds where a key issue is homogeneous freezing; and deep convective clouds where some of the key questions relate to aerosol influences on liquid, ice, and liquid-ice pathways for precipitation formation, cold pool formation, and scavenging. These processes influence the short- and longwave forcing of the system and hence climate.

7.4.1.2 Advances and Challenges in Observing Aerosol-Cloud Interactions

Since AR4, progress has been made in understanding how measurement artefacts affect retrievals of both aerosol (Jeong and Li, 2010; Kahn et al., 2005; Tanré et al., 1996; Tanré et al., 1997) and cloud properties (Platnick et al., 2003) in broken cloud fields. Two key issues are that measurements classified as "cloud-free" may not be, and that aerosol measured in the vicinity of clouds is significantly different than it would be were the cloud field, and its proximate cause (high humidity), not present (e.g., Loeb and Schuster, 2008). The latter results from humidification effects on aerosol optical properties (Charlson et al., 2007; Su et al., 2008; Tackett and Di Girolamo, 2009; Twohy et al., 2009), contamination by undetectable cloud fragments (Koren et al., 2007) and the remote effects of radiation scattered by cloud edges on aerosol retrieval (Várnai and Marshak, 2009; Wen et al., 2007).

While passive satellite retrievals are unable to distinguish aerosol layers above or below clouds from those intermingling with the cloud field, newer active space-based remote sensing has begun to address this problem (Anderson et al., 2005; Huffman et al., 2007; Stephens et al., 2002). Spectral polarization and multi-angular measurements can discriminate between cloud droplets and aerosol particles and thus improve estimates of aerosol loading and absorption (Deuzé et al., 2001; Mishchenko et al., 2007). Field studies (Rauber et al., 2007; Vogelmann et al., 2012; Wood et al., 2011b) and laboratory investigations (e.g.,

Stratmann et al., 2009) of aerosol-cloud interactions also continue to make important contributions to our understanding of how aerosols impact cloud processes, and how clouds in turn modify aerosols. The latter occurs along a number of pathways including aqueous chemistry, which adds non-volatile mass to drops (e.g., Schwartz and Freiberg, 1981), coalescence scavenging, whereby drop collision-coalescence diminishes the drop (and aerosol) number concentration (Hudson, 1993), new particle formation in the vicinity of clouds (Clarke et al., 1999) and aerosol removal by rain (see also Section 7.3). As a result, our understanding of the distribution and properties of the aerosol in the vicinity of clouds continues to improve apace with an appreciation of the limits of this understanding (Anderson et al., 2009).

The observational challenge of inferring causality from correlation remains a large and limiting one. Because the aerosol is a strong function of air-mass history and origin, and is strongly influenced by cloud and precipitation processes (Anderson et al., 2009; Clarke et al., 1999; Petters et al., 2006), and both are affected by meteorology (Engström and Ekman, 2010), correlations between the aerosol and cloud, or precipitation, cannot be taken as generally indicating a cloud response to the aerosol (e.g., Painemal and Zuidema, 2010). Furthermore, attempts to control for other important factors (air-mass history or cloud dynamical processes) are limited by a lack of understanding of cloud controlling factors in the first place (Anderson et al., 2009; Siebesma et al., 2009; Stevens and Brenguier, 2009). These problems greatly undermine confidence in observationally-based inferences of aerosol effects on clouds and precipitation.

7.4.1.3 Advances and Challenges in Modelling Aerosol-Cloud Interactions

Fine-scale models, capable of resolving cloud-scale circulations have greatly advanced as a tool for testing the physical mechanisms proposed to govern aerosol-cloud-precipitation interactions (Ackerman et al., 2009; vanZanten et al., 2011). A general finding from explicit numerical simulations of clouds is that various aerosol impact mechanisms tend to be mediated (and often buffered) by interactions across scales not included in the idealized models that gave rise to the original idea (Stevens and Feingold, 2009). Specific examples involve the interplay between the drop-size distribution and mixing processes that determine cloud macrostructure (Ackerman et al., 2004; Bretherton et al., 2007; Small et al., 2009; Stevens et al., 1998; Wood, 2007), or the dependence of precipitation development in stratiform clouds on details of the vertical structure of the cloud (Wood, 2007). As a result it is likely that the physical system is less sensitive to aerosol perturbations than are large-scale models, which do not represent all of these compensating processes.

At larger scales, regional models allow for a much broader range of scale interactions and timescales long enough for robust features to emerge (Bangert et al., 2011; Seifert et al., 2012). Regional models allow exploration of aerosol-cloud interactions in the context of non-idealized meteorology, variability in land surface, and diurnal/monthly cycles (Tao et al., 2012). These advantages must be weighed against their inability to resolve the fine-scale cloud processes discussed above. Regional models have brought to light the possibility of aerosol gradients manifesting changes in circulation patterns via numerous mechanisms including gradients in heating rates (Lau et al., 2006; Section 7.3.4.2), changes in the radiative properties of cloud anvils (van den Heever et al., 2011; see Section 7.6), or changes in the spatial distribution of precipitation (Lee, 2012; Section 7.6).

The representation of aerosol effects in global models has also advanced. Most global models now represent an increasing number of hypothesized aerosol-cloud interactions, and are undergoing evaluation through comparisons to data and to other models (Quaas et al., 2009). Historically, aerosol-cloud interactions in climate models have largely been introduced based on simple constructs (e.g., Albrecht, 1989; Pincus and Baker, 1994; Twomey, 1977). There has been significant progress on droplet activation (e.g., Ghan et al., 2011) and ice nucleation (Barahona and Nenes, 2008; DeMott et al., 2010) parameterizations, however these still depend heavily on unresolved (climate model) physics such as updraught velocity. Similarly, parameterizations of aerosol influences on cloud amount cannot account for known non-monotonic responses (Section 7.4.3.2). Global models are now beginning to represent effects in convective, ice and mixed-phase clouds (e.g., Lohmann, 2008; Section 7.6; Song and Zhang, 2011). In addition "superparameterisation" approaches (Section 7.2.2.1.2) hold promise for treating aerosol-cloud interactions more comprehensively, with recent results supporting the notion that aerosol forcing is smaller than simulated by standard climate models (Wang et al., 2011b; see Section 7.5.3). Nevertheless, we caution that for both liquid-only and mixed-phase clouds, the inability of GCMs to resolve cloud-scale updraught

velocities and associated cooling rates is a pervasive concern for aerosol-cloud interactions, even for models with grid sizes on the order of kilometres.

Although advances have been considerable, the challenges remain formidable. The representation of clouds in large-scale models remains primitive (Section 7.2.3) and even if large-scale models were able to represent clouds with greater fidelity, fine-scale modelling suggests that the outcome of an aerosol perturbation depends on the details of the interaction of clouds, turbulence, radiation and precipitation processes on a range of scales not represented by large-scale models (vanZanten et al., 2011). For this reason it is not surprising that large-scale models exhibit a range of manifestations of aerosol-cloud interactions, which limits quantitative inference (Quaas et al., 2009). This emphasises the need to incorporate into climate models the lessons learned from cloud-scale models, in a physically consistent way.

7.4.1.4 Combined Modelling and Observational Approaches

Combined approaches, which attempt to maximize the respective advantage of models and data, are beginning to add to understanding of aerosol-cloud interactions. These include inversions of the observed historical record using large-scale modelling studies, but also the use of reanalysis and chemical transport models to help interpret satellite records (Chameides et al., 2002; Koren et al., 2010; Mauger and Norris, 2010), field study data to help constrain fine-scale modelling studies (Ackerman et al., 2009; vanZanten et al., 2011), or satellite/surface-based climatologies to constrain large-scale modelling (Quaas et al., 2009).

7.4.2 Radiative Forcing due to Aerosol-Cloud Interactions (RFaci)

7.4.2.1 The Physical Basis

The cloud albedo effect (Twomey, 1977), or RFaci, is the mechanism by which an increase in aerosol number concentration leads to an increase in liquid cloud albedo (reflectance of incoming solar radiation) by increasing the cloud droplet number concentration and hence increasing total droplet surface area, with the liquid water content and cloud geometrical thickness held fixed. Although only the change in the droplet concentration is considered in the original concept of the cloud albedo effect, a change in the shape of the droplet size distribution that is directly induced by the aerosols, may also play a role (e.g., Feingold et al., 1997; Liu and Daum, 2002). In the Arctic, anthropogenic aerosols may influence the longwave emissivity of thin liquid clouds and generate a positive forcing at the surface (Garrett and Zhao, 2006; Lubin and Vogelmann, 2006). This line of research is at a stage of relative infancy and is not covered further in this assessment.

The physical basis of RFaci is fairly well understood, with research since AR4 generally reinforcing earlier work. Detailed in-situ aircraft observations show that droplet concentrations observed just above the cloud base generally agree with those predicted given the aerosol and updraught observed below the cloud (e.g., Fountoukis et al., 2007). Vertical profiles of cloud effective radius also agree with those predicted by models that take into account the effect of entrainment (Lu et al., 2008), although uncertainties still remain in estimating the shape of the droplet size distribution (Brenguier et al., 2011), and the degree of non-adiabaticity within clouds. Multi-dimensional radiative transfer calculations have also been applied to estimate cloud albedo instead of using the traditional two-stream approximation to find that the latter could overestimate the albedo effect under certain conditions (Duda et al., 1996; Zuidema et al., 2008).

7.4.2.2 Observational Evidence for Aerosol-Cloud Interactions

At low AOD (i.e., less than about 0.3) there is ample observational evidence for increases in aerosol resulting in an increase in drop concentration and decrease in drop size (for constant liquid water) but uncertainties remain regarding the magnitude of this effect, and its sensitivity to spatial averaging. Based on simple metrics, there is a large range of physically plausible responses, with aircraft measurements (e.g., Hegg et al., 2012; Lu et al., 2007; Lu et al., 2008; Twohy et al., 2005) tending to show stronger responses than satellite-derived responses (McComiskey and Feingold, 2008; Nakajima and Schulz, 2009). At high AOD, droplet concentration tends to saturate and, if the aerosol is absorbing, there may be reductions in droplet concentration and cloudiness (Koren et al., 2008). This effect is part of AFaci (Section 7.4.3.2).

Since clouds experience rapid adjustments to liquid water and depth when influenced by aerosol perturbations, RFaci is a hypothetical construct. Hence while an aerosol influence on cloud microphysics is observable, the radiative forcing associated with the "constant liquid water RFaci" is generally not (Section 7.4.3.2).

7.4.2.3 Advances in Process Level Understanding

At the heart of the albedo effect lie two fundamental issues. The first is droplet activation and its sensitivity to aerosol and meteorological parameters. The primary controls on droplet concentration are the aerosol number concentration (particularly at diameters greater than about 60 nm) and cooling rate (proportional to updraught velocity). Aerosol size distribution can play an important role under high aerosol loadings, whereas aerosol composition tends to be much less important, except perhaps under very polluted conditions and low updraught velocities (e.g., Ervens et al., 2005). The relative unimportance of composition is partially because aging makes particles more hygroscopic, but also because of the self-regulation of the supersaturation field that determines drop activation (e.g., higher hygroscopicity, which initially favours activation, leads to higher water vapour uptake, which then lowers supersaturation and suppresses activation). The second issue is the presence of condensed water that strongly determines how much energy can be reflected; there is no RFaci unless clouds are present. Simple arguments show that in a relative sense the amount of reflected energy is approximately two-and-a-half times more sensitive to changes in the liquid water path than to changes in droplet concentration (Boers and Mitchell, 1994). Since both these parameters experience similar ranges of variability, the magnitude of aerosol-cloud related forcing rests mostly on dynamical factors such as turbulent strength and entrainment that control cloud amount, and a few key aerosol parameters such as aerosol number concentration and size distribution, and to a much lesser extent, composition.

7.4.3 Forcing Associated with Adjustments in Liquid Clouds (AFaci)

7.4.3.1 The Physical Basis for Adjustments in Liquid Clouds

The adjustments giving rise to AFaci are multi-faceted and are often associated with changes in cloud lifetime or cloud water, previously referred to as 'lifetime' effects (Figure 7.2). However this old nomenclature is misleading because it assumes a relationship between cloud lifetime and cloud amount or water content. Moreover, the effect of the aerosol on cloud amount may have nothing to do with cloud lifetime per se (e.g., Pincus and Baker, 1994).

The traditional view has been that adjustment effects associated with aerosol-cloud-precipitation interactions will add to the initial albedo increase by increasing cloud amount. The chain of reasoning involves three steps: first that droplet concentrations depend on the number of available CCN; second that precipitation development is regulated by the droplet concentration; and third that the development of precipitation reduces cloud amount (Stevens and Feingold, 2009).

Of the three steps the first has ample support in both observations and theory (Section 7.4.2). More problematic are the second two links in the chain of reasoning. The physical basis for a pervasive, positive dependence of cloud amount on the available CCN is weak. Although increased droplet concentrations inhibit the initial development of precipitation in single clouds and stratocumulus (see Section 7.4.3.2.1), it is not clear that such an effect operates in an evolving, broken cloud field. In the trade-cumulus regime, some modelling studies suggest the opposite, with increased aerosol concentrations actually promoting the development of deeper clouds and invigorating precipitation (Stevens and Seifert, 2008; see discussion of similar responses in deep convective clouds in Section 7.6). Others have shown alternating cycles of larger *and* smaller cloud water in both aerosol-perturbed stratocumulus (Sandu et al., 2008) and trade cumulus (Lee et al., 2012), pointing to the important role of environmental feedback. Although the original studies that hypothesized cloud amount effects (Albrecht, 1989; Liou and Ou, 1989) are often taken as demonstrative of this point, there is limited unambiguous observational evidence (exceptions to be given below). Many climate models assume such an effect *a priori,* which likely influences their forcing estimates.

7.4.3.2 Observational Evidence of Adjustments in Liquid Clouds

Since AFaci subsumes RFaci, and because RFaci is hard to observe, we now discuss observations of aerosol-perturbed cloud fields more generally.

7.4.3.2.1 Stratocumulus

The cloud albedo effect is best manifested in so-called ship tracks, which are bright lines of clouds behind ships. As shown during the Monterey Area Ship Track (MAST) experiment, many ship tracks are characterized by an increase in the droplet concentration resulting from the increase in aerosol number concentration and an absence of drizzle size drops, which leads to a decrease in the droplet radius and an increase in the cloud albedo (Durkee et al., 2000), all else equal. Coakley and Walsh (2002) showed that cloud water responses can be of different sign. This is supported by more recent shiptrack analyses based on the new A-Train satellites (Christensen and Stephens, 2011); liquid water decreases weakly (−6%) in overcast clouds in response to ship-track intrusions but increases significantly (39%) in precipitating, broken stratocumulus clouds where aerosol intrusions result in larger cloud fraction. Adjustments are therefore key to understanding radiative response. A-Train satellites studies of long-term degassing of low-lying volcanic aerosol on stratocumulus point to smaller drop sizes but ambiguous changes in cloud fraction and cloud water (Gasso, 2008). The global radiative forcing of visible ship tracks has been estimated from satellite and found to be insignificant at about –0.5 mW m^{-2} (Schreier et al., 2007), although there is some concern that this analysis may not have identified all shiptracks. Nevertheless, this result is supported by two years of data downwind of shipping lanes that were unable to distinguish aerosol influences from meteorological influences on cloud microphysical or macrophysical properties (Peters et al., 2011b). Counter evidence of shiptracks significantly increasing the cloud fraction and albedo of broken cloud scenes are also emerging (Goren and Rosenfeld, 2012).

The development of precipitation in stratocumulus, whether due to aerosol or meteorological influence can, in some instances, change a highly reflective closed-cellular cloud field to a weakly reflective broken open-cellular field (Comstock et al., 2005; Savic-Jovcic and Stevens, 2008; Sharon et al., 2006; Stevens et al., 2005b; vanZanten et al., 2005; Wang and Feingold, 2009a). In some cases, compact regions (pockets) of open-cellular convection become surrounded by regions of closed-cellular convection. It is, however, noteworthy that observed precipitation rates can be similar in both open and closed-cell environments (Wood et al., 2011a). The lack of any apparent difference in the large-scale environment of the open cells, versus the surrounding closed cellular convection, suggests the potential for multiple equilibria (Baker and Charlson, 1990; Feingold et al., 2010). Therefore in the stratocumulus regime, the onset of precipitation may lead to a chain of events that leads to a large-scale reduction of cloudiness in agreement with Liou and Ou (1989) and Albrecht (1989). The transition may be bidirectional: ship tracks passing through open-cell regions also appear to revert the cloud field to a closed-cell regime inducing a potentially strong AFaci (Christensen and Stephens, 2011; Goren and Rosenfeld, 2012; Wang et al., 2011a).

7.4.3.2.2 Trade-cumulus

Precipitation from shallow convective clouds proves difficult to observe in trade cumuli, as the clouds are small, and not easily observed by space-based remote sensing techniques (Stephens et al., 2008). A recent A-Train satellite study of trade cumuli influenced by aerosol associated with slow volcanic degassing points to smaller droplet size, decreased precipitation efficiency, increased cloud amount, and higher cloud tops (Yuan et al., 2011). Other studies show that in the trade cumulus regime cloudiness tends to increase with precipitation amount, most likely because processes that favour precipitation development also favour clouds (Nuijens et al., 2009) and because precipitating trade cumuli tend to regenerate through colliding outflows (Zuidema et al., 2012).

While observationally-based assessments of aerosol-cloud interactions have a long history, a more recent development is assessment of the ability of detailed models to reproduce the radiative fingerprints of aerosol-cloud interactions in cumulus cloud fields (Schmidt et al., 2009). This involves comparison between measurements of the irradiance field with the same field calculated in a fine-scale model that represents aerosol-cloud interactions. Such an approach identifies key forcing parameters (e.g., cloud-field properties, aerosol hygroscopicity and absorption) and provides the link between aerosol-cloud interactions and AFaci.

7.4.3.3 Advances in Process Level Understanding

Since AR4, there has been progress towards understanding some basic processes relevant to AFaci. One question is how susceptible precipitation is to droplet concentration, and by inference to the available aerosol. Some studies point to the drop effective radius as a threshold indicator of the onset of drizzle (Rosenfeld and Gutman, 1994; Wang et al., 2011a). Others focus on the sensitivity of the conversion of cloud-water to rain-water (autoconversion) and find that it scales with the *square* of the inverse of the droplet concentration(Khairoutdinov and Kogan, 2000). However theoretical work that incorporates a fuller description of rain formation processes suggests that this strongly over-estimates the sensitivity of rain formation in shallow clouds (Stevens and Seifert, 2008), and that rain formation scales with approximately the inverse *square-root* of the droplet concentration (Kostinski, 2008; Seifert and Stevens, 2010). Observational studies also suggest a weaker scaling law (approximately the inverse of drop concentration; Comstock et al., 2005; Pawlowska and Brenguier, 2003; vanZanten et al., 2005). Note that thicker, liquid clouds generate rain via accretion of cloud drops by raindrops, a process that is relatively insensitive to droplet concentration, and therefore to aerosol perturbations (e.g., Khairoutdinov and Kogan, 2000).

The balance of evidence suggests that autoconversion likely scales with approximately the inverse square root of droplet concentration and that liquid water path has significantly more leverage over precipitation than does droplet concentration. Some of the effects that reduce and even eliminate the sensitivity of rain formation to the autoconversion process have begun to be incorporated in parameterizations used by large-scale models (Posselt and Lohmann, 2009).

Small-scale studies (Ackerman et al., 2004; Small et al., 2009; Xue et al., 2008) and A-Train satellite observations (Christensen and Stephens, 2011; Lebsock et al., 2008) tend to confirm two responses of the cloud liquid water to increasing aerosol. Under clean conditions when clouds are prone to precipitation, an increase in the aerosol tends to increase cloud amount. Under non-precipitating conditions, clouds tend to thin in response to increasing aerosol. Treatment of the subtlety of these responses and associated detail in small-scale cloud processes is not currently feasible in GCMs, nor will it be in the foreseeable future.

Since AR4, cloud resolving model simulation has begun to stress the importance of scale interactions when addressing aerosol-cloud interactions. Large model domains (order 100 km) allow mesoscale circulations to develop in response to changes in the aerosol. These dynamical responses may have a significant impact on cloud morphology and radiative forcing. Examples include the dramatic changes in cloud morphology associated with changes in cellular structure discussed above and the cloud-free shadows that appear alongside ship tracks (Wang and Feingold, 2009b). Similar examples of large-scale changes in circulation associated with aerosol, and associated influence on precipitation are discussed in Section 7.6.4. These underscore the imprudence of applying simplistic rules for aerosol-cloud-precipitation interactions in GCMs.

7.4.3.4 Advances in and Insights Gained from Large-Scale Modelling Studies

Regional models are increasingly including representation of aerosol-cloud interactions using sophisticated microphysical models (Bangert et al., 2011; Seifert et al., 2012; Yang et al., 2011) and offer an important middle ground between fine-scale, idealized simulations and GCMs. Some of these models are operational weather forecast models that undergo regular evaluation. Yang et al. (2011) show improved simulations of stratocumulus fields when aerosol-cloud interactions are introduced. Regional models are increasingly being used in conjunction with satellite observations to provide the meteorological context for aerosol-cloud interactions (see Section 7.4.1.4) with some (e.g., Painemal and Zuidema, 2010) suggesting that droplet concentration differences, are primarily driven by synoptic scale influences rather than aerosol.

It appears increasingly likely that cloud adjustments, which almost certainly exist locally, vary from one cloud regime to the next. As such it requires models to correctly represent the distribution of cloud regimes evincing such effects, and knowledge of how such effects manifest themselves across these regimes. Because diverse effects offer the possibility of compensating one another, at least globally, it seems possible that AFaci may be less important than previously thought (Stevens and Feingold, 2009).

7.4.4 Adjustments in Cold Clouds

7.4.4.1 The Physical Basis for Adjustments in Cold Clouds

Mixed-phase clouds, containing both liquid water and ice particles, exist at temperatures between 0°C and –38°C. At warmer temperatures ice melts rapidly, whereas at colder temperatures liquid water freezes homogeneously. The formation of ice in mixed-phase clouds depends on heterogeneous freezing, initiated by ice nuclei (IN; Section 7.3.3.4 and Figure 7.15), usually insoluble aerosol particles. In spite of their very low concentrations (on the order of 1 l^{-1}), IN have an important influence on mixed-phase clouds. Mineral dust particles have been identified as good IN but far less is known about the IN ability of other aerosol types, and their preferred modes of nucleation. For example, the ice nucleating ability of black carbon particles remains controversial (Hoose and Möhler, 2012). In the case of cirrus (ice-only) clouds forming via homogeneous freezing at temperatures colder than –38°C, soluble matter can hinder glaciation by depressing the freezing temperature of super-cooled drops (e.g., Baker and Peter, 2008; Girard et al., 2004). Hence anthropogenic perturbations to the aerosol have the potential to affect glaciation, water and ice optical properties, and their radiative effect.

Because the equilibrium vapour pressure with respect to ice is lower than that with respect to liquid, the initiation of ice in a supercooled liquid cloud will cause vapour to diffuse rapidly toward ice particles at the expense of the liquid water (Wegener-Bergeron-Findeisen process; e.g., Hudson et al., 2010; Verheggen et al., 2007). This favours the depositional growth of large ice crystals, which may sediment away from the water-saturated region of the atmosphere, influencing the subsequent evolution of the cloud. Hence anthropogenic perturbations to the IN can influence the rate at which ice forms, which in turn may regulate cloud amount (Lohmann, 2002a; Storelvmo et al., 2011; see also Section 7.2.3.2.2) and upper tropospheric humidity.

Finally, the ice-phase provides enthalpy to the environment, which influences cloud dynamics, as well as alternate, complex pathways for precipitation to develop (e.g., Zubler et al., 2011and Section 7.6).

7.4.4.2 Observations of Aerosol Effects on Arctic Ice and Mixed-Phase Stratiform Clouds

Arctic mixed-phase clouds have received a great deal of attention since AR4, with major field programs conducted in 2004 (Verlinde et al., 2007) and 2009 (Brock et al., 2011; Jacob et al., 2010; McFarquhar et al., 2011), in addition to long-term monitoring at Barrow, Alaska (Shupe et al., 2008) and analysis of earlier field experiments (Uttal et al., 2002). Mixed-phase Arctic clouds persist for extended periods of time (days and even weeks; Zuidema et al., 2005), in spite of the inherent instability of the ice-water mix. We focus here on the role of the aerosol and refer to Section 7.2.3.2.2 for a discussion of meteorological aspects. In spite of their low concentrations, IN have an important influence on cloud persistence, with clouds tending to glaciate and disappear rapidly when IN concentrations are relatively high and/or updraught velocities too small to sustain a liquid water layer (e.g., Ovchinnikov et al., 2011). The details of the heterogeneous ice-nucleation mechanism remain controversial but there is increasing evidence that ice forms in Arctic stratus via the liquid phase (immersion freezing) so that the CCN population also plays an important role (de Boer et al., 2011; Lance et al., 2011). If ice indeed forms via the liquid phase this represents a self-regulating feedback that helps sustain the clouds: as ice forms, water is depleted, which restricts further ice formation and competition for water vapour via the Wegener-Bergeron-Findeisen process.

7.4.4.3 Advances in Process Level Understanding

Since AR4 research on ice-microphysical processes has been very active as evidenced by activity in the abovementioned field experiments. The persistence of some mixed-phase stratiform clouds has prompted efforts to explain this phenomenon in a theoretical framework (Korolev and Field, 2008). Cloud persistence may require a level of understanding of very detailed processes. For example, ice particle growth by vapour diffusion depends strongly on particle habit (Harrington et al., 2009), the details of which may have similar influence on glaciation times to the choice of different ice nucleation mechanism (Ervens et al., 2011). A recent review (Morrison et al., 2012) discusses the myriad processes that create a resilient mixed-phase cloud system, invoking the ideas of "buffering" seen in liquid clouds (Stevens and Feingold, 2009). Bistability has also been observed in the mixed-phase Arctic cloud system; the resilient cloud state is sometimes interrupted by a cloud-free state (Stramler et al., 2011), however there is much uncertainty regarding the meteorological and microphysical conditions determining which of these states is preferred.

Significant effort has been expended on heterogeneous freezing parameterizations employed in cloud or larger-scale models. Korolev (2007) developed a theoretically based parameterization of the Wegener-Bergeron-Findeisen process that has lately been employed in different GCMs (Lohmann and Hoose, 2009; Storelvmo et al., 2008b). Other parameterizations remain empirical (e.g., DeMott et al., 2010; Gettelman et al., 2010; Hoose et al., 2008; Lohmann and Diehl, 2006; Phillips et al., 2008; Salzmann et al., 2010; Storelvmo et al., 2008a), although some recent work attempts to represent the processes explicitly (Jacobson, 2003) or ground the development of parameterisations in concepts derived from classical nucleation theory (Hoose et al., 2010b). The details of how these processes are treated have important implications for tropical anvils (Fan et al., 2010).

Ice nucleation in cirrus clouds (at temperatures less than –35°C) depends crucially on the cloud updraught velocity and hence the supersaturation with respect to ice. For homogeneous nucleation, the onset relative humidities have been parameterized using results of parcel model simulations (e.g., Barahona and Nenes, 2009; Sassen and Dodd, 1988), airborne measurements in cirrus or wave clouds (Heymsfield et al., 1998; Heymsfield and Miloshevich, 1995), extensions of classical homogeneous ice nucleation theory (Khvorostyanov and Sassen, 1998; Khvorostyanov and Curry, 2009), and data from laboratory measurements (e.g., Bertram et al., 2000; Friedman et al., 2011; Koop et al., 2000; Magee et al., 2006; Mohler et al., 2003). If IN are present, then heterogeneous nucleation is the preferred freezing pathway because it occurs at lower onset relative humidities (or higher onset temperatures) than homogeneous nucleation. The onset relative humidities (or temperatures) for heterogeneous nucleation depend on the type and size of the involved ice nuclei (Figure 7.15 and Section 7.3.3.4).

7.4.4.4 Advances in and Insights Gained from Large-Scale Modelling Studies

Since the AR4 mixed-phase and ice clouds have received significant attention, with effort on representation of both heterogeneous (mixed-phase clouds) and homogeneous (cirrus) freezing processes. The physics of cirrus clouds usually only involve ice-phase microphysical processes and are somewhat simpler than mixed-phase clouds. Nevertheless, representation of aerosol-cloud interactions in mixed-phase and ice clouds is considerably less advanced than that involving liquid-only clouds.

For realistic concentrations of bacteria, biological particles have been found to play a negligible role for heterogeneous freezing in GCMs (Diehl and Wurzler, 2010; Hoose et al., 2010a; 2010b; Phillips et al., 2009; Sesartic et al., 2011). However some investigators (Ariya et al., 2009; Sun et al., 2010) argue that biological particles even in low concentrations may still be important because they can trigger secondary ice production via ice multiplication. Anthropogenic changes to the biosphere could conceivably also reduce the prevalence of biological IN. Our poor understanding of the climatology and lifecycle of aerosol particles that can serve as IN complicates attempts to assess what constitutes an anthropogenic perturbation to the IN population, let alone the effect of such a perturbation. BC can impact background cirrus by affecting ice nucleation properties but its effect remains uncertain (Kärcher et al., 2007). The numerous GCM studies that have evaluated AFaci for ice clouds are summarised in Section 7.5.

7.4.5 Impact of Cosmic Rays on Aerosols and Clouds

High solar acti0vity leads to variations in the strength and three-dimensional structure of the heliosphere, which reduces the flux of galactic cosmic rays (GCR) impinging upon the Earth's atmosphere by increasing the deflection of low energy GCR. As GCR is the primary source of atmospheric ionization, it has been suggested that GCR may act to amplify relative small variations in solar activity into climatologically significant effects (Ney, 1959), via a hypothesised relationship between ionization and cloudiness (e.g., Dickinson, 1975; Kirkby, 2007). There have been many studies aiming to test this hypothesis since AR4, which fall in two categories: i) studies that seek to establish a causal relationship between cosmic rays and aerosols/clouds by looking at correlations between the two quantities on timescales of days to decades, and ii) studies that test through observations or modelling one of the physical mechanisms that have been put forward. We assess these two categories of studies in the next two sections.

7.4.5.1 Correlations Between Cosmic Rays and Properties of Aerosols and Clouds

Many empirical relationships have been reported between GCR or cosmogenic isotope archives and some aspects of the climate system (e.g., Bond et al., 2001; Dengel et al., 2009; Ram and Stolz, 1999). The forcing from changes in total solar irradiance alone does not seem to account for these observations, implying the existence of an amplifying mechanism such as the hypothesized GCR-cloud link. We focus here on observed relationships between GCR and aerosol and cloud properties. Such relationships have focused on decadal variations in GCR induced by the 11-year solar cycle, shorter variations associated with the quasi-periodic oscillation in solar activity centred on 1.68 years or sudden and large variations known as Forbush decrease events. It should be noted that GCR co-vary with other solar parameters such as solar and UV irradiance, which makes any attribution of cloud changes to GCR problematic (Laken et al., 2011).

Some studies have shown co-variation between GCR and low-level cloud cover using global satellite data over periods of typically 5–10 years (Marsh and Svensmark, 2000; Pallé Bagó and Butler, 2000). Such correlations have not proved to be robust when extending the time period under consideration (Agee et al., 2012), restricting the analysis to particular cloud types (Kernthaler et al., 1999) or locations (Udelhofen and Cess, 2001; Usoskin and Kovaltsov, 2008). The purported correlations have also been attributed to ENSO variability (Farrar, 2000; Laken et al., 2012) and artefacts of the satellite data cannot be ruled out (Pallé, 2005). Statistically significant, but weak, correlations between diffuse fraction and cosmic rays have been found at some locations in the UK over the 1951 to 2000 period (Harrison and Stephenson, 2006). Harrison (2008) also found a unique 1.68-year periodicity in surface radiation for two different UK sites between 1978 and 1990, potentially indicative of a cosmic ray effect. Svensmark et al. (2009) found large global reductions in the aerosol Ångström exponent from AERONET, liquid water path from SSM/I, and cloud cover from MODIS and ISCCP after large Forbush decreases, but these results were not corroborated by other studies who found no statistically significant links between GCR and clouds at the global scale (Čalogović et al., 2010; Kristjánsson et al., 2008; Laken and Čalogović, 2011). Although some studies found small but significant positive correlations between GCR and high- and mid-altitude clouds (Laken et al., 2010; Rohs et al., 2010), these variations were very weak, and the results were highly sensitive to how the Forbush events were selected and composited (Laken et al., 2009).

7.4.5.2 Physical Mechanisms Linking Cosmic Rays to Cloudiness

The most widely studied mechanism proposed to explain the possible link between GCR and cloudiness is the "ion-aerosol clear air" mechanism, in which atmospheric ions produced by GCR facilitate aerosol nucleation and growth ultimately impacting CCN concentrations and cloud properties (Carslaw et al., 2002; Usoskin and Kovaltsov, 2008). The variability of atmospheric ionization rates due to GCR changes can be considered relatively well quantified (Bazilevskaya et al., 2008), whereas resulting changes in aerosol nucleation rates are very poorly known (Enghoff and Svensmark, 2008; Kazil et al., 2008). The Cosmics Leaving OUtdoor Droplets (CLOUD) experiment at CERN indicates that GCR-induced ionization enhances water–sulphuric acid nucleation in the middle and upper troposphere, but is very unlikely to give a significant contribution to nucleation taking place in the continental boundary layer (Kirkby et al., 2011). Field measurements qualitatively support this view but cannot provide any firm conclusion on the role of ions due to the scarcity and other limitations of free-troposphere measurements (Arnold, 2006; Mirme et al., 2010), and due to difficulties in separating GCR-induced nucleation from other nucleation pathways in continental boundary layers (Hirsikko et al., 2011). If strong enough, the signal from GCR-induced nucleation should be detectable at the Earth's surface because a big fraction of CCN in the global boundary layer is expected to originate from nucleation taking place in the free troposphere (Merikanto et al., 2009). Based on surface aerosol measurements at one site, Kulmala et al. (2010) found no connection between GCR and new particle formation or any other aerosol property over a solar cycle (1996–2008). Our understanding of the "ion-aerosol clear air" mechanism as a whole relies on a few model investigations that simulate GCR changes over a solar cycle (Kazil et al., 2012; Pierce and Adams, 2009a; Snow-Kropla et al., 2011) or during strong Forbush decreases (Bondo et al., 2010; Snow-Kropla et al., 2011). Although all model studies found a detectable connection between GCR variations and either CCN changes or column aerosol properties, the response appears to be too weak to cause a significant radiative effect because GCR are unable to effectively raise CCN and droplet concentrations (Kazil et al., 2012).

A second pathway linking GCR to cloudiness has been proposed through the global electric circuit (GEC). A small direct current is able to flow vertically between the ionosphere (maintained at approximately 250 kV by thunderstorms and electrified clouds) and the Earth's surface over fair-weather regions because of GCR-

induced atmospheric ionization. Charges can accumulate at the upper and lower cloud boundaries as a result of the effective scavenging of ions by cloud droplets (Tinsley, 2000). This creates conductivity gradients at the cloud edges (Nicoll and Harrison, 2010), and may influence droplet-droplet collision (Khain et al., 2004), cloud droplet-particle collisions (Tinsley, 2000), and cloud droplet formation processes (Harrison and Ambaum, 2008). These microphysical effects may potentially influence cloud properties both directly and indirectly. Although Harrison and Ambaum (2010) observed a small reduction in downward LW radiation which they associated with variations in surface current density, supporting observations are extremely limited. Our current understanding of the relationship between cloud properties and the GEC remains very low, and there is no evidence yet that associated cloud processes could be of climatic significance.

7.4.5.3 Synthesis

Although there is some evidence that ionization from cosmic rays may enhance aerosol nucleation in the free troposphere, there is medium evidence and high agreement that the cosmic ray-ionization mechanism is too weak to influence global concentrations of CCN or their change over the last century or during a solar cycle in any climatically significant way. The lack of trend in the cosmic ray intensity over the last 50 years (Agee et al., 2012; McCracken and Beer, 2007) provides another strong argument against the hypothesis of a major contribution of cosmic rays to ongoing climate change.

7.5 Radiative Forcing and Adjusted Forcing by Anthropogenic Aerosols

In this section, aerosol forcing estimates are synthesized and updated from AR4. As depicted in Figure 7.2, RF refers to the instantaneous radiative forcing either due to aerosol-radiation interactions (ari), formerly known as the direct aerosol forcing, or aerosol-cloud interactions (aci), formerly known as the indirect aerosol forcing. AF refers to the adjusted forcing (also referred to as radiative flux perturbation) and can be estimated from Hansen-style experiments with fixed sea-surface temperatures (see Sections 7.1 and 8.1). It includes rapid adjustments, such as changes to the cloud lifetime, changes in lapse-rate due to absorbing aerosols and aerosol microphysical effects on mixed-phase, ice and convective clouds. AF can again be caused by ari, aci or the sum of ari and aci.

Chapter 2 of AR4 (Forster et al., 2007) assessed RFari to be –0.5 ± 0.4 W m^{-2} and broke this down into components associated with several species. Land albedo changes associated with black carbon (BC) on snow were assessed to be +0.1 ± 0.1 W m^{-2}. The RFaci was assessed to be –0.70 W m^{-2} with a –1.8 to –0.3 W m^{-2} uncertainty range. These uncertainty estimates were based on a combination of model results and remote observations. The semi-direct effect and other aerosol indirect effects were assessed in Chapter 7 (Denman et al., 2007) to contribute additional uncertainty. The combined total aerosol forcing was given as two distinct ranges: –0.2 to –2.3 W m^{-2} from models and a –0.1 to –1.7 W m^{-2} range from inverse estimates.

For consistency with Chapter 8, all quoted ranges represent a 5% to 95% uncertainty range and we evaluate the forcings between 1750 and ~2010. Note that for several aerosol species (such as biomass burning) this does not quite equate to the anthropogenic effect as emissions started to be influenced by humans before the Industrial Revolution. Many studies estimate aerosol forcings between 1850 and present day and conversion to a forcing between 1750 and present-day contributes to increase the uncertainty (Bellouin et al., 2008).

7.5.1 Estimates of RF and AF from Aerosol-Radiation Interactions (RFari and AFari)

7.5.1.1 Radiative Forcing and Adjusted Forcing from All Aerosols

Building on our understanding of aerosol processes and their radiative effects (Section 7.3), this section assesses RFari and AFari. The subsection additionally assesses the forcings from absorbing aerosol (BC and dust) on both snow and ice.

Observations can give useful constraints to aspects of the global RFari estimates (Section 7.3.4, Anderson et al., 2005; Kahn, 2012). Estimates of RFari are either taken from global aerosol models directly (Schulz et al., 2006) or based mostly on observations, but using supplemental information from models (Loeb and Su, 2010; Myhre, 2009). Three studies (Bellouin et al., 2008; Myhre, 2009; Zhao et al., 2008) improved satellite-based RFari estimate over those quoted in AR4. The most complete analysis of the globally-averaged all-sky

preindustrial-to-present RF (Myhre, 2009) estimated an RFari of –0.3 ± 0.2 W m^{-2}. There is medium confidence in this best estimate, but the uncertainty range is likely underestimated (Loeb and Su, 2010).

Lohmann et al. (2010) found RFari in five GCMs ranging from –0.1 to –0.4 W m^{-2}. A second phase of AeroCom model results gives an RFari median of –0.39 W m^{-2}, with a model range of about –0.1 to –0.6 W m^{-2}, after their forcings for 1850-2000 had been scaled by emissions to represent 1750–2010 changes (Myhre et al., 2012). Figure 7.17 shows the zonal mean total RFari for AeroCom phase II models and the 1750–2010 RFari from all models are shown in Figure 7.19. Robust features are the maximum negative RF around 10°N–50°N, in the region with highest aerosol concentrations and a positive RF at high latitudes due to the higher surface albedo there.

Remote sensing data, observations of fine-mode aerosol properties and a better knowledge of bulk aerosol optical properties make the estimate of total RFari more robust than the RF for individual species (see Forster et al., 2007). The best estimate of total RFari is taken to be –0.4 W m^{-2}, based on combining the AeroCom median with the refined satellite-based estimates. The methodology of Loeb and Su (2010) is combined with an uncertainty analysis of aerosol optical properties to give an overall assessment for the RFari of –0.4 W m^{-2}, with a 5-95% range of –0.7 to –0.1 W m^{-2}. This is also consistent with the uncertainty analysis of Bellouin et al. (2012) and Ma et al. (2012b). Uncertainties in the radiative transfer also contribute to the overall uncertainty (Randles et al., 2012; Stier et al., 2012), while uncertainties in the vertical distribution are important for absorbing aerosols (Samset et al., 2012; Section 7.3.3).

The assessed RFari of –0.4 ± 0.3 W m^{-2} has a smaller magnitude and smaller range than in AR4. There is also increased confidence in this assessment due to more robust satellite-based estimates and their better agreement with models.

[INSERT FIGURE 7.17 HERE]

Figure 7.17: Annual zonal mean RFari (in W m^{-2}) due to all anthropogenic aerosols from the different AeroCom II models. No adjustment for missing species in certain models has been applied. The multi-model mean is shown with a black solid line. Adapted from Myhre et al. (2012).

AFari adds the radiative effects from rapid adjustments onto RFari. Studies have evaluated the rapid adjustments separately as a semi-direct effect (see Section 7.3.5) and/or the AFari has been directly evaluated. Rapid adjustments are principally caused by cloud changes. There is high confidence that the local heating caused by absorbing aerosols can cause cloudiness to increase or decrease depending on their conditions. However, there is low confidence in determining the sign and magnitude of the rapid adjustments at the global scale as current models differ in their responses and are known to inadequately represent some of the important relevant cloud processes (see Section 7.3.5). Existing estimates of AFari nevertheless rely on such global models. Five GCMs were analysed for RFari and AFari in Lohmann et al. (2010). Their rapid adjustments ranged from –0.3 to +0.1 W m^{-2}. In a further study, Takemura and Uchida (2011) found a rapid adjustment of +0.06 W m^{-2}. The sensitivity analysis of Ghan et al. (2012) found a –0.1 W m^{-2} to +0.1 W m^{-2} range over model variants, where an improved aging of the mixing state led to small negative rapid adjustment of around –0.1 W m^{-2}. Bond et al. (2012) assessed scaled RF and efficacy estimates from seven earlier studies focusing on BC and found a range of rapid adjustments between –0.2 W m^{-2} and –0.01 W m^{-2}. There is a potential additional rapid adjustment term from the effect of cloud drop inclusions (see Section 7.3.4.2). Based on the Ghan et al. (2011) and Jacobson (2012), Bond et al. (2012) estimate an additional AFari of +0.2 W m^{-2}, with an uncertainty range of –0.1 to +0.7 W m^{-2}, however there is low evidence for this effect and we do not include it in our assessment. Overall a best estimate for the rapid adjustment is taken to be –0.1 W m^{-2}, with a 5% to 95% uncertainty range of –0.3 to +0.1 W m^{-2}. The uncertainties are added in quadrature to the estimate of RFari to give an assessment for AFari of –0.5 ± 0.4 W m^{-2}.

7.5.1.2 Radiative Forcing by Species

AeroComII studies have calculated aerosol distributions using 1850 and 2000 simulations with the same meteorology to isolate RFari for individual aerosol types (SO_4, BC fossil-fuel, OC fossil-fuel, biomass burning or BB, SOA, NO_3). Unless otherwise noted in the text below the best estimate and 5–95% ranges for individual types quoted in Figure 7.18 are solely based on the AeroComII range (Myhre et al., 2012) and the estimates have been scaled by emissions to derive 1750–2010 RFari values. Note that although global

numbers are presented here these RF estimates all exhibit large regional variations and individual aerosol species can contribute significantly to regional climate change despite rather small RF estimates (e.g., Wang et al., 2010b).

For sulphate AeroComII models give a RF median and 5–95% uncertainty range of –0.35 ± 0.2 W m^{-2}, for the 1850–2000 period and –0.37± 0.2 W m^{-2} for the 1750–2010 period. This estimate and uncertainty range are consistent with the AR4 estimate of –0.4 ± 0.2 W m^{-2}, which is retained as the best estimate for AR5.

RF from BC is evaluated in different ways in the literature. The BC RF in this report is from fossil fuel and biofuel sources, while open burning sources are attached to the BB aerosol, which also includes other organic species (see Section 7.3.2). The radiative effect from all anthropogenic plus natural sources of BC derived using an analysis of AERONET level 2.0 (e.g., Ramanathan and Carmichael, 2008) is likely biased high due to the inability of AERONET to measure small optical depths (Section 7.3.4, Bond et al., 2012). Bond et al. (2012) analysed BC forcing across 18 model variants, including 8 AeroComII models, using and improved AERONET scaling and accounting for model bias in the BC vertical profile. Scaling for absorption AOD in the models to account for a low bias in emissions (see Section 7.3.2) typically led to 50% or larger underestimates in RF, whilst BC at too high altitudes in models led to a RF overestimate of around 15% (Zarzycki and Bond, 2010; Section 7.3.3). Bond et al. (2012) also performed an uncertainty analysis, principally of the scaling approach and forcing efficiency with each contributing roughly a ±40% (2 standard deviation) uncertainty. RFs from Bond et al. (2012) were assessed to be +0.17, +0.12 and +0.15 W m^{-2} from fossil fuel, biofuel and open burning sources, respectively. AeroComII models give a BC RFari from fossil fuel and biofuel of +0.19 ± 0.013 W m^{-2} for the 1850–2000 period and +0.24 ± 0.19 W m^{-2} for the 1750–2010 period (Myhre et al., 2012). The Bond et al. (2012) scaling is used to derive the best estimate of BC RFari of +0.3 W m^{-2} and a ±0.2 W m^{-2} uncertainty range is adopted, based on both the AeroComII range and the Bond et al. (2012) bottom-up uncertainty analysis.

Biomass burning aerosol RFari, which includes both BC and OA species, is estimated from AeroComII models as –0.01 ± 0.08 W m^{-2}, and an estimate of +0.0 (–0.1 to +0.1) W m^{-2} is adopted. Note here that the BB RFari is close to zero, but consists of rather strong RFari from BC and OA as shown in Figure 7.18. The SOA RFari estimate is –0.08 ± 0.2 W m^{-2} and the POM from fossil fuel estimate is –0.05 ± 0.04 W m^{-2}. For OA from natural burning and for SOA the natural radiative effects can be an order of magnitude larger than the RF (see Sections 7.3.2, Section 7.3.3, and O'Donnell et al., 2011) and they could thus contribute to climate feedback (see Section 7.3.6).

The AeroComII RF estimate is used for nitrate aerosol, giving an RFari of –0.13 ± 0.1 W m^{-2}, but comprises a relatively large 1850 to 1750 correction term. This is in good agreement with earlier estimates (e.g., Adams et al., 2001; Bauer et al., 2007; Myhre et al., 2009). In the AeroComII models ammonium aerosol is included within the sulphate and nitrate estimates.

Anthropogenic sources of mineral aerosols can result from changes in land use and water use or climate change. Estimates of the RF from anthropogenic mineral aerosols are highly uncertain, because natural and anthropogenic sources of mineral aerosols are often located close to each other (Ginoux et al., 2012a; Mahowald et al., 2009). Using a compilation of observations of dust records over the 20th century with model simulations, Mahowald et al. (2010) deduced a 1750–2000 change in mineral aerosol RFari including both natural and anthropogenic changes of –0.14 ± 0.11 W m^{-2}. This is consistent within the AR4 estimate of –0.1 ± 0.2 W m^{-2} (Forster et al., 2007) which is retained here. Note that some of this forcing could be due to feedback processes (see Section 7.3.6).

[INSERT FIGURE 7.18 HERE]

Figure 7.18: Mean (solid line), median (dashed line), one standard deviation (box) and full (min-max) range (whiskers) for RFari (in W m^{-2}) from different aerosol types from AeroCom II models. The forcings are for the 1850 to 2000 period. Adapted from Myhre et al. (2012).

7.5.1.3 Absorbing Aerosol on Snow and Sea-Ice

Forster et al. (2007) estimated the RF for surface albedo changes from BC deposited on snow to be +0.10 ± 0.10 W m^{-2}, with a low level of understanding, based largely on studies from Hansen and Nazarenko (2004)

and Jacobson (2004). Since AR4, observations of BC in snow have been conducted using several different measurement techniques (e.g., Doherty et al., 2010; Forsström et al., 2009; Huang et al., 2011; Kaspari et al., 2011; McConnell et al., 2007; Ming et al., 2009; Xu et al., 2009), providing data with which to constrain models. Laboratory measurements have confirmed the albedo reduction due to BC in snow (Hadley and Kirchstetter, 2012). The albedo effects of non-BC constituents have also been investigated but not rigorously quantified. Global modelling studies since AR4 have quantified present-day radiative effects from BC on snow of +0.02 to +0.08 W m^{-2} (Flanner et al., 2009; Flanner et al., 2007; Hansen et al., 2007; Koch et al., 2009a; Rypdal et al., 2009; Skeie et al., 2011; Wang et al., 2011c). These studies apply different BC emission inventories and atmospheric aerosol representations, include forcing from different combinations of terrestrial snow, sea-ice, and snow on sea-ice, and include different indirect effects such as snow grain size evolution and melt-induced accumulation of impurities at the snow surface, observed on Tibetan glaciers (Xu et al., 2012). The forcing operates mostly on terrestrial snow and is largest during March–May, when boreal snow and ice are exposed to strong insolation (Flanner et al., 2007). All climate change studies exploring this forcing find that it warms the Arctic. Estimates of the change in global mean surface temperature per unit forcing are 1.7–4.5 times greater for snow and sea-ice forcing than for CO_2 forcing (Bellouin and Boucher, 2010; Flanner et al., 2009; Flanner et al., 2007; Hansen and Nazarenko, 2004; Hansen et al., 2005). The Koch et al. (2009a) estimate is not included in this range due to the low signal to noise ratio in their study. The greater response of global-mean temperature occurs primarily because all of the forcing energy is deposited directly into the cryosphere, whose evolution drives a positive albedo feedback on climate. Key sources of forcing uncertainty include BC concentrations in snow and ice, BC mixing state and optical properties, snow and ice coverage and patchiness, co-presence of other light-absorbing particles in the snow pack, snow effective grain size and its influence on albedo perturbation, the masking of snow surfaces by clouds and vegetation, and the accumulation of BC at the top of snowpack caused by melting and sublimation. Bond et al. (2012) derive a 1750–2010 snow and sea-ice RF estimate of +0.046 (+0.015 to +0.094) W m^{-2} for BC by 1) considering forcing ranges from all relevant global studies, 2) accounting for biases caused by a) modelled Arctic BC-in-snow concentrations using measurements from Doherty et al. (2010), and b) exclusion of soil dust, which reduces BC forcing by approximately 20%, 3) combining in quadrature individual uncertainty terms from Flanner et al. (2007) plus that originating from the co-presence of dust, and 4) scaling the present-day radiative contributions from BB, biofuel, and fossil fuel BC emissions according to their 1750–2010 changes. Here, we adopt an estimate of +0.04 (+0.02 to +0.09) W m^{-2} and note that the surface temperature change is roughly three (two to four) times more responsive to this RF relative to CO_2.

7.5.2 Estimates of RF and AF from Aerosol-Cloud Interactions (RFaci and AFaci)

RFaci and AFaci can be estimated in different ways. Both refer to changes in TOA radiation since pre-industrial times but whether it is estimated from changes in SW radiation, net radiation or cloud radiative forcing varies among publications. In this section and in Figure 7.19 we refer to estimates of the change in net TOA radiation whenever possible. If that estimate is not available we use, in order of preference, the change in net SW radiation, the change in net cloud forcing and last, the change in SW cloud forcing. Given that the LW RFaci is negligible and that RFaci is limited to cloudy skies, the different ways to estimate RFaci are comparable. However, AFaci has contributions from clear-sky conditions and LW radiation, especially if aerosol effects on mixed-phase and ice clouds are considered or if the atmospheric circulation responds to changes in the SW forcing.

Despite the consolidation in our understanding of the physical basis of the indirect forcing there still remain large uncertainties in quantification, because of the difficulties in representing relevant aerosol properties, clouds, and aerosol-cloud interactions in climate models as discussed in Section 7.4. Ensemble-mean globally-averaged model estimates of RFaci have thus remained rather constant over time (Figure 7.19) and amount to roughly –1 W m^{-2}. This estimate is obtained from the average over all published estimates, treating each of them as equal (taking one value for the best estimate per model and paper). The –1 W m^{-2} estimate is slightly more negative than the estimate of RFaci in AR4 where the reported value of –0.7 W m^{-2} was obtained from putting more emphasis of the newest results at that time (Forster et al., 2007). Whereas early models used offline three-dimensional sulphate fields, state-of-the art GCMs have their own aerosol schemes and consider sea salt, mineral dust and carbonaceous aerosols in addition to sulphate. There does not seem to be a systematic tendency for models that use a parameterization based on cloud parcel models instead of empirical relationships between the aerosol mass/number concentration and the cloud droplet

number concentration to simulate a larger or smaller RFaci. Sensitivity studies show that RFaci is larger if the background aerosol concentration is low (Chen and Penner, 2005) as this increases the cloud susceptibility. As shown by Storelvmo et al. (2009) different empirical relationships that are used to bypass cloud activation can cause a difference of 1.3 W m^{-2} in RFaci. RFaci depends strongly on the assumed minimum droplet concentration because that determines the susceptibility of the cloud (Hoose et al., 2009). Models that use autoconversion rates of cloud droplets to form rain drops which depend inversely on the droplet concentration automatically simulate an increase in cloud lifetime and cloud liquid water. In small-scale studies no increase in cloud lifetime is found because smaller droplets also evaporate more readily (Jiang et al., 2006), a process that is not yet considered in GCMs. AFaci tends to be less negative if changes to the cloud droplet size distribution (dispersion) are considered (e.g., Rotstayn and Liu, 2005) or if a prognostic equation for precipitation is introduced (Posselt and Lohmann, 2009) because that shifts the emphasis from autoconversion to accretion between cloud droplet and rain drops in better agreement with what can be inferred from observations and large-eddy simulations (Wood, 2005).

Recent estimates of RFaci using satellite-based observations are systematically weaker (–0.4 W m^{-2} in Figure 7.19) than the estimates, which were derived from GCM calculations based on parameterization of physical processes or in-situ observations (Lohmann and Lesins, 2002; Quaas et al., 2008; Quaas et al., 2009). The satellite-based data show lower susceptibility of cloud effective radius or droplet number concentration to aerosol optical depth or number concentration than do in-situ observations or detailed cloud parcel model calculations (McComiskey and Feingold, 2008), leading to the differences in the estimate of RFaci. This result is at least partly due to scale-related averaging biases in satellite retrievals (McComiskey and Feingold, 2012). It is also generally difficult to separate the RFaci from the rapid cloud response and meteorological effects in both observations and fully coupled numerical model calculations (e.g., George and Wood, 2010; Lohmann et al., 2010; Mauger and Norris, 2010; Painemal and Zuidema, 2010). Penner et al. (2011) have recently questioned the applicability of present day (satellite-based) observations of cloud-aerosol susceptibility to present-day minus preindustrial calculations in climate models. Their work suggests that RFaci may be significantly higher than suggested by Quaas et al. (2008).

There is conflicting evidence for the importance of AFaci associated with cirrus, ranging from a statistically significant impact on cirrus coverage (Hendricks et al., 2005) to a very small effect (Liu et al., 2009). Penner et al. (2009) obtained a rather large (unadjusted) forcing of anthropogenic ice-forming aerosol on upper tropospheric clouds; however, they ignored potential compensating effects on lower lying clouds. The climate impact of anthropogenic lead-containing mineral dust particles, among the most efficient ice-forming substances, has been investigated. In the extreme scenario in which 100% of ice-forming mineral dust particles in cirrus clouds contained lead, up to +0.8 W m^{-2} more longwave radiation was emitted to space as compared to pure mineral dust particles (Cziczo et al., 2009b). A new study based on two GCMs and different ways to deduce AFaci on cirrus clouds estimates that effect to be +0.27 ± 0.1 W m^{-2} (Gettelman et al., 2012b), which partially offsets the total AFaci.

A complementary approach to GCM-based estimates of AF/RF is to infer AF/RF as a residual using the observed temperature record over land, and estimates of the ocean heat uptake and the evolution of greenhouse gas and solar RF (Anderson et al., 2003; Hegerl et al., 2007). These approaches, called inverse estimates, normally involve models of intermediate complexity. The only inverse study that obtained RFaci bracketed it to be between 0 and –1.2 W m^{-2} (Knutti et al., 2002). Both RFaci estimates constrained by satellite observations and the ensemble-mean model estimate of –1 W m^{-2} fit into this range.

In conclusion, there are different rapid adjustments that contribute to the AF through changes in cloud condensate, cloud cover, cloud phase or precipitation efficiency (Section 7.4). These adjustments can either increase or decrease RFaci. While adjustments in both directions occur in CRMs (Section 7.4), climate models do not always include the processes leading to compensation effects and positive adjustments. For this reason we defer our assessment of RFaci and AFaci to Section 7.5.3.

7.5.3 Estimates of AF from Combined Aerosol-Radiation and Aerosol-Cloud Interactions (AFari+aci)

The first GCM estimates of AFari+aci only included aci in liquid stratiform clouds. Its mean value of –1.5 W m^{-2} is only slightly less negative than the mean AFaci suggesting that ari play a secondary role once aci are considered. AFari+aci is much more variable if secondary processes (+SEC) such as aci on mixed-phase or

convective clouds are additionally included in GCMs (Figure 7.19). The model average to –1.4 W m^{-2} is dominated by a few large negative estimates. Thus, the median value of –1.1 W m^{-2} may be more meaningful. The spread between the GCMs studies that also include aci in mixed-phase clouds (+MPC) can be explained by differences in the frequency of glaciation of supercooled clouds. If more IN are available in present-day conditions, supercooled clouds glaciate more readily and precipitate (see Section 7.4.4.1). In these cases an additional cooling stems from more LW radiation being emitted to space. If on the contrary more IN become coated with soluble material and become less efficient, supercooled clouds remain longer in the atmosphere, which enhances AFaci of liquid clouds but leads to a small positive LW effect that slightly compensates for the SW cooling.

Regional and global models systematically misrepresent the distribution of clouds, and cloud processes, especially those for shallow maritime clouds. One persistent shortcoming of global models is the tendency to only treat aerosol-cloud interactions in terms of stratiform but not convective clouds. In fact most GCMs neglect the radiative effect of convective clouds entirely. Recent efforts to consistently address both types of cloud representations represent a significant advance in large scale-modelling (Jacobson, 2003; Lohmann, 2008; Suzuki et al., 2008). Nonetheless our understanding of aerosol-cloud interactions is incomplete, and what is well-understood, is incompletely represented in large-scale models. For these reasons, and because lifetime effects depend critically on the interplay of uncertainly parameterized physical processes, global model-based estimates of lifetime effects remain uncertain. This is reflected in the large spread of climate model estimates of AFari+aci that also consider aci in convective clouds (+CNV). One of the most reliable estimate in the +CNV category may be the estimate of –1.1 W m^{-2} to the farthest right because it is obtained from a multi-scale modelling framework approach (Wang et al., 2011b), which resolves convection. Using satellite retrievals to estimate AFari+aci leads to the least negative average AFari+aci of –0.7 W m^{-2} (Figure 7.19).

An inverse estimate that is obtained purely from energy balance arguments bounds AFari+aci (including unknown residuals that are assumed to be small) since 1950 to be between –0.7 to –1.5 W m^{-2} (Murphy et al., 2009), which is the same range as obtained from all inverse estimates of AFari+aci (Figure 7.19).

We produce a best estimate and 5–95% uncertainty range for AFari+aci in the following way. The global CMIP5 models and inverse estimates are grouped together and a bootstrapping method is used to estimate a mean and standard deviation of –0.98 and 0.32 W m^{-2}. Processing the satellite-based estimates in the same way leads to a mean and standard deviation of–0.73 and 0.30 W m^{-2}, respectively, with the caveat that the method applied to a small sample may underestimate the variance. We combine these two estimates into a best estimate and a 5 to 95% range for RFari+aci of –0.9 (–1.5 to –0.3) W m^{-2}, accounting for a small 1850 to 1750 correction term. This estimate is significantly lower than the AR4 estimate but is consistent with several new lines of evidence. Firstly the best estimate is close to the estimate of –1.1 W m^{-2} from the multi-scale modelling framework approach (Wang et al., 2011b). Secondly climate model studies that include missing processes such as aci on mixed-phase clouds or by putting more emphasis on accretion instead of autoconversion by treating rain as a prognostic variable arrive at smaller AFari+aci estimates than those which ignore them. Thirdly those AFari+aci studies taking satellite data into account, and therefore are observationally based, yield the least negative forcing. Fourthly the average AFari+aci from the CMIP5/ACCMIP models also amounts to about –1 W m^{-2} (see Table 7.5).

The AFaci is estimated as the residual between AFari+aci and AFari. We further assume that AFari and AFaci are additive and uncertainties are independent, which yields to our assessment of AFaci of –0.4 (–0.9 to 0) W m^{-2}. Models indicate that RFaci is less than AFaci, which implies an estimate of –0.3 (–0.7 to 0) W m^{-2}, again less negative than the AR4 estimate for the same reasons as given above.

[INSERT FIGURE 7.19 HERE]

Figure 7.19: Upper panel: GCM, satellite and inverse estimates of RFari, RFaci, AFaci and AFari+aci. Each symbol represents the best estimate per model and paper as detailed in Table 7.4. The RFaci studies are divided into those from GCMs published prior to TAR, AR4 and AR5, those including satellite data (SAT) and the inverse estimate (INV). AFaci and AFari+aci studies from GCMs on liquid stratiform clouds are also divided into those published prior to AR4 and AR5 and from the CMIP5/ACCMIP models. GCM estimates that include adjustments beyond aci in liquid stratifrom clouds are marked +MPC when including aci in mixed-phase clouds and are marked +CNV when including aci in convective clouds. For RFaci from inverse estimates the range instead of the best estimate is given because it is only one study.

Lower panel: Box whisker plots of GCM, satellite and inverse estimates of RFari, RFaci, AFaci and AFari+aci. They are grouped into RFari from CMIP5/ACCMIP GCMs, RFaci from GCMs (TAR, AR4, AR5) and satellites (SAT), AFaci from GCMs, AFari+aci from GCMs taking aci only on liquid stratiform clouds (AR4+AR5) and including secondary processes (aci on mixed-phase or convective clouds) into account (+SEC), AFari+aci studies from the CMIP5 models, satellites (SAT) and inverse estimates of AFari+aci. Displayed are the averages (cross sign), median values (middle line), 33% and 67% percentiles (box boundaries) and 5% and 95% percentiles (ends of vertical lines) except for the inverse estimates, which is an expert assessment of the combined estimate of multiple inverse estimates. References for the individual estimates are provided in Table 7.4.

[INSERT TABLE 7.4 HERE]
Table 7.4: List of references for each category of estimates displayed in Figure 7.19.

[INSERT TABLE 7.5 HERE]
Table 7.5: Estimates of aerosol AF (in W m^{-2}) in some of the CMIP5 models. The AF are estimated from fixed-SST experiments using atmosphere-only version of the models listed. Different models include different aerosol effects.

7.6 Links to Precipitation

7.6.1 Introduction

Precipitation is limited by the availability of moisture and energy. Energy, which is required to evaporate water from the surface, is provided by the differential heating, through radiative processes, of the surface relative to the atmosphere. Evaporation cools the surface and, by making water available for condensation (which returns to the surface as precipitation), warms the atmosphere by an equal amount (Figure 7.20; Trenberth et al., 2009). The oceans provide a huge reservoir of moisture, but without the energetic imbalances set by radiative processes, there would be no driving force for the hydrological cycle. These basic constraints are most powerful when applied globally, but also help define how the structure of atmospheric circulations moderates their influence on regional scales (Neelin and Held, 1987; Raymond et al., 2009).

[INSERT FIGURE 7.20 HERE]
Figure 7.20: Illustration of major drivers affecting precipitation. Radiative drivers cool the atmosphere, warm the surface, and thereby provide the energy for evaporation and condensation/precipitation. Circulations organize and distribute precipitation. The ability of changes in the position or strength of circulation features to change the distribution of precipitation is referred to as a dynamic effect, the ability of warmer circulations to transport more water vapour and thereby change the amount of precipitation is referred to as a thermodynamic effect. The immediate effect of warming, greenhouse gases, clouds and aerosols on precipitation is indicated by blue or red if their change over the 20th century is thought to have changed a precipitation driver in a way that will increase, respectively decrease, precipitation. Grey indicates that changes are unknown or have multiple effects of different sign.

Precipitation fields simulated by the current generation of climate models still exhibit substantial biases (Liepert and Previdi, 2012; Stephens et al., 2010; Chapter 9). Nonetheless, it is possible to identify robust features in simulated response of precipitation to changes in precipitation drivers. In almost every case the Clausius-Clapeyron relation, which governs water phase changes, underlies these robust features.

7.6.2 The Effects of Global Warming on Large Scale Precipitation Trends

Atmospheric specific humidity is strongly expected to increase by about 7.5% K^{-1} in the column average (see Section 7.2.4.1). Precipitation however increases much less rapidly with temperature because the net evaporation is energetically limited. This limitation arises because the spectroscopic properties of water vapour demand that the fractional increase in its ability to absorb (and emit) infrared radiation must increase less rapidly than the fractional increase in concentration (Stephens and Hu, 2010).

Globally-averaged precipitation increases with global mean surface temperature at about 2% K^{-1} (Held and Soden (2006) and Richter and Xie (2008); for the CMIP3 models analysed by Andrews et al. (2009) the response is 1.4–3.4% K^{-1}), but not uniformly, as atmospheric circulations tend to increase the precipitation in the wettest latitudes, and dry latitudes may even see a precipitation decrease (Allen and Ingram, 2002; Held and Soden, 2006). This tendency of wet regions to get wetter and dry regions to get drier is moderated by a

weakening in the tropical overturning circulation (Figure 7.20). On smaller scales the signal is less clear due to model-specific regional circulation shifts (Neelin et al., 2006), but there is some evidence that the sub-tropical dry zones are expanding, both as a result of the tropical convergence zones narrowing (Chou et al., 2009; Neelin et al., 2006), and the storm tracks moving poleward (Allen et al., 2012) and strengthening (O'Gorman and Schneider, 2008).

The "wet-get-wetter" and "dry-get-drier" response that is evident at large scales over oceans, can be understood as a simple consequence of the sharp increase in atmospheric water vapour combined with the result that changes in atmospheric circulations are significantly smaller in a relative sense (Held and Soden, 2006). Wet regions are wet because they import moisture from dry regions, increasingly so with warmer temperatures. This thermodynamic effect is evident in trends in of 20th century precipitation (Allan and Soden, 2007; Zhang et al., 2007b; see Section 2.3.1), and has withstood additional analysis and scrutiny since AR4 (Chou et al., 2009; Muller and O'Gorman, 2011; Seager et al., 2010), increasing our confidence in the effect.

The wet-get-wetter response is mitigated by the anticipated reduction in the overturning rate of the atmosphere (which can be understood partly as a consequence of the change in the dry static stability of the atmosphere with warming, Figure 7.20, see also Section 7.2). This argument is less robust in dry regions because of the opposing effects of increased horizontal vapour divergence by the circulation and gains from local surface evaporation, primarily over the ocean (Bony et al., 2012; Chou et al., 2009), but can still be used to understand the GCM land responses to some extent (Muller and O'Gorman, 2011). The non-uniform nature of surface warming (e.g., land areas warm more and differently than neighbouring oceans, Joshi et al., 2008) induces regional circulation shifts that affect precipitation trends. Low understanding of soil-moisture-precipitation feedbacks, whose sign remains uncertain, also complicates local responses to warming (Hohenegger et al., 2009). In summary, the effect of warming on precipitation on the scale of individual catchments remains highly uncertain, even though some broad-scale responses are robust and relatively well understood.

7.6.3 Radiative Forcing of the Hydrological Cycle

As much as half of the total change in precipitation can be related directly to the radiative effects of the CO_2, irrespective of whether it causes any surface warming (Andrews et al., 2009; Bony et al., 2012). These hydrological adjustments to radiative forcing are rapid, and can be linked to rapid adjustments of clouds (Wyant et al., 2012; also Section 7.2).

[INSERT FIGURE 7.21 HERE]

Figure 7.21: Illustration of the response of the large-scale overturning to increasing CO_2 concentrations (adapted from Bony et al., 2012). Approximately half of the response is evident before any warming is felt, but additional warming continues to slow down the circulation and adds linearly to the rapid adjustment. The rapid adjustment is different over land and ocean, with the increase in CO_2 initially causing an intensification of the circulation over land. The robustness of the result is illustrated by the common behaviour of 15 CMIP5 models, irrespective of the details of their configuration.

In the absence of a compensating temperature change, an increase in any well-mixed greenhouse gas reduces the net radiative cooling rate of the atmosphere. This reduces the rainfall rate and the strength of the overturning circulation. The dynamic effects are similar to those that result from the effect of atmospheric warming on the lapse rate, which also reduces the strength of the overturning circulation (e.g., Section 7.6.2) and are robustly evident over a wide range of models and model configurations (Bony et al., 2012; see also Figure 7.21). These circulation changes are more pronounced over the ocean, because asymmetries in the land-sea response to changing concentrations of greenhouse gases (Joshi et al., 2008) amplify the maritime and dampen or even reverse the terrestrial signal (Bony et al., 2012; Wyant et al., 2012).

The response of the hydrological cycle to the partitioning of radiation between the surface and atmosphere partly explains why forcings having the same AF do not produce the same precipitation responses. Increased solar forcing does not strongly affect the net atmospheric cooling, and thus the hydrological cycle feels only the associated warming with little rapid adjustment (Andrews et al., 2009), despite a small atmospheric absorption of additional solar radiation (Takahashi, 2009). As a result, solar radiation management schemes

that maintain a constant surface temperature will lead to a reduction in globally averaged precipitation and potentially substantially different regional distributions (Schmidt et al., 2012b; Section 7.7).

Changes in cloud radiative effects, and the radiative forcing from aerosol particles are also effective in changing the profile of radiative heating, and thus influence the hydrological cycle. Cloud effects can be large, but have been less studied than those of aerosols. To the extent that aerosol particles only scatter radiation, their global effect is expected to be analogous to that associated with changes in the solar irradiance. Absorbing aerosols act more like CO_2 however, as they heat and stabilize the troposphere thereby reducing precipitation in a way that partially offsets their overall warming effect (Andrews et al., 2009). The impact of non-well-mixed precipitation drivers such as clouds, aerosols and tropospheric ozone can depend sensitively on their height and geographic distribution (Allen et al., 2012; Ming et al., 2010; Shindell et al., 2012b), because of the impact of spatially non-uniform heating on atmospheric circulations of all scales, and associated adjustments of cloud cover which can further alter the circulations (Section 7.2).

7.6.4 Aerosol-Cloud Interactions

In contrast to aerosol-radiation interactions, aerosol-cloud interactions do not directly influence the radiant streams of energy that drive the climate system, and thus are not expected to have any influence on the global mean precipitation rate. But because such interactions affect the microphysical structure of clouds they may influence how precipitation is distributed.

There is a growing body of literature suggesting that aerosol-cloud interactions affect the dynamics of individual convective clouds and storms, but in a variety of different ways that may be situation dependent, and remain poorly understood. An increase in cloud condensation nuclei may affect the cloud microphysical development thereby changing where and how much ice forms in convective clouds (Khain et al., 2005; Rosenfeld and Woodley, 2001), or how much cloud water is available for detrainment and evaporation after shallow convection (Stevens and Seifert, 2008). These changes tend to affect the vertical distribution of latent heating in ways that would support the invigoration of convection (Tao et al., 2012). Some support for these ideas is provided by observations (Devasthale et al., 2005; Koren et al., 2010; Koren et al., 2008), but the interpretation of the observational evidence is difficult for reasons discussed extensively in Section 7.4.1.2. Modelling studies suggest that aerosol-cloud interactions accompanying increased aerosol loading may either invigorate or suppress storms, depending on environmental factors such as vertical wind shear (Fan et al., 2009). For the more studied cases in which invigoration is present, the degree of invigoration depends sensitively on a number of factors, including the representation of cloud and aerosol microphysics (Ekman et al., 2011), as well as the types of clouds and storms being simulated (Khain, 2009; Seifert and Beheng, 2006). Studies that have looked at the effect of aerosol-cloud interactions in more of a climate context, wherein convection is allowed to equilibrate with its forcing, find that invigoration effects are minor (van den Heever et al., 2011) or negligible (Morrison and Grabowski, 2011), suggesting that convective intensity is also limited by energetic constraints (e.g., Chou et al., 2009; Raymond et al., 2009).

Because precipitation development in clouds is a time dependent process, which proceeds at rates that are partly determined by the cloud microphysical structure (Seifert and Zängl, 2010), aerosol-cloud interactions may lead to shifts in topographic precipitation to the leeward side of mountains when precipitation is suppressed, or to the windward side in cases when it is more readily initiated. Orographic clouds show a reduction in the annual precipitation over topographical barriers downwind of major urban areas in some studies (Givati and Rosenfeld, 2004; Jirak and Cotton, 2006) but not in others (Halfon et al., 2009). Even in cases where effects are reported, the interpretation of the data remains controversial (Alpert et al., 2008; Levin and Cotton, 2009).

The idea that precipitation can respond in a variety of different, often compensating, ways to a microphysical perturbation from the ambient aerosol (as also discussed in Section 7.4) receives support from studies using high-resolution numerical weather prediction methods. Although large aerosol perturbations may affect the day-to-day predictions of summer season rainfall over Germany, no systematic effect of aerosol-cloud interactions on precipitation is evident (Seifert et al., 2012). Likewise, although weekly cycles in aerosol properties are readily apparent, a robust effect on precipitation or storm intensity has proven difficult to detect (Barmet et al., 2009; Bäumer et al., 2008; Stjern, 2011; Tuttle and Carbone, 2011; Yuter et al., 2012).

7.6.5 The Physical Basis for Changes in Precipitation Extremes

The physical basis for an effect of aerosol-cloud interactions on precipitation extremes was discussed in the previous section. Here we briefly discuss process understanding of the effect of warming on precipitation extremes; observed trends supporting these conclusions are presented in Section 2.7.

Precipitation within individual storms is expected to increase with the available moisture content in the atmosphere rather than with the global precipitation (Allen and Ingram, 2002; Held and Soden, 2006). Global models provide robust support for these ideas, particularly in the extra-tropics (O'Gorman and Schneider, 2009), although the increase in the surface humidity, where the air is warmer, proves to be a better indicator of changes in extremes than changes in column humidity. When these effects are combined with a weakening of the overturning mass circulation, individual storms are expected to become more intense. On this issue global model results are less robust (Kharin et al., 2007; O'Gorman and Schneider, 2009). However, experiments designed to mimic the conditions of the tropical atmosphere under climate change using large-eddy simulation (Romps, 2011) and cloud-resolving models (Muller et al., 2011) provide support for the thermodynamic scaling based on surface saturation humidity, for which precipitation extremes increase by 7–8% K^{-1}.

Inferences from observed variations in particular regions suggest a dependence on temperature that might be twice as large as the thermodynamic arguments predict (Lenderink et al., 2011; Lenderink and Van Meijgaard, 2008) and may be different at short time scales (e.g., an hour or less) than at daily or storm-duration time scales (Haerter et al., 2010; Hardwick Jones et al., 2010). It is possible that in a warmer climate individual storms are deeper and drive more convergence (Chou et al., 2009; Romps, 2011; Sugiyama et al., 2010); however, a problem with regional observational approaches to this question is that the atmosphere is typically more convectively unstable during regionally hotter weather, exaggerating the effect (e.g., Haerter and Berg, 2009) relative to that in a globally warmer climate where convective instability should not differ much from today (Section 7.2.4.2). From this combination of evidence we conclude that while it is very likely that precipitation extremes will increase with warming, by how much remains uncertain and may vary with time scale.

Following the AR4 studies have continued to show that extremes in precipitation are associated with the coincidence of particular weather patterns (e.g., Lavers et al., 2011). We currently lack an adequate basic understanding of what controls the return time and persistence of such rare events.

7.7 Solar Radiation Management and Related Techniques

7.7.1 Introduction

Geoengineering is the deliberate large-scale intervention in the Earth system to counter undesirable impacts of climate change on the planet (e.g., Keith, 2000; Royal Society, 2009). One class of proposed geoengineering methods is Solar Radiation Management (SRM), which aims to counter the warming associated with increasing greenhouse gas concentrations by reducing the amount of solar energy absorbed by the climate system. A related technique seeks to deliberately decrease the greenhouse effect in the climate system by altering high-level cloudiness. Another class of geoengineering methods, known as Carbon Dioxide Reduction (CDR), is discussed in Chapter 6. The potential impacts of SRM are discussed in Section 19.5.4 of the WGII AR5. Some of the issues relating to cost, implementation, governance, ethics, economics, laws, and politics are assessed in Chapter 6 of the WGIII contribution to AR5. Here we assess proposed geoengineering methods that have the potential to influence components of the energy budget by at least a few tenths of a W m^{-2} in the global mean without presuming their technological feasibility. It should be noted that no technology for SRM has been fully developed and can be considered ready for large-scale deployment. The physical underpinnings of specific methods are discussed in Section 7.7.2 followed by an assessment of their impact on climate in Section 7.7.3.

7.7.2 Assessment of Proposed SRM Methods

7.7.2.1 Stratospheric Aerosols

Observations of the aftermaths of major volcanic eruptions such as Pinatubo (June, 1991) demonstrate that an increase in the amount of stratospheric aerosols cools the planet. Some proposed SRM techniques increase stratospheric aerosol in a similar way to explosive volcanic eruptions (Budyko, 1974; Crutzen, 2006). Most stratospheric aerosol SRM research to date has explored the possibility of forming sulphuric acid aerosols by injecting sulphur containing gases into the stratosphere, Other particles composed of black carbon (Crutzen, 2006; Keith, 2010; Kravitz et al., 2012b) or metal oxides (Keith, 2010) have been suggested with the potential for larger RFs, but they are not assessed further here because the literature on them is too limited.

The RF from stratospheric aerosols will depend on the injection strategy: chemical species (gaseous SO_2, H_2SO_4 or sprayed aerosols), location(s), rate, and frequency of injection. The injection strategy effects particle size - an important factor influencing the mass scattering efficiency, and sedimentation rate. These properties are important to SRM, changing the reflectivity of the aerosol and its loss rate. Particle size may also have other physiochemical effects (some mentioned below). The eventual aerosol size distribution is controlled by the balance between new particle formation, deposition of vapour on pre-existing particles, evaporation of particles, coagulation, and sedimentation that changes as particles grow larger. Models that include more comprehensive representations of aerosol microphysics (English et al., 2012; Heckendorn et al., 2009; Pierce et al., 2010) found smaller aerosol burdens, larger particles and weaker RF than the earlier studies that assumed a fixed particle size (e.g., Rasch et al., 2008a). This is because coagulation and condensation of sulphuric acid on pre-existing particles both contribute to increase particle size when the injection rate is increased. Pierce et al. (2010) suggested that the injection of H_2SO_4, a condensable vapour, from an aircraft could produce larger forcings with lower sulfur loadings than SO_2 injection. Recent modelling studies agree that emissions of sulfate aerosol precursors of 10 MtS yr^{-1} or greater would be needed to achieve forcing stronger than –4 W m^{-2} (estimated as the mean of experiments reported by Heckendorn et al. (2009), Niemeier et al. (2011) and Pierce et al. (2010)).

A variety of potential side effects have been identified. Tilmes et al. (2009; 2008) found that SRM by stratospheric aerosols would lead to an increase of chemical ozone loss for the Arctic, a delay of the recovery of the Antarctic ozone hole by 30–70 years, changes in ozone abundance (column ozone depletion of 3–10% in polar latitudes and increases of 3–5% in the tropics) and discernable shifts in tropopause altitude (lifting by 1 km) from radiative heating associated with the ozone changes. The change in ozone could increase UV radiation reaching the surface, although attenuation by the aerosols may partially compensate (Vogelmann et al., 1992). A decrease in direct radiation and increase in diffuse radiation reaching the Earth's surface could increase photosynthesis in terrestrial ecosystems (Mercado et al., 2009; see Chapter 6) and impact some solar energy technologies (see WGII AR5, Section 19.5.4). Kravitz et al. (2009) explored rain acidification from stratospheric geoengineering and concluded that acid deposition rates would be orders of magnitude lower than those that impact most ecosystems. These impacts remain poorly quantified and there may be additional ones, for instance on tropospheric photochemistry and cirrus cloud microphysics.

7.7.2.2 Cloud Brightening

Boundary layer clouds act to cool the planet, and relatively small changes in cloud albedo or extent can have profound effects on the Earth's radiation budget (e.g., Slingo, 1990). Examples of cloud brightening include shiptracks produced in marine stratocumulus clouds by emissions of particles from ships and changes in trade cumulus cloud properties produced by a relatively weak but continuous volcanic eruption of SO_2 (Yuan et al., 2011), as discussed in Section 7.4.3.2. Latham (1990) suggested that it might be possible to deliberately increase cloud albedo by introducing additional sea salt particles into the marine boundary layer, to act as cloud condensation nuclei and "brighten" clouds through the aerosol-cloud interaction first described by Twomey (1974) and discussed in Section 7.4.

Changes in cloud morphology (e.g., from open to closed cells) or switching from low to high liquid water content clouds have the potential to create large AF locally. Marine stratocumulus clouds (with relatively weak precipitation) are thought to be an optimal cloud type for brightening because of their relatively low values of droplet concentration and the longer lifetime of sea-salt particles in non-precipitating environments. However these clouds occupy a relatively small fraction of the planet and large local RF (30 to 100 W m^{-2}) would be required to produce a globally-averaged RF of the order of –1 to –5 W m^{-2}.

Latham et al. (2008), Jones et al. (2009) and Rasch et al. (2009) explored the impact of changing droplet concentration without an explicit examination of the complex interactions that govern the way aerosols affect clouds. Their studies show that about –1 W m^{-2} of AF could be produced by increasing droplet concentration over about 5% of the ocean surface area in marine stratocumulus regions. Forcing as strong as –4 W m^{-2} was produced by increasing droplet concentration over 75% of the ocean surface, although it is not clear whether such increases are achievable. There is less agreement among models when a more complete treatment of aerosol-cloud interactions is considered. Korhonen et al. (2010b) concluded that increases in droplet concentration would be much smaller than previous studies had assumed. In contrast, Partanen et al. (2012) used the same seeding mechanism in a different model to find much larger increases in droplet concentration, with an AF as strong as –5 W m^{-2}. Wang et al. (2011a) used very high resolution simulations to demonstrate that cloud brightening is sensitive to cloud-dynamical feedbacks that are missing in current global models. They also explored aerosol injection strategies and concluded that rates initially proposed for cloud seeding would be insufficient to produce droplet concentration values needed for large-scale cloud brightening. These studies highlight the limitations of our understanding of aerosol-cloud interactions, and the resulting uncertainty in estimates of the AF that can be produced with cloud brightening SRM.

Changes in clouds due to aerosols are often swamped by meteorological variability (Wood et al., 2011b) making detection of aerosol effects on clouds extremely difficult. Total AF from anthropogenic aerosols is assessed to be –0.9 (–1.5 to –0.3) W m^{-2} in Section 7.5, that is at least 5 times smaller than the AF that climate models assume is achievable with SRM.

While aerosol seeding over oceans was originally proposed to brighten clouds, Hill and Ming (2012) and Partanen et al. (2012) found that aerosol-radiation interactions (the aerosol direct effect) could also be important, adding 30 to 50% to the AF from aerosol-cloud interactions, sometimes dominating the forcing in certain regions.

7.7.2.3 Surface Albedo Changes

Planetary albedo might also be increased by engineering local changes to the albedo of urban areas, croplands, grasslands, deserts and the ocean surfaces.

Hamwey (2007) estimated the potential RF from whitening roofs and pavements at –0.17 W m^{-2} and calculations by Akbari et al. (2012) suggest a global-mean equilibrium cooling between 0.01 to 0.07°C. However, more detailed radiative transfer calculations (Lenton and Vaughan, 2009; Oleson et al., 2010), overestimation of the surface area of the built environment that would be available for whitening, and possible atmospheric feedbacks (Jacobson and Ten Hoeve, 2012) suggest that these are somewhat overestimated.

The surface albedo of the world's grassland and/or cropland could be modified by replacing native species with other natural or bioengineered species (Hamwey, 2007). A 25% increase in grassland albedo could give an RF of –0.5 W m^{-2} (Lenton and Vaughan, 2009), with the maximum effect in summer mid-latitudes. (Doughty et al., 2011; Ridgwell et al., 2009). Ridgwell et al. (2009) estimated a global-mean surface cooling of 0.11°C for a +0.04 increase in cropland albedo. Potential effects in low-latitude regions are a reduction in soil moisture, cloud cover and precipitation. The possibility for increasing crop and grassland albedo across a wide variety of species remains largely non-quantified. Irvine et al. (2011) tested the impact of increasing desert albedo up to 0.80 in a single model. This cooled surface temperature by –1.1°C (versus –0.22°C and −0.11°C for their largest crop and urban albedo change).

The low albedo and large extent of ocean surfaces mean that only a small increase in albedo could be sufficient to offset several W m^{-2} of RF by greenhouse gases. Methods have been proposed (Evans et al., 2010; Seitz, 2011) to increase the fraction of the oceans covered with foam which is known to be very reflective (Whitlock et al., 1982). Neither the extent of foam generation and persistence required for a significant climate impact, nor the impact of artificial foam on the world's ocean (including ocean biology, air-sea fluxes of latent heat, sensible heat, trace gases, aerosols, ocean circulation, and surface emissivity) have been assessed quantitatively in the peer-reviewed literature.

7.7.2.4 Cirrus Thinning

Thin high cirrus clouds are relatively transparent to incoming sunlight, but absorb some of the infrared energy leaving the Earth's surface. Their overall radiative effect is to warm the climate (see Section 7.2.1.2). Reducing the coverage or longwave opacity of these clouds would therefore produce a negative AF. Cirrus cloud coverage and optical thickness are affected by ice crystal fall speeds, which depend on ice crystal size. Mitchell and Finnegan (2009) suggested seeding the upper troposphere with efficient IN that would trigger ice nucleation at higher temperatures than in the unperturbed atmosphere. The engineered ice crystals would grow preferentially and sediment out, resulting in thinner cirrus and reducing the water vapour available for normal particle formation. This strategy depends upon details of the cirrus nucleation processes that remain poorly understood (Section 7.4.4), but climate model simulations suggest that small changes in ice nucleation and the subsequent competition of ice particles for water vapour responses could produce responses in AF of order −5 W m^{-2} (e.g., Lohmann et al., 2008).

7.7.3 Climate Response to SRM Methods

The many ways that SRM can be implemented make quantitative model evaluation and intercomparison difficult, motivating idealised experiments to explore climate model responses. One such experiment consists of an artificial reduction of the total solar irradiance, which approximates the radiative impact of space mirrors (Early, 1989), but represents the radiative impact of other SRM methods less accurately. This results in a global cooling. Balancing the RF from a CO_2 increase with a reduction in the total solar irradiance results in a residual surface temperature change that is generally positive at mid- and high-latitudes, especially over continents, and generally negative in the Tropics (Bala et al., 2008; Kravitz et al., 2012a; Lunt et al., 2008; Schmidt et al., 2012b; Figures 7.22a-b and 7.23a-d). This is a robust prediction of climate models, and can be understood in terms of the difference between the relatively uniform longwave forcing (associated with greenhouse gases) and the latitudinally and seasonally varying shortwave forcing (from SRM). The residual changes in surface temperature are nevertheless much smaller than the warming due to the CO_2 RF alone. These features can be seen in Figure 7.23a-d showing results from the recent Geoengineering Model Intercomparison Project (Kravitz et al., 2011). The substantial warming from 4xCO_2 AF at high latitudes (4°C–18°C) is reduced substantially through idealized SRM leaving residual changes, particularly a warming of 0°C–3°C near the winter pole. While increasing CO_2 concentrations lead to a positive RF that warms the entire troposphere, SRM produces a negative RF that tends to cool the surface. The combination of RF used to balance the globally-averaged surface temperature increases atmospheric stability, reducing the evaporative flux, leading to a reduction in global precipitation rate as seen in Figures 7.22c-d and Figures 7.23e-g (Andrews et al., 2010; Bala et al., 2008; Schmidt et al., 2012b) and discussed in Section 7.6 Other factors can also modulate the climate response in evaporation, soil moisture and precipitation, such as the enhanced closure of stomata with increased CO_2 concentrations. Although models agree on the globally and annually averaged impact on precipitation, there is less agreement in the spatial pattern of the changes but some residual patterns in the idealized experiments are quite robust, for example the ~5% reduction in precipitation over SE Asia and the Pacific Warm Pool in JJA. Precipitation changes are substantially more varied between model simulations using more complex strategies for SRM as described below.

[INSERT FIGURE 7.22 HERE]

Figure 7.22: Zonally- and annually-averaged change in surface air temperature (°C) for (a) an abrupt 4 × CO_2 experiment and (b) the GeoMIP G1 experiment for 11 coupled atmosphere-ocean general circulation models. (c) and (d) Same as (a) and (b) but for the change in precipitation (mm day^{-1}). In the GeoMIP G1 experiment (Kravitz et al., 2011) an abrupt fourfold increase in CO_2 concentration is balanced by a reduction in total solar irradiance to produce a top of atmosphere flux imbalance of less than ±0.1 W m^{-2} during the first 10 years of the simulation. All changes are relative to the pre-industrial control experiment and averaged over years 21–50.

Idealized experiments have also been conducted in which solar radiation is reduced only over the ocean (e.g., to approximate the effects of marine cloud seeding or increased sea foam). Other studies have explored albedo changes over land (e.g., to represent a surface albedo increase through plant albedo or brightening desert regions) and over particular latitudinal bands (Caldeira and Wood, 2008) or regions (Irvine et al., 2010; Irvine et al., 2011). Bala et al. (2010) found that although global-mean precipitation might decrease, precipitation and runoff over land could increase because of the RF gradient between ocean and land. In

contrast, increasing the albedo of desert areas may result in reduction in rainfall over the Indian and Sahel regions (Irvine et al., 2010).

[INSERT FIGURE 7.23 HERE]

Figure 7.23: Multi-model mean of the change in surface air temperature (°C) averaged over December, January and February months for (a) the abrupt 4 × CO_2 simulation and (b) the GeoMIP G1 experiment. (c-d) same as (a-b) but for the June, July and August months. (e-h) same as (a-d) but for the change in precipitation (mm day^{-1}). All changes are relative to the pre-industrial control experiment and averaged over years 21-50. Stippling denotes agreement on the sign of the temperature anomaly in at least 75% of the models in panels.

High CO_2 concentrations from anthropogenic emissions will persist in the atmosphere for a long time (for more than a thousand years in the absence of CDR). If SRM were used to counter positive forcing, it would be needed as long as the CO_2 concentrations were high. If greenhouse gas concentrations increase, then the scale of SRM to offset the resulting warming would need to increase, with amplifying residual effects from increasingly imperfect compensation. Figure 7.24 shows the globally averaged warming and precipitation changes associated with a 1% yr^{-1} CO_2 increase (GeoMIP experiment G2), with and without SRM, followed by termination of SRM at year 50. While the rate of temperature change varies by a factor of 2–3 between models, all GeoMIP models return to temperature levels consistent with CO_2 forcing within one to two decades. The associated very rapid warming would have significant impact on ecosystem and human adaptation. Other strategies could be considered that use SRM with mitigation to try to avoid transitions across climate thresholds or to keep temperatures below a threshold in combination with greenhouse gas emissions reductions. Such scenarios would not necessarily be subject to the "termination effect" as described above and SRM might be used for shorter times, perhaps less than a century (Smith and Rasch, 2012; Wigley, 2006).

[INSERT FIGURE 7.24 HERE]

Figure 7.24: Timeseries of surface temperature (°C, left) and precipitation change (mm day^{-1}, right) for GeoMIP experiment G2, relative to each model's 1 × CO_2 reference simulation. Solid lines are simulations using SRM to balance a 1% yr^{-1} increase in CO_2 concentration until year 50 after which SRM is stopped. Dashed lines are for 1% CO_2 increase simulations with no SRM.

Several modelling studies (Jones et al., 2010; Rasch et al., 2008b; Robock et al., 2008) examined the model response to SRM in less idealized scenarios with stratospheric aerosol SRM when the forcing is sufficient to counter the effects of a doubling CO_2 on globally-averaged surface temperature. The results show that changes in temperature, winds and precipitation are similar to those obtained in idealized studies described above, with a residual warming at high latitudes, and a reduction in global-mean precipitation. Similar responses have been observed following volcanic eruptions like Pinatubo (Trenberth and Dai, 2007). Each of these studies used a somewhat different experimental design, and there are significant disagreements in regional responses that may be due to the experimental design, model differences, or larger differences in forcing produced by different representation of the stratospheric aerosol production, transport, and loss processes.

Jones et al. (2009), Rasch et al. (2009), and Hill and Ming (2012) used coupled ocean/atmosphere/sea ice models to assess the climate impacts of cloud brightening due to droplet concentration changes. A global cooling was achieved, in spite of the heterogeneous RF associated with cooling by subtropical and midlatitude cloud systems in all three models, but temperature and precipitation signatures that differed substantially. One common feature was the cooling over the seeded regions (the marine stratocumulus regions) and a warmer North Pacific adjacent to a cooler northwestern Canada, a feature reminiscent of La Niña.

7.7.4 Synthesis

Multiple, consistent and independent lines of evidence (from theory, model studies and observations) suggest that some SRM strategies may be able to counter a portion of the global warming due to anthropogenic greenhouse gases. In particular SRM by stratospheric aerosols appears to be scalable to counter at least a twofold increase in CO_2 concentration, but models disagree on the amount of material that would need to be injected to achieve this. SRM by marine cloud brightening has received somewhat less attention, and issues are less well understood because of the high level of uncertainty about aerosol-cloud interactions, and there

is as yet no consensus on whether it will be possible to achieve a significant RF. It does not appear that SRM strategies that change land albedo (whiter rooftops and paving, vegetation changes) can produce sufficient RF to counter the warming expected from a doubling of CO_2. Much less attention has been devoted to other SRM strategies, so it is not yet possible to assess their efficacy, scalability, viability and consequences.

There is high agreement among models that the compensation between greenhouse gas warming and SRM cooling is imprecise and that some regional impacts would remain, but the models disagree on the details. Models consistently indicate that, if feasible, a geoengineered climate with SRM and high atmospheric CO_2 levels would be much closer to 20th century climate than a world with elevated CO_2 concentrations and no SRM (Lunt et al., 2008; Moreno-Cruz et al., 2011). A wide range of side effects has been identified for SRM methods. Some are common to all SRM methods (e.g., a global decrease in precipitation for no temperature change in the global-mean). Others are particular to a specific SRM method (e.g., the high latitude stratospheric ozone depletion from stratospheric aerosol SRM). SRM will not address the issue of ocean acidification from increasing CO_2 and may have other impacts on the climate system. If SRM were terminated at a high CO_2 concentration, the global average temperature would rapidly (within a decade or two) approach temperatures consistent with that CO_2 forcing, severely stressing ecosystem and human adaptation.

[START FAQ 7.1 HERE]

FAQ 7.1: How do Clouds Affect Climate and Climate Change?

Clouds strongly affect the current climate, but observations alone cannot yet tell us how they will affect a future, warmer climate. Comprehensive prediction of clouds requires a global climate model. Such models produce cloud fields that roughly resemble those observed, but are far from perfect. Climate models vary in how they predict clouds will change in a warmer climate, but based on all available evidence, it seems likely that the net cloud-climate feedback is positive, and will not significantly limit global warming.

Since the 1970s, scientists have recognised the critical importance of cloudiness for climate change. Clouds affect the climate system in a variety of ways. They produce precipitation (rain and snow) that is necessary for most life on land. They warm the atmosphere as water vapour condenses and releases latent heat. They strongly affect the flows of both solar and infrared radiation through the atmosphere. Finally, they are intimately associated with powerful vertical motions that can carry air from near the surface to the upper troposphere in less than an hour. These strong, vertical currents carry energy, moisture, momentum, and various chemical constituents, including aerosol particles. For decades, climate scientists have been using observations to study how clouds change with the daily weather, with the seasonal cycle, and with year-to-year changes, such as those associated with El Niño.

Each of the various cloud processes has the potential to change as the climate state evolves. Cloud feedbacks are of intense interest in the context of anthropogenic climate change. Any change in a cloud process that is caused by climate change—and in turn influences climate—represents a cloud-climate feedback. Because clouds interact so strongly with both infrared and visible radiation, relative changes in cloudiness of only a few per cent can have a potent effect on the climate system.

Many types of possible cloud-climate feedbacks have been identified. Broadly speaking, they would occur through changes in cloud amount, cloud-top height, and/or cloud optical properties. We still are not sure what types of cloud feedbacks will actually occur, nor how significant they will be for climate change. Nevertheless, all the models used for the past two IPCC assessments produce cloud feedbacks that either enhance anthropogenic greenhouse warming or have little overall effect. Feedbacks are not "put into" these models, but are an aspect of the solutions to the model equations describing the atmosphere and other parts of the climate system. The differences in the strength of the cloud feedbacks produced by these models explain why they react more or less sensitively to changes in greenhouse gas concentrations.

Low clouds reflect a lot of solar radiation back to space, but have only a weak effect on the infrared radiation emitted by the Earth. As a result, they tend to cool the Earth in the present climate. High clouds efficiently reflect sunlight, but also strongly reduce the amount of emitted infrared radiation. This compensation makes the surface temperature somewhat less sensitive to changes in high cloud amount than to changes in low

cloud amount. In a future climate, warmed by increasing greenhouse gases, most IPCC-assessed climate models simulate a decrease in low-cloud amount, which would increase the warming, but the extent of this decrease is quite model-dependent.

Although surface temperature is relatively insensitive to changes in high cloud amount, changes in the altitude of a given amount of high clouds can more strongly affect surface temperature. Higher cloud tops increase the greenhouse effect, while reflecting a similar amount of solar radiation. There is strong evidence that high clouds rise further in a warmer climate. This acts as an important positive feedback by preventing some of the additional infrared radiative energy emitted by the surface from leaving the climate system.

There are other ways clouds may change in a warmer climate. More clouds may be made of liquid drops, and fewer made of ice crystals, changing the overall amount of light reflected. Changing amounts of aerosol particles could cause changes in cloud reflectivity, independent of any caused by greenhouse gases (see FAQ 7.2). Changes in wind patterns and storm tracks could also affect the regional and seasonal distribution of cloudiness and precipitation. Some studies suggest that the signal of one such expected trend—a poleward migration of the clouds associated with mid-latitude storm tracks—is already detectable in the observational record. However, because clouds are quite variable from year to year, there is as yet no broadly accepted way to infer global cloud feedback more generally from observations.

[END FAQ 7.1 HERE]

[START FAQ 7.2 HERE]

FAQ 7.2: How do Aerosols Affect Climate and Climate Change?

Atmospheric aerosols are small particles suspended in the atmosphere. They come from natural and anthropogenic sources, and can affect the climate in multiple and equivocal ways through their interactions with radiation and clouds. Overall, it seems very likely that anthropogenic variations in atmospheric aerosols have exerted a cooling influence on the Earth, which has diminished anthropogenic greenhouse warming.

Atmospheric aerosols have a typical lifetime of one day to two weeks in the troposphere, and about one year in the stratosphere. They vary greatly in size, chemical composition and shape. Some aerosols, such as dust and sea spray, are mostly or entirely of natural origin, while other aerosols, such as sulphates and smoke, come from both natural and anthropogenic sources.

Aerosols affect climate in many ways. First, they scatter and absorb sunlight, which modifies the Earth's radiative balance (see FAQ.7.2, Figure 1). Aerosol scattering generally makes the planet more reflective, and tends to cool the climate, while aerosol absorption has opposite effects, and tends to warm the climate system. The balance between cooling and warming depends on aerosol properties and environmental conditions. Many observational studies have quantified local radiative effects from anthropogenic and natural aerosols, but predicting their global impact requires satellite data and models. Most studies agree that the overall radiative effect from anthropogenic aerosols is to cool the planet. One of the remaining uncertainties, however, comes from soot, an absorbing aerosol which is more difficult to measure than scattering aerosols, and induces a specific cloud response.

[INSERT FAQ 7.2, FIGURE 1 HERE]

FAQ 7.2, Figure 1: Overview of aerosol-radiation interactions and their impact on climate. The left panels show the instantaneous radiative effects of aerosols, while the right panels show their overall impact after the climate system has responded to their radiative effects.

Aerosols also serve as condensation and freezing sites, where cloud droplets and ice particles form (see FAQ.7.2, Figure 2). You might assume that more cloud condensation nuclei would increase the amount of low clouds, but cloud formation is largely limited by dynamical processes, so that the net effect on clouds of more aerosols is quite subtle, and remains uncertain. A robust result is that more aerosols generally produce liquid clouds, which are brighter because they have more numerous, smaller cloud droplets. There are many other pathways for aerosol-cloud interactions, particularly in ice—or mixed liquid and ice—clouds, where

phase changes are sensitive to aerosols. Quantifying the overall impact of aerosols on cloud amounts and properties is understandably difficult. Available studies, based on climate models and satellite observations, generally indicate that the net effect of anthropogenic aerosols on cloud is to cool the climate system.

[INSERT FAQ 7.2, FIGURE 2 HERE]

FAQ 7.2, Figure 2: Overview of aerosol-cloud interactions and their impact on climate. The left and right panels represent a clean and a polluted low-level cloud, respectively.

Since aerosols are distributed unevenly in the atmosphere, they can heat and cool the climate system in patterns that can drive small changes in the weather. These effects are complex, and hard to simulate with current models, but several studies suggest significant effects on precipitation in certain regions.

Because of their short lifetime, the abundance of aerosols—and their climate effects—have varied over time, in rough concert with anthropogenic emissions of aerosols and their gaseous precursors. Since anthropogenic emissions have increased substantially over the industrial period, this has very likely counteracted some of the warming that would otherwise have occurred from increased concentrations of long-lived greenhouse gases. Aerosols from volcanic eruptions, such as those of El Chichón and Pinatubo, have also caused sporadic cooling periods.

Over the last two decades, anthropogenic aerosol emissions have decreased in industrialised countries, but increased in developing countries. It is therefore difficult to assess whether the global impact of aerosols has been to cool or warm the planet over this recent period. It is very likely, however, that emissions of anthropogenic aerosols will ultimately decrease, augmenting greenhouse-gas induced warming.

[END FAQ 7.2 HERE]

[START FAQ 7.3 HERE]

FAQ 7.3: Could Geoengineering Counteract Climate Change and What Side Effects Might Occur?

Geoengineering—also called climate engineering—is defined as a deliberate large-scale manipulation of the climate system to counteract the consequences of increasing greenhouse gas emissions. Two distinct categories of geoengineering methods are usually considered: Solar Radiation Management, also called Sunlight Reflection Methods (SRM, assessed in Chapter 7) and Carbon Dioxide Removal (CDR, assessed in Chapter 6). Each operates on different physical principles, and acts in different ways. While both methods are likely to counter some effects of greenhouse gases, they also carry risks and side effects.

Carbon Dioxide Removal (CDR) Methods

By definition, CDR methods are designed to remove CO_2 from the atmosphere, often through a manipulation of natural carbon cycle processes. The carbon withdrawn from the atmosphere would then be stored in land, ocean or geological reservoirs, where it would have little or no impact on the Earth's energy budget. Some proposed CDR methods would rely on biological processes, such as afforestation/reforestation, carbon sequestration in soils through biochar, bioenergy associated with carbon capture and storage (BECCS) and ocean fertilisation. Others would rely on geochemical processes, such as accelerated weathering of silicate and carbonate rocks—on land or in the ocean—to remove CO_2 from the atmosphere, or directly capture it in industrial facilities (see FAQ.7.3, Figure 1). The captured CO_2 would then be stored in organic form in land reservoirs, and in inorganic form in ocean and geological reservoirs.

[INSERT FAQ 7.3, FIGURE 1 HERE]

FAQ 7.3, Figure 1: Overview of some carbon dioxide removal methods. (a) nutrients are added to the ocean, which increases oceanic productivity in the surface ocean and transports a fraction of the resulting biogenic carbon downward, (b) alkalinity from solid minerals is added to the ocean, which causes more atmospheric CO_2 to dissolve in the ocean, (c) the weathering rate of silicate rocks is increased, and the dissolved carbonate minerals are transported to the ocean, (d) alkalinity from mined silicate rocks is extracted, then combined with atmospheric CO_2 to produce solid carbonate minerals, (e) atmospheric CO_2 is captured chemically, and stored either underground or in the ocean, (f) biomass is burned at an electric power plant with carbon capture, and the captured CO_2 is stored either underground or in the ocean and (g) CO_2 is captured through afforestation and reforestation to be stored in land ecosystems.

In general, insofar as CDR methods are effective at removing CO_2 from the atmosphere and keeping the removed carbon away from the atmosphere, they are believed to pose a low risk of unintended climatic side effects. If deployed, they would counter the root cause of CO_2-induced climate change by reducing atmospheric carbon dioxide concentrations, thus reducing the associated radiative forcing and ocean acidification.

One main issue relates to the capacity and permanence of storage reservoirs. Permanent carbon storage by CDR would decrease climate warming in the long term. However, non-permanent storage strategies, which would eventually see the CO_2 returned to the atmosphere, would only reduce climate change for some limited time. Geological reservoirs could permanently store several thousand PgC, while oceans may also be able to store a further few thousand PgC. In contrast, the estimated capacity of the terrestrial biosphere is only 150 to 200 PgC, which represents only about 10% of the existing living biomass and soil carbon pools.

It is well known that the land and ocean carbon pools act as a buffer for CO_2 emitted to, and removed from, the atmosphere. At present, about 50% of the CO_2 emitted into the atmosphere from fossil fuel burning is taken up by the land and ocean carbon pools. Should CDR be deployed, the uptake would be reduced or even reverse into a carbon source over a period of several decades. Therefore, to offset past anthropogenic CO_2 emissions, CDR techniques would need to remove not just the CO_2 that accumulated in the atmosphere, but also the anthropogenic carbon previously taken up by terrestrial and oceanic sinks.

Any given biological or chemical weathering CDR method is estimated to be able to remove a maximum of 100 PgC (equivalent to about 50 parts per million by volume [ppm] of atmospheric CO_2) over a century. However, that maximum potential cannot typically be achieved, due to constraints such as competing demands for land. Furthermore, buffering could reduce the effective potential to about 25 ppm.

The atmospheric concentration of CO_2 has risen by more than 75 ppm in the last 50 years. Assuming a maximum CDR sequestration rate of 100 PgC per century as discussed above, any single biological or chemical weathering CDR method would take about three centuries to remove the CO_2 emitted in the last 50 years, making it difficult—even for a suite of biological methods—to mitigate climate change rapidly. Direct air capture methods could in principle operate much more rapidly, but are limited by cost, energy use and environmental constraints.

CDR could have climatic and environmental side effects. For instance, it would tend to counter the general increase in plant productivity expected in a world with higher CO_2 concentrations. A large-scale increase in vegetation coverage, for instance through afforestation or energy crops, could alter surface characteristics, such as surface reflectivity and turbulent fluxes. Many modelling studies have shown that afforestation in seasonally snow-covered boreal regions could accelerate global warming, whereas afforestation in the tropics may be more effective at slowing global warming.

Ocean-based CDR methods, which rely on enhanced biological production, could have many biogeochemical side effects, most of them being largely unknown, given the complexity of marine ecosystem communities. Macronutrients such as nitrogen and phosphorus would decrease in regions where marine productivity is artificially enhanced, likely leading to a shortage of nutrients downstream and a decrease in productivity. Ocean-based biological CDR methods might also have impact on ocean oxygen levels, and stimulate increased production of DMS, isoprene, and non-CO_2 greenhouse gases such as N_2O and CH_4. Finally acidification of the deep ocean might occur, caused by the respiration associated with the organic matter that is exported downwards.

Solar Radiation Management (SRM) Methods

The globally-averaged temperature of the planet is controlled by the amount of sunlight absorbed by the Earth's atmosphere and surface, and by the existence of a greenhouse effect, by which gases and clouds make the atmosphere opaque in the infrared spectrum where terrestrial radiation is emitted. If less incoming sunlight reaches the surface, because of an increase in the reflectivity of the planet, or if energy is emitted to space from a lower altitude because of a less opaque atmosphere in the infrared, the average global surface temperature will be less.

Suggested geoengineering methods which manage the Earth's radiative budget are based on this fundamental physical principle (see FAQ7.3, Figure 2). These methods propose to either reduce sunlight reaching the Earth—using mirrors in space—or increase the reflectivity of the planet by making the atmosphere, clouds or the surface more reflective. Another technique proposes to suppress cirrus clouds, as these absorb some of the terrestrial radiation emitted by the Earth.

[INSERT FAQ 7.3, FIGURE 2 HERE]

FAQ 7.3, Figure 2: Overview of some proposed solar radiation management (SRM) schemes to reflect sunlight to space that would otherwise be absorbed. Illustrated methods, counter-clockwise from upper left, are (a) reflectors in space, (b) aerosols in the stratosphere, (c) enhanced reflectivity of marine clouds, (d) making the ocean surface more reflective, (e) growing more reflective crops, and (f) whitening of roofs and other built structures.

Basic physics tells us that if any of these methods produce a net flux change of energy from Earth to space, the planet will cool. The picture is complicated, however, because of the many complex physical processes which govern the interactions between the flow of energy, the atmospheric circulation, weather and the resulting climate.

While the average surface temperature of the planet responds to the energy budget in a rather straightforward way, the temperature at any given location and time is influenced by many other factors. The amount of cooling from SRM will not in general equal the amount of warming caused by greenhouse gases at each location and time. For example, SRM will only change heating rates during the daytime, whereas changes in greenhouse gases affect heating rates during both day and night. This inexact compensation will have some influence on the diurnal cycle of surface temperature, even if the average surface temperature is unchanged. There may be other important changes: a uniform stratospheric aerosol loading might offset global mean CO_2-induced warming, but some regions will cool less than others and polar regions could be left with some residual warming.

If deployed, SRM could theoretically counteract anthropogenic climate change rapidly, cooling the Earth to pre-industrial levels within one or two decades. We know this from climate models but also from the observed rapid cooling of about 0.5 K that followed the eruption of Mt Pinatubo in 1991.

Climate consists of many factors besides surface temperature. Consequences for other climate features, such as precipitation, soil moisture, river flow, snowpack and sea ice, may also be important. Both models and theory show that compensating an increased greenhouse effect with SRM will not counter the globally-averaged surface temperature and rainfall equally, and there could be large regional changes. Such imprecise compensation in regional and global climate patterns makes it very unlikely that solar radiation management will produce a future climate that is "just like" the one we experience today, or have experienced in the past. However, climate models indicate that a geoengineered climate with SRM and high atmospheric CO_2 levels could be much closer to 20th century climate than a future climate with elevated CO_2 concentrations and no SRM.

SRM techniques will have other side effects: radiation management by stratospheric sulphate aerosols can induce stratospheric ozone depletion, especially while chlorine from CFC emissions still resides in the atmosphere, possibly increasing dangerous ultraviolet radiation reaching the surface. It can also alter the ratio of direct to diffuse sunlight reaching the surface, which is known to affect terrestrial ecosystems. Finally, SRM will not mitigate the ocean acidification associated with increasing atmospheric CO_2 concentrations.

Without CDR, high CO_2 concentrations from anthropogenic emissions will persist in the atmosphere for as long as a thousand years, and SRM would have to be maintained for a similar period to remain effective at counteracting global warming. Stopping SRM while CO_2 concentrations were still high would lead to a very rapid warming over one or two decades, severely stressing ecosystem and human adaptation.

As greenhouse gas concentrations increase, the scale of any SRM deployment would have to increase too, in order to keep pace with the greenhouse effect. This would exacerbate the residual climate change and the risk of abrupt termination. SRM could conceivably help avoid transitions across climate thresholds or tipping

points that might, at some point, be unavoidable otherwise. Nevertheless, its side effects make it a high-risk strategy for staving off climate change.

[END FAQ 7.3 HERE]

References

Abbatt, J.P.D., Benz, S., Cziczo, D.J., Kanji, Z., Lohmann, U. and Mohler, O., 2006. Solid ammonium sulfate aerosols as ice nuclei: A pathway for cirrus cloud formation. Science, **313**(5794): 1770-1773.

Abdul-Razzak, H. and Ghan, S., 2000. A parameterization of aerosol activation 2. Multiple aerosol types. J. Geophys. Res., **105**: 6837-6844.

Ackerman, A.S., Kirkpatrick, M.P., Stevens, D.E. and Toon, O.B., 2004. The impact of humidity above stratiform clouds on indirect aerosol climate forcing. Nature, **432**(7020): 1014-1017.

Ackerman, A.S., Toon, O.B., Stevens, D.E. and Coakley, J.A., 2003. Enhancement of cloud cover and suppression of nocturnal drizzle in stratocumulus polluted by haze. Geophysical Research Letters, **30**(7): 1381.

Ackerman, A.S., vanZanten, M.C., Stevens, B., Savic-Jovcic, V., Bretherton, C.S., Chlond, A., Golaz, J.-C., Jiang, H., Khairoutdinov, M., Krueger, S.K., Lewellen, D.C., Lock, A., Moeng, C.-H., Nakamura, K., Petters, M.D., Snider, J.R., Weinbrecht, S. and Zulauf, M., 2009. Large-eddy simulations of a drizzling, stratocumulus-topped marine boundary layer. Monthly Weather Review, **137**(3): 1083-1110.

Adachi, K., Chung, S.H. and Buseck, P.R., 2010. Shapes of soot aerosol particles and implications for their effects on climate. Journal of Geophysical Research, **115**(D15): D15206.

Adams, P.J., Seinfeld, J.H., Koch, D., Mickley, L. and Jacob, D., 2001. General circulation model assessment of direct radiative forcing by the sulfate-nitrate-ammonium-water inorganic aerosol system. Journal of Geophysical Research, **106**(D1): 1097-1111.

Agee, E.M., Kiefer, K. and Cornett, E., 2012. Relationship of lower troposphere cloud cover and cosmic rays: An updated perspective. Journal of Climate(25): 1057-1060.

Ahern, H.E., Walsh, K.A., Hill, T.C.J. and Moffett, B.F., 2007. Fluorescent pseudomonads isolated from Hebridean cloud and rain water produce biosurfactants but do not cause ice nucleation. Biogeosciences, **4**(1): 115-124.

Akbari, H., Matthews, H.D. and Seto, D., 2012. The long-term effect of increasing the albedo of urban areas. Environ. Res. Lett., **7**: 024004.

Albrecht, B.A., 1989. Aerosols, cloud microphysics, and fractional cloudiness. Science, **245**(4923): 1227-1230.

Alexander, D.T.L., Crozier, P.A. and Anderson, J.R., 2008. Brown carbon spheres in East Asian outflow and their optical properties. Science, **321**(5890): 833-836.

Allan, R. and Soden, B., 2007. Large discrepancy between observed and simulated precipitation trends in the ascending and descending branches of the tropical circulation. Geophysical Research Letters, **34**(18): L18705.

Allen, M.R. and Ingram, W.J., 2002. Constraints on future changes in climate and the hydrologic cycle. Nature, **419**(6903): 224-232.

Allen, R., Sherwood, S., Norris, J. and Zender, C., 2012. Recent Northern Hemisphere tropical expansion primarily driven by black carbon and tropospheric ozone. Nature, **485**(7398): 350-354.

Allen, R.J. and Sherwood, S.C., 2010. Aerosol-cloud semi-direct effect and land-sea temperature contrast in a GCM. Geophysical Research Letters, **37**: L07702.

Alpert, P., Halfon, N. and Levin, Z., 2008. Does air pollution really suppress precipitation in Israel? Journal of Applied Meteorology and Climatology, **47**: 933–943.

Anderson, T.L., Ackerman, A., Hartmann, D.L., Isaac, G.A., Kinne, S., Masunaga, H., Norris, J.R., Poschl, U., Schmidt, K.S., Slingo, A. and Takayabu., Y.N., 2009. Temporal and spatial variability of clouds and related aerosol. In: R.J.a.H. Charlson, J. (Editor), Clouds in the Perturbed Climate System: Their Relationship to Energy Balance, Atmospheric Dynamics, and Precipitation. MIT Press, Cambridge, pp. 127-148.

Anderson, T.L., Charlson, R.J., Bellouin, N., Boucher, O., Chin, M., Christopher, S.A., Haywood, J., Kaufman, Y.J., Kinne, S., Ogren, J.A., Remer, L.A., Takemura, T., Tanré, D., Torres, O., Trepte, C.R., Wielicki, B.A., Winker, D.M. and Yu, H.B., 2005. An "A-Train" strategy for quantifying direct climate forcing by anthropogenic aerosols. Bulletin of the American Meteorological Society, **86**(12): 1795-1809.

Anderson, T.L., Charlson, R.J., Schwartz, S.E., Knutti, R., Boucher, O., Rodhe, H. and Heintzenberg, J., 2003. Climate forcing by aerosols - a hazy picture. Science, **300**: 1103-1104.

Andreae, M.O. and Gelencser, A., 2006. Black carbon or brown carbon? The nature of light-absorbing carbonaceous aerosols. Atmospheric Chemistry and Physics, **6**: 3131-3148.

Andrews, T., Forster, P. and Gregory, J., 2009. A surface energy perspective on climate change. Journal of Climate, **22**(10): 2557-2570.

Andrews, T. and Forster, P.M., 2008. CO_2 forcing induces semi-direct effects with consequences for climate feedback interpretations. Geophysical Research Letters, **35**: L04802.

Andrews, T., Forster, P.M., Boucher, O., Bellouin, N. and Jones, A., 2010. Precipitation, radiative forcing and global temperature change. Geophysical Research Letters, **37**: L14701.

Andrews, T., Gregory, J.M., Webb, M.J. and Taylor, K.E., 2012. Forcing, feedbacks and climate sensitivity in CMIP5 coupled atmosphere-ocean climate models. Geophysical Research Letters, **39**: L09712.

Andronova, N.G. and Schlesinger, M.E., 2001. Objective estimation of the probability density function for climate sensitivity. Journal of Geophysical Research, **106**(D19): 22605-22611.

Ansmann, A., Tesche, M., Althausen, D., Muller, D., Seifert, P., Freudenthaler, V., Heese, B., Wiegner, M., Pisani, G., Knippertz, P. and Dubovik, O., 2008. Influence of Saharan dust on cloud glaciation in southern Morocco during the Saharan Mineral Dust Experiment. Journal of Geophysical Research, **113**(D4): D04210.

Arakawa, A., 1975. Modeling clouds and cloud processes for use in climate models, *The physical basis of climate and climate modelling*. ICSU/WMO, Geneva, pp. 181-197.
Arakawa, A., 2004. The cumulus parameterization problem: Past, present, and future. Journal of Climate, **17**(13): 2493-2525.
Archuleta, C.M., DeMott, P.J. and Kreidenweis, S.M., 2005. Ice nucleation by surrogates for atmospheric mineral dust and mineral dust/sulfate particles at cirrus temperatures. Atmospheric Chemistry and Physics, **5**: 2617-2634.
Ariya, P.A., Sun, J., Eltouny, N.A., Hudson, E.D., Hayes, C.T. and Kos, G., 2009. Physical and chemical characterization of bioaerosols - Implications for nucleation processes. International Reviews in Physical Chemistry, **28**(1): 1-32.
Arneth, A., Miller, P.A., Scholze, M., Hickler, T., Schurgers, G., Smith, B. and Prentice, I.C., 2007. CO_2 inhibition of global terrestrial isoprene emissions: Potential implications for atmospheric chemistry. Geophysical Research Letters, **34**: L18813.
Arneth, A., Monson, R.K., Schurgers, G., Niinemets, U. and Palmer, P.I., 2008. Why are estimates of global terrestrial isoprene emissions so similar (and why is this not so for monoterpenes)? Atmospheric Chemistry and Physics, **8**: 4605-4620.
Arnold, F., 2006. Atmospheric aerosol and cloud condensation nuclei formation: A possible influence of cosmic rays? Space Science Reviews, **125**(1-4): 169-186.
Artaxo, P., Fernandes, E.T., J, V.M., Yamasoe, M.A., Hobbs, P.V., Maenhaut, W., Longo, K.M. and Castanho, A., 1998. Large-scale aerosol source apportionment in Amazonia. Journal of Geophysical Research, **103**(D24): 31837-31847.
Artaxo, P., Martins, J.V., Yamasoe, M.A., Procopio, A.S., Pauliquevis, T.M., Andreae, M.O., Guyon, P., Gatti, L.V. and Leal, A.M.C., 2002. Physical and chemical properties of aerosols in the wet and dry seasons in Rondônia, Amazonia. Journal of Geophysical Research, **107**(D20): 8081.
Asmi, E., Kivekas, N., Kerminen, V., Komppula, M., Hyvarinen, A., Hatakka, J., Viisanen, Y. and Lihavainen, H., 2011. Secondary new particle formation in Northern Finland Pallas site between the years 2000 and 2010. Atmospheric Chemistry and Physics, **11**(24): 12959-12972.
Aw, J. and Kleeman, M.J., 2003. Evaluating the first-order effect of intraannual temperature variability on urban air pollution. Journal of Geophysical Research, **108**(D12): 4365.
Ayers, G.P. and Cainey, J.M., 2007. The CLAW hypothesis: a review of the major developments. Environmental Chemistry, **4**(6): 366-374.
Baker, M.B. and Charlson, R.J., 1990. Bistability of CCN concentrations and thermodynamics in the cloud-topped boundary-layer. Nature, **345**(6271): 142-145.
Baker, M.B. and Peter, T., 2008. Small-scale cloud processes and climate. Nature, **451**(7176): 299-300.
Bala, G., Caldeira, K. and Nemani, R., 2010. Fast versus slow response in climate change: implications for the global hydrological cycle. Climate Dynamics, **35**: 423-434.
Bala, G., Duffy, P.B. and Taylor, K.E., 2008. Impact of geoengineering schemes on the global hydrological cycle. Proc. Natl. Acad. Sci. U S A, **105**: 7664–7669.
Bangert, M., Kottmeier, C., Vogel, B. and Vogel, H., 2011. Regional scale effects of the aerosol cloud interaction simulated with an online coupled comprehensive chemistry model. Atmospheric Chemistry and Physics, **11**(9): 4411-4423.
Barahona, D. and Nenes, A., 2008. Parameterization of cirrus cloud formation in large-scale models: Homogeneous nucleation. Journal of Geophysical Research, **113**(D11): D11211.
Barahona, D. and Nenes, A., 2009. Parameterizing the competition between homogeneous and heterogeneous freezing in ice cloud formation - polydisperse ice nuclei. Atmospheric Chemistry and Physics, **9**(16): 5933-5948.
Barahona, D., Sotiropoulou, R. and Nenes, A., 2011. Global distribution of cloud droplet number concentration, autoconversion rate, and aerosol indirect effect under diabatic droplet activation. Journal of Geophysical Research, **116**: D09203.
Barker, H.W., Cole, J.N.S., Morcrette, J.J., Pincus, R., Raisaenen, P., von Salzen, K. and Vaillancourt, P.A., 2008. The Monte Carlo Independent Column Approximation: An assessment using several global atmospheric models. Quarterly Journal of the Royal Meteorological Society, **134**(635): 1463-1478.
Barmet, P., Kuster, T., Muhlbauer, A. and Lohmann, U., 2009. Weekly cycle in particulate matter versus weekly cycle in precipitation over Switzerland. Journal of Geophysical Research, **114**: D05206.
Bauer, S., Bierwirth, E., Esselborn, M., Petzold, A., Macke, A., Trautmann, T. and Wendisch, M., 2011. Airborne spectral radiation measurements to derive solar radiative forcing of Saharan dust mixed with biomass burning smoke particles. Tellus, **63B**(4): 742-750.
Bauer, S.E., Koch, D., Unger, N., Metzger, S.M., Shindell, D.T. and Streets, D.G., 2007. Nitrate aerosols today and in 2030: a global simulation including aerosols and tropospheric ozone. Atmospheric Chemistry and Physics, **7**(19): 5043-5059.
Bäumer, D., Rinke, R. and Vogel, B., 2008. Weekly periodicities of aerosol optical thickness over Central Europe – evidence of an anthropogenic direct aerosol effect. Atmospheric Chemistry and Physics, **8**: 83-90.
Baustian, K.J., Wise, M.E. and Tolbert, M.A., 2010. Depositional ice nucleation on solid ammonium sulfate and glutaric acid particles. Atmospheric Chemistry and Physics, **10**(5): 2307-2317.

Bazilevskaya, G.A., Usoskin, I.G., Fluckiger, E.O., Harrison, R.G., Desorgher, L., Butikofer, R., Krainev, M.B., Makhmutov, V.S., Stozhkov, Y.I., Svirzhevskaya, A.K., Svirzhevsky, N.S. and Kovaltsov, G.A., 2008. Cosmic ray induced ion production in the atmosphere. Space Science Reviews, **137**(1-4): 149-173.

Bechtold, P., Kohler, M., Jung, T., Doblas-Reyes, F., Leutbecher, M., Rodwell, M., Vitart, F. and Balsamo, G., 2008. Advances in simulating atmospheric variability with the ECMWF model: From synoptic to decadal time-scales. Quarterly Journal of the Royal Meteorological Society, **134**: 1337-1351.

Bellouin, N. and Boucher, O., 2010. Climate response and efficacy of snow forcing in the HadGEM2-AML climate model, *Hadley Centre Technical Note N°82,* Met Office, United Kingdom.

Bellouin, N., Boucher, O., Haywood, J. and Reddy, M.S., 2005. Global estimate of aerosol direct radiative forcing from satellite measurements. Nature, **438**: 1138-1141.

Bellouin, N., Jones, A., Haywood, J. and Christopher, S.A., 2008. Updated estimate of aerosol direct radiative forcing from satellite observations and comparison against the Hadley Centre climate model. Journal of Geophysical Research, **113**(D10): D10205.

Bellouin, N., Quaas, J., Morcrette, J.-J. and Boucher, O., 2012. Estimates of aerosol radiative forcing from the MACC re-analysis. Atmospheric Chemistry and Physics: submitted.

Bellouin, N., Rae, J., Johnson, C., Haywood, J., Jones, A. and Boucher, O., 2011. Aerosol forcing in the Climate Model Intercomparison Project (CMIP5) simulations by HadGEM2-ES and the role of ammonium nitrate. Journal of Geophysical Research, **116**: D20206.

Bender, F.A.-M., Ramanathan, V. and Tselioudis, G., 2012. Changes in extratropical storm track cloudiness 1983–2008: observational support for a poleward shift. Climate Dynamics, **38**: 2037-2053.

Benedetti, A., Morcrette, J.-J., Boucher, O., Dethof, A., Engelen, R.J., Fischer, M., Flentjes, H., Huneeus, N., Jones, L., Kaiser, J.W., Kinne, S., Mangold, A., Razinger, M., Simmons, A.J., Suttie, M. and the GEMS-AER team, 2009. Aerosol analysis and forecast in the ECMWF Integrated Forecast System. Part II : Data assimilation. Journal of Geophysical Research, **114**: D13205.

Benedict, J.J. and Randall, D.A., 2009. Structure of the Madden-Julian Oscillation in the Superparameterized CAM. Journal of the Atmospheric Sciences, **66**: 3277-3296.

Bennartz, R., 2007. Global assessment of marine boundary layer cloud droplet number concentration from satellite. Journal of Geophysical Research, **112**(D2): D02201.

Bergamo, A., Tafuro, A.M., Kinne, S., De Tomasi, F. and Perrone, M.R., 2008. Monthly-averaged anthropogenic aerosol direct radiative forcing over the Mediterranian based on AERONET aerosol properties. Atmospheric Chemistry and Physics, **8**(23): 6995-7014.

Bergstrom, R., Schmidt, K., Coddington, O., Pilewskie, P., Guan, H., Livingston, J., Redemann, J. and Russell, P., 2010. Aerosol spectral absorption in the Mexico City area: results from airborne measurements during MILAGRO/INTEX B. Atmospheric Chemistry and Physics: 6333-6343.

Bertram, A.K., Koop, T., Molina, L.T. and Molina, M.J., 2000. Ice formation in $(NH_4)_2SO_4$-H_2O particles. Journal of Physical Chemistry A, **104**(3): 584-588.

Bi, X., Zhang, G.H., Li, L., Wang, X.M., Li, M., Sheng, G.Y., Fu, J.M. and Zhou, Z., 2011. Mixing state of biomass burning particles by single particle aerosol mass spectrometer in the urban area of PRD, China. Atmospheric Environment, **45**(20): 3447-3453.

Blossey, P.N., Bretherton, C.S., Cetrone, J. and Kharoutdinov, M., 2007. Cloud-resolving model simulations of KWAJEX: Model sensitivities and comparisons with satellite and radar observations. Journal of the Atmospheric Sciences, **64**(5): 1488-1508.

Boers, R. and Mitchell, R.M., 1994. Absorption feedback in stratocumulus clouds - Influence on cloud-top albedo. Tellus, **46A**(3): 229-241.

Bond, G., Kromer, B., Beer, J., Muscheler, R., Evans, M.N., Showers, W., Hoffmann, S., Lotti-Bond, R., Hajdas, I. and Bonani, G., 2001. Persistent solar influence on North Atlantic climate during the Holocene. Science, **294**: 2130-2136.

Bond, T.C. and Bergstrom, R.W., 2006. Light absorption by carbonaceous particles: An investigative review. Aerosol Science and Technology, **40**(1): 27-67.

Bond, T.C., Doherty, S.J., Fahey, D.W., Forster, P.M., Berntsen, T.K., Boucher, O., DeAngelo, B.J., Flanner, M.G., Ghan, S.J., Kärcher, B., Koch, D., Kinne, S., Kondo, Y., Lohmann, U., Quinn, P.K., Sarofim, M.C., Schultz, M., Schulz, M., Venkataraman, C., Zhang, H., Zhang, S., Bellouin, N., Guttikunda, S.K., Hopke, P.K., Jacobson, M.Z., Kaiser, J.W., Klimont, Z., Lohmann, U., Schwarz, J.P., Shindell, D., Storelvmo, T., Warren, S.G. and C. S. Zender, 2012. Bounding the role of black carbon in the climate system: A scientific assessment. Journal of Geophysical Research, **submitted**.

Bondo, T., Enghoff, M.B. and Svensmark, H., 2010. Model of optical response of marine aerosols to Forbush decreases. Atmospheric Chemistry and Physics, **10**: 2765-2776.

Bony, S., Bellon, G., Fermapin, S., Klocke, D., Sherwood, S. and Denvil, S., 2012. Direct effect of carbon dioxide on tropical atmospheric circulation and regional rainfall. Nature Geoscience: submitted.

Bony, S., Colman, R., Kattsov, V.M., Allan, R.P., Bretherton, C.S., Dufresne, J.L., Hall, A., Hallegatte, S., Holland, M.M., Ingram, W., Randall, D.A., Soden, B.J., Tselioudis, G. and Webb, M.J., 2006. How well do we understand and evaluate climate change feedback processes? Journal of Climate, **19**(15): 3445-3482.

Bony, S. and Dufresne, J.-L., 2005. Marine boundary layer clouds at the heart of tropical cloud feedback uncertainties in climate models. Geophysical Research Letters, **32**(20): L20806.
Bony, S., Dufresne, J.L., Le Treut, H., Morcrette, J.J. and Senior, C., 2004. On dynamic and thermodynamic components of cloud changes. Climate Dynamics, **22**(2-3): 71-86.
Bopp, L., Boucher, O., Aumont, O., Belviso, S., Dufresne, J.L., Pham, M. and Monfray, P., 2004. Will marine dimethylsulfide emissions amplify or alleviate global warming? A model study. Canadian Journal of Fisheries and Aquatic Sciences, **61**: 826-835.
Boucher, O., 1999. Air traffic may increase cirrus cloudiness. Nature, **397**: 30-31.
Boucher, O. and Lohmann, U., 1995. The sulfate-CCN-cloud albedo effect - A sensitivity study with 2 general circulation models. Tellus, **47B**(3): 281-300.
Boucher, O., Myhre, G. and Myhre, A., 2004. Direct influence of irrigation on atmospheric water vapour and climate. Climate Dynamics, **22**: 597–603.
Bourotte, C., Curi-Amarante, A.-P., Forti, M.-C., Pereira, L.A.A., Braga, A.L. and Lotufo, P.A., 2007. Association between ionic composition of fine and coarse aerosol soluble fraction and peak expiratory flow of asthmatic patients in Sao Paulo city (Brazil). Atmospheric Environment, **41**: 2036–2048.
Boutle, I.A. and Abel, S.J., 2012. Microphysical controls on the stratocumulus topped boundary-layer structure during VOCALS-REx. Atmospheric Chemistry and Physics, **12**(6): 2849-2863.
Brenguier, J.L., 1993. Observations of cloud microstructure at the centimeter scale. Journal of Applied Meteorology, **32**(4): 783-793.
Brenguier, J.L., Burnet, F. and Geoffroy, O., 2011. Cloud optical thickness and liquid water path - does the k coefficient vary with droplet concentration? Atmospheric Chemistry and Physics, **11**(18): 9771-9786.
Brenninkmeijer, C.A.M., Crutzen, P., Boumard, F., Dauer, T., Dix, B., Ebinghaus, R., Filippi, D., Fischer, H., Franke, H., Friess, U., Heintzenberg, J., Helleis, F., Hermann, M., Kock, H.H., Koeppel, C., Lelieveld, J., Leuenberger, M., Martinsson, B.G., Miemczyk, S., Moret, H.P., Nguyen, H.N., Nyfeler, P., Oram, D., O'Sullivan, D., Penkett, S., Platt, U., Pupek, M., Ramonet, M., Randa, B., Reichelt, M., Rhee, T.S., Rohwer, J., Rosenfeld, K., Scharffe, D., Schlager, H., Schumann, U., Slemr, F., Sprung, D., Stock, P., Thaler, R., Valentino, F., Velthoven, P.v., Waibel, A., Wandel, A., Waschitschek, K., Wiedensohler, A., Xueref-Remy, I., Zahn, A., Zech, U. and Ziereis, H., 2007. Civil Aircraft for the regular investigation of the atmosphere based on an instrumented container: The new CARIBIC system. Atmospheric Chemistry and Physics, **7**: 4953-4976.
Bretherton, C.S., Blossey, P.N. and Jones, C.R., 2012. A large-eddy simulation of mechanisms of boundary layer cloud response to climate change. Journal of Advances in Modeling Earth Systems: submitted.
Bretherton, C.S., Blossey, P.N. and Uchida, J., 2007. Cloud droplet sedimentation, entrainment efficiency, and subtropical stratocumulus albedo. Geophysical Research Letters, **34**(3): L03813.
Brient, F. and Bony, S., 2012. Interpretation of the positive low-cloud feedback predicted by a climate model under global warming. Climate Dynamics, **Online first**.
Brioude, J., Cooper, O.R., Feingold, G., Trainer, M., Freitas, S.R., Kowal, D., Ayers, J.K., Prins, E., Minnis, P., McKeen, S.A., Frost, G.J. and Hsie, E.Y., 2009. Effect of biomass burning on marine stratocumulus clouds off the California coast. Atmospheric Chemistry and Physics, **9**(22): 8841-8856.
Brock, C.A., Cozic, J., Bahreini, R., Froyd, K.D., Middlebrook, A.M., McComiskey, A., Brioude, J., Cooper, O.R., Stohl, A., Aikin, K.C., de Gouw, J.A., Fahey, D.W., Ferrare, R.A., Gao, R.S., Gore, W., Holloway, J.S., Huebler, G., Jefferson, A., Lack, D.A., Lance, S., Moore, R.H., Murphy, D.M., Nenes, A., Novelli, P.C., Nowak, J.B., Ogren, J.A., Peischl, J., Pierce, R.B., Pilewskie, P., Quinn, P.K., Ryerson, T.B., Schmidt, K.S., Schwarz, J.P., Sodemann, H., Spackman, J.R., Stark, H., Thomson, D.S., Thornberry, T., Veres, P., Watts, L.A., Warneke, C. and Wollny, A.G., 2011. Characteristics, sources, and transport of aerosols measured in spring 2008 during the aerosol, radiation, and cloud processes affecting Arctic Climate (ARCPAC) Project. Atmospheric Chemistry and Physics, **11**(6): 2423-2453.
Bryan, G.H., Wyngaard, J.C. and Fritsch, J.M., 2003. Resolution requirements for the simulation of deep moist convection. Monthly Weather Review, **131**(10): 2394-2416.
Budyko, M.I., 1974. Izmeniya Klimata. Gidrometeoizdat, Leningrad.
Bundke, U., Nillius, B., Jaenicke, R., Wetter, T., Klein, H. and Bingemer, H., 2008. The fast Ice Nucleus chamber FINCH. Atmospheric Research, **90**(2-4): 180-186.
Burkhardt, U. and Kärcher, B., 2009. Process-based simulation of contrail cirrus in a global climate model. Journal of Geophysical Research, **114**: D16201.
Burkhardt, U. and Kärcher, B., 2011. Global radiative forcing from contrail cirrus. Nature Climate Change, **1**: 54-58.
Burrows, S.M., Butler, T., Jöckel, P., Tost, H., Kerkweg, A., Pöschl, U. and Lawrence, M.G., 2009. Bacteria in the global atmosphere – Part 2: Modeling of emissions and transport between different ecosystems. Atmospheric Chemistry and Physics, **9**: 9281-9297.
Cahalan, R.F., Ridgway, W., Wiscombe, W.J., Bell, T.L. and Snider, J.B., 1994. The albedo of fractal stratocumulus clouds. Journal of the Atmospheric Sciences, **51**(16): 2434-2455.
Caldeira, K. and Wood, L., 2008. Global and Arctic climate engineering: numerical model studies. Philosophical Transactions of the Royal Society A, **366**(1882): 4039-4056.
Caldwell, P. and Bretherton, C.S., 2009. Response of a subtropical stratocumulus-capped mixed layer to climate and aerosol changes. Journal of Climate, **22**: 20-38

Čalogović, J., Albert, C., Arnold, F., Beer, J., Desorgher, L. and Flueckiger, E.O., 2010. Sudden cosmic ray decreases: No change of global cloud cover. Geophysical Research Letters, **37**: L03802.
Cameron-Smith, P., Elliott, S., Maltrud, M., Erickson, D. and Wingenter, O., 2011. Changes in dimethyl sulfide oceanic distribution due to climate change. Geophysical Research Letters, **38**: L07704.
Carlton, A., Pinder, R., Bhave, P. and Pouliot, G., 2010. To what extent can biogenic SOA be controlled? Environmental Science & Technology, **44**(9): 3376-3380.
Carrico, C.M., Bergin, M.H., Shrestha, A.B., Dibb, J.E., Gomes, L. and Harris, J.M., 2003. The importance of carbon and mineral dust to seasonal aerosol properties in the Nepal Himalaya. Atmospheric Environment, **37**(20): 2811-2824.
Carslaw, K., Boucher, O., Spracklen, D., Mann, G., Rae, J., Woodward, S. and Kulmala, M., 2010. A review of natural aerosol interactions and feedbacks within the Earth system. Atmospheric Chemistry and Physics, **10**: 1701-1737.
Carslaw, K.S., Harrison, R.G. and Kirkby, J., 2002. Cosmic rays, clouds, and climate. Science, **298**(5599): 1732-1737.
Celis, J.E., Morales, J.R., Zarorc, C.A. and Inzunza, J.C., 2004. A study of the particulate matter PM_{10} composition in the atmosphere of Chillán, Chile. Chemosphere, **54**(4): 541-550.
Cess, R.D., 1975. Global climate change - Investigation of atmospheric feedback mechanisms. Tellus, **27**(3): 193-198.
Cess, R.D., Potter, G.L., Blanchet, J.P., Boer, G.J., Delgenio, A.D., Deque, M., Dymnikov, V., Galin, V., Gates, W.L., Ghan, S.J., Kiehl, J.T., Lacis, A.A., Letreut, H., Li, Z.X., Liang, X.Z., McAvaney, B.J., Meleshko, V.P., Mitchell, J.F.B., Morcrette, J.J., Randall, D.A., Rikus, L., Roeckner, E., Royer, J.F., Schlese, U., Sheinin, D.A., Slingo, A., Sokolov, A.P., Taylor, K.E., Washington, W.M., Wetherald, R.T., Yagai, I. and Zhang, M.H., 1990. Intercomparison and interpretation of climate feedback processes in 19 atmospheric general circulation models. Journal of Geophysical Research, **95**(D10): 16601-16615.
Cess, R.D., Potter, G.L., Blanchet, J.P., Boer, G.J., Ghan, S.J., Kiehl, J.T., Le Treut, H., Li, Z.X., Liang, X.Z., Mitchell, J.F.B., Morcrette, J.-J., Randall, D.A., Riches, M.R., Roeckner, E., Schlese, U., Slingo, A., Taylor, K.E., Washington, W.M., Wetherald, R.T. and Yagai, I., 1989. Interpretation of cloud-climate feedbacks as produced by 14 atmospheric general circulation models. Science, **245**(4917): 513-516.
Chae, J.H. and Sherwood, S.C., 2010. Insights into cloud-top height and dynamics from the seasonal cycle of cloud-top heights observed by MISR in the West Pacific region. Journal of the Atmospheric Sciences, **67**: 248-261.
Chakraborty, A. and Gupta, T., 2010. Chemical characterization and source apportionment of submicron (PM1) aerosol in Kanpur region, India. Aerosol and Air Quality Research, **10**: 433-445.
Chameides, W.L., Luo, C., Saylor, R., Streets, D., Huang, Y., Bergin, M. and Giorgi, F., 2002. Correlation between model-calculated anthropogenic aerosols and satellite-derived cloud optical depths: Indication of indirect effect? Journal of Geophysical Research, **107**(D10): 4085.
Chan, M.A. and Comiso, J.C., 2011. Cloud features detected by MODIS but not by CloudSat and CALIOP. Geophysical Research Letters, **38**: L24813.
Chan, Y.C., Simpson, R.W., Mctainsh, G.H., Vowles, P.D., Cohen, D.D. and Bailey, G.M., 1997. Characterisation of chemical species in $PM_{2.5}$ and PM_{10} aerosols in Brisbane, Australia. Atmospheric Environment, **31**(22): 3773-3785.
Chand, D., Wood, R., Anderson, T.L., Satheesh, S.K. and Charlson, R.J., 2009. Satellite-derived direct radiative effect of aerosols dependent on cloud cover. Nature Geoscience, **2**: 181-184.
Chang, F. and Coakley, J., 2007. Relationships between marine stratus cloud optical depth and temperature: Inferences from AVHRR observations. Journal of Climate, **20**: 2022-2036.
Chang, L., Schwartz, S., McGraw, R. and Lewis, E., 2009. Sensitivity of aerosol properties to new particle formation mechanism and to primary emissions in a continental-scale chemical transport model. Journal of Geophysical Research, **114**: D07203.
Charlson, R.J., Ackerman, A.S., Bender, F.A.M., Anderson, T.L. and Liu, Z., 2007. On the climate forcing consequences of the albedo continuum between cloudy and clear air. Tellus, **59B**(4): 715-727.
Charney, J.G., 1979. *Carbon dioxide and climate: A scientific assessment*, Washington, D. C.
Chen, L., Shi, G., Qin, S., Yang, S. and Zhang, P., 2011. Direct radiative forcing of anthropogenic aerosols over oceans from satellite observations. Advances in Atmospheric Sciences, **28**(4): 973-984.
Chen, W.T., Lee, Y.H., Adams, P.J., Nenes, A. and Seinfeld, J.H., 2010. Will black carbon mitigation dampen aerosol indirect forcing? Geophysical Research Letters, **37**: L09801.
Chen, Y., Li, Q., Kahn, R.A., Randerson, J.T. and Diner, D.J., 2009. Quantifying aerosol direct radiative effect with Multiangle Imaging Spectroradiometer observations: Top-of-atmosphere albedo change by aerosols based on land surface types. Journal of Geophysical Research, **114**: D02109.
Chen, Y. and Penner, J.E., 2005. Uncertainty analysis for estimates of the first indirect aerosol effect. Atmospheric Chemistry and Physics, **5**: 2935-2948.
Cheng, A. and Xu, K.-M., 2008. Simulation of boundary-layer cumulus and stratocumulus clouds using a cloud-resolving model with low- and third-order turbulence closures. Journal of the Meteorological Society of Japan, **86**: 67-86.
Cheng, A. and Xu, K.M., 2006. Simulation of shallow cumuli and their transition to deep convective clouds by cloud-resolving models with different third-order turbulence closures. Quarterly Journal of the Royal Meteorological Society, **132**(615): 359-382.

Cheng, Z.L., Lam, K.S., Chan, L.Y. and Cheng, K.K., 2000. Chemical characteristics of aerosols at coastal station in Hong Kong. I. Seasonal variation of major ions, halogens and mineral dusts between 1995 and 1996. Atmospheric Environment, **34**: 2771-2783.

Chepfer, H., Bony, S., Winker, D., Chiriaco, M., Dufresne, J.-L. and Sèze, G., 2008. Use of CALIPSO lidar observations to evaluate the cloudiness simulated by a climate model. Geophysical Research Letters, **35**: L15704.

Chikira, M. and Sugiyama, M., 2010. A cumulus parameterization with state-dependent entrainment rate. Part I: Description and sensitivity to temperature and humidity profiles. Journal of the Atmospheric Sciences, **67**: 2171-2193.

Choi, Y.S., Lindzen, R.S., Ho, C.H. and Kim, J., 2010. Space observations of cold-cloud phase change. Proceedings of the National Academy of Sciences of the United States of America, **107**(25): 11211-11216.

Chou, C., Neelin, J., Chen, C. and Tu, J., 2009. Evaluating the "Rich-Get-Richer" mechanism in tropical precipitation change under global warming. Journal of Climate, **22**(8): 1982-2005.

Chow, J.C., Waston, J.G., Lowenthal, D.H., Solomon, P.A., Magliano, K.L., Ziman, S.D. and Richards, L.W., 1993. PM_{10} and $PM_{2.5}$ compositions in California's San Joaquin Valley. Aerosol Science and Technology, **18**: 105-128.

Christensen, M.W. and Stephens, G.L., 2011. Microphysical and macrophysical responses of marine stratocumulus polluted by underlying ships: Evidence of cloud deepening. Journal of Geophysical Research, **116**: D03201.

Christopher, S.A., Johnson, B., Jones, T.A. and Haywood, J., 2009. Vertical and spatial distribution of dust from aircraft and satellite measurements during the GERBILS field campaign. Geophysical Research Letters, **36**: L06806.

Chuang, C.C., Penner, J.E., Prospero, J.M., Grant, K.E., Rau, G.H. and Kawamoto, K., 2002. Cloud susceptibility and the first aerosol indirect forcing: Sensitivity to black carbon and aerosol concentrations. Journal of Geophysical Research, **107**(D21): 4564.

Chuang, C.C., Penner, J.E., Taylor, K.E., Grossman, A.S. and Walton, J.J., 1997. An assessment of the radiative effects of anthropogenic sulfate. Journal of Geophysical Research, **102**(D3): 3761-3778.

Church, J.A., White, N.J., Konikow, L.F., Domingues, C.M., Cogley, J.G., Rignot, E., Gregory, J.M., van den Broeke, M.R., Monaghan, A.J. and Velicogna, I., 2011. Revisiting the Earth's sea-level and energy budgets from 1961 to 2008. Geophysical Research Letters, **38**: L18601.

Clarke, A.D., Kapustin, V.N., Eisele, F.L., Weber, R.J. and McMurry, P.H., 1999. Particle production near marine clouds: Sulfuric acid and predictions from classical binary nucleation. Geophysical Research Letters, **26**(16): 2425-2428.

Clement, A.C., Burgman, R. and Norris, J.R., 2009. Observational and model evidence for positive low-level cloud feedback. Science, **325**(5939): 460-464.

Coakley, J.A. and Walsh, C.D., 2002. Limits to the aerosol indirect radiative effect derived from observations of ship tracks. Journal of the Atmospheric Sciences, **59**(3): 668-680.

Collins, M., Booth, B.B., Bhaskaran, B., Harris, G.R., Murphy, J.M., Sexton, D.M.H. and Webb, M.J., 2011. Climate model errors, feedbacks and forcings: a comparison of perturbed physics and multi-model ensembles. Climate Dynamics, **36**(9-10): 1737-1766.

Colman, R.A. and McAvaney, B.J., 2011. On tropospheric adjustment to forcing and climate feedbacks. Climate Dynamics, **36**(9-10): 1649-1658.

Comstock, K.K., Bretherton, C.S. and Yuter, S.E., 2005. Mesoscale variability and drizzle in Southeast Pacific stratocumulus. Journal of the Atmospheric Sciences, **62**(10): 3792-3807.

Connolly, P.J., Mohler, O., Field, P.R., Saathoff, H., Burgess, R., Choularton, T. and Gallagher, M., 2009. Studies of heterogeneous freezing by three different desert dust samples. Atmospheric Chemistry and Physics, **9**(8): 2805-2824.

Couvreux, F., Hourdin, F. and Rio, C., 2010. Resolved versus parametrized boundary-layer plumes. Part I: A parametrization-oriented conditional sampling in large-eddy simulations. Boundary-Layer Meteorology, **134**(3): 441-458.

Cozic, J., Mertes, S., Verheggen, B., Cziczo, D.J., Gallavardin, S.J., Walter, S., Baltensperger, U. and Weingartner, E., 2008. Black carbon enrichment in atmospheric ice particle residuals observed in lower tropospheric mixed phase clouds. Journal of Geophysical Research, **113**(D15): D15209.

Crawford, I., Mohler, O., Schnaiter, M., Saathoff, H., Liu, D., McMeeking, G., Linke, C., Flynn, M., Bower, K.N., Connolly, P.J., Gallagher, M.W. and Coe, H., 2011. Studies of propane flame soot acting as heterogeneous ice nuclei in conjunction with single particle soot photometer measurements. Atmospheric Chemistry and Physics, **11**(18): 9549-9561.

Cross, E.S., Onasch, T.B., Ahern, A., Wrobel, W., Slowik, J.G., Olfert, J., Lack, D.A., Massoli, P., Cappa, C.D., Schwarz, J.P., Spackman, J.R., Fahey, D.W., Sedlacek, A., Trimborn, A., Jayne, J.T., Freedman, A., Williams, L.R., Ng, N.L., Mazzoleni, C., Dubey, M., Brem, B., Kok, G., Subramanian, R., Freitag, S., Clarke, A., Thornhill, D., Marr, L.C., Kolb, C.E., Worsnop, D.R. and Davidovits, P., 2010. Soot Particle Studies—Instrument Inter-Comparison—Project Overview. Aerosol Science and Technology, **44**(8): 592-611.

Crucifix, M., 2006. Does the Last Glacial Maximum constrain climate sensitivity? Geophysical Research Letters, **33**(18): L18701.

Crutzen, P.J., 2006. Albedo enhancement by stratospheric sulfur injections: A contribution to resolve a policy dilemma? Climatic Change, **77**: 211-220.

Cziczo, D.J., Froyd, K.D., Gallavardin, S.J., Moehler, O., Benz, S., Saathoff, H. and Murphy, D.M., 2009a. Deactivation of ice nuclei due to atmospherically relevant surface coatings. Environmental Research Letters, **4**(4): 044013.

Cziczo, D.J., Stetzer, O., Worringen, A., Ebert, M., Weinbruch, S., Kamphus, M., Gallavardin, S.J., Curtius, J., Borrmann, S., Froyd, K.D., Mertes, S., Mohler, O. and Lohmann, U., 2009b. Inadvertent climate modification due to anthropogenic lead. Nature Geoscience, **2**(5): 333-336.

Dai, A.G., Wang, J.H., Thorne, P.W., Parker, D.E., Haimberger, L. and Wang, X.L.L., 2011. A new approach to homogenize daily radiosonde humidity data. Journal of Climate, **24**(4): 965-991.

Davies, R. and Molloy, M., 2012. Global cloud height fluctuations measured by MISR on Terra from 2000 to 2010. Geophysical Research Letters, **39**: L03701.

Dawson, J.P., Adams, P.J. and Pandis, S.N., 2007. Sensitivity of PM2.5 to climate in the Eastern US: a modeling case study. Atmospheric Chemistry and Physics, **7**(16): 4295-4309.

de Boer, G., Morrison, H., Shupe, M.D. and Hildner, R., 2011. Evidence of liquid dependent ice nucleation in high-latitude stratiform clouds from surface remote sensors. Geophysical Research Letters, **38**: L01803.

De Gouw, J. and Jimenez, J., 2009. Organic aerosols in the Earth's atmosphere. Environmental Science & Technology, **43**(20): 7614-7618.

de Gouw, J.A., Middlebrook, A.M., Warneke, C., Goldan, P.D., Kuster, W.C., Roberts, J.M., Fehsenfeld, F.C., Worsnop, D.R., Canagaratna, M.R., Pszenny, A.A.P., Keene, W.C., Marchewka, M., Bertman, S.B. and Bates, T.S., 2005. Budget of organic carbon in a polluted atmosphere: Results from the New England Air Quality Study in 2002. Journal of Geophysical Research, **110**: D16305.

de Graaf, M., Tilstra, L., Wang, P. and Stammes, P., 2012. Retrieval of the aerosol direct radiative effect over clouds from spaceborne spectrometry. Journal of Geophysical Research, **117**: D07207.

de Leeuw, G., Andreas, E.L., Anguelova, M.D., Fairall, C.W., Lewis, E.R., O'Dowd, C., Schulz, M. and Schwartz, S.E., 2011. Production flux of sea spray aerosol. Reviews of Geophysics, **49**: RG2001.

Deboudt, K., Flament, P., Choel, M., Gloter, A., Sobanska, S. and Colliex, C., 2010. Mixing state of aerosols and direct observation of carbonaceous and marine coatings on African dust by individual particle analysis. Journal of Geophysical Research, **115**: D24207.

Decesari, S., Facchini, M.C., Carbone, C., Giulianelli, L., Rinaldi, M., Finessi, E., Fuzzi, S., Marinoni, A., Cristofanelli, P., Duchi, R., nasoni, P., Vuillermoz, E., ozic, J., Jaffrezo, J.L. and Laj, P., 2010. Chemical composition of PM_{10} and PM_1 at the high-altitude Himalayan station Nepal Climate Observatory-Pyramid (NCO-P) (5079 m.a.s.l.). Atmospheric Chemistry and Physics, **10**: 4583-4596.

Del Genio, A.D., Chen, Y.-H., Kim, D. and Yao, M.-S., 2012. The MJO transition from shallow to deep convection in CloudSat/CALIPSO data and GISS GCM simulations. Journal of Climate, **25**: 3755-3770.

Del Genio, A.D., Yao, M.-S. and Jonas, J., 2007. Will moist convection be stronger in a warmer climate? Geophysical Research Letters, **34**: L16703.

DeMott, C.A., Stan, C., Randall, D.A., Kinter III, J.L. and Khairoutdinov, M., 2011. The Asian Monsoon in the super-parameterized CCSM and its relation to tropical wave activity. Journal of Climate, **24**: 5134–5156.

DeMott, P.J., 1990. An exploratory study of ice nucleation by soot aerosols. Journal of Applied Meteorology, **29**(10): 1072-1079.

DeMott, P.J., Chen, Y., Kreidenweis, S.M., Rogers, D.C. and Sherman, D.E., 1999. Ice formation by black carbon particles. Geophysical Research Letters, **26**(16): 2429-2432.

DeMott, P.J., Prenni, A.J., Liu, X., Kreidenweis, S.M., Petters, M.D., Twohy, C.H., Richardson, M.S., Eidhammer, T. and Rogers, D.C., 2010. Predicting global atmospheric ice nuclei distributions and their impacts on climate. Proceedings of the National Academy of Sciences of the United States of America, **107**(25): 11217-11222.

Dengel, S., Aeby, D. and Grace, J., 2009. A relationship between galactic cosmic radiation and tree rings. New Phytologist, **184**(3): 545-551.

Denman, K.L., Brasseur, G., Chidthaisong, A., Ciais, P., Cox, P.M., Dickinson, R.E., Hauglustaine, D., Heinze, C., Holland, E., Jacob, D., Lohmann, U., Ramachandran, S., da Silva Dias, P.L., Wofsy, S.C. and Zhang, X., 2007. Couplings Between Changes in the Climate System and Biogeochemistry, Climate Change 2007: The Physical Science Basis. Contribution of Working Group I to the Fourth Assessment Report of the Intergovernmental Panel on Climate Change. Cambridge University Press, Cambridge, United Kingdom and New York, NY, USA.

Derbyshire, S.H., Beau, I., Bechtold, P., Grandpeix, J.-Y., Piriou, J.-M., Redelsperger, J.-L. and Soares, P.M.M., 2004. Sensitivity of moist convection to environmental humidity. Quarterly Journal of the Royal Meteorological Society, **130**(604): 3055-3079.

Després, V., Huffman, J., Burrows, S., Hoose, C., Safatov, A., Buryak, G., Frohlich-Nowoisky, J., Elbert, W., Andreae, M., Pöschl, U. and Jaenicke, R., 2012. Primary biological aerosol particles in the atmosphere: a review. Tellus, **64B**: 15598.

Dessler, A.E., 2010. A determination of the cloud feedback from climate variations over the past decade. Science, **330**(6010): 1523-1527.

Dessler, A.E., 2011. Cloud variations and the Earth's energy budget. Geophysical Research Letters, **38**: L19701.

Dessler, A.E. and Davis, S.M., 2010. Trends in tropospheric humidity from reanalysis systems. Journal of Geophysical Research, **115**: D19127.

Dessler, A.E. and Wong, S., 2009. Estimates of the water vapor climate feedback during El Nino-Southern Oscillation. Journal of Climate, **22**(23): 6404-6412.
Deuzé, J.-L., Bréon, F.-M., Devaux, C., Goloub, P., Herman, M., Lafrance, B., Maignan, F., Marchand, A., Nadal, F., Perry, G. and Tanré, D., 2001. Remote sensing of aerosols over land surfaces from POLDER-ADEOS-1 polarized measurements. Journal of Geophysical Research, **106**(D5): 4913-4926.
Devasthale, A., Kruger, O. and Graßl, H., 2005. Change in cloud-top temperatures over Europe. IEEE Geoscience and Remote Sensing Letters, **2**(3): 333-336.
Di Biagio, C., di Sarra, A. and Meloni, D., 2010. Large atmospheric shortwave radiative forcing by Mediterranean aerosols derived from simultaneous ground-based and spaceborne observations and dependence on the aerosol type and single scattering albedo. Journal of Geophysical Research, **115**: D10209.
Dickinson, R., 1975. Solar variability and the lower atmosphere. Bulletin of the American Meteorological Society, **56**: 1240-1248.
Diehl, K. and Mitra, S.K., 1998. A laboratory study of the effects of a kerosene-burner exhaust on ice nucleation and the evaporation rate of ice crystals. Atmospheric Environment, **32**(18): 3145-3151.
Diehl, K., Quick, C., Matthias-Maser, S., Mitra, S.K. and Jaenicke, R., 2001. The ice nucleating ability of pollen - Part I: Laboratory studies in deposition and condensation freezing modes. Atmospheric Research, **58**(2): 75-87.
Diehl, K. and Wurzler, S., 2010. Air parcel model simulations of a convective cloud: Bacteria acting as immersion ice nuclei. Atmospheric Environment, **44**(36): 4622-4628.
Doherty, S.J., Warren, S.G., Grenfell, T.C., Clarke, A.D. and Brandt, R.E., 2010. Light-absorbing impurities in Arctic snow. Atmospheric Chemistry and Physics, **10**(23): 11647-11680.
Donahue, N.M., Epstein, S.A., Pandis, S.N. and Robinson, A.L., 2011. A two-dimensional volatility basis set: 1. Organic-aerosol mixing thermodynamics. Atmospheric Chemistry and Physics, **11**(7): 3303-3318.
Donner, L.J., Wyman, B.L., Hemler, R.S., Horowitz, L.W., Ming, Y., Zhao, M., Golaz, J.-C., Ginoux, P., Lin, S.-J., Schwarzkopf, M.D., Austin, J., Alaka, G., Cooke, W.F., Delworth, T.L., Freidenreich, S.M., Gordon, C.T., Griffies, S.M., Held, I.M., Hurlin, W.J., Klein, S.A., Knutson, T.R., Langenhorst, A.R., Lee, H.-C., Lin, Y., Magi, B.I., Malyshev, S.L., Milly, P.C.D., Naik, V., Nath, M.J., Pincus, R., Ploshay, J.J., Ramaswamy, V., Seman, C.J., Shevliakova, E., Sirutis, J.J., Stern, W.F., Stouffer, R.J., Wilson, R.J., Winton, M., Wittenberg, A.T. and Zeng, F., 2011. The dynamical core, physical parameterizations, and basic simulation characteristics of the atmospheric component AM3 of the GFDL global coupled model CM3. Journal of Climate, **24**: 3484–3519
Doughty, C.E., Field, C.B. and McMillan, A.M.S., 2011. Can crop albedo be increased through the modification of leaf trichomes, and could this cool regional climate? Climatic Change, **104**(2): 379-387.
Dubovik, O., Herman, M., Holdak, A., Lapyonok, T., Tanré, D., Deuzé, J.L., Ducos, F., Sinyuk, A. and Lopatin, A., 2011. Statistically optimized inversion algorithm for enhanced retrieval of aerosol properties from spectral multi-angle polarimetric satellite observations. Atmospheric Measurement Techniques, **4**(5): 975-1018.
Dubovik, O., Lapyonok, T., Kaufman, Y.J., Chin, M., Ginoux, P., Kahn, R.A. and Sinyuk, A., 2008. Retrieving global aerosol sources from satellites using inverse modeling. Atmospheric Chemistry and Physics, **8**: 209–250.
Dubovik, O., Sinyuk, A., Lapyonok, T., Holben, B.N., Mishchenko, M., Yang, P., Eck, T.F., Volten, H., Munoz, O., Veihelmann, B., van der Zande, W.J., Leon, J.F., Sorokin, M. and Slutsker, I., 2006. Application of spheroid models to account for aerosol particle nonsphericity in remote sensing of desert dust. Journal of Geophysical Research, **111**(D11): D11208.
Duda, D.P., Stephens, G.L., Stevens, B. and Cotton, W.R., 1996. Effects of aerosol and horizontal inhomogeneity on the broadband albedo of marine stratus: Numerical simulations. Journal of the Atmospheric Sciences, **53**(24): 3757-3769.
Dufresne, J.-L., Quaas, J., Boucher, O., Denvil, S. and Fairhead, L., 2005. Contrasts in the effects on climate of anthropogenic sulfate aerosols between the 20th and the 21st century. Geophysical Research Letters, **32**(21): L21703.
Dufresne, J.L. and Bony, S., 2008. An assessment of the primary sources of spread of global warming estimates from coupled atmosphere-ocean models. Journal of Climate, **21**(19): 5135-5144.
Duplissy, J., Gysel, M., Alfarra, M.R., Dommen, J., Metzger, A., Prevot, A.S.H., Weingartner, E., Laaksonen, A., Raatikainen, T., Good, N., Turner, S.F., McFiggans, G. and Baltensperger, U., 2008. Cloud forming potential of secondary organic aerosol under near atmospheric conditions. Geophysical Research Letters, **35**(3): L03818.
Durkee, P.A., Noone, K.J. and Bluth, R.T., 2000. The Monterey Area Ship Track experiment. Journal of the Atmospheric Sciences, **57**(16): 2523-2541.
Dusek, U., Frank, G.P., Hildebrandt, L., Curtius, J., Schneider, J., Walter, S., Chand, D., Drewnick, F., Hings, S., Jung, D., Borrmann, S. and Andreae, M.O., 2006. Size matters more than chemistry for cloud-nucleating ability of aerosol particles. Science, **312**(5778): 1375-1378.
Dymarska, M., Murray, B.J., Sun, L.M., Eastwood, M.L., Knopf, D.A. and Bertram, A.K., 2006. Deposition ice nucleation on soot at temperatures relevant for the lower troposphere. Journal of Geophysical Research, **111**(D4): D04204.
Early, J.T., 1989. Space-based solar shield to offset greenhouse effect. Journal of the British Interplanetary Society, **42**: 567-569.

Easter, R.C., Ghan, S.J., Zhang, Y., Saylor, R.D., Chapman, E.G., Laulainen, N.S., Abdul-Razzak, H., Leung, L.R., Bian, X.D. and Zaveri, R.A., 2004. MIRAGE: Model description and evaluation of aerosols and trace gases. Journal of Geophysical Research, **109**: D20210.

Eastman, R. and Warren, S.G., 2010. Interannual variations of Arctic cloud types in relation to sea ice. Journal of Climate, **23**(15): 4216-4232.

Eitzen, Z.A., Xu, K.M. and Wong, T., 2009. Cloud and radiative characteristics of tropical deep convective systems in extended cloud objects from CERES observations. Journal of Climate, **22**(22): 5983-6000.

Ekman, A.M.L., Engström, A. and Söderberg, A., 2011. Impact of two-way aerosol–cloud interaction and changes in aerosol size distribution on simulated aerosol-induced deep convective cloud sensitivity. Journal of the Atmospheric Sciences, **68**(685–698).

Enghoff, M.B. and Svensmark, H., 2008. The role of atmospheric ions in aerosol nucleation - a review. Atmospheric Chemistry and Physics, **8**: 4911-4923.

Engling, G. and Gelencsér, A., 2010. Atmospheric Brown Clouds: From local air pollution to climate change. Elements, **6**: 223-228.

English, J.T., Toon, O.B. and Mills, M.J., 2012. Microphysical simulations of sulfur burdens from stratospheric sulfur geoengineering. Atmospheric Physics and Chemistry, **12**: 4775-4793.

Engström, A. and Ekman, A.M.L., 2010. Impact of meteorological factors on the correlation between aerosol optical depth and cloud fraction. Geophysical Research Letters, **37**: L18814.

Ervens, B., Cubison, M., Andrews, E., Feingold, G., Ogren, J.A., Jimenez, J.L., DeCarlo, P. and Nenes, A., 2007. Prediction of cloud condensation nucleus number concentration using measurements of aerosol size distributions and composition and light scattering enhancement due to humidity. Journal of Geophysical Research, **112**(D10): D10S32.

Ervens, B., Feingold, G. and Kreidenweis, S.M., 2005. Influence of water-soluble organic carbon on cloud drop number concentration. Journal of Geophysical Research, **110**(D18): D18211.

Ervens, B., Feingold, G., Sulia, K. and Harrington, J., 2011. The impact of microphysical parameters, ice nucleation mode, and habit growth on the ice/liquid partitioning in mixed-phase Arctic clouds. Journal of Geophysical Research, **116**: D17205.

Evan, A. and Norris, J., 2012. On global changes in effective cloud height. Geophysical Research Letters: submitted.

Evans, J.R.G., Stride, E.P.J., Edirisinghe, M.J., Andrews, D.J. and Simons, R.R., 2010. Can oceanic foams limit global warming? Climate Research, **42**(2): 155-160.

Facchini, M.C., Rinaldi, M., Decesari, S., Carbone, C., Finessi, E., Mircea, M., Fuzzi, S., Ceburnis, D., Flanagan, R., Nilsson, E.D., de Leeuw, G., Martino, M., Woeltjen, J. and O'Dowd, C.D., 2008. Primary submicron marine aerosol dominated by insoluble organic colloids and aggregates. Geophysical Research Letters, **35**(17): L17814.

Fan, J., Yuan, T., Comstock, J.M., Ghan, S., Khain, A., Leung, L.R., Li, Z., Martins, V.J. and Ovchinnikov, M., 2009. Dominant role by vertical wind shear in regulating aerosol effects on deep convective clouds. Journal of Geophysical Research, **114**: D22206.

Fan, J., Zhang, R., Li, G., Nielsen-Gammon, J. and Li, Z., 2005. Simulations of fine particulate matter (PM2.5) in Houston, Texas. Journal of Geophysical Research, **110**(D16): D16203.

Fan, J.W., Comstock, J.M. and Ovchinnikov, M., 2010. The cloud condensation nuclei and ice nuclei effects on tropical anvil characteristics and water vapor of the tropical tropopause layer. Environmental Research Letters, **5**(4): 6.

Farina, S.C., Adams, P.J. and Pandis, S.N., 2010. Modeling global secondary organic aerosol formation and processing with the volatility basis set: Implications for anthropogenic secondary organic aerosol. Journal of Geophysical Research, **115**: D09202.

Farrar, P.D., 2000. Are cosmic rays influencing oceanic cloud coverage – or is it only El Niño? Climatic Change, **47**(1-2): 7-15.

Favez, O., Cachier, H., Sciarea, J., Alfaro, S.C., El-Araby, T.M., Harhash, M.A. and Magdy M. Abdelwahab, 2008. Seasonality of major aerosol species and their transformations in Cairo megacity. Atmospheric Environment, **42**: 1503–1516.

Feichter, J., Lohmann, U. and Schult, I., 1997. The atmospheric sulfur cycle in ECHAM-4 and its impact on the shortwave radiation. Climate Dynamics, **13**(4): 235-246.

Feingold, G., Boers, R., Stevens, B. and Cotton, W.R., 1997. A modeling study of the effect of drizzle on cloud optical depth and susceptibility. Journal of Geophysical Research, **102**(D12): 13527-13534.

Feingold, G., Jiang, H.L. and Harrington, J.Y., 2005. On smoke suppression of clouds in Amazonia. Geophysical Research Letters, **32**(2): L02804.

Feingold, G., Koren, I., Wang, H., Xue, H. and Brewer, W.A., 2010. Precipitation-generated oscillations in open cellular cloud fields. Nature, **466**(7308): 849-852.

Feng, J., 2008. A size-resolved model and a four-mode parameterization of dry deposition of atmospheric aerosols. Journal of Geophysical Research, **113**: D12201.

Field, P.R., Mohler, O., Connolly, P., Kramer, M., Cotton, R., Heymsfield, A.J., Saathoff, H. and Schnaiter, M., 2006. Some ice nucleation characteristics of Asian and Saharan desert dust. Atmospheric Chemistry and Physics, **6**: 2991-3006.

Flanner, M.G., Zender, C.S., Hess, P.G., Mahowald, N.M., Painter, T.H., Ramanathan, V. and Rasch, P.J., 2009. Springtime warming and reduced snow cover from carbonaceous particles. Atmospheric Chemistry and Physics, **9**(7): 2481-2497.

Flanner, M.G., Zender, C.S., Randerson, J.T. and Rasch, P.J., 2007. Present-day climate forcing and response from black carbon in snow. Journal of Geophysical Research, **112**(D11): D11202.

Fletcher, J.K. and Bretherton, C.S., 2010. Evaluating boundary layer-based mass flux closures using cloud-resolving model simulations of deep convection. Journal of the Atmospheric Sciences, **67**(7): 2212-2225.

Flowers, B.A., Dubey, M.K., Mazzoleni, C., Stone, E.A., Schauer, J.J., Kim, S.W. and Yoon, S.C., 2010. Optical-chemical-microphysical relationships and closure studies for mixed carbonaceous aerosols observed at Jeju Island; 3-laser photoacoustic spectrometer, particle sizing, and filter analysis. Atmospheric Chemistry and Physics, **10**(21): 10387-10398.

Forest, C.E., Stone, P.H. and Sokolov, A.P., 2006. Estimated PDFs of climate system properties including natural and anthropogenic forcings. Geophysical Research Letters, **33**(1): L01705.

Forest, C.E., Stone, P.H., Sokolov, A.P., Allen, M.R. and Webster, M.D., 2002. Quantifying uncertainties in climate system properties with the use of recent climate observations. Science, **295**(5552): 113-117.

Fornea, A.P., Brooks, S.D., Dooley, J.B. and Saha, A., 2009. Heterogeneous freezing of ice on atmospheric aerosols containing ash, soot, and soil. Journal of Geophysical Research, **114**: D13201.

Forsström, S., Ström, J., Pedersen, C.A., Isaksson, E. and Gerland, S., 2009. Elemental carbon distribution in Svalbard snow. Journal of Geophysical Research, **114**: D19112.

Forster, P., Ramaswamy, V., Artaxo, P., Berntsen, T., Betts, R., Fahey, D.W., Haywood, J., Lean, J., Lowe, D.C., Myhre, G., Nganga, J., Prinn, R., Raga, G., Schulz, M. and Van Dorland, R., 2007. Changes in Atmospheric Constituents and in Radiative Forcing, Climate Change 2007: The Physical Science Basis. Contribution of Working Group I to the Fourth Assessment Report of the Intergovernmental Panel on Climate Change. Cambridge University Press, Cambridge, United Kingdom and New York, NY, USA.

Forster, P.M.D. and Gregory, J.M., 2006. The climate sensitivity and its components diagnosed from Earth Radiation Budget data. Journal of Climate, **19**(1): 39-52.

Fountoukis, C., Nenes, A., Meskhidze, N., Bahreini, R., Conant, W.C., Jonsson, H., Murphy, S., Sorooshian, A., Varutbangkul, V., Brechtel, F., Flagan, R.C. and Seinfeld, J.H., 2007. Aerosol-cloud drop concentration closure for clouds sampled during the International Consortium for Atmospheric Research on Transport and Transformation 2004 campaign. Journal of Geophysical Research, **112**(D10): D10S30.

Fowler, L.D. and Randall, D.A., 2002. Interactions between cloud microphysics and cumulus convection in a general circulation model. Journal of the Atmospheric Sciences, **59**: 3074-3098.

Freney, E.J., Adachi, K. and Buseck, P.R., 2010. Internally mixed atmospheric aerosol particles: Hygroscopic growth and light scattering. Journal of Geophysical Research, **115**: D19210.

Fridlind, A.M., Ackerman, A.S., McFarquhar, G., Zhang, G., Poellot, M.R., DeMott, P.J., Prenni, A.J. and Heymsfield, A.J., 2007. Ice properties of single-layer stratocumulus during the Mixed-Phase Arctic Cloud Experiment: 2. Model results. Journal of Geophysical Research, **112**(D24): D24202.

Friedman, B., Kulkarni, G., Beranek, J., Zelenyuk, A., Thornton, J.A. and Cziczo, D.J., 2011. Ice nucleation and droplet formation by bare and coated soot particles. Journal of Geophysical Research-Atmospheres, **116**: D17203.

Frömming, C., Ponater, M., Burkhardt, U., Stenke, A., Pechtl, S. and Sausen, R., 2011. Sensitivity of contrail coverage and contrail radiative forcing to selected key parameters. Atmospheric Environment, **45**: 1483-1490.

Fuzzi, S., Decesari, S., Facchini, M.C., Cavalli, F., Emblico, L., Mircea, M., Andreae, M.O., Trebs, I., Hoffer, A.s., Guyon, P., Artaxo, P., Rizzo, L.V., Lara, L.L., Pauliquevis, T., Maenhaut, W., Raes, N., Chi, X., Mayol-Bracero, O.L., Soto-Garcı, L.L., Claeys, M., Kourtchev, I., Rissler, J., Swietlicki, E., Tagliavini, E., Schkolnik, G., Falkovich, A.H., Rudich, Y., Fisch, G. and Gatti, L.V., 2007. Overview of the inorganic and organic composition of size-segregated aerosol in Rondonia, Brazil, from the biomass-burning period to the onset of the wet season. Journal of Geophysical Research, **112**: D01201.

Gagen, M., Zorita, E., McCarroll, D., Young, G.H.F., Grudd, H., Jalkanen, R., Loader, N.J., Robertson, I. and Kirchhefer, A., 2011. Cloud response to summer temperatures in Fennoscandia over the last thousand years. Geophysical Research Letters, **38**: L05701.

Galewsky, J. and Hurley, J.V., 2010. An advection-condensation model for subtropical water vapor isotopic ratios. Journal of Geophysical Research, **115**: D16116.

Gao, R.S., Schwarz, J.P., Kelly, K.K., Fahey, D.W., Watts, L.A., Thompson, T.L., Spackman, J.R., Slowik, J.G., Cross, E.S., Han, J.H., Davidovits, P., Onasch, T.B. and Worsnop, D.R., 2007. A novel method for estimating light-scattering properties of soot aerosols using a modified single-particle soot photometer. Aerosol Science and Technology, **41**(2): 125-135.

Garrett, T.J. and Zhao, C.F., 2006. Increased Arctic cloud longwave emissivity associated with pollution from mid-latitudes. Nature, **440**(7085): 787-789.

Garvert, M.F., Woods, C.P., Colle, B.A., Mass, C.F., Hobbs, P.V., Stoelinga, M.T. and Wolfe, J.B., 2005. The 13-14 December 2001 IMPROVE-2 event. Part II: Comparisons of MM5 model simulations of clouds and precipitation with observations. Journal of the Atmospheric Sciences, **62**(10): 3520-3534.

Gasso, S., 2008. Satellite observations of the impact of weak volcanic activity on marine clouds. Journal of Geophysical Research, **113**(D14): D14S19.

Geogdzhayev, I.V., Mishchenko, M.I., Rossow, W.B., Cairns, B. and Lacis, A.A., 2002. Global two-channel AVHRR retrievals of aerosol properties over the ocean for the period of NOAA-9 observations and preliminary retrievals using NOAA-7 and NOAA-11 data. Journal of the Atmospheric Sciences, **59**: 262-278.

George, R.C. and Wood, R., 2010. Subseasonal variability of low cloud radiative properties over the southeast Pacific Ocean. Atmospheric Chemistry and Physics, **10**(8): 4047-4063.

Gerasopoulos, E., Koulouri, E., Kalivitis, N., Kouvarakis, G., Saarikoski, S., Makela, T., Hillamo, R. and Mihalopoulos, N., 2007. Size-segregated mass distributions of aerosols over Eastern Mediterranean: seasonal variability and comparison with AERONET columnar size-distributions. Atmospheric Chemistry and Physics, **7**(10): 2551-2561.

Gettelman, A., Fasullo, J.T. and Kay, J.E., 2012a. Spatial decomposition of climate feedbacks in the Community Earth System Model. Journal of Climate, **submitted**.

Gettelman, A. and Fu, Q., 2008. Observed and simulated upper-tropospheric water vapor feedback. Journal of Climate, **21**: 3282-3289.

Gettelman, A., Liu, X., Barahona, D., Lohmann, U. and Chen, C., 2012b. Climate impacts of cirrus ice nucleation. Journal of Geophysical Research: submitted.

Gettelman, A., Liu, X., Ghan, S.J., Morrison, H., Park, S., Conley, A.J., Klein, S.A., Boyle, J., Mitchell, D.L. and Li, J.L.F., 2010. Global simulations of ice nucleation and ice supersaturation with an improved cloud scheme in the Community Atmosphere Model. Journal of Geophysical Research, **115**: D18216.

Ghan, S., Easter, R., Hudson, J. and Bréon, F.M., 2001. Evaluation of aerosol indirect radiative forcing in MIRAGE. Journal of Geophysical Research, **106**: 5317-5334.

Ghan, S.J., Abdul-Razzak, H., Nenes, A., Ming, Y., Liu, X. and Ovchinnikov, M., 2011. Droplet nucleation: Physically-based parameterizations and comparative evaluation. Journal of Advances in Modeling Earth Systems, **3**: M10001.

Ghan, S.J., Liu, X., Easter, R.C., Zaveri, R., Rasch, P.J., Yoon, J.-H. and Eaton, B., 2012. Toward a minimal representation of aerosols in climate models: Comparative decomposition of aerosol direct, semi-direct and indirect radiative forcing. Journal of Climate: in press.

Ginoux, P., Clarisse, L., Clerbaux, C., Coheur, P.-F., Dubovik, O., Hsu, N.C. and Damme, M.V., 2012a. Mixing of dust and NH_3 observed globally over anthropogenic dust sources Atmospheric Chemistry and Physics, **12**: in press.

Ginoux, P., Prospero, J.M., Gill, T.E., Hsu, N.C. and Zhao, M., 2012b. Global-scale attribution of anthropogenic and natural dust sources and their emission rates based on MODIS Deep Blue aerosol products. Reviews of Geophysics, **50**: RG3005.

Gioda, A., Amaral, B.S., Monteiro, I.L.G. and Saint'Pierre, T.D., 2011. Chemical composition, sources, solubility, and transport of aerosol trace elements in a tropical region. Journal of Environmental Monitoring, **13**: 2134-2142.

Girard, E., Blanchet, J.-P. and Dubois, Y., 2004. Effects of arctic sulphuric acid aerosols on wintertime low-level atmospheric ice crystals, humidity and temperature at Alert, Nunavut. Atmospheric Research, **73**: 131-148.

Givati, A. and Rosenfeld, D., 2004. Quantifying precipitation suppression due to air pollution. Journal of Applied Meteorology, **43**(7): 1038-1056.

Good, N., Topping, D.O., Allan, J.D., Flynn, M., Fuentes, E., Irwin, M., Williams, P.I., Coe, H. and McFiggans, G., 2010. Consistency between parameterisations of aerosol hygroscopicity and CCN activity during the RHaMBLe discovery cruise. Atmospheric Chemistry and Physics, **10**(7): 3189-3203.

Gorbunov, B., Baklanov, A., Kakutkina, N., Windsor, H.L. and Toumi, R., 2001. Ice nucleation on soot particles. Journal of Aerosol Science, **32**(2): 199-215.

Gordon, N.D. and Norris, J.R., 2010. Cluster analysis of midlatitude oceanic cloud regimes: mean properties and temperature sensitivity. Atmospheric Chemistry and Physics, **10**(13): 6435-6459.

Goren, T. and Rosenfeld, D., 2012. Satellite observations of ship emission fully clouding broken marine stratocumulus over large areas. Journal of Geophysical Research, **accepted**.

Graber, E.R. and Rudich, Y., 2006. Atmospheric HULIS: How humic-like are they? A comprehensive and critical review. Atmospheric Chemistry and Physics, **6**: 729-753.

Grabowski, W.W. and Smolarkiewicz, P.K., 1999. CRCP: a Cloud Resolving Convection Parameterization for modeling the tropical convecting atmosphere. Physica D, **133**: 171-178.

Grabowski, W.W., Wu, X., Moncrieff, M.W. and Hall, W.D., 1998. Cloud-resolving modeling of cloud systems during Phase III of GATE. Part II: Effects of resolution and the third spatial dimension. Journal of the Atmospheric Sciences, **55**(21): 3264–3282.

Grandpeix, J.Y. and Lafore, J.P., 2010. A density current parameterization coupled with Emanuel's convection scheme. Part I: The models. Journal of the Atmospheric Sciences, **67**(4): 881-897.

Granier, C., Bessagnet, B., Bond, T., D'Angiola, A., Denier van der Gon, H., Frost, G.J., Heil, A., Kaiser, J.W., Kinne, S., Klimont, Z., Kloster, S., Lamarque, J.-F., Liousse, C., Masui, T., Meleux, F., Mieville, A., Ohara, T., Raut, J.-C., Riahi, K., Schultz, M.G., Smith, S.J., Thompson, A., van Aardenne, J., van der Werf, G.R. and van Vuuren, D.P., 2011. Evolution of anthropogenic and biomass burning emissions of air pollutants at global and regional scales during the 1980-2010 period. Climatic Change, **109**: 163-190.

Gregory, J. and Webb, M., 2008. Tropospheric adjustment induces a cloud component in CO_2 forcing. Journal of Climate, **21**: 58-71.

Gregory, J.M., Stouffer, R.J., Raper, S.C.B., Stott, P.A. and Rayner, N.A., 2002. An observationally based estimate of the climate sensitivity. Journal of Climate, **15**(22): 3117-3121.
Grote, R. and Niinemets, U., 2008. Modeling volatile isoprenoid emissions - a story with split ends. Plant Biology, **10**: 8-28.
Guenther, A., Karl, T., Harley, P., Wiedinmyer, C., Palmer, P.I. and Geron, C., 2006. Estimates of global terrestrial isoprene emissions using MEGAN (Model of Emissions of Gases and Aerosols from Nature). Atmospheric Chemistry and Physics, **6**: 3181-3210.
Gullu, H.G., Ölmez, I. and Tuncel, G., 2000. Temporal variability of atmospheric trace element concentrations over the eastern Mediterranean Sea. Spectrochimica Acta, **B55**: 1135-1150.
Hadley, O.L. and Kirchstetter, T.W., 2012. Black-carbon reduction of snow albedo. Nature Climate Change, **2**: 437-440.
Haerter, J.O. and Berg, P., 2009. Unexpected rise in extreme precipitation caused by a shift in rain type? Nature Geoscience, **2**: 372-373.
Haerter, J.O., Berg, P. and Hagemann, S., 2010. Heavy rain intensity distributions on varying time scales and at different temperatures. Journal of Geophysical Research, **115**: D17102.
Haerter, J.O., Roeckner, E., Tomassini, L. and von Storch, J.S., 2009. Parametric uncertainty effects on aerosol radiative forcing. Geophysical Research Letters, **36**: L15707.
Hagler, G.S.W., Bergin, M.H., Salmon, L.G., Yu, J.Z., Wan, E.C.H., Zheng, M., Zeng, L.M., Kiang, C.S., Zhang, Y.H., Lau, A.K.H. and Schauer, J., 2006. Source areas and chemical composition of fine particulate matter in the Pearl River Delta region of China. Atmospheric Environment, **40**: 3802-3815.
Halfon, N., Levin, Z. and Alpert, P., 2009. Temporal rainfall fluctuations in Israel and their possible link to urban and air pollution effects. Environmental Research Letters, **4**(2): 025001.
Halloran, P.R., Bell, T.G. and Totterdell, I.J., 2010. Can we trust empirical marine DMS parameterisations within projections of future climate? Biogeosciences, **7**(5): 1645-1656.
Hallquist, M., Wenger, J.C., Baltensperger, U., Rudich, Y., Simpson, D., Claeys, M., Dommen, J., Donahue, N.M., George, C., Goldstein, A.H., Hamilton, J.F., Herrmann, H., Hoffmann, T., Iinuma, Y., Jang, M., Jenkin, M.E., Jimenez, J.L., Kiendler-Scharr, A., Maenhaut, W., McFiggans, G., Mentel, T.F., Monod, A., Prevot, A.S.H., Seinfeld, J.H., Surratt, J.D., Szmigielski, R. and Wildt, J., 2009. The formation, properties and impact of secondary organic aerosol: current and emerging issues. Atmospheric Chemistry and Physics, **9**: 5155-5236.
Hamwey, R.M., 2007. Active amplification of the terrestrial albedo to mitigate climate change: An exploratory study. Mitigation and Adaptation Strategies for Global Change, **12**(4): 419-439.
Han, Y.-J., Kim, T.-S. and Kim, H., 2008. Ionic constituents and source analysis of $PM_{2.5}$ in three Korean cities. Atmospheric Environment, **42**: 4735–4746.
Hand, V.L., Capes, G., Vaughan, D.J., Formenti, P., Haywood, J.M. and Coe, H., 2010. Evidence of internal mixing of African dust and biomass burning particles by individual particle analysis using electron beam techniques. Journal of Geophysical Research, **115**: D13301.
Hansell, R., Tsay, S., Ji, Q., Hsu, N., Jeong, M., Wang, S., Reid, J., Liou, K. and Ou, S., 2010. An assessment of the surface longwave direct radiative effect of airborne Saharan dust during the NAMMA field campaign. Journal of the Atmospheric Sciences, **67**(4): 1048-1065.
Hansen, J., Lacis, A., Rind, D., Russell, G., Stone, P., Fung, I., Ruedy, R. and Lerner, J., 1984. Climate sensitivity: Analysis of feedback mechanisms. In: J.E. Hansen and T. Takahashi (Editors), Geophysical Monograph 29. American Geophysical Union, Washington, DC, pp. 130–163.
Hansen, J. and Nazarenko, L., 2004. Soot climate forcing via snow and ice albedos. Proceedings of the National Academy of Sciences of the United States of America, **101**(2): 423-428.
Hansen, J., Sato, M., Kharecha, P., Russell, G., Lea, D. and Siddall, M., 2007. Climate change and trace gases. Philosophical Transactions of the Royal Society a-Mathematical Physical and Engineering Sciences, **365**(1856): 1925-1954.
Hansen, J., Sato, M., Kharecha, P. and von Schuckmann, K., 2011. Earth's energy imbalance and implications. Atmospheric Chemistry and Physics, **11**: 13421-13449.
Hansen, J., Sato, M., Ruedy, R., Nazarenko, L., Lacis, A., Schmidt, G.A., Russell, G., Aleinov, I., Bauer, M., Bauer, S., Bell, N., Cairns, B., Canuto, V., Chandler, M., Cheng, Y., Del Genio, A., Faluvegi, G., Fleming, E., Friend, A., Hall, T., Jackman, C., Kelley, M., Kiang, N., Koch, D., Lean, J., Lerner, J., Lo, K., Menon, S., Miller, R., Minnis, P., Novakov, T., Oinas, V., Perlwitz, J., Rind, D., Romanou, A., Shindell, D., Stone, P., Sun, S., Tausnev, N., Thresher, D., Wielicki, B., Wong, T., Yao, M. and Zhang, S., 2005. Efficacy of climate forcings. Journal of Geophysical Research, **110**(D18): D18104.
Hara, K., Yamagata, S., Yamanouchi, T., Sato, K., Herber, A., Iwasaka, Y., Nagatani, M. and Nakata, H., 2003. Mixing states of individual aerosol particles in spring Arctic troposphere during ASTAR 2000 campaign. Journal of Geophysical Research, **108**: 4209.
Hardwick Jones, R., Westra, S. and Sharma, A., 2010. Observed relationships between extreme sub-daily precipitation, surface temperature, and relative humidity. Geophysical Research Letters, **37**: L22805.
Harrington, J.Y., Lamb, D. and Carver, R., 2009. Parameterization of surface kinetic effects for bulk microphysical models: Influences on simulated cirrus dynamics and structure. Journal of Geophysical Research, **114**: D06212.
Harrison, R. and Ambaum, M., 2008. Enhancement of cloud formation by droplet charging. Proceedings of the Royal Society A, **464**: 2561-2573.

Harrison, R.G., 2008. Discrimination between cosmic ray and solar irradiance effects on clouds, and evidence for geophysical modulation of cloud thickness. Proceedings of the Royal Society A, **464**: 2575-2590.
Harrison, R.G. and Ambaum, M.H.P., 2010. Observing Forbush decreases in cloud at Shetland. Journal of Atmospheric and Solar-Terrestrial Physics, **72**(18): 1408-1414.
Harrison, R.G. and Stephenson, D.B., 2006. Empirical evidence for a nonlinear effect of galactic cosmic rays on clouds. Proceedings of the Royal Society A, **462**: 1221-1233.
Hartmann, D.L. and Larson, K., 2002. An important constraint on tropical cloud - climate feedback. Geophysical Research Letters, **29**(20): 1951.
Harvey, L.D.D. and Kaufmann, R.K., 2002. Simultaneously constraining climate sensitivity and aerosol radiative forcing. Journal of Climate, **15**(20): 2837-2861.
Haynes, J.M., Jakob, C., Rossow, W.B., Tselioudis, G. and Brown, J., 2011. Major characteristics of Southern Ocean cloud regimes and their effects on the energy budget. Journal of Climate, **24**(19): 5061-5080.
Haywood, J. and Boucher, O., 2000. Estimates of the direct and indirect radiative forcing due to tropospheric aerosols: A review. Reviews of Geophysics, **38**: 513-543.
Haywood, J. and Schulz, M., 2007. Causes of the reduction in uncertainty in the anthropogenic radiative forcing of climate between IPCC (2001) and IPCC (2007). Geophysical Research Letters, **34**(20): L20701.
Haywood, J.M., Allan, R.P., Bornemann, J., Forster, P.M., Francis, P.N., Milton, S., Radel, G., Rap, A., Shine, K.P. and Thorpe, R., 2009. A case study of the radiative forcing of persistent contrails evolving into contrail-induced cirrus. Journal of Geophysical Research, **114**: D24201.
Haywood, J.M., Johnson, B.T., Osborne, S.R., Baran, A.J., Brooks, M., Milton, S.F., Mulcahy, J., Walters, D., Allan, R.P., Klaver, A., Formenti, P., Brindley, H.E., Christopher, S. and Gupta, P., 2011. Motivation, rationale and key results from the GERBILS Saharan dust measurement campaign. Quarterly Journal of the Royal Meteorological Society, **137**(658): 1106-1116.
Heald, C., Coe, H., Jimenez, J., Weber, R., Bahreini, R., Middlebrook, A., Russell, L., Jolleys, M., Fu, T., Allan, J., Bower, K., Capes, G., Crosier, J., Morgan, W., Robinson, N., Williams, P., Cubison, M., DeCarlo, P. and Dunlea, E., 2011. Exploring the vertical profile of atmospheric organic aerosol: comparing 17 aircraft field campaigns with a global model. Atmospheric Chemistry and Physics, **11**(24): 12673-12696.
Heald, C.L., Henze, D.K., Horowitz, L.W., Feddema, J., Lamarque, J.F., Guenther, A., Hess, P.G., Vitt, F., Seinfeld, J.H., Goldstein, A.H. and Fung, I., 2008. Predicted change in global secondary organic aerosol concentrations in response to future climate, emissions, and land use change. Journal of Geophysical Research, **113**: D05211.
Heald, C.L., Jacob, D.J., Park, R.J., Russell, L.M., Huebert, B.J., Seinfeld, J.H., Liao, H. and Weber, R.J., 2005. A large organic aerosol source in the free troposphere missing from current models. Geophysical Research Letters, **32**: L18809.
Heald, C.L., Ridley, D.A., Kreidenweis, S.M. and Drury, E.E., 2010. Satellite observations cap the atmospheric organic aerosol budget. Geophysical Research Letters, **37**: L24808.
Heald, C.L. and Spracklen, D.V., 2009. Atmospheric budget of primary biological aerosol particles from fungal spores. Geophysical Research Letters, **36**: L09806.
Heckendorn, P., Weisenstein, D., Fueglistaler, S., Luo, B.P., Rozanov, E., Schraner, M., Thomason, L.W. and Peter, T., 2009. The impact of geoengineering aerosols on stratospheric temperature and ozone. Environmental Research Letters, **4**: 045108.
Hegerl, G.C., Crowley, T.J., Allen, M., Hyde, W.T., Pollack, H.N., Smerdon, J. and Zorita, E., 2007. Detection of human influence on a new, validated 1500-year temperature reconstruction. Journal of Climate, **20**(4): 650-666.
Hegg, D.A., Covert, D.S., Jonsson, H.H. and Woods, R.K., 2012. A simple relationship between cloud drop number concentration and precursor aerosol concentration for the regions of Earth's large marine stratocumulus decks. Atmospheric Chemistry and Physics, **12**(3): 1229-1238.
Held, I.M. and Shell, K.M., 2012. Using relative humidity as a state variable in climate feedback analysis. Journal of Climate, **25**(8): 2578-2582.
Held, I.M. and Soden, B.J., 2006. Robust responses of the hydrological cycle to global warming. Journal of Climate, **19**(21): 5686-5699.
Hendricks, J., Karcher, B., Lohmann, U. and Ponater, M., 2005. Do aircraft black carbon emissions affect cirrus clouds on the global scale? Geophysical Research Letters, **32**(12): L12814.
Hennigan, C., Bergin, M., Russell, A., Nenes, A. and Weber, R., 2009. Gas/particle partitioning of water-soluble organic aerosol in Atlanta. Atmospheric Chemistry and Physics, **9**(11): 3613-3628.
Heymsfield, A., Baumgardner, D., DeMott, P., Forster, P., Gierens, K. and Kärcher, B., 2010. Contrail microphysics. Bulletin of the American Meteorological Society, **91**: 465-472.
Heymsfield, A.J., McFarquhar, G.M., Collins, W.D., Goldstein, J.A., Valero, F.P.J., Spinhirne, J., Hart, W. and Pilewskie, P., 1998. Cloud properties leading to highly reflective tropical cirrus: Interpretations from CEPEX, TOGA COARE, and Kwajalein, Marshall Islands. Journal of Geophysical Research, **103**(D8): 8805-8812.
Heymsfield, A.J. and Miloshevich, L.M., 1995. Relative humidity and temperature influences on cirrus formation and evolution: Observations from wave clouds and FIRE II. Journal of the Atmospheric Sciences, **52**(23): 4302-4326.
Hill, A.A. and Dobbie, S., 2008. The impact of aerosols on non-precipitating marine stratocumulus. II: The semi-direct effect. Quarterly Journal of the Royal Meteorological Society, **134**(634): 1155-1165.

Hill, S. and Ming, Y., 2012. Nonlinear climate response to regional brightening of tropical marine stratocumulus. Geophysical Research Letters, **39**: L15707.
Hirsikko, A., Nieminen, T., Gagne, S., Lehtipalo, K., Manninen, H.E., Ehn, M., Horrak, U., Kerminen, V.M., Laakso, L., McMurry, P.H., Mirme, A., Mirme, S., Petaja, T., Tammet, H., Vakkari, V., Vana, M. and Kulmala, M., 2011. Atmospheric ions and nucleation: a review of observations. Atmospheric Chemistry and Physics, **11**(2): 767-798.
Hogan, R.J., O'Connor, E.J. and Illingworth, A.J., 2009. Verification of cloud-fraction forecasts. Quarterly Journal of the Royal Meteorological Society, **135**(643): 1494-1511.
Hohenegger, C. and Bretherton, C.S., 2011. Simulating deep convection with a shallow convection scheme. Atmospheric Chemistry and Physics, **11**(20): 10389-10406.
Hohenegger, C., Brockhaus, P., Bretherton, C.S. and Schär, C., 2009. The soil moisture–precipitation feedback in simulations with explicit and parameterized convection. Journal of Climate, **22**: 5003–5020.
Hohenegger, C., Brockhaus, P. and Schar, C., 2008. Towards climate simulations at cloud-resolving scales. Meteorologische Zeitschrift, **17**(4): 383-394.
Holben, B.N., Eck, T.F., Slutsker, I., Tanré, D., Buis, J.P., Setzer, A., Vermote, E., Reagan, J.A., Kaufman, Y.J., Nakajima, T., Lavenu, F., Jankowiak, I. and Smirnov, A., 1998. AERONET - A federated instrument network and data archive for aerosol characterization. Remote Sensing of Environment, **66**: 1-16.
Holben, B.N., Tanré, D., Smirnov, A., Eck, T.F., Slutsker, I., Abuhassan, N., Newcomb, W.W., Schafer, J.S., Chatenet, B., Lavenu, F., Kaufman, Y.J., Castle, J.V., Setzer, A., Markham, B., Clark, D., Frouin, R., Halthore, R., Karneli, A., O'Neill, N.T., Pietras, C., Pinker, R.T., Voss, K. and Zibordi, G., 2001. An emerging ground-based aerosol climatology: Aerosol optical depth from AERONET. Journal of Geophysical Research, **106**(D11): 12067-12097.
Hoose, C., Kristjansson, J.E. and Burrows, S.M., 2010a. How important is biological ice nucleation in clouds on a global scale? Environmental Research Letters, **5**(2): 024009.
Hoose, C., Kristjansson, J.E., Chen, J.P. and Hazra, A., 2010b. A classical-theory-based parameterization of heterogeneous ice nucleation by mineral dust, soot, and biological particles in a global climate model. Journal of the Atmospheric Sciences, **67**(8): 2483-2503.
Hoose, C., Kristjansson, J.E., Iversen, T., Kirkevåg, A., Seland, O. and Gettelman, A., 2009. Constraining cloud droplet number concentration in GCMs suppresses the aerosol indirect effect. Geophysical Research Letters, **36**: L12807.
Hoose, C., Lohmann, U., Erdin, R. and Tegen, I., 2008. The global influence of dust mineralogical composition on heterogeneous ice nucleation in mixed-phase clouds. Environmental Research Letters, **3**(2): 025003.
Hoose, C. and Möhler, O., 2012. Heterogeneous ice nucleation on atmospheric aerosols: a review of results from laboratory experiments. Atmospheric Chemistry and Physics Discussions, **12**: 12531-12621.
Hourdin, F., Grandpeix, J.-Y., Rio, C., Bony, S., Jam, A., Cheruy, F., Rochetin, N., Fairhead, L., Idelkadi, A., Musat, I., Dufresne, J.-L., Lahellec, A., Lefebvre, M.-P. and Roehrig, R., 2012. LMDZ5B: the atmospheric component of the IPSL climate model with revisited parameterizations for clouds and convection. Climate Dynamics, **Online first**.
Hu, M., He, L.Y., Zhang, Y.H., Wang, M., Pyo Kim, Y. and Moon, K.C., 2002. Seasonal variation of ionic species in fine particles at Qingdao. Atmospheric Environment, **36**: 5853-5859.
Huang, J., Fu, Q., Zhang, W., Wang, X., Zhang, R., Ye, H. and Warren, S.G., 2011. Dust and black carbon in seasonal snow across Northern China. Bulletin of the American Meteorological Society, **92**(2): 175-181.
Huber, M. and Knutti, R., 2011. Probabilistic climate projections with an intermediate complexity model. Part II: Application to observational datasets. Climate Dynamics: submitted.
Hudson, J.G., 1993. Cloud condensation nuclei near marine cumulus. Journal of Geophysical Research, **98**(D2): 2693-2702.
Hudson, J.G., Noble, S. and Jha, V., 2010. Comparisons of CCN with supercooled clouds. Journal of the Atmospheric Sciences, **67**(9): 3006-3018.
Hueglin, C., Gehrig, R., Baltensperger, U., Gysel, M., Monn, C. and Vonmont, H., 2005. Chemical characterisation of $PM_{2.5}$, PM_{10} and coarse particles at urban, near-city and rural sites in Switzerland. Atmospheric Environment, **39**: 637-651.
Huffman, G.J., Adler, R.F., Bolvin, D.T., Gu, G., Nelkin, E.J., Bowman, K.P., Hong, Y., Stocker, E.F. and Wolff, D.B., 2007. The TRMM multisatellite precipitation analysis (TMPA): Quasi-global, multiyear, combined-sensor precipitation estimates at fine scales. Journal of Hydrometeorology, **8**(1): 38-55.
Huneeus, N., Chevallier, F. and Boucher, O., 2012. Estimating aerosol emissions by assimilating observed aerosol optical depth in a global aerosol model. Atmospheric Chemistry and Physics, **12**: 4585-4606.
Huneeus, N., Schulz, M., Balkanski, Y., Griesfeller, J., Prospero, J., Kinne, S., Bauer, S., Boucher, O., Chin, M., Dentener, F., Diehl, T., Easter, R., Fillmore, D., Ghan, S., Ginoux, P., Grini, A., Horowitz, L., Koch, D., Krol, M.C., Landing, W., Liu, X., Mahowald, N., Miller, R., Morcrette, J.-J., Myhre, G., Penner, J., Perlwitz, J., Stier, P., Takemura, T. and Zender, C.S., 2011. Global dust model intercomparison in AeroCom phase I. Atmospheric Chemistry and Physics, **11**: 7781-7816.
Hurley, J.V. and Galewsky, J., 2010a. A last-saturation diagnosis of subtropical water vapor response to global warming. Geophysical Research Letters, **37**: L06702.
Hurley, J.V. and Galewsky, J., 2010b. A last saturation analysis of ENSO humidity variability in the Subtropical Pacific. Journal of Climate, **23**(4): 918-931.

Iannone, R., Chernoff, D.I., Pringle, A., Martin, S.T. and Bertram, A.K., 2011. The ice nucleation ability of one of the most abundant types of fungal spores found in the atmosphere. Atmospheric Chemistry and Physics, **11**(3): 1191-1201.

Iga, S., Tomita, H., Tsushima, Y. and Satoh, M., 2011. Sensitivity of Hadley Circulation to physical parameters and resolution through changing upper-tropospheric ice clouds using a global cloud-system resolving model. Journal of Climate, **24**: 2666-2679.

Illingworth, A.J., Hogan, R.J., O'Connor, E.J., Bouniol, D., Brooks, M.E., Delanoe, J., Donovan, D.P., Eastment, J.D., Gaussiat, N., Goddard, J.W.F., Haeffelin, M., Baltink, H.K., Krasnov, O.A., Pelon, J., Piriou, J.M., Protat, A., Russchenberg, H.W.J., Seifert, A., Tompkins, A.M., van Zadelhoff, G.J., Vinit, F., Willen, U., Wilson, D.R. and Wrench, C.L., 2007. Cloudnet - Continuous evaluation of cloud profiles in seven operational models using ground-based observations. Bulletin of the American Meteorological Society, **88**(6): 883-898.

Ingram, W., 2010. A very simple model for the water vapour feedback on climate change. Quarterly Journal of the Royal Meteorological Society, **136**(646): 30-40.

Ingram, W., 2012a. A new way of quantifying GCM water vapour feedback. Climate Dynamics, **Online**.

Ingram, W., 2012b. Some implications of a new approach to the water vapour feedback. Climate Dynamics, **in press**.

Inoue, T., Satoh, M., Hagihara, Y., Miura, H. and Schmetz, J., 2010. Comparison of high-level clouds represented in a global cloud system-resolving model with CALIPSO/CloudSat and geostationary satellite observations. Journal of Geophysical Research, **115**: D00H22.

Irvine, P.J., Ridgwell, A. and Lunt, D.J., 2010. Assessing the regional disparities in geoengineering impacts. Geophysical Research Letters, **37**: L18702.

Irvine, P.J., Ridgwell, A. and Lunt, D.J., 2011. Climatic effects of surface albedo geoengineering. Journal of Geophysical Research, **116**: D24112.

Irwin, M., Good, N., Crosier, J., Choularton, T.W. and McFiggans, G., 2010. Reconciliation of measurements of hygroscopic growth and critical supersaturation of aerosol particles in central Germany. Atmospheric Chemistry and Physics, **10**(23): 11737-11752.

Ito, K., Xue, N. and Thurston, G., 2004. Spatial variation of $PM_{2.5}$ chemical species and source-apportioned mass concentrations in New York City. Atmospheric Environment, **38**: 5269-5282.

Jacob, D.J., Crawford, J.H., Maring, H., Clarke, A.D., Dibb, J.E., Emmons, L.K., Ferrare, R.A., Hostetler, C.A., Russell, P.B., Singh, H.B., Thompson, A.M., Shaw, G.E., McCauley, E., Pederson, J.R. and Fisher, J.A., 2010. The Arctic Research of the Composition of the Troposphere from Aircraft and Satellites (ARCTAS) mission: design, execution, and first results. Atmospheric Chemistry and Physics, **10**(11): 5191-5212.

Jacobson, M., 2001. Global direct radiative forcing due to multicomponent anthropogenic and natural aerosols. Journal of Geophysical Research, **106**: 1551-1568.

Jacobson, M.Z., 2003. Development of mixed-phase clouds from multiple aerosol size distributions and the effect of the clouds on aerosol removal. Journal of Geophysical Research, **108**(D8): 4245.

Jacobson, M.Z., 2004. Climate response of fossil fuel and biofuel soot, accounting for soot's feedback to snow and sea ice albedo and emissivity. Journal of Geophysical Research, **109**: D21201.

Jacobson, M.Z., 2006. Effects of externally-through-internally-mixed soot inclusions within clouds and precipitation on global climate. Journal of Physical Chemistry A, **110**(21): 6860-6873.

Jacobson, M.Z., 2012. Investigating cloud absorption effects: Global absorption properties of black carbon, tar balls, and soil dust in clouds and aerosols. J. Geophys. Res., **117**(D6): D06205.

Jacobson, M.Z. and Streets, D.G., 2009. Influence of future anthropogenic emissions on climate, natural emissions, and air quality. Journal of Geophysical Research, **114**: D08118.

Jacobson, M.Z. and Ten Hoeve, J.E., 2012. Effects of urban surfaces and white roofs on global and regional climate. Journal of Climate, **25**: 1028-1044.

Jaeglé, L., Quinn, P.K., Bates, T.S., Alexander, B. and Lin, J.T., 2011. Global distribution of sea salt aerosols: new constraints from in situ and remote sensing observations. Atmospheric Chemistry and Physics, **11**(7): 3137-3157.

Jeong, M.-J. and Li, Z., 2010. Separating real and apparent effects of cloud, humidity, and dynamics on aerosol optical thickness near cloud edges. Journal of Geophysical Research, **115**: D00K32.

Jeong, M., Tsay, S., Ji, Q., Hsu, N., Hansell, R. and Lee, J., 2008. Ground-based measurements of airborne Saharan dust in marine environment during the NAMMA field experiment. Geophysical Research Letters, **35**(20).

Jeong, M.J. and Li, Z.Q., 2005. Quality, compatibility, and synergy analyses of global aerosol products derived from the Advanced Very High Resolution Radiometer and Total Ozone Mapping Spectrometer. Journal of Geophysical Research, **110**: D10S08.

Jethva, H., Satheesh, S.K., Srinivasan, J. and Moorthy, K.K., 2009. How good is the assumption about visible surface reflectance in MODIS aerosol retrieval over land? A comparison with aircraft measurements over an urban site in India. IEEE Transactions on Geoscience and Remote Sensing, **47**(7): 1990-1998.

Jiang, H.L., Xue, H.W., Teller, A., Feingold, G. and Levin, Z., 2006. Aerosol effects on the lifetime of shallow cumulus. Geophysical Research Letters, **33**(14): L14806.

Jimenez, J.L., Canagaratna, M.R., Donahue, N.M., Prevot, A.S.H., Zhang, Q., Kroll, J.H., DeCarlo, P.F., Allan, J.D., Coe, H., Ng, N.L., Aiken, A.C., Docherty, K.S., Ulbrich, I.M., Grieshop, A.P., Robinson, A.L., Duplissy, J., Smith, J.D., Wilson, K.R., Lanz, V.A., Hueglin, C., Sun, Y.L., Tian, J., Laaksonen, A., Raatikainen, T., Rautiainen, J., Vaattovaara, P., Ehn, M., Kulmala, M., Tomlinson, J.M., Collins, D.R., Cubison, M.J., Dunlea,

E.J., Huffman, J.A., Onasch, T.B., Alfarra, M.R., Williams, P.I., Bower, K., Kondo, Y., Schneider, J., Drewnick, F., Borrmann, S., Weimer, S., Demerjian, K., Salcedo, D., Cottrell, L., Griffin, R., Takami, A., Miyoshi, T., Hatakeyama, S., Shimono, A., Sun, J.Y., Zhang, Y.M., Dzepina, K., Kimmel, J.R., Sueper, D., Jayne, J.T., Herndon, S.C., Trimborn, A.M., Williams, L.R., Wood, E.C., Middlebrook, A.M., Kolb, C.E., Baltensperger, U. and Worsnop, D.R., 2009. Evolution of organic aerosols in the atmosphere. Science, **326**(5959): 1525-1529.

Jirak, I.L. and Cotton, W.R., 2006. Effect of air pollution on precipitation along the front range of the Rocky Mountains. Journal of Applied Meteorology and Climatology, **45**(1): 236-245.

Johns, T.C., Durman, C.F., Banks, H.T., Roberts, M.J., McLaren, A.J., Ridley, J.K., Senior, C.A., Williams, K.D., Jones, A., Rickard, G.J., Cusack, S., Ingram, W.J., Crucifix, M., Sexton, D.M.H., Joshi, M.M., Dong, B.W., Spencer, H., Hill, R.S.R., Gregory, J.M., Keen, A.B., Pardaens, A.K., Lowe, J.A., Bodas-Salcedo, A., Stark, S. and Searl, Y., 2006. The new Hadley Centre Climate Model (HadGEM1): Evaluation of coupled simulations. Journal of Climate, **19**(7): 1327-1353.

Johnson, B.T., Shine, K.P. and Forster, P.M., 2004. The semi-direct aerosol effect: Impact of absorbing aerosols on marine stratocumulus. Quarterly Journal of the Royal Meteorological Society, **130**(599): 1407-1422.

Johnson, N.C. and Xie, S.P., 2010. Changes in the sea surface temperature threshold for tropical convection. Nature Geoscience, **3**(12): 842-845.

Jones, A., Haywood, J. and Boucher, O., 2009. Climate impacts of geoengineering marine stratocumulus clouds. Journal of Geophysical Research, **114**: D10106.

Jones, A., Haywood, J., Boucher, O., Kravitz, B. and Robock, A., 2010. Geoengineering by stratospheric SO_2 injection: results from the Met Office HadGEM2 climate model and comparison with the Goddard Institute for Space Studies ModelE. Atmospheric Chemistry and Physics, **10**: 5999-6006.

Jones, A., Haywood, J.M. and Boucher, O., 2007. Aerosol forcing, climate response and climate sensitivity in the Hadley Centre climate model. Journal of Geophysical Research, **112**: D20211.

Jones, A., Roberts, D.L. and Slingo, A., 1994. A climate model study of indirect radiative forcing by anthropogenic sulfate aerosols. Nature, **370**(6489): 450-453.

Jones, A., Roberts, D.L., Woodage, M.J. and Johnson, C.E., 2001. Indirect sulphate aerosol forcing in a climate model with an interactive sulphur cycle. Journal of Geophysical Research, **106**(D17): 20293-20310.

Joshi, M.M., Gregory, J.M., Webb, M.J., Sexton, D.M.H. and Johns, T.C., 2008. Mechanisms for the land/sea warming contrast exhibited by simulations of climate change. Climate Dynamics, **30**(5): 455-465.

Joshi, M.M., Webb, M.J., Maycock, A.C. and Collins, M., 2010. Stratospheric water vapour and high climate sensitivity in a version of the HadSM3 climate model. Atmospheric Chemistry and Physics, **10**(15): 7161-7167.

Kahn, R., 2012. Reducing the uncertainties in direct aerosol radiative forcing. Surveys in Geophysics, **33**: 701-721.

Kahn, R.A., Gaitley, B.J., Martonchik, J.V., Diner, D.J., Crean, K.A. and Holben, B., 2005. Multiangle Imaging Spectroradiometer (MISR) global aerosol optical depth validation based on 2 years of coincident Aerosol Robotic Network (AERONET) observations. Journal of Geophysical Research, **110**(D10): D10S04.

Kahn, R.A., Garay, M.J., Nelson, D.L., Yau, K.K., Bull, M.A., Gaitley, B.J., Martonchik, J.V. and Levy, R.C., 2007. Satellite-derived aerosol optical depth over dark water from MISR and MODIS: Comparisons with AERONET and implications for climatological studies. Journal of Geophysical Research, **112**: D18205.

Kanakidou, M., Seinfeld, J.H., Pandis, S.N., Barnes, I., Dentener, F.J., Facchini, M.C., Van Dingenen, R., Ervens, B., Nenes, A., Nielsen, C.J., Swietlicki, E., Putaud, J.P., Balkanski, Y., Fuzzi, S., Horth, J., Moortgat, G.K., Winterhalter, R., Myhre, C.E.L., Tsigaridis, K., Vignati, E., Stephanou, E.G., and Wilson, J., 2005. Organic aerosol and global climate modelling: a review. Atmospheric Chemistry and Physics, **5**: 1053-1123.

Kanji, Z.A. and Abbatt, J.P.D., 2006. Laboratory studies of ice formation via deposition mode nucleation onto mineral dust and n-hexane soot samples. Journal of Geophysical Research, **111**(D16): D16204.

Kanji, Z.A., DeMott, P.J., Mohler, O. and Abbatt, J.P.D., 2011. Results from the University of Toronto continuous flow diffusion chamber at ICIS 2007: instrument intercomparison and ice onsets for different aerosol types. Atmospheric Chemistry and Physics, **11**(1): 31-41.

Kanji, Z.A., Florea, O. and Abbatt, J.P.D., 2008. Ice formation via deposition nucleation on mineral dust and organics: dependence of onset relative humidity on total particulate surface area. Environmental Research Letters, **3**(2): 025004.

Kärcher, B., Burkhardt, U., Ponater, M. and Frömming, C., 2010. Importance of representing optical depth variability for estimates of global line-shaped contrail radiative forcing. Proceedings of the National Academy of Sciences of the USA, **107**(45): 19181–19184.

Kärcher, B., Mohler, O., DeMott, P.J., Pechtl, S. and Yu, F., 2007. Insights into the role of soot aerosols in cirrus cloud formation. Atmospheric Chemistry and Physics, **7**(16): 4203-4227.

Kaspari, S.D., Schwikowski, M., Gysel, M., Flanner, M.G., Kang, S., Hou, S. and Mayewski, P.A., 2011. Recent increase in black carbon concentrations from a Mt. Everest ice core spanning 1860-2000 AD. Geophysical Research Letters, **38**: L04703.

Kato, S., Rose, F.G., Sun-Mack, S., Miller, W.F., Chen, Y., Rutan, D.A., Stephens, G.L., Loeb, N.G., Minnis, P., Wielicki, B.A., Winker, D.M., Charlock, T.P., Stackhouse, P.W., Xu, K.M. and Collins, W.D., 2011. Improvements of top-of-atmosphere and surface irradiance computations with CALIPSO-, CloudSat-, and MODIS-derived cloud and aerosol properties. Journal of Geophysical Research, **116**: D19209.

Kaufman, Y.J. and Chou, M.D., 1993. Model simulations of the competing climatic effects of SO_2 and CO_2. Journal of Climate, **6**(7): 1241-1252.
Kay, J.E. and Gettelman, A., 2009. Cloud influence on and response to seasonal Arctic sea ice loss. Journal of Geophysical Research, **114**: D18204.
Kay, J.E., Hillman, B.R., Klein, S.A., Zhang, Y., Medeiros, B., Pincus, R., Gettelman, A., Eaton, B., Boyle, J., Marchand, R. and Ackerman, T.P., 2012. Exposing global cloud biases in the Community Atmosphere Model (CAM) using satellite observations and their corresponding instrument simulators. Journal of Climate, **Online**.
Kay, J.E., L'Ecuyer, T., Gettelman, A., Stephens, G. and O'Dell, C., 2008. The contribution of cloud and radiation anomalies to the 2007 Arctic sea ice extent minimum. Geophysical Research Letters, **35**: L08503.
Kay, J.E., Raeder, K., Gettelman, A. and Anderson, J., 2011. The boundary layer response to recent Arctic sea ice loss and implications for high-latitude climate feedbacks. Journal of Climate, **24**(2): 428-447.
Kazil, J., Harrison, R.G. and Lovejoy, E.R., 2008. Tropospheric new particle formation and the role of ions. Space Science Reviews, **137**: 241-255.
Kazil, J., Stier, P., Zhang, K., Quaas, J., Kinne, S., O'Donnell, D., Rast, S., Esch, M., Ferrachat, S., Lohmann, U. and Feichter, J., 2010. Aerosol nucleation and its role for clouds and Earth's radiative forcing in the aerosol-climate model ECHAM5-HAM. Atmospheric Chemistry and Physics, **10**: 10733-10752.
Kazil, J., Zhang, K., Stier, P., Feichter, J., Lohmann, U. and O'Brien, K., 2012. The present-day decadal solar cycle modulation of Earth's radiative forcing via charged H_2SO_4/H_2O aerosol nucleation. Geophysical Research Letters, **39**: L02805.
Keith, D.W., 2000. Geoengineering the climate: History and prospect. Annual Review of Energy Environment, **25**: 245-284.
Keith, D.W., 2010. Photophoretic levitation of engineered aerosols for geoengineering. Proceedings of the National Academy of Sciences of the United States of America, **107**: 16428-16431.
Kerkweg, A., Buchholz, J., Ganzeveld, L., Pozzer, A., Tost, H. and Jöckel, P., 2006. Technical Note: An implementation of the dry removal processes DRY DEPositionand SEDImentation in the Modular Earth Submodel System (MESSy). Atmospheric Chemistry and Physics, **6**: 4617–4632.
Kerminen, V.M., Petaja, T., Manninen, H.E., Paasonen, P., Nieminen, T., Sipila, M., Junninen, H., Ehn, M., Gagne, S., Laakso, L., Riipinen, I., Vehkamaki, H., Kurten, T., Ortega, I.K., Dal Maso, M., Brus, D., Hyvarinen, A., Lihavainen, H., Leppa, J., Lehtinen, K.E.J., Mirme, A., Mirme, S., Horrak, U., Berndt, T., Stratmann, F., Birmili, W., Wiedensohler, A., Metzger, A., Dommen, J., Baltensperger, U., Kiendler-Scharr, A., Mentel, T.F., Wildt, J., Winkler, P.M., Wagner, P.E., Petzold, A., Minikin, A., Plass-Dulmer, C., Poschl, U., Laaksonen, A. and Kulmala, M., 2010. Atmospheric nucleation: highlights of the EUCAARI project and future directions. Atmospheric Chemistry and Physics, **10**: 10829-10848.
Kernthaler, S.C., Toumi, R. and Haigh, J.D., 1999. Some doubts concerning a link between cosmic ray fluxes and global cloudiness. Geophysical Research Letters, **26**: 863-865.
Khain, A., Arkhipov, M., Pinsky, M., Feldman, Y. and Ryabov, Y., 2004. Rain enhancement and fog elimination by seeding with charged droplets. Part 1: Theory and numerical simulations. Journal of Applied Meteorology, **43**: 1513–1529.
Khain, A., Rosenfeld, D. and Pokrovsky, A., 2005. Aerosol impact on the dynamics and microphysics of deep convective clouds. Quarterly Journal of the Royal Meteorological Society, **131**(611): 2639-2663.
Khain, A.P., 2009. Notes on state-of-the-art investigations of aerosol effects on precipitation: a critical review. Environmental Research Letters, **4**(1): 015004.
Khairoutdinov, M. and Kogan, Y., 2000. A new cloud physics parameterization in a large-eddy simulation model of marine stratocumulus. Monthly Weather Review, **128**(1): 229-243.
Khairoutdinov, M., Randall, D. and DeMott, C., 2005. Simulations of the atmospheric general circulation using a cloud-resolving model as a superparameterization of physical processes. Journal of the Atmospheric Sciences, **62**: 2136-2154.
Khairoutdinov, M.F., Krueger, S.K., Moeng, C.-H., Bogenschutz, P.A. and Randall, D.A., 2009. Large-eddy simulation of maritime deep tropical convection. Journal of Advances in Modeling Earth Systems, **1**: 15.
Khairoutdinov, M.F. and Randall, D.A., 2001. A cloud resolving model as a cloud parameterization in the NCAR Community Climate System Model: Preliminary results. Geophysical Research Letters, **28**: 3617-3620.
Khan, M.F., Shirasuna, Y., Hirano, K. and Masunaga, S., 2010. Characterization of PM2.5, PM2.5–10 and PMN10 in ambient air, Yokohama, Japan. Atmospheric Research, **96**: 159–172.
Khare, P. and Baruah, B.P., 2010. Elemental characterization and source identification of $PM_{2.5}$ using multivariate analysis at the suburban site of North-East India. Atmospheric Research, **98**: 148-162.
Kharin, V., Zwiers, F., Zhang, X. and Hegerl, G., 2007. Changes in temperature and precipitation extremes in the IPCC ensemble of global coupled model simulations. Journal of Climate, **20**(8): 1419-1444.
Khvorostyanov, V. and Sassen, K., 1998. Toward the theory of homogeneous nucleation and its parameterization for cloud models. Geophysical Research Letters, **25**(16): 3155-3158.
Khvorostyanov, V.I. and Curry, J.A., 2009. Critical humidities of homogeneous and heterogeneous ice nucleation: Inferences from extended classical nucleation theory. Journal of Geophysical Research, **114**: D04207.
Kiehl, J.T., 1994. On the observed near cancellation between longwave and shortwave cloud forcing in tropical regions. Journal of Climate, **7**(4): 559-565.

Kiehl, J.T., Schneider, T.L., Rasch, P.J., Barth, M.C. and Wong, J., 2000. Radiative forcing due to sulfate aerosols from simulations with the National Center for Atmospheric Research Community Climate Model, Version 3. Journal of Geophysical Research, **105**(D1): 1441-1457.

Kim, B.M., Teffera, S. and Zeldin, M.D., 2000. Characterization of $PM_{2.5}$ and PM_{10} in the South Coast air basin of Southern California: Part 1- Spatial variations. Journal of the Air & Waste Management Association, **50**: 2034-2044.

Kim, D., Sobel, A.H., Del Genio, A.D., Chen, Y., Camargo, S.J., Yao, M.-S., Kelley, M. and Nazarenko, L., 2012. The tropical subseasonal variability simulated in the NASA GISS General Circulation Model. Journal of Climate, **25**: 4641–4659.

Kim, H.-S., Huh, J.-B., Hopke, P.K., Holsen, T.M. and Yi, S.-M., 2007. Characteristics of the major chemical constituents of $PM_{2.5}$ and smog events in Seoul, Korea in 2003 and 2004. Atmospheric Environment, **41**: 6762-6770.

Kim, J.M., Lee, K., Yang, E.J., Shin, K., Noh, J.H., Park, K.T., Hyun, B., Jeong, H.J., Kim, J.H., Kim, K.Y., Kim, M., Kim, H.C., Jang, P.G. and Jang, M.C., 2010. Enhanced production of oceanic dimethylsulfide resulting from CO_2-induced grazing activity in a high CO_2 world. Environmental Science & Technology, **44**(21): 8140-8143.

King, S.M., Rosenoern, T., Shilling, J.E., Chen, Q., Wang, Z., Biskos, G., McKinney, K.A., Poschl, U. and Martin, S.T., 2010. Cloud droplet activation of mixed organic-sulfate particles produced by the photooxidation of isoprene. Atmospheric Chemistry and Physics, **10**(8): 3953-3964.

Kirchstetter, T.W., Novakov, T. and Hobbs, P.V., 2004. Evidence that the spectral dependence of light absorption by aerosols is affected by organic carbon. Journal of Geophysical Research, **109**: D21208.

Kirkby, J., 2007. Cosmic rays and climate. Surveys in Geophysics, **28**: 333-375.

Kirkby, J., Curtius, J., Almeida, J., Dunne, E., Duplissy, J., Ehrhart, S., Franchin, A., Gagne, S., Ickes, L., Kurten, A., Kupc, A., Metzger, A., Riccobono, F., Rondo, L., Schobesberger, S., Tsagkogeorgas, G., Wimmer, D., Amorim, A., Bianchi, F., Breitenlechner, M., David, A., Dommen, J., Downard, A., Ehn, M., Flagan, R.C., Haider, S., Hansel, A., Hauser, D., Jud, W., Junninen, H., Kreissl, F., Kvashin, A., Laaksonen, A., Lehtipalo, K., Lima, J., Lovejoy, E.R., Makhmutov, V., Mathot, S., Mikkila, J., Minginette, P., Mogo, S., Nieminen, T., Onnela, A., Pereira, P., Petaja, T., Schnitzhofer, R., Seinfeld, J.H., Sipila, M., Stozhkov, Y., Stratmann, F., Tome, A., Vanhanen, J., Viisanen, Y., Vrtala, A., Wagner, P.E., Walther, H., Weingartner, E., Wex, H., Winkler, P.M., Carslaw, K.S., Worsnop, D.R., Baltensperger, U. and Kulmala, M., 2011. Role of sulphuric acid, ammonia and galactic cosmic rays in atmospheric aerosol nucleation. Nature, **476**(7361): 429-433.

Kirkevåg, A., Iversen, T., Seland, O., Debernard, J.B., Storelvmo, T. and Kristjansson, J.E., 2008. Aerosol-cloud-climate interactions in the climate model CAM-Oslo. Tellus, **60A**(3): 492-512.

Kleeman, M.J., 2008. A preliminary assessment of the sensitivity of air quality in California to global change. Climatic Change, **87**: S273-S292.

Kleidman, R.G., Smirnov, A., Levy, R.C., Mattoo, S. and Tanré, D., 2012. Evaluation and wind speed dependence of MODIS aerosol retrievals over open ocean. IEEE Transactions on Geoscience and Remote Sensing, **50**: 429-435.

Klein, S.A. and Hartmann, D.L., 1993. The seasonal cycle of low stratiform clouds. Journal of Climate, **6**: 1587-1606.

Klein, S.A., McCoy, R.B., Morrison, H., Ackerman, A.S., Avramov, A., de Boer, G., Chen, M.X., Cole, J.N.S., Del Genio, A.D., Falk, M., Foster, M.J., Fridlind, A., Golaz, J.C., Hashino, T., Harrington, J.Y., Hoose, C., Khairoutdinov, M.F., Larson, V.E., Liu, X.H., Luo, Y.L., McFarquhar, G.M., Menon, S., Neggers, R.A.J., Park, S., Poellot, M.R., Schmidt, J.M., Sednev, I., Shipway, B.J., Shupe, M.D., Spangenbery, D.A., Sud, Y.C., Turner, D.D., Veron, D.E., von Salzen, K., Walker, G.K., Wang, Z.E., Wolf, A.B., Xie, S.C., Xu, K.M., Yang, F.L. and Zhang, G., 2009. Intercomparison of model simulations of mixed-phase clouds observed during the ARM Mixed-Phase Arctic Cloud Experiment. I: Single-layer cloud. Quarterly Journal of the Royal Meteorological Society, **135**(641): 979-1002.

Klocke, D., Pincus, R. and Quaas, J., 2011. On Constraining Estimates of Climate Sensitivity with Present-Day Observations through Model Weighting. Journal of Climate, **24**(23): 6092-6099.

Kloster, S., Mahowald, N.M., Randerson, J.T., Thornton, P.E., Hoffman, F.M., Levis, S., Lawrence, P.J., Feddema, J.J., Oleson, K.W. and Lawrence, D.M., 2010. Fire dynamics during the 20th century simulated by the Community Land Model. Biogeosciences, **7**(6): 1877-1902.

Knopf, D.A. and Koop, T., 2006. Heterogeneous nucleation of ice on surrogates of mineral dust. Journal of Geophysical Research, **111**(D12): D12201.

Knutti, R., Stocker, T.F., Joos, F. and Plattner, G.K., 2002. Constraints on radiative forcing and future climate change from observations and climate model ensembles. Nature, **416**(6882): 719-723.

Kocak, M., Mihalopoulos, N. and Kubilay, N., 2007. Chemical composition of the fine and coarse fraction of aerosols in the northeastern Mediterranean. Atmospheric Environment, **41**(34): 7351-7368.

Koch, D. and Del Genio, A.D., 2010. Black carbon semi-direct effects on cloud cover: review and synthesis. Atmospheric Chemistry and Physics, **10**: 7685-7696.

Koch, D., Menon, S., Genio, A.D., Ruedy, R., Alienov, I. and Schmidt, G.A., 2009a. Distinguishing aerosol impacts on climate over the past century. Journal of Climate, **22**: 2659–2677.

Koch, D., Schulz, M., Kinne, S., McNaughton, C., Spackman, J.R., Balkanski, Y., Bauer, S., Berntsen, T., Bond, T.C., Boucher, O., Chin, M., Clarke, A., Luca, N.D., Dentener, F., Diehl, T., Dubovik, O., Easter, R., Fahey, D.W., Feichter, J., Fillmore, D., Freitag, S., Ghan, S., Ginoux, P., Gong, S., Horowitz, L., Iversen, T., Kirkevåg, A.,

Klimont, Z., Kondo, Y., Krol, M., Liu, X., Miller, R., Montanaro, V., Moteki, N., Myhre, G., Penner, J.E., Perlwitz, J., Pitari, G., Reddy, S., Sahu, L., Sakamoto, H., Schuster, G., Schwarz, J.P., Seland, O., Stier, P., Takegawa, N., Takemura, T., Textor, C., Aardenne, J.A.v. and Zhao, Y., 2009b. Evaluation of black carbon estimations in global aerosol models. Atmospheric Chemistry and Physics, **9**: 9001-9026.

Koehler, K.A., Kreidenweis, S.M., DeMott, P.J., Petters, M.D., Prenni, A.J. and Mohler, O., 2010. Laboratory investigations of the impact of mineral dust aerosol on cold cloud formation. Atmospheric Chemistry and Physics, **10**(23): 11955-11968.

Koffi, B., Schulz, M., Bréon, F.M., Griesfeller, J., Winker, D., Balkanski, Y., Bauer, S., Berntsen, T., Chin, M., Collins, W.D., Dentener, F., Diehl, T., Easter, R., Ghan, S., Ginoux, P., Gong, S., Horowitz, L.W., Iversen, T., Kirkevåg, A., Koch, D., Krol, M., Myhre, G., Stier, P. and Takemura, T., 2012. Application of the CALIOP layer product to evaluate the vertical distribution of aerosols estimated by global models: Part 1. AeroCom phase I results. Journal of Geophysical Research, **117**: D10201.

Köhler, M., Ahlgrimm, M. and Beljaars, A., 2011. Unified treatment of dry convective and stratocumulus-topped boundary layers in the ECMWF model. Quarterly Journal of the Royal Meteorological Society, **137**(654): 43-57.

Kok, J.F., 2011. A scaling theory for the size distribution of emitted dust aerosols suggests climate models underestimate the size of the global dust cycle. Proceedings of the National Academy of Sciences of the United States of America, **108**(3): 1016-1021.

Kokhanovsky, A.A., Deuzé, J.L., Diner, D.J., Dubovik, O., Ducos, F., Emde, C., Garay, M.J., Grainger, R.G., Heckel, A., Herman, M., Katsev, I.L., Keller, J., Levy, R., North, P.R.J., Prikhach, A.S., Rozanov, V.V., Sayer, A.M., Ota, Y., Tanré, D., Thomas, G.E. and Zege, E.P., 2010. The inter-comparison of major satellite aerosol retrieval algorithms using simulated intensity and polarization characteristics of reflected light. Atmospheric Measurement Techniques, **3**: 909-932.

Koop, T., Luo, B.P., Tsias, A. and Peter, T., 2000. Water activity as the determinant for homogeneous ice nucleation in aqueous solutions. Nature, **406**(6796): 611-614.

Koren, I., Feingold, G. and Remer, L.A., 2010. The invigoration of deep convective clouds over the Atlantic: aerosol effect, meteorology or retrieval artifact? Atmospheric Chemistry and Physics, **10**(18): 8855-8872.

Koren, I., Kaufman, Y., Remer, L. and Martins, J., 2004. Measurement of the effect of Amazon smoke on inhibition of cloud formation. Science, **303**(5662): 1342-1345.

Koren, I., Martins, J.V., Remer, L.A. and Afargan, H., 2008. Smoke invigoration versus inhibition of clouds over the Amazon. Science, **321**(5891): 946-949.

Koren, I., Remer, L.A., Kaufman, Y.J., Rudich, Y. and Martins, J.V., 2007. On the twilight zone between clouds and aerosols. Geophysical Research Letters, **34**(8): L08805.

Korhonen, H., Carslaw, K.S., Forster, P.M., Mikkonen, S., Gordon, N.D. and Kokkola, H., 2010a. Aerosol climate feedback due to decadal increases in Southern Hemisphere wind speeds. Geophysical Research Letters, **37**: L02805.

Korhonen, H., Carslaw, K.S. and Romakkaniemi, S., 2010b. Enhancement of marine cloud albedo via controlled sea spray injections: a global model study of the influence of emission rates, microphysics and transport. Atmospheric Chemistry and Physics, **10**: 4133-4143.

Korolev, A., 2007. Limitations of the Wegener-Bergeron-Findeisen mechanism in the evolution of mixed-phase clouds. Journal of the Atmospheric Sciences, **64**(9): 3372-3375.

Korolev, A. and Field, P.R., 2008. The effect of dynamics on mixed-phase clouds: Theoretical considerations. Journal of the Atmospheric Sciences, **65**(1): 66-86.

Korolev, A.V., Emery, E.F., Strapp, J.W., Cober, S.G., Isaac, G.A., Wasey, M. and Marcotte, D., 2011. Small ice particles in tropospheric clouds: Fact or artifact? Airborne Icing Instrumentation Evaluation Experiment. Bulletin of the American Meteorological Society, **92**(8): 967-973.

Kostinski, A.B., 2008. Drizzle rates versus cloud depths for marine stratocumuli. Environmental Research Letters, **3**(4): 045019.

Kravitz, B., Caldeira, K., Boucher, O., Robock, A., Rasch, P.J., Alterskjær, K., Bou Karam, D., Cole, J.N.S., Curry, C.L., Haywood, J.M., Irvine, P.J., Ji, D., Jones, A., Lunt, D.J., Kristjánsson, J.E., Moore, J., Niemeier, U., Schmidt, H., Schulz, M., Singh, B., Tilmes, S., Watanabe, S. and Yoon, J.-H., 2012a. Climate model response from the Geoengineering Model Intercomparison Project (GeoMIP). Nature Climate Change, **submitted**.

Kravitz, B., Robock, A., Boucher, O., Schmidt, H., Talylor, K., Stinchikov, G. and Schulz, M., 2011. The Geoengineering Model Intercomparison Project (GeoMIP). Atmospheric Science Letters, **12**: 162-167.

Kravitz, B., Robock, A., Oman, L., Stenchikov, G. and Marquardt, A., 2009. Sulfuric acid deposition from stratospheric geoengineering with sulfate aerosols. Journal of Geophysical Research, **114**: D14109.

Kravitz, B., Robock, A., Shindell, D. and Miller, M., 2012b. Sensitivity of stratospheric geoengineering with black carbon to aerosol size and altitude of injection. Journal of Geophysical Research, **117**: D09203.

Kristjansson, J.E., 2002. Studies of the aerosol indirect effect from sulfate and black carbon aerosols. Journal of Geophysical Research, **107**(D15): 4246.

Kristjansson, J.E., Iversen, T., Kirkevag, A., Seland, O. and Debernard, J., 2005. Response of the climate system to aerosol direct and indirect forcing: Role of cloud feedbacks. Journal of Geophysical Research, **110**(D24): D24206.

Kristjánsson, J.E., Stjern, C.W., Stordal, F., Fjæraa, A.M., Myhre, G. and Jónasson, K., 2008. Cosmic rays, cloud condensation nuclei and clouds – a reassessment using MODIS data. Atmospheric Chemistry and Physics, **8**: 7373-7387.

Krueger, S.K., McLean, G.T. and Fu, Q., 1995. Numerical simulation of the stratus-to-cumulus transition in the subtropical marine boundary layer. 1. Boundary-layer structure. Journal of the Atmospheric Sciences, **52**(16): 2839-2850.

Kuang, Z. and Hartmann, D., 2007. Testing the fixed anvil temperature hypothesis in a cloud-resolving model. Journal of Climate, **20**: 2051-2057.

Kuang, Z.M., 2008. Modeling the interaction between cumulus convection and linear gravity waves using a limited-domain cloud system-resolving model. Journal of the Atmospheric Sciences, **65**(2): 576-591.

Kuang, Z.M. and Bretherton, C.S., 2006. A mass-flux scheme view of a high-resolution simulation of a transition from shallow to deep cumulus convection. Journal of the Atmospheric Sciences, **63**(7): 1895-1909.

Kubar, T.L., Hartmann, D.L. and Wood, R., 2007. Radiative and convective driving of tropical high clouds. Jounal of Climate, **20**: 5510–5526.

Kueppers, L.M., Snyder, M.A. and Sloan, L.C., 2007. Irrigation cooling effect: Regional climate forcing by land-use change. Geophysical Research Letters, **34**: L03703.

Kulkarni, G. and Dobbie, S., 2010. Ice nucleation properties of mineral dust particles: determination of onset RH(i), IN active fraction, nucleation time-lag, and the effect of active sites on contact angles. Atmospheric Chemistry and Physics, **10**(1): 95-105.

Kulmala, M. and Kerminen, V.M., 2008. On the formation and growth of atmospheric nanoparticles. Atmospheric Research, **90**(2-4): 132-150.

Kulmala, M., Riipinen, I., Nieminen, T., Hulkkonen, M., Sogacheva, L., Manninen, H.E., Paasonen, P., Petäjä, T., Maso, M.D., Aalto, P.P., Viljanen, A., Usoskin, I., Vainio, R., Mirme, S., Mirme, A., Miniki, A., Petzold, A., Hõrrak, U., Plaß-Dülmer, C., Birmili, W. and Kerminen, V.-M., 2010. Atmospheric data over a solar cycle: no connection between galactic cosmic rays and new particle formation. Atmospheric Chemistry and Physics, **10**: 1885-1898.

Kumar, P., Sokolik, I.N. and Nenes, A., 2011. Measurements of cloud condensation nuclei activity and droplet activation kinetics of fresh unprocessed regional dust samples and minerals. Atmospheric Chemistry and Physics, **11**: 3527-3541.

Kumar, R., Srivastava, S.S. and Kumari, K.M., 2007. Characteristics of aerosols over suburban and urban site of semiarid region in India: Seasonal and spatial variations. Aerosol and Air Quality Research, **7**(4): 531-549.

Kurten, T., Loukonen, V., Vehkamaki, H. and Kulmala, M., 2008. Amines are likely to enhance neutral and ion-induced sulfuric acid-water nucleation in the atmosphere more effectively than ammonia. Atmospheric Chemistry and Physics, **8**(14): 4095-4103.

Kvalevåg, M.M. and Myhre, G., 2007. Human impact on direct and diffuse solar radiation during the industrial era. Journal of Climate, **20**(19): 4874-4883.

Laken, B., Kniveton, D. and Wolfendale, A., 2011. Forbush decreases, solar irradiance variations, and anomalous cloud changes. Journal of Geophysical Research, **116**: D09201.

Laken, B., Pallé, E. and Miyahara, H., 2012. A decade of the Moderate Resolution Imaging Spectroradiometer: is a solar–cloud link detectable? Journal of Climate, **25**: 4430-4440.

Laken, B., Wolfendale, A. and Kniveton, D., 2009. Cosmic ray decreases and changes in the liquid water cloud fraction over the oceans. Geophysical Research Letters, **36**: L23803.

Laken, B.A. and Čalogović, J., 2011. Solar irradiance, cosmic rays and cloudiness over daily timescales. Geophysical Research Letters, **38**: L24811.

Laken, B.A., Kniveton, D.R. and Frogley, M.R., 2010. Cosmic rays linked to rapid mid-latitude cloud changes. Atmospheric Chemistry and Physics, **10**: 10941–10948.

Lance, S., Shupe, M.D., Feingold, G., Brock, C.A., Cozic, J., Holloway, J.S., Moore, R.H., Nenes, A., Schwarz, J.P., Spackman, J.R., Froyd, K.D., Murphy, D.M., Brioude, J., Cooper, O.R., Stohl, A. and Burkhart, J.F., 2011. Cloud condensation nuclei as a modulator of ice processes in Arctic mixed-phase clouds. Atmospheric Chemistry and Physics, **11**(15): 8003-8015.

Lanz, V.A., Alfarra, M.R., Baltensperger, U., Buchmann, B., Hueglin, C. and Prévôt, A.S.H., 2007. Source apportionment of submicron organic aerosols at an urban site by factor analytical modelling of aerosol mass spectra. Atmospheric Chemistry and Physics, **7**(6): 1503-1522.

Larson, V.E., Wood, R., Field, P.R., Golaz, J.-C., Vonder Haar, T.H. and Cotton, W.R., 2001. Systematic Biases in the Microphysics and Thermodynamics of Numerical Models That Ignore Subgrid-Scale Variability. Journal of the Atmospheric Sciences, **58**(9): 1117–1128.

Latham, J., 1990. Control of global warming? Nature, **347**: 339-340.

Latham, J., Rasch, P.J., Chen, C.C., Kettles, L., Gadian, A., Gettelman, A., Morrison, H., Bower, K. and Choularton, T., 2008. Global temperature stabilization via controlled albedo enhancement of low-level maritime clouds. Philosophical Transactions Royal Society London, **366**(1882): 3969-3987.

Lathière, J., Hewitt, C.N. and Beerling, D.J., 2010. Sensitivity of isoprene emissions from the terrestrial biosphere to 20th century changes in atmospheric CO_2 concentration, climate, and land use. Global Biogeochemical Cycles, **24**: GB1004.

Lau, K.M., Kim, M.K. and Kim, K.M., 2006. Asian summer monsoon anomalies induced by aerosol direct forcing: the role of the Tibetan Plateau. Climate Dynamics, **26**(7-8): 855-864.
Lavers, D., Allan, R., Wood, E., Villarini, G., Brayshaw, D. and Wade, A., 2011. Winter floods in Britain are connected to atmospheric rivers. Geophysical Research Letters, **38**: L23803.
Lebel, T., Parker, D.J., Flamant, C., Bourles, B., Marticorena, B., Mougin, E., Peugeot, C., Diedhiou, A., Haywood, J.M., Ngamini, J.B., Polcher, J., Redelsperger, J.L. and Thorncroft, C.D., 2010. The AMMA field campaigns: Multiscale and multidisciplinary observations in the West African region. Quarterly Journal of the Royal Meteorological Society, **136**: 8-33.
Lebsock, M.D., Kummerow, C. and Stephens, G.L., 2010. An observed tropical oceanic radiative-convective cloud feedback. Journal of Climate, **23**: 2065-2078.
Lebsock, M.D., Stephens, G.L. and Kummerow, C., 2008. Multisensor satellite observations of aerosol effects on warm clouds. Journal of Geophysical Research, **113**(D15): D15205.
Lee, D., Fahey, D., Forster, P., Newton, P., Wit, R., Lim, L., Owen, B. and Sausen, R., 2009. Aviation and global climate change in the 21st century. Atmospheric Environment, **43**: 3520-3537.
Lee, H.S. and Kang, B.W., 2001. Chemical characteristics of principal $PM_{2.5}$ species in Chongju, South Korea. Atmospheric Environment, **35**: 739-749.
Lee, L.A., Carslaw, K.S., Pringle, K., Mann, G.W. and Spracklen, D.V., 2011. Emulation of a complex global aerosol model to quantify sensitivity to uncertain parameters. Atmospheric Chemistry and Physics, **11**: 12253-12273.
Lee, S.-S., Feingold, G. and Chuang, P.Y., 2012. Effect of aerosol on cloud-environment interactions in trade cumulus. Journal of the Atmospheric Sciences.
Lee, S.S., 2012. Effect of aerosol on circulations and precipitation in deep convective clouds. Journal of the Atmospheric Sciences, **69**(6): 1957-1974.
Lenderink, G., Mok, H., Lee, T. and van Oldenborgh, G., 2011. Scaling and trends of hourly precipitation extremes in two different climate zones - Hong Kong and the Netherlands. Hydrology and Earth System Sciences, **15**(9): 3033-3041.
Lenderink, G. and Van Meijgaard, E., 2008. Increase in hourly precipitation extremes beyond expectations from temperature changes. Nature Geoscience, **1**(8): 511-514.
Lenschow, P., Abraham, H.J., Kutzner, K., Lutz, M., Preu, J.D. and Reichenbacher, W., 2001. Some ideas about the sources of PM_{10}. Atmospheric Environment, **35**: 23-33.
Lenton, T.M. and Vaughan, N.E., 2009. The radiative forcing potential of different climate geoengineering options. Atmospheric Chemistry and Physics, **9**: 5539-5561.
Levin, Z. and Cotton, W.R., 2009. Aerosol Pollution Impact on Precipitation: A Scientific Review. Springer Verlag, 386 pp. pp.
Levy, R.C., Remer, L.A., Kleidman, R.G., Mattoo, S., Ichoku, C., Kahn, R. and Eck, T.F., 2010. Global evaluation of the Collection 5 MODIS dark-target aerosol products over land. Atmospheric Chemistry and Physics, **10**: 10399-10420.
Li, J., Pósfai, M., Hobbs, P.V. and Buseck, P.R., 2003. Individual aerosol particles from biomass burning in southern Africa: 2, Compositions and aging of inorganic particles. Journal of Geophysical Research, **108**(D13): 8484.
Li, Z., Lee, K.-H., Wang, Y., Xin, J. and Hao, W.-M., 2010. First observation-based estimates of cloud-free aerosol radiative forcing across China. Journal of Geophysical Research, **115**: D00K18.
Liao, H., Chen, W.T. and Seinfeld, J.H., 2006. Role of climate change in global predictions of future tropospheric ozone and aerosols. Journal of Geophysical Research, **111**(D12): D12304.
Liao, H., Zhang, Y., Chen, W.T., Raes, F. and Seinfeld, J.H., 2009. Effect of chemistry-aerosol-climate coupling on predictions of future climate and future levels of tropospheric ozone and aerosols. Journal of Geophysical Research, **114**: D10306.
Libardoni, A.G. and Forest, C.E., 2011. Sensitivity of distributions of climate system properties to the surface temperature dataset. Geophysical Research Letters, **38**: L22705.
Liepert, B. and Previdi, M., 2012. Inter-model variability and biases of the global water cycle in CMIP3 coupled climate models. Environmental Research Letters, **7**(1).
Lin, G., Penner, J.E., Sillman, S., Taraborrelli, D. and Lelieveld, J., 2012. Global modeling of SOA formation from dicarbonyls, epoxides, organic nitrates and peroxides. Atmospheric Chemistry and Physics, **12**: 4743-4774.
Lindzen, R.S. and Choi, Y.-S., 2011. On the observational determination of climate sensitivity and its implications. Asia-Pacific Journal of Atmospheric Sciences, **47**(4): 377-390.
Liou, K.N. and Ou, S.C., 1989. The role of cloud microphysical processes in climate - An assessment from a one-dimensional perspective. Journal of Geophysical Research, **94**(D6): 8599-8607.
Liu, W., Wang, Y., Russell, A. and Edgerton, E.S., 2005. Atmospheric aerosol over two urban-rural pairs in the southeastern United States: Chemical composition and possible sources. Atmospheric Environment, **39**: 4453-4470.
Liu, X., Easter, R.C., Ghan, S.J., Zaveri, R., Rasch, P., Shi, X., Lamarque, J.F., Gettelman, A., Morrison, H., Vitt, F., Conley, A., Park, S., Neale, R., Hannay, C., Ekman, A.M.L., Hess, P., Mahowald, N., Collins, W., Iacono, M.J., Bretherton, C.S., Flanner, M.G. and Mitchell, D., 2012. Toward a minimal representation of aerosols in climate models: description and evaluation in the Community Atmosphere Model CAM5. Geoscientific Model Development, **5**: 709-739.

Liu, X., Penner, J., Ghan, S. and Wang, M., 2007. Inclusion of ice microphysics in the NCAR community atmospheric model version 3 (CAM3). Journal of Climate, **20**: 4526-4547.
Liu, X.H., Penner, J.E. and Wang, M.H., 2009. Influence of anthropogenic sulfate and black carbon on upper tropospheric clouds in the NCAR CAM3 model coupled to the IMPACT global aerosol model. Journal of Geophysical Research, **114**: D03204.
Liu, Y. and Daum, P.H., 2002. Anthropogenic aerosols: Indirect warming effect from dispersion forcing. Nature, **419**: 580-581.
Liu, Y., Key, J.R. and Wang, X., 2008. The influence of changes in cloud cover on recent surface temperature trends in the Arctic. Journal of Climate, **21**(4): 705-715.
Lobell, D., Bala, G., Mirin, A., Phillips, T., Maxwell, R. and Rotman, D., 2009. Regional differences in the influence of irrigation on climate. J. Climate, **22**: 2248–2255.
Lock, A.P., 2009. Factors influencing cloud area at the capping inversion for shallow cumulus clouds. Quarterly Journal of the Royal Meteorological Society, **135**(641): 941-952.
Lodhi, A., Ghauri, B., Khan, M.R., Rahmana, S. and Shafiquea, S., 2009. Particulate matter ($PM_{2.5}$) concentration and source apportionment in Lahore. Journal of the Brazilian Chemical Society, **20**(10): 1811-1820.
Loeb, N.G. and Manalo-Smith, N., 2005. Top-of-atmosphere direct radiative effect of aerosols over global oceans from merged CERES and MODIS observations. Journal of Climate, **18**: 3506-3526.
Loeb, N.G. and Schuster, G.L., 2008. An observational study of the relationship between cloud, aerosol and meteorology in broken low-level cloud conditions. Journal of Geophysical Research, **113**(D14): D14214.
Loeb, N.G. and Su, W.Y., 2010. Direct aerosol radiative forcing uncertainty based on a radiative perturbation analysis. Journal of Climate, **23**: 5288-5293.
Loeb, N.G., Wielicki, B.A., Doelling, D.R., Smith, G.L., Keyes, D.F., Kato, S., Manalo-Smith, N. and Wong, T., 2009. Toward optimal closure of the Earth's top-of-atmosphere radiation budget. Journal of Climate, **22**(3): 748-766.
Logan, T., Xi, B., Dong, X., Obrecht, R., Li, Z. and Cribb, M., 2010. A study of Asian dust plumes using satellite, surface, and aircraft measurements during the INTEX-B field experiment. Journal of Geophysical Research, **115**: D00K25.
Lohmann, U., 2002a. A glaciation indirect aerosol effect caused by soot aerosols. Geophysical Research Letters, **29**(4): 1052.
Lohmann, U., 2002b. Possible aerosol effects on ice clouds via contact nucleation. Journal of the Atmospheric Sciences, **59**(3): 647-656.
Lohmann, U., 2004. Can anthropogenic aerosols decrease the snowfall rate? Journal of the Atmospheric Sciences, **61**(20): 2457-2468.
Lohmann, U., 2008. Global anthropogenic aerosol effects on convective clouds in ECHAM5-HAM. Atmospheric Chemistry and Physics, **8**: 2115-2131.
Lohmann, U. and Diehl, K., 2006. Sensitivity studies of the importance of dust ice nuclei for the indirect aerosol effect on stratiform mixed-phase clouds. Journal of the Atmospheric Sciences, **63**(3): 968-982.
Lohmann, U. and Feichter, J., 1997. Impact of sulfate aerosols on albedo and lifetime of clouds: A sensitivity study with the ECHAM4 GCM. Journal of Geophysical Research, **102**(D12): 13685-13700.
Lohmann, U. and Feichter, J., 2001. Can the direct and semi-direct aerosol effect compete with the indirect effect on a global scale? Geophysical Research Letters, **28**(1): 159-161.
Lohmann, U. and Feichter, J., 2005. Global indirect aerosol effects: a review. Atmospheric Chemistry and Physics, **5**: 715-737.
Lohmann, U., Feichter, J., Penner, J. and Leaitch, R., 2000. Indirect effect of sulfate and carbonaceous aerosols: A mechanistic treatment. Journal of Geophysical Research, **105**(D10): 12193-12206.
Lohmann, U. and Ferrachat, S., 2010. Impact of parametric uncertainties on the present-day climate and on the anthropogenic aerosol effect. Atmospheric Chemistry and Physics, **10**(23): 11373-11383.
Lohmann, U. and Hoose, C., 2009. Sensitivity studies of different aerosol indirect effects in mixed-phase clouds. Atmospheric Chemistry and Physics, **9**: 8917-8934.
Lohmann, U. and Kärcher, B., 2002. First interactive simulations of cirrus clouds formed by homogeneous freezing in the ECHAM general circulation model. Journal of Geophysical Research, **107**: 4105.
Lohmann, U. and Lesins, G., 2002. Stronger constraints on the anthropogenic indirect aerosol effect. Science, **298**(5595): 1012-1015.
Lohmann, U., Rotstayn, L., Storelvmo, T., Jones, A., Menon, S., Quaas, J., Ekman, A.M.L., Koch, D. and Ruedy, R., 2010. Total aerosol effect: radiative forcing or radiative flux perturbation? Atmospheric Chemistry and Physics, **10**(7): 3235-3246.
Lohmann, U., Spichtinger, P., Jess, S., Peter, T. and Smit, H., 2008. Cirrus cloud formation and ice supersaturated regions in a global climate model. Environmental Research Letters, **3**: 045022.
Lohmann, U., Stier, P., Hoose, C., Ferrachat, S., Kloster, S., Roeckner, E. and Zhang, J., 2007. Cloud microphysics and aerosol indirect effects in the global climate model ECHAM5-HAM. Atmospheric Chemistry and Physics, **7**(13): 3425-3446.
Lonati, G., Giugliano, M., Butelli, P., Romele, L. and Tardivo, R., 2005. Major chemical components of $PM_{2.5}$ in Milan (Italy). Atmospheric Environment, **39**: 1925-1934.

Lu, M.-L., Conant, W.C., Jonsson, H.H., Varutbangkul, V., Flagan, R.C. and Seinfeld, J.H., 2007. The marine stratus/stratocumulus experiment (MASE): aerosol-cloud relationships in marine stratocumulus. Journal of Geophysical Research, **112**(D10): D10209.

Lu, M.-L., Feingold, G., Jonsson, H.H., Chuang, P.Y., Gates, H., Flagan, R.C. and Seinfeld, J.H., 2008. Aerosol-cloud relationships in continental shallow cumulus. Journal of Geophysical Research, **113**(D15): D15201.

Lubin, D. and Vogelmann, A.M., 2006. A climatologically significant aerosol longwave indirect effect in the Arctic. Nature, **439**(7075): 453-456.

Lüönd, F., Stetzer, O., Welti, A. and Lohmann, U., 2010. Experimental study on the ice nucleation ability of size-selected kaolinite particles in the immersion mode. Journal of Geophysical Research, **115**: D14201.

Lunt, D., Ridgwell, A., Valdes, P. and Seale, A., 2008. "Sunshade World": A fully coupled GCM evaluation of the climatic impacts of geoengineering. Geophysical Research Letters, **35**(12): L12710.

Lyapustin, A., Gatebe, C., Kahn, R., Brandt, R., Redemann, J., Russell, P., King, M., Pedersen, C., Gerland, S., Poudyal, R., Marshak, A., Wang, Y., Schaaf, C., Hall, D. and Kokhanovsky, A., 2010. Analysis of snow bidirectional reflectance from ARCTAS Spring-2008 Campaign. Atmospheric Chemistry and Physics, **10**: 4359-4375.

Ma, H.Y., Kohler, M., Li, J.L.F., Farrara, J.D., Mechoso, C.R., Forbes, R.M. and Waliser, D.E., 2012a. Evaluation of an ice cloud parameterization based on a dynamical-microphysical lifetime concept using CloudSat observations and the ERA-Interim reanalysis. Journal of Geophysical Research, **117**: D05210.

Ma, X., Yu, F. and Luo, G., 2012b. Aerosol direct radiative forcing based on GEOS-Chem-APM and uncertainties. Atmospheric Chemistry and Physics, **12**: 5563-5581.

Mace, G.G., Zhang, Q.Q., Vaughan, M., Marchand, R., Stephens, G., Trepte, C. and Winker, D., 2009. A description of hydrometeor layer occurrence statistics derived from the first year of merged Cloudsat and CALIPSO data. Journal of Geophysical Research, **114**: D00A26.

Maenhaut, W., Fernandez-Jimenez, M.-T., Vanderzalm, J.L., Hooper, B., Hooper, M.A. and Tapper, N.J., 2000. Aerosol composition at Jabiru, Australia, and impact of biomass burning. Journal of Aerosol Science, **31**(Suppl. 1): 745-746.

Maenhaut, W., Salma, I. and Cafrneyer, J., 1996. Regional atmospheric aerosol composition and sources in the eastern Transvaal, South Africa, and impact of biomass burning. Journal of Geophysical Research, **101**(D19): 23613-23650.

Magee, N., Moyle, A.M. and Lamb, D., 2006. Experimental determination of the deposition coefficient of small cirrus-like ice crystals near −50°C. Geophysical Research Letters, **33**(17): L17813.

Mahowald, N.M., Engelstaedter, S., Luo, C., Sealy, A., Artaxo, P., Benitez-Nelson, C., Bonnet, S., Chen, Y., Chuang, P.Y., Cohen, D.D., Dulac, F., Herut, B., Johansen, A.M., Kubilay, N., Losno, R., Maenhaut, W., Paytan, A., Prospero, J.A., Shank, L.M. and Siefert, R.L., 2009. Atmospheric iron deposition: Global distribution, variability, and human perturbations. Annual Review of Marine Science, **1**: 245-278.

Mahowald, N.M., Kloster, S., Engelstaedter, S., Moore, J.K., Mukhopadhyay, S., McConnell, J.R., Albani, S., Doney, S.C., Bhattacharya, A., Curran, M.A.J., Flanner, M.G., Hoffman, F.M., Lawrence, D.M., Lindsay, K., Mayewski, P.A., Neff, J., Rothenberg, D., Thomas, E., Thornton, P.E. and Zender, C.S., 2010. Observed 20th century desert dust variability: impact on climate and biogeochemistry. Atmospheric Chemistry and Physics, **10**(22): 10875-10893.

Mahowald, N.M., Lamarque, J.F., Tie, X.X. and Wolff, E., 2006a. Sea-salt aerosol response to climate change: Last Glacial Maximum, preindustrial, and doubled carbon dioxide climates. Journal of Geophysical Research, **111**(D5): D05303.

Mahowald, N.M., Muhs, D.R., Levis, S., Rasch, P.J., Yoshioka, M., Zender, C.S. and Luo, C., 2006b. Change in atmospheric mineral aerosols in response to climate: Last glacial period, preindustrial, modern, and doubled carbon dioxide climates. Journal of Geophysical Research, **111**(D10): D10202.

Makkonen, R., Asmi, A., Kerminen, V., Boy, M., Arneth, A., Hari, P. and Kulmala, M., 2012. Air pollution control and decreasing new particle formation lead to strong climate warming. Atmospheric Chemistry and Physics, **12**(3): 1515-1524.

Malm, W.C. and Schichtel, B.A., 2004. Spatial and monthly trends in speciated fine particle concentration in the United States. Journal of Geophysical Research, **109**: D03306.

Malm, W.C., Sisler, J.F., Huffman, D., Eldred, R.A. and Cahill, T.A., 1994. Spatial and seasonal trends in particle concentration and optical extinction in the United States. Journal of Geophysical Research, **99**: 1347-1370.

Mangold, A., Wagner, R., Saathoff, H., Schurath, U., Giesemann, C., Ebert, V., Kramer, M. and Mohler, O., 2005. Experimental investigation of ice nucleation by different types of aerosols in the aerosol chamber AIDA: implications to microphysics of cirrus clouds. Meteorologische Zeitschrift, **14**(4): 485-497.

Manninen, H.E., Nieminen, T., Asmi, E., Gagne, S., Hakkinen, S., Lehtipalo, K., Aalto, P., Vana, M., Mirme, A., Mirme, S., Horrak, U., Plass-Dulmer, C., Stange, G., Kiss, G., Hoffer, A., Toeroe, N., Moerman, M., Henzing, B., de Leeuw, G., Brinkenberg, M., Kouvarakis, G.N., Bougiatioti, A., Mihalopoulos, N., O'Dowd, C., Ceburnis, D., Arneth, A., Svenningsson, B., Swietlicki, E., Tarozzi, L., Decesari, S., Facchini, M.C., Birmili, W., Sonntag, A., Wiedensohler, A., Boulon, J., Sellegri, K., Laj, P., Gysel, M., Bukowiecki, N., Weingartner, E., Wehrle, G., Laaksonen, A., Hamed, A., Joutsensaari, J., Petaja, T., Kerminen, V.M. and Kulmala, M., 2010. EUCAARI ion spectrometer measurements at 12 European sites - analysis of new particle formation events. Atmospheric Chemistry and Physics, **10**(16): 7907-7927.

Mapes, B. and Neale, R., 2011. Parameterizing convective organization to escape the entrainment dilemma. Journal of Advances in Modeling Earth Systems, **3**: M06004.
Mariani, R.L. and Mello, W.Z.d., 2007. PM2.5–10, PM2.5 and associated water-soluble inorganic species at a coastal urban site in the metropolitan region of Rio de Janeiro. Atmospheric Environment, **41**: 2887–2892.
Markowicz, K.M. and Witek, M.L., 2011. Simulations of contrail optical properties and radiative forcing for various crystal shapes. J. Appl. Meteor. Climatol., **50**: 1740–1755.
Marlon, J.R., Bartlein, P.J., Carcaillet, C., Gavin, D.G., Harrison, S.P., Higuera, P.E., Joos, F., Power, M.J. and Prentice, I.C., 2008. Climate and human influences on global biomass burning over the past two millennia. Nature Geoscience, **1**(10): 697-702.
Marsh, N.D. and Svensmark, H., 2000. Low cloud properties influenced by cosmic rays. Physical Review Letters, **85**: 5004-5007.
Martin, S.T., Andreae, M.O., Althausen, D., Artaxo, P., Baars, H., Borrmann, S., Chen, Q., Farmer, D.K., Guenther, A., Gunthe, S.S., Jimenez, J.L., Karl, T., Longo, K., Manzi, A., Müller, T., Pauliquevis, T., Petters, M.D., Prenni, A.J., Pöschl, U., Rizzo, L.V., Schneider, J., Smith, J.N., Swietlicki, E., Tota, J., Wang, J., Wiedensohler, A. and Zorn, S.R., 2010a. An overview of the Amazonian Aerosol Characterization Experiment 2008 (AMAZE-08). Atmospheric Chemistry and Physics, **10**: 11415-11438.
Martin, S.T., Andreae, M.O., Artaxo, P., Baumgardner, D., Chen, Q., Goldstein, A.H., Guenther, A., Heald, C.L., Mayol-Bracero, O.L., McMurry, P.H., Pauliquevis, T., Pöschl, U., Prather, K.A., Roberts, G.C., Saleska, S.R., Dias, M.A.S., Spracklen, D.V., Swietlicki, E. and Trebs, I., 2010b. Sources and properties of Amazonian aerosol particles. Review of Geophysics, **48**: RG2002.
Mauger, G.S. and Norris, J.R., 2010. Assessing the impact of meteorological history on subtropical cloud fraction. Journal of Climate, **23**(11): 2926-2940.
May, P.T., Mather, J.H., Vaughan, G., Jakob, C., McFarquhar, G.M., Bower, K.N. and Mace, G.G., 2008. The tropical warm pool international cloud experiment. Bulletin of the American Meteorological Society, **89**(5): 629-645.
McComiskey, A. and Feingold, G., 2008. Quantifying error in the radiative forcing of the first aerosol indirect effect. Geophysical Research Letters, **35**(2): L02810.
McComiskey, A. and Feingold, G., 2012. The scale problem in quantifying aerosol indirect effects. Atmospheric Chemistry and Physics, **12**: 1031-1049.
McConnell, J.R., Edwards, R., Kok, G.L., Flanner, M.G., Zender, C.S., Saltzman, E.S., Banta, J.R., Pasteris, D.R., Carter, M.M. and Kahl, J.D.W., 2007. 20th-century industrial black carbon emissions altered Arctic climate forcing. Science, **317**: 1381-1384.
McCracken, K.G. and Beer, J., 2007. Long-term changes in the cosmic ray intensity at Earth, 1428–2005. J. Geophys. Res. , **112**: A10101.
McFarquhar, G.M., Ghan, S., Verlinde, J., Korolev, A., Strapp, J.W., Schmid, B., Tomlinson, J.M., Wolde, M., Brooks, S.D., Cziczo, D., Dubey, M.K., Fan, J., Flynn, C., Gultepe, I., Hubbe, J., Gilles, M.K., Laskin, A., Lawson, P., Leaitch, W.R., Liu, P., Liu, X., Lubin, D., Mazzoleni, C., Macdonald, A.-M., Moffet, R.C., Morrison, H., Ovchinnikov, M., Shupe, M.D., Turner, D.D., Xie, S., Zelenyuk, A., Bae, K., Freer, M. and Glen, A., 2011. Indirect and semi-direct aerosol campaign: The impact of Arctic aerosols on clouds. Bulletin of the American Meteorological Society, **92**(2): 183-201.
McMeeking, G.R., Hamburger, T., Liu, D., Flynn, M., Morgan, W.T., Northway, M., Highwood, E.J., Krejci, R., Allan, J.D., Minikin, A. and Coe, H., 2010. Black carbon measurements in the boundary layer over western and northern Europe. Atmospheric Chemistry and Physics, **10**: 9393-9414.
Medeiros, B., Stevens, B., Held, I.M., Zhao, M., Williamson, D.L., Olson, J.G. and Bretherton, C.S., 2008. Aquaplanets, climate sensitivity, and low clouds. Journal of Climate, **21**(19): 4974-4991.
Meehl, G.A., Stocker, T.F., Collins, W.D., Friedlingstein, P., Gaye, A.T., Gregory, J.M., Kitoh, A., Knutti, R., Murphy, J.M., Noda, A., Raper, S.C.B., Watterson, I.G., Weaver, A.J. and Zhao, Z.-C., 2007. Global Climate Projections, Climate Change 2007: The Physical Science Basis. Contribution of Working Group I to the Fourth Assessment Report of the Intergovernmental Panel on Climate Change. Cambridge University Press, Cambridge, United Kingdom and New York, NY, USA.
Menon, S., Del Genio, A.D., Koch, D. and Tselioudis, G., 2002. GCM Simulations of the aerosol indirect effect: Sensitivity to cloud parameterization and aerosol burden. Journal of the Atmospheric Sciences, **59**(3): 692-713.
Menon, S. and DelGenio, A., 2007. Evaluating the impacts of carbonaceous aerosols on clouds and climate. In: S.M. E., H.S. Kheshgi, J. Smith, F.C. de la Chesnaye, J.M. Reilly, T. Wilson and C. Kolstad (Editors), Human-Induced Climate Change: An Interdisciplinary Assessment. Cambridge University Press.
Menon, S. and Rotstayn, L., 2006. The radiative influence of aerosol effects on liquid-phase cumulus and stratiform clouds based on sensitivity studies with two climate models. Climate Dynamics, **27**(4): 345-356.
Mercado, L.M., Bellouin, N., Sitch, S., Boucher, O., Huntingford, C., Wild, M. and Cox, P.M., 2009. Impact of changes in diffuse radiation on the global land carbon sink. Nature, **458**(7241): 1014-1017.
Merikanto, J., Spracklen, D.V., Mann, G.W., Pickering, S.J. and Carslaw, K.S., 2009. Impact of nucleation on global CCN. Atmospheric Chemistry and Physics, **9**: 8601-8616.
Metzger, A., Verheggen, B., Dommen, J., Duplissy, J., Prevot, A.S.H., Weingartner, E., Riipinen, I., Kulmala, M., Spracklen, D.V., Carslaw, K.S. and Baltensperger, U., 2010. Evidence for the role of organics in aerosol particle

formation under atmospheric conditions. Proceedings of the National Academy of Sciences of the United States of America, **107**(15): 6646-6651.
Miller, R.L., 1997. Tropical thermostats and low cloud cover. Journal of Climate, **10**(3): 409-440.
Ming, J., Xiao, C.D., Cachier, H., Qin, D.H., Qin, X., Li, Z.Q. and Pu, J.C., 2009. Black Carbon (BC) in the snow of glaciers in west China and its potential effects on albedos. Atmospheric Research, **92**(1): 114-123.
Ming, J., Zhang, D., Kang, S. and Tian, W., 2007a. Aerosol and fresh snow chemistry in the East Rongbuk Glacier on the northern slope of Mt. Qomolangma (Everest). Journal of Geophysical Research, **112**: D15307.
Ming, Y., Ramaswamy, V., Donner, L.J., Phillips, V.T.J., Klein, S.A., Ginoux, P.A. and Horowitz, L.W., 2007b. Modeling the interactions between aerosols and liquid water clouds with a self-consistent cloud scheme in a general circulation model. Journal of the Atmospheric Sciences, **64**: 1189-1209.
Ming, Y., Ramaswamy, V., Ginoux, P.A., Horowitz, L.W. and Russell, L.M., 2005. Geophysical Fluid Dynamics Laboratory general circulation model investigation of the indirect radiative effects of anthropogenic sulfate aerosol. Journal of Geophysical Research, **110**(D22): D22206.
Ming, Y., Ramaswamy, V. and Persad, G., 2010. Two opposing effects of absorbing aerosols on global-mean precipitation. Geophysical Research Letters, **37**: L13701.
Mirme, S., Mirme, A., Minikin, A., Petzold, A., Horrak, U., Kerminen, V.M. and Kulmala, M., 2010. Atmospheric sub-3 nm particles at high altitudes. Atmospheric Chemistry and Physics, **10**(2): 437-451.
Mishchenko, M.I., Cairns, B., Kopp, G., Schueler, C.F., Fafaul, B.A., Hansen, J.E., Hooker, R.J., Itchkawich, T., Maring, H.B. and Travis, L.D., 2007. Accurate monitoring of terrestrial aerosols and total solar irradiance - Introducing the Glory mission. Bulletin of the American Meteorological Society, **88**(5): 677-691.
Mitchell, D.L., d'Entremont, R.P. and Lawson, R.P., 2010. Inferring cirrus size distributions through satellite remote sensing and microphysical databases. Journal of the Atmospheric Sciences, **67**(4): 1106-1125.
Mitchell, D.L. and Finnegan, W., 2009. Modification of cirrus clouds to reduce global warming. Environmental Research Letters, **4**: 045102.
Mkoma, S.L., 2008. Physico-chemical characterisation of atmospheric aerosol in Tanzania, with emphasis on the carbonaceous aerosol components and on chemical mass closure, Ghent University.
Mkoma, S.L., Maenhaut, W., Chi, X., Wang, W. and Raes, N., 2009a. Chemical composition and mass closure for PM10 aerosols during the 2005 dry season at a rural site in Morogoro, Tanzania. X-Ray Spectrom, **38**: 293–300.
Mkoma, S.L., Maenhaut, W., Chi, X.G., Wang, W. and Raes, N., 2009b. Characterisation of PM_{10} atmospheric aerosols for the wet season 2005 at two sites in East Africa. Atmospheric Environment, **43**: 631–639.
Mohler, O., Buttner, S., Linke, C., Schnaiter, M., Saathoff, H., Stetzer, O., Wagner, R., Kramer, M., Mangold, A., Ebert, V. and Schurath, U., 2005. Effect of sulfuric acid coating on heterogeneous ice nucleation by soot aerosol particles. Journal of Geophysical Research, **110**(D11): D11210.
Mohler, O., Field, P.R., Connolly, P., Benz, S., Saathoff, H., Schnaiter, M., Wagner, R., Cotton, R., Kramer, M., Mangold, A. and Heymsfield, A.J., 2006. Efficiency of the deposition mode ice nucleation on mineral dust particles. Atmospheric Chemistry and Physics, **6**: 3007-3021.
Mohler, O., Georgakopoulos, D.G., Morris, C.E., Benz, S., Ebert, V., Hunsmann, S., Saathoff, H., Schnaiter, M. and Wagner, R., 2008. Heterogeneous ice nucleation activity of bacteria: new laboratory experiments at simulated cloud conditions. Biogeosciences, **5**(5): 1425-1435.
Mohler, O., Stetzer, O., Schaefers, S., Linke, C., Schnaiter, M., Tiede, R., Saathoff, H., Kramer, M., Mangold, A., Budz, P., Zink, P., Schreiner, J., Mauersberger, K., Haag, W., Kärcher, B. and Schurath, U., 2003. Experimental investigation of homogeneous freezing of sulphuric acid particles in the aerosol chamber AIDA. Atmospheric Chemistry and Physics, **3**: 211-223.
Moorthy, K., Satheesh, S., Babu, S. and Dutt, C., 2008. Integrated campaign for aerosols, gases and radiation budget (ICARB): An overview. Journal of Earth System Science, **117**: 243-262.
Moosmüller, H., Chakrabarty, R. and Arnott, W., 2009. Aerosol light absorption and its measurement: A review. Journal of Quantitative Spectroscopy & Radiative Transfer, **110**: 844-878.
Morales, J.A., Pirela, D., Nava, M.G.d., Borrego, B.S.d., Velasquez, H. and Duran, J., 1998. Inorganic water soluble ions in atmospheric particles over Maracaibo Lake Basin in the western region of Venezuela. Atmospheric Research, **46**: 307–320.
Morcrette, J.-J., Boucher, O., Jones, L., Salmond, D., Bechtold, P., Beljaars, A., Benedetti, A., Bonet, A., Kaiser, J.W., Razinger, M., Schulz, M., Serrar, S., Simmons, A.J., Sofiev, M., Suttie, M., Tompkins, A.M. and Untch, A., 2009. Aerosol analysis and forecast in the ECMWF Integrated Forecast System. Part I: Forward modelling. Journal of Geophysical Research, **114**: D06206.
Moreno-Cruz, J.B., Ricke, K.W. and Keith, D.W., 2011. A simple model to account for regional inequalities in the effectiveness of solar radation management. Climatic Change, **110**(3-4): 649-668.
Morrison, H., de Boer, G., Feingold, G., Harrington, J., Shupe, M.D. and Sulia, K., 2012. Resilience of persistent Arctic mixed-phase clouds. Nature Geoscience, **5**(1): 11-17.
Morrison, H. and Gettelman, A., 2008. A new two-moment bulk stratiform cloud microphysics scheme in the community atmosphere model, version 3 (CAM3). Part I: Description and numerical tests. Journal of Climate, **21**: 3642-3659.

Morrison, H. and Grabowski, W.W., 2011. Cloud-system resolving model simulations of aerosol indirect effects on tropical deep convection and its thermodynamic environment. Atmospheric Chemistry and Physics, **11**: 10503-10523.

Mortazavi, R., Hayes, C.T. and Ariya, P.A., 2008. Ice nucleation activity of bacteria isolated from snow compared with organic and inorganic substrates. Environmental Chemistry, **5**(6): 373-381.

Moteki, N. and Kondo, Y., 2010. Dependence of laser-induced incandescence on physical properties of black carbon aerosols: Measurements and theoretical interpretation. Aerosol Science and Technology, **44**: 663-675.

Moteki, N., Kondo, Y., Miyazaki, Y., Takegawa, N., Komazaki, Y., Kurata, G., Shirai, T., Blake, D.R., Miyakawa, T. and Koike, M., 2007. Evolution of mixing state of black carbon particles: Aircraft measurements over the western Pacific in March 2004. Geophysical Research Letters, **34**: L11803.

Mouillot, F., Narasimha, A., Balkanski, Y., Lamarque, J.F. and Field, C.B., 2006. Global carbon emissions from biomass burning in the 20th century. Geophysical Research Letters, **33**(1): L01801.

Muller, C. and O'Gorman, P., 2011. An energetic perspective on the regional response of precipitation to climate change. Nature Climate Change, **1**(5): 266-271.

Muller, C.J., O'Gorman, P.A. and Back, L.E., 2011. Intensification of precipitation extremes with warming in a cloud-resolving model. Journal of Climate, **24**(11): 2784-2800.

Muller, J., Stavrakou, T., Wallens, S., De Smedt, I., Van Roozendael, M., Potosnak, M., Rinne, J., Munger, B., Goldstein, A. and Guenther, A., 2008. Global isoprene emissions estimated using MEGAN, ECMWF analyses and a detailed canopy environment model. Atmospheric Chemistry and Physics, **8**(5): 1329-1341.

Murphy, D.M., Solomon, S., Portmann, R.W., Rosenlof, K.H., Forster, P.M. and Wong, T., 2009. An observationally based energy balance for the Earth since 1950. Journal of Geophysical Research, **114**: D17107.

Murray, B.J., Broadley, S.L., Wilson, T.W., Atkinson, J.D. and Wills, R.H., 2011. Heterogeneous freezing of water droplets containing kaolinite particles. Atmospheric Chemistry and Physics, **11**(9): 4191-4207.

Myhre, G., 2009. Consistency between satellite-derived and modeled estimates of the direct aerosol effect. Science, **325**(5937): 187-190.

Myhre, G., Bellouin, N., Berglen, T.F., Berntsen, T.K., Boucher, O., Grini, A., Isaksen, I.S.A., Johnsrud, M., Mishchenko, M.I., Stordal, F. and Tanré, D., 2007. Comparison of the radiative properties and direct radiative effect of aerosols from a global aerosol model and remote sensing data over ocean. Tellus, **59B**(1): 115-129.

Myhre, G., Berglen, T.F., Johnsrud, M., Hoyle, C.R., Berntsen, T.K., Christopher, S.A., Fahey, D.W., Isaksen, I.S.A., Jones, T.A., Kahn, R.A., Loeb, N., Quinn, P., Remer, L., Schwarz, J.P. and Yttri, K.E., 2009. Modelled radiative forcing of the direct aerosol effect with multi-observation evaluation. Atmospheric Chemistry and Physics, **9**(4): 1365-1392.

Myhre, G., Samset, B.H., Skeie, R.B., Berntsen, T.K., Zhang, H., Wang, Z., Kirkevåg, A., T.Iversen, Seland, Ø., Ghan, S.J., Liu, X., Easter, R.C., Rasch, P.J., Yoon, J.-H., Yu, F., Luo, G., Ma, X., Bauer, S., Tsigaridis, K., H. Bian, Steenrod, S.D., Diehl, T., Chin, M., Lin, G., Penner, J., Balkanski, Y., Schulz, M., Hauglustaine, D., Bellouin, N., Zhang, K., Stier, P., Lamarque, J.-F., Takemura, T. and Kinne, S., 2012. Radiative forcing of the direct aerosol effect from AeroCom Phase II simulations. Atmospheric Chemistry and Physics: Submitted.

Nakajima, T. and Schulz, M., 2009. What do we know about large scale changes of aerosols, clouds, and the radiative budget? In: R.J. Charlson and J. Heintzenberg (Editors), Clouds in the Perturbed Climate System: Their Relationship to Energy Balance, Atmospheric Dynamics, and Precipitation. MIT Press, Cambridge, pp. 401-430.

Nakajima, T., Yoon, S.C., Ramanathan, V., Shi, G.Y., Takemura, T., Higurashi, A., Takamura, T., Aoki, K., Sohn, B.J., Kim, S.W., Tsuruta, H., Sugimoto, N., Shimizu, A., Tanimoto, H., Sawa, Y., Lin, N.H., Lee, C.T., Goto, D. and Schutgens, N., 2007. Overview of the Atmospheric Brown Cloud East Asian Regional Experiment 2005 and a study of the aerosol direct radiative forcing in East Asia. Journal of Geophysical Research, **112**(D24): D24S91.

Naud, C.M., Del Genio, A., Mace, G.G., Benson, S., Clothiaux, E.E. and Kollias, P., 2008. Impact of dynamics and atmospheric state on cloud vertical overlap. Journal of Climate, **21**(8): 1758-1770.

Naud, C.M., Del Genio, A.D., Bauer, M. and Kovari, W., 2010. Cloud Vertical Distribution across Warm and Cold Fronts in CloudSat-CALIPSO Data and a General Circulation Model. Journal of Climate, **23**(12): 3397-3415.

Neale, R.B., Richter, J.H. and Jochum, M., 2008. The impact of convection on ENSO: From a delayed oscillator to a series of events. Journal of Climate, **21**: 5904-5924.

Neelin, J. and Held, I., 1987. Modeling tropical convergence based on the moist static energy budget. Monthly Weather Review, **115**(1): 3-12.

Neelin, J.D., Münnich, M., Su, H., Meyerson, J.E. and Holloway, C.E., 2006. Tropical drying trends in global warming models and observations. Proceedings of the National Academy of Sciences of the United States of America, **103**(16): 6110-6115.

Neggers, R.A.J., 2009. A dual mass flux framework for boundary layer convection. Part II: Clouds. Journal of the Atmospheric Sciences, **66**: 1489-1506.

Neggers, R.A.J., Kohler, M. and Beljaars, A.C.M., 2009. A dual mass flux framework for boundary layer convection. Part I: Transport. Journal of the Atmospheric Sciences, **66**: 1465-1487.

Neggers, R.A.J., Siebesma, A.P. and Heus, T., 2012. Continuous single-column model evaluation at a permanent meteorological supersite. Bulletin of the American Meteorological Society, **early online release**.

Ney, E., 1959. Cosmic radiation and the weather. Nature, **183**: 451–452.

Nicoll, K. and Harrison, R.G., 2010. Experimental determination of layer cloud edge charging from cosmic ray ionization. Geophysical Research Letters, **37**: L13802.
Niedermeier, D., Hartmann, S., Shaw, R.A., Covert, D., Mentel, T.F., Schneider, J., Poulain, L., Reitz, P., Spindler, C., Clauss, T., Kiselev, A., Hallbauer, E., Wex, H., Mildenberger, K. and Stratmann, F., 2010. Heterogeneous freezing of droplets with immersed mineral dust particles - measurements and parameterization. Atmospheric Chemistry and Physics, **10**(8): 3601-3614.
Niemand, M., Möhler, O., Vogel, B., Vogel, H., Hoose, C., Connolly, P., Klein, H., Bingemer, H., DeMott, P., Skrotzki, J. and Leisner, T., 2012. A particle-surface-area-based parameterization of immersion freezing on desert dust particles. Journal of the Atmospheric Sciences: Early online release.
Niemeier, U., Schmidt, H. and Timmreck, C., 2011. The dependency of geoengineered sulfate aerosol on the emission strategy. Atmospheric Science Letters, **12**(2): 189-194.
Norris, J.R., Evan, A.T., Allen, R.J., Zelinka, M.D., O'Dell, C.W. and Klein, S.A., 2012. Evidence for climate change in the satellite cloud record. Science: submitted.
Nuijens, L., Stevens, B. and Siebesma, A.P., 2009. The environment of precipitating shallow cumulus convection. Journal of the Atmospheric Sciences, **66**(7): 1962-1979.
Nyanganyura, D., Maenhaut, W., Mathuthu, M., Makarau, A. and Meixner, F.X., 2007. The chemical composition of tropospheric aerosols and their contributing sources to a continental background site in northern Zimbabwe from 1994 to 2000. Atmospheric Environment, **41**: 2644–2659.
O'Dell, C.W., Wentz, F.J. and Bennartz, R., 2008. Cloud liquid water path from satellite-based passive microwave observations: A new climatology over the global oceans. Journal of Climate, **21**(8): 1721-1739.
O'Donnell, D., Tsigaridis, K. and Feichter, J., 2011. Estimating the direct and indirect effects of secondary organic aerosols using ECHAM5-HAM. Atmospheric Chemistry and Physics, **11**(16): 8635-8659.
O'Dowd, C., Monahan, C. and Dall'Osto, M., 2010. On the occurrence of open ocean particle production and growth events. Geophysical Research Letters, **37**: L19805.
O'Gorman, P. and Schneider, T., 2008. The hydrological cycle over a wide range of climates simulated with an idealized GCM. Journal of Climate, **21**(15): 3815-3832.
O'Gorman, P. and Schneider, T., 2009. The physical basis for increases in precipitation extremes in simulations of 21st-century climate change. Proceedings of the National Academy of Sciences of the United States of America, **106**(35): 14773-14777.
Oanh, N.T.K., Upadhyay, N., Zhuang, Y.-H., Hao, Z.-P., Murthy, D.V.S., Lestari, P., Villarin, J.T., Chengchua, K., Cof, H.X., Dung, N.T. and Lindgren, E.S., 2006. Particulate air pollution in six Asian cities: Spatial and temporal distributions, and associated sources. Atmospheric Environment, **40**: 3367-3380.
Oleson, K.W., Bonan, G.B. and Feddema, J., 2010. Effects of white roofs on urban temperature in a global climate model. Geophysical Research Letters, **37**: L03701.
Omar, A.H., Winker, D.M., Kittaka, C., Vaughan, M.A., Liu, Z., Hu, Y., Trepte, C.R., Rogers, R.R., Ferrare, R.A., Lee, K.-P., Kuehn, R.E. and Hostetler, C.A., 2009. The CALIPSO automated aerosol classification and lidar ratio selection algorithm. Journal of Atmospheric and Oceanic Technology, **26**(10): 1994-2014.
Oouchi, K., Noda, A.T., Satoh, M., Wang, B., Xie, S.P., Takahashi, H.G. and Yasunari, T., 2009. Asian summer monsoon simulated by a global cloud-system-resolving model: Diurnal to intra-seasonal variability. Geophysical Research Letters, **36**: L11815.
Osborne, S.R., Barana, A.J., Johnson, B.T., Haywood, J.M., Hesse, E. and Newman, S., 2011. Short-wave and long-wave radiative properties of Saharan dust aerosol. Quarterly Journal of the Royal Meteorological Society, **137**(658): 1149-1167.
Oshima, N., Kondo, Y., Moteki, N., Takegawa, N., Koike, M., Kita, K., Matsui, H., Kajino, M., Nakamura, H., Jung, J.S. and Kim, Y.J., 2012. Wet removal of black carbon in Asian outflow: Aerosol Radiative Forcing in East Asia (A-FORCE) aircraft campaign. Journal of Geophysical Research: submitted.
Ovadnevaite, J., Ceburnis, D., Martucci, G., Bialek, J., Monahan, C., Rinaldi, M., Facchini, M.C., Berresheim, H., Worsnop, D.R. and O'Dowd, C., 2011. Primary marine organic aerosol: A dichotomy of low hygroscopicity and high CCN activity. Geophysical Research Letters, **38**: L21806.
Ovchinnikov, M., Korolev, A. and Fan, J., 2011. Effects of ice number concentration on dynamics of a shallow mixed-phase stratiform cloud. Journal of Geophysical Research, **116**: D00T06.
Paasonen, P., Nieminen, T., Asmi, E., Manninen, H.E., Petaja, T., Plass-Dulmer, C., Flentje, H., Birmili, W., Wiedensohler, A., Horrak, U., Metzger, A., Hamed, A., Laaksonen, A., Facchini, M.C., Kerminen, V.M. and Kulmala, M., 2010. On the roles of sulphuric acid and low-volatility organic vapours in the initial steps of atmospheric new particle formation. Atmospheric Chemistry and Physics, **10**: 11223-11242.
Pacifico, F., Harrison, S.P., Jones, C.D. and Sitch, S., 2009. Isoprene emissions and climate. Atmospheric Environment, **43**(39): 6121-6135.
Painemal, D. and Zuidema, P., 2010. Microphysical variability in southeast Pacific Stratocumulus clouds: synoptic conditions and radiative response. Atmospheric Chemistry and Physics, **10**(13): 6255-6269.
Pallé Bagó, E. and Butler, C.J., 2000. The influence of cosmic rays on terrestrial clouds and global warming. Astronomy & Geophysics, **41**: 4.18-4.22.
Pallé, E., 2005. Possible satellite perspective effects on the reported correlations between solar activity and clouds. Geophysical Research Letters, **32**: L03802.

Palm, S.P., Strey, S.T., Spinhirne, J. and Markus, T., 2010. Influence of Arctic sea ice extent on polar cloud fraction and vertical structure and implications for regional climate. Journal of Geophysical Research, **115**: D21209.
Paltridge, G., Arking, A. and Pook, M., 2009. Trends in middle- and upper-level tropospheric humidity from NCEP reanalysis data. Theoretical and Applied Climatology, **98**: 351-359.
Paltridge, G.W., 1980. Cloud-radiation feedback to climate. Quarterly Journal of the Royal Meteorological Society, **106**(450): 895-899.
Paredes-Miranda, G., Arnott, W., Jimenez, J., Aiken, A., Gaffney, J. and Marley, N., 2009. Primary and secondary contributions to aerosol light scattering and absorption in Mexico City during the MILAGRO 2006 campaign. Atmospheric Chemistry and Physics, **9**: 3721-3730.
Park, S. and Bretherton, C.S., 2009. The University of Washington shallow convection and moist turbulence schemes and their impact on climate simulations with the Community Atmosphere Model. Journal of Climate, **22**: 3449-3469.
Partanen, A.-I., Kokkola, H., Romakkaniemi, S., Kerminen, V.-M., Lehtinen, K., Bergman, T., Arola, A. and Korhonen, H., 2012. Direct and indirect effects of sea spray geoengineering and the role of injected particle size. Journal of Geophysical Research, **117**: D02203.
Pawlowska, H. and Brenguier, J.L., 2003. An observational study of drizzle formation in stratocumulus clouds for general circulation model (GCM) parameterizations. Journal of Geophysical Research, **108**(D15): 8630.
Pechony, O. and Shindell, D.T., 2010. Driving forces of global wildfires over the past millennium and the forthcoming century. Proceedings of the National Academy of Sciences of the United States of America, **107**(45): 19167-19170.
Peng, Y.R. and Lohmann, U., 2003. Sensitivity study of the spectral dispersion of the cloud droplet size distribution on the indirect aerosol effect. Geophysical Research Letters, **30**(10): 1507.
Penner, J.E., Chen, Y., Wang, M. and Liu, X., 2009. Possible influence of anthropogenic aerosols on cirrus clouds and anthropogenic forcing. Atmospheric Chemistry and Physics, **9**(3): 879-896.
Penner, J.E., Quaas, J., Storelvmo, T., Takemura, T., Boucher, O., Guo, H., Kirkevag, A., Kristjansson, J.E. and Seland, O., 2006. Model intercomparison of indirect aerosol effects. Atmospheric Chemistry and Physics, **6**: 3391-3405.
Penner, J.E., Xu, L. and Wang, M.H., 2011. Satellite methods underestimate indirect climate forcing by aerosols. Proceedings of the National Academy of Sciences of the United States of America, **108**(33): 13404-13408.
Penner, J.E., Zhang, S.Y. and Chuang, C.C., 2003. Soot and smoke aerosol may not warm climate. Journal of Geophysical Research, **108**(D21): 4657.
Perez, N., Pey, J., Querol, X., Alastuey, A., Lopez, J.M. and Viana, M., 2008. Partitioning of major and trace components in PM10-PM2.5-PM1 at an urban site in Southern Europe. Atmospheric Environment, **42**: 1677-1691.
Peters, K., Quaas, J. and Bellouin, N., 2011a. Effects of absorbing aerosols in cloudy skies: a satellite study over the Atlantic Ocean. Atmospheric Chemistry and Physics, **11**(4): 1393-1404.
Peters, K., Quaas, J. and Grassl, H., 2011b. A search for large-scale effects of ship emissions on clouds and radiation in satellite data. Journal of Geophysical Research, **116**: D24205.
Petroff, A. and Zhang, L., 2010. Development and validation of a size-resolved particle dry deposition scheme for application in aerosol transport models. Geoscientific Model Development, **3**(2): 753-769.
Petters, M.D. and Kreidenweis, S.M., 2007. A single parameter representation of hygroscopic growth and cloud condensation nucleus activity. Atmospheric Chemistry and Physics, **7**: 1961-1971.
Petters, M.D., Parsons, M.T., Prenni, A.J., DeMott, P.J., Kreidenweis, S.M., Carrico, C.M., Sullivan, A.P., McMeeking, G.R., Levin, E., Wold, C.E., Collett, J.L. and Moosmuller, H., 2009. Ice nuclei emissions from biomass burning. Journal of Geophysical Research, **114**: D07209.
Petters, M.D., Snider, J.R., Stevens, B., Vali, G., Faloona, I. and Russell, L.M., 2006. Accumulation mode aerosol, pockets of open cells, and particle nucleation in the remote subtropical Pacific marine boundary layer. Journal of Geophysical Research, **111**(D2): D02206.
Phillips, V.T.J., Andronache, C., Christner, B., Morris, C.E., Sands, D.C., Bansemer, A., Lauer, A., McNaughton, C. and Seman, C., 2009. Potential impacts from biological aerosols on ensembles of continental clouds simulated numerically. Biogeosciences, **6**(6): 987-1014.
Phillips, V.T.J., DeMott, P.J. and Andronache, C., 2008. An empirical parameterization of heterogeneous ice nucleation for multiple chemical species of aerosol. Journal of the Atmospheric Sciences, **65**(9): 2757-2783.
Pierce, J.R. and Adams, P.J., 2009a. Can cosmic rays affect cloud condensation nuclei by altering new particle formation rates? Geophysical Research Letters, **36**: L09820.
Pierce, J.R. and Adams, P.J., 2009b. Uncertainty in global CCN concentrations from uncertain aerosol nucleation and primary emission rates. Atmospheric Chemistry and Physics, **9**(4): 1339-1356.
Pierce, J.R., Weisenstein, D.K., Heckendorn, P., Peter, T. and Keith, D.W., 2010. Efficient formation of stratospheric aerosol for climate engineering by emission of condensible vapor from aircraft. Geophysical Research Letters, **37**(18): L18805.
Pincus, R. and Baker, M.B., 1994. Effect of precipitation on the albedo susceptibility of clouds in the marine boundary-layer. Nature, **372**(6503): 250-252.
Pincus, R., Hemler, R. and Klein, S.A., 2006. Using stochastically generated subcolumns to represent cloud structure in a large-scale model. Monthly Weather Review, **134**(12): 3644-3656.

Pincus, R. and Klein, S.A., 2000. Unresolved spatial variability and microphysical process rates in large-scale models. Journal of Geophysical Research, **105**(D22): 27059-27065.

Platnick, S., King, M.D., Ackerman, S.A., Menzel, W.P., Baum, B.A., Riedi, J.C. and Frey, R.A., 2003. The MODIS cloud products: Algorithms and examples from Terra. IEEE Transactions on Geoscience and Remote Sensing, **41**(2): 459-473.

Pöschl, U., Martin, S., Sinha, B., Chen, Q., Gunthe, S., Huffman, J., Borrmann, S., Farmer, D., Garland, R., Helas, G., Jimenez, J., King, S., Manzi, A., Mikhailov, E., Pauliquevis, T., Petters, M., Prenni, A., Roldin, P., Rose, D., Schneider, J., Su, H., Zorn, S., Artaxo, P. and Andreae, M., 2010. Rainforest aerosols as biogenic nuclei of clouds and precipitation in the Amazon. Science, **329**: 1513-1516.

Pósfai, M., Simonics, R., Li, J., Hobbs, P. and Buseck, P., 2003. Individual aerosol particles from biomass burning in southern Africa: 1. Compositions and size distributions of carbonaceous particles. Journal of Geophysical Research, **108**: 8483.

Posselt, R. and Lohmann, U., 2008. Influence of giant CCN on warm rain processes in the ECHAM5 GCM. Atmospheric Chemistry and Physics, **8**(14): 3769-3788.

Posselt, R. and Lohmann, U., 2009. Sensitivity of the total anthropogenic aerosol effect to the treatment of rain in a global climate model. Geophysical Research Letters, **36**: L02805.

Pratt, K.A. and Prather, K.A., 2010. Aircraft measurements of vertical profiles of aerosol mixing states. Journal of Geophysical Research, **115**: D11305.

Prenni, A.J., Harrington, J.Y., Tjernstrom, M., DeMott, P.J., Avramov, A., Long, C.N., Kreidenweis, S.M., Olsson, P.Q. and Verlinde, J., 2007. Can ice-nucleating aerosols affect arctic seasonal climate? Bulletin of the American Meteorological Society, **88**(4): 541-550.

Pringle, K., Tost, H., Pozzer, A., Poschl, U. and Lelieveld, J., 2010. Global distribution of the effective aerosol hygroscopicity parameter for CCN activation. Atmospheric Chemistry and Physics, **10**: 5241-5255.

Prisle, N.L., Raatikainen, T., Laaksonen, A. and Bilde, M., 2010. Surfactants in cloud droplet activation: mixed organic-inorganic particles. Atmospheric Chemistry and Physics, **10**(12): 5663-5683.

Prisle, N.L., Raatikainen, T., Sorjamaa, R., Svenningsson, B., Laaksonen, A. and Bilde, M., 2008. Surfactant partitioning in cloud droplet activation: a study of C8, C10, C12 and C14 normal fatty acid sodium salts. Tellus, **60B**(3): 416-431.

Pritchard, M.S. and Somerville, R.C.J., 2010. Assessing the diurnal cycle of precipitation in a multi-scale climate model. J. Adv. Model. Earth Syst., **1**: Art. #12.

Puma, M.J. and Cook, B.I., 2010. Effects of irrigation on global climate during the 20th century. Journal of Geophysical Research, **115**: D16120.

Putaud, J.-P., Raes, F., Dingenen, R.V., Bruggemann, E., Facchini, M.C., Decesari, S., Fuzzi, S., Gehrig, R., Huglin, C., Laj, P., Lorbeer, G., Maenhaut, W., Mihalopoulos, N., Mulller, K., Querol, X., Rodriguez, S., Schneider, J., Spindler, G., Brink, H.t., Torseth, K. and Wiedensohler, A., 2004. European aerosol phenomenology-2: chemical characteristics of particulate matter at kerbside, urban, rural and background sites in Europe. Atmospheric Environment, **38**: 2579-2595.

Putman, W.M. and Suarez, M., 2011. Cloud-system resolving simulations with the NASA Goddard Earth Observing System global atmospheric model (GEOS-5). Geophysical Research Letters, **38**: L16809.

Puxbaum, H., Gomiscek, B., Kalina, M., Bauer, H., Salam, A., Stopper, S., Preining, O. and Hauck, H., 2004. A dual site study of PM2.5 and PM10 aerosol chemistry in the larger region of Vienna, Austria. Atmos. Environ., **38**: 3949-3958.

Pye, H., Liao, H., Wu, S., Mickley, L., Jacob, D., Henze, D. and Seinfeld, J., 2009. Effect of changes in climate and emissions on future sulfate-nitrate-ammonium aerosol levels in the United States. Journal of Geophysical Research, **114**: D01205.

Qu, W.J., Zhang, X.Y., Arimoto, R., Wang, D., Wang, Y.Q., Yan, L.W. and Li, Y., 2008. Chemical composition of the background aerosol at two sites in southwestern and northwestern China: potential influences of regional transport. Tellus, **60B**: 657-673.

Quaas, J. and Boucher, O., 2005. Constraining the first aerosol indirect radiative forcing in the LMDZ GCM using POLDER and MODIS satellite data. Geophysical Research Letters, **32**(17): L17814.

Quaas, J., Boucher, O., Bellouin, N. and Kinne, S., 2008. Satellite-based estimate of the direct and indirect aerosol climate forcing. Journal of Geophysical Research, **113**: D05204.

Quaas, J., Boucher, O. and Bréon, F.M., 2004. Aerosol indirect effects in POLDER satellite data and the Laboratoire de Meteorologie Dynamique-Zoom (LMDZ) general circulation model. Journal of Geophysical Research, **109**(D8): D08205.

Quaas, J., Boucher, O. and Lohmann, U., 2006. Constraining the total aerosol indirect effect in the LMDZ and ECHAM4 GCMs using MODIS satellite data. Atmospheric Chemistry and Physics, **6**: 947-955.

Quaas, J., Ming, Y., Menon, S., Takemura, T., Wang, M., Penner, J.E., Gettelman, A., Lohmann, U., Bellouin, N., Boucher, O., Sayer, A.M., Thomas, G.E., McComiskey, A., Feingold, G., Hoose, C., Kristjansson, J.E., Liu, X., Balkanski, Y., Donner, L.J., Ginoux, P.A., Stier, P., Grandey, B., Feichter, J., Sednev, I., Bauer, S.E., Koch, D., Grainger, R.G., Kirkevag, A., Iversen, T., Seland, O., Easter, R., Ghan, S., Rasch, P., Morrison, H., Lamarque, J., Iacono, M., Kinne, S. and Schulz, M., 2009. Aerosol indirect effects - general circulation model intercomparison and evaluation with satellite data. Atmospheric Chemistry and Physics, **9**: 8697-8717.

Querol, X., Alastuey, A., Moreno, N., Alvarez-Ayuso, E., Garcıa-Sanchez, A., Cama, J., Ayora, C. and Simon, M., 2006. Immobilization of heavy metals in polluted soils by the addition of zeolitic material synthesized from coal fly ash. Chemosphere, **62**: 171–180.

Querol, X., Alastuey, A., Moreno, T., Viana, M.M., Castillo, S., Pey, J., Rodrıguez, S., Artinano, B., Salvador, P., Sanchez, M., Santos, S.G.D., Garraleta, M.D.H., Fernandez-Patier, R., Moreno-Grau, S., Minguillon, M.C., Monfort, E., Sanz, M.J., Palomo-Marın, R., Pinilla-Gil, E. and Cuevas, E., 2008. Spatial and temporal variations in airborne particulate matter (PM10 and PM2.5) across Spain 1999-2005. Atmospheric Environment, **42**: 3964-3979.

Querol, X., Alastuey, A., Pey, J., Cusack, M., Pérez, N., Mihalopoulos, N., Theodosi, C., Gerasopoulos, E., Kubilay, N. and Koçak, M., 2009. Variability in regional background aerosols within the Mediterranean. Atmospheric Chemistry and Physics, **9**: 4575-4591.

Querol, X., Alastuey, A., Rodrıguez, S., Plana, F., Ruiz, C.R., Cots, N., Massague, G. and Puig, O., 2001. PM10 and PM2.5 source apportionment in the Barcelona Metropolitan Area, Catalonia, Spain. Atmospheric Environment, **35/36**: 6407-6419.

Querol, X., Alastuey, A., Ruiz, C.R., Artinano, B., Hansson, H.C., Harrison, R.M., Buringh, E., ten Brink, H.M., Lutz, M., Bruckmann, P., Straehl, P. and Schneider, J., 2004. Speciation and origin of PM10 and PM2.5 in selected European cities. Atmospheric Environment, **38**: 6547-6555.

Quinn, P.K. and Bates, T.S., 2011. The case against climate regulation via oceanic phytoplankton sulphur emissions. Nature, **480**(7375): 51-56.

Racherla, P. and Adams, P., 2006. Sensitivity of global tropospheric ozone and fine particulate matter concentrations to climate change. Journal of Geophysical Research, **111**(D24): D24103.

Radhi, M., Box, M.A., Box, G.P., Mitchell, R.M., Cohen, D.D., Stelcer, E. and Keywood, M.D., 2010. Optical, physical and chemical characteristics of Australian continental aerosols: results from a field experiment. Atmospheric Chemistry and Physics, **10**: 5925–5942.

Rae, J.G.L., Johnson, C.E., Bellouin, N., Boucher, O., Haywood, J.M. and Jones, A., 2007. Sensitivity of global sulphate aerosol production to changes in oxidant concentrations and climate. Journal of Geophysical Research, **112**: D10312.

Raes, F., Liao, H., Chen, W.-T. and Seinfeld, J.H., 2010. Atmospheric chemistry-climate feedbacks. Journal of Geophysical Research, **115**: D12121.

Ram, K., Sarin, M.M. and Hegde, P., 2010. Long-term record of aerosol optical properties and chemical composition from a high-altitude site (Manora Peak) in Central Himalaya. Atmospheric Chemistry and Physics, **10**: 11791-11803.

Ram, M. and Stolz, M.R., 1999. Possible solar influences on the dust profile of the GISP2 Ice Core from central Greenland. Geophysical Research Letters, **26**: 1043–1046.

Raman, R.S., Ramachandran, S. and Rastogi, N., 2010. Source identification of ambient aerosols over an urban region in western India. Journal of Environmental Monitoring, **12**: 1330-1340.

Ramanathan, V. and Carmichael, G., 2008. Global and regional climate changes due to black carbon. Nature Geoscience, **1**(4): 221-227.

Randall, D., Khairoutdinov, M., Arakawa, A. and Grabowski, W., 2003. Breaking the cloud parameterization deadlock. Bulletin of the American Meteorological Society, **84**(11): 1547-1564.

Randall, D.A., Wood, R.A., Bony, S., Colman, R., Fichefet, T., Fyfe, J., Kattsov, V., Pitman, A., Shukla, J., Srinivasan, J., Stouffer, R.J., Sumi, A. and Taylor, K.E., 2007. Climate Models and Their Evaluation, Climate Change 2007: The Physical Science Basis. Contribution of Working Group I to the Fourth Assessment Report of the Intergovernmental Panel on Climate Change. Cambridge University Press, Cambridge, United Kingdom and New York, NY, USA.

Randles, C.A., Kinne, S., Myhre, G., Schulz, M., Stier, P., Fischer, J., Doppler, L., Highwood, E., Ryder, C., Harris, B., Huttunen, J., Ma, Y., Pinker, R.T., Mayer, B., Neubauer, D., Hitzenberger, R., Oreopoulos, L., Lee, D., Pitari, G., Di Genova, G., Rose, F.G., Kato, S., Rumbold, S.T., Vardavas, I., Hatzianastassiou, N., Matsoukas, C., Yu, H., Zhang, F., Zhang, H. and Lu, P., 2012. Intercomparison of shortwave radiative transfer schemes in global aerosol modeling: Results from the AeroCom Radiative Transfer Experiment. Atmospheric Chemistry and Physics, **submitted**.

Rap, A., Forster, P., Jones, A., Boucher, O., Haywood, J., Bellouin, N. and De Leon, R., 2010a. Parameterization of contrails in the UK Met Office Climate Model. Journal of Geophysical Research, **115**: D10205.

Rap, A., Forster, P.M., Haywood, J.M., Jones, A. and Boucher, O., 2010b. Estimating the climate impact of linear contrails using the UK Met Office climate model. Geophysical Research Letters, **37**: L20703.

Rasch, P.J., Chen, C.C. and Latham, J.L., 2009. Geo-engineering by cloud seeding: influence on sea-ice and the climate system. Environmental Research Letters, **4**: 045112.

Rasch, P.J., Crutzen, P.J. and Coleman, D.B., 2008a. Exploring the geoengineering of climate using stratospheric sulfate aerosols: The role of particle size. Geophysical Research Letters, **35**(2): L02809.

Rasch, P.J., Tilmes, S., Turco, R.P., Robock, A., Oman, L., Chen, C.C., Stenchikov, G.L. and Garcia, R.R., 2008b. An overview of geoengineering of climate using stratospheric sulphate aerosols. Philosophical Transactions Royal Society London A, **366**(1882): 4007-4037.

Rastogi, N. and Sarin, M.M., 2005. Long-term characterization of ionic species in aerosols from urban and high-altitude sites in western India: Role of mineral dust and anthropogenic sources. Atmospheric Environment, **39**: 5541-5554.

Rauber, R.M., Stevens, B., Ochs, H.T., III, Knight, C., Albrecht, B.A., Blyth, A.M., Fairall, C.W., Jensen, J.B., Lasher-Trapp, S.G., Mayol-Bracero, O.L., Vali, G., Anderson, J.R., Baker, B.A., Bandy, A.R., Burnet, E., Brenguier, J.L., Brewer, W.A., Brown, P.R.A., Chuang, P., Cotton, W.R., Girolamo, L.D., Geerts, B., Gerber, H., Goke, S., Gomes, L., Heikes, B.G., Hudson, J.G., Kollias, P., Lawson, R.P., Krueger, S.K., Lenschow, D.H., Nuijens, L., O'Sullivan, D.W., Rilling, R.A., Rogers, D.C., Siebesma, A.P., Snodgrass, E., Stith, J.L., Thornton, D.C., Tucker, S., Twohy, C.H. and Zuidema, P., 2007. Rain in shallow cumulus over the ocean - The RICO campaign. Bulletin of the American Meteorological Society, **88**(12): 1912-1928.

Raymond, D., Sessions, S., Sobel, A. and Fuchs, Z., 2009. The mechanics of gross moist stability. Journal of Advances in Modeling Earth Systems, **1**: Art. #9.

Reddington, C., Carslaw, K., Spracklen, D., Frontoso, M., Collins, L., Merikanto, J., Minikin, A., Hamburger, T., Coe, H., Kulmala, M., Aalto, P., Flentje, H., Plass-Duelmer, C., Birmili, W., Wiedensohler, A., Wehner, B., Tuch, T., Sonntag, A., O'Dowd, C., Jennings, S., Dupuy, R., Baltensperger, U., Weingartner, E., Hansson, H., Tunved, P., Laj, P., Sellegri, K., Boulon, J., Putaud, J., Gruening, C., Swietlicki, E., Roldin, P., Henzing, J., Moerman, M., Mihalopoulos, N., Kouvarakis, G., Zdimal, V., Zikova, N., Marinoni, A., Bonasoni, P. and Duchi, R., 2011. Primary versus secondary contributions to particle number concentrations in the European boundary layer. Atmospheric Chemistry and Physics, **11**(23): 12007-12036.

Reddy, M.S., Boucher, O., Balkanski, Y. and Schulz, M., 2005. Aerosol optical depths and direct radiative perturbations by species and source type. Geophysical Research Letters, **32**(12): L12803.

Remer, L.A., Kaufman, Y.J., Tanre, D., Mattoo, S., Chu, D.A., Martins, J.V., Li, R.R., Ichoku, C., Levy, R.C., Kleidman, R.G., Eck, T.F., Vermote, E. and Holben, B.N., 2005. The MODIS aerosol algorithm, products, and validation. Journal of the Atmospheric Sciences, **62**(4): 947-973.

Rengarajan, R., Sarin, M.M. and Sudheer, A.K., 2007. Carbonaceous and inorganic species in atmospheric aerosols during wintertime over urban and high-altitude sites in North India. Journal of Geophysical Research, **112**: D21307.

Richter, I. and Xie, S., 2008. Muted precipitation increase in global warming simulations: A surface evaporation perspective. Journal of Geophysical Research, **113**: D24118.

Richter, J.H. and Rasch, P.J., 2008. Effects of convective momentum transport on the atmospheric circulation in the community atmosphere model, version 3. Journal of Climate, **21**: 1487-1499.

Ridgwell, A., Singarayer, J., Hetherington, A. and Valdes, P., 2009. Tackling regional climate change by leaf albedo bio-geoengineering. Current Biology, **19**(2): 146-150.

Rieck, M., Nuijens, L. and Stevens, B., 2012. Marine boundary-layer cloud feedbacks in a constant relative humidity atmosphere. Journal of the Atmospheric Sciences, **69**: 2538–2550.

Riipinen, I., Pierce, J., Yli-Juuti, T., Nieminen, T., Hakkinen, S., Ehn, M., Junninen, H., Lehtipalo, K., Petaja, T., Slowik, J., Chang, R., Shantz, N., Abbatt, J., Leaitch, W., Kerminen, V., Worsnop, D., Pandis, S., Donahue, N. and Kulmala, M., 2011. Organic condensation: a vital link connecting aerosol formation to cloud condensation nuclei (CCN) concentrations. Atmospheric Chemistry and Physics, **11**(8): 3865-3878.

Rinaldi, M., Decesari , S., Carbone, C., Finessi, E., Fuzzi, S., Ceburnis, D., O'Dowd , C., Sciare, J., Burrows, J., Vrekoussis, M., Ervens, B., Tsigaridis, K. and Facchini, M.C., 2011. Evidence of a natural marine source of oxalic acid and a possible link to glyoxal. Journal of Geophysical Research, **116**: D16204.

Rinaldi, M., Facchini, M.C., Decesari, S., Carbone, C., Finessi, E., Mircea, M., Fuzzi, S., Ceburnis, D., Ehn, M., Kulmala, M., de Leeuw, G. and O'Dowd, C.D., 2009. On the representativeness of coastal aerosol studies to open ocean studies: Mace Head – a case study. Atmospheric Chemistry and Physics, **9**: 9635-9646.

Ringer, M.A., McAvaney, B.J., Andronova, N., Buja, L.E., Esch, M., Ingram, W.J., Li, B., Quaas, J., Roeckner, E., Senior, C.A., Soden, B.J., Volodin, E.M., Webb, M.J. and Williams, K.D., 2006. Global mean cloud feedbacks in idealized climate change experiments. Geophysical Research Letters, **33**(7): L07718.

Rio, C. and Hourdin, F., 2008. A thermal plume model for the convective boundary layer: Representation of cumulus clouds. Journal of the Atmospheric Sciences, **65**(2): 407-425.

Rio, C., Hourdin, F., Grandpeix, J.Y. and Lafore, J.P., 2009. Shifting the diurnal cycle of parameterized deep convection over land. Geophysical Research Letters, **36**: L07809.

Roberts, G.C., Day, D.A., Russell, L.M., Dunlea, E.J., Jimenez, J.L., Tomlinson, J.M., Collins, D.R., Shinozuka, Y. and Clarke, A.D., 2010. Characterization of particle cloud droplet activity and composition in the free troposphere and the boundary layer during INTEX-B. Atmospheric Chemistry and Physics, **10**(14): 6627-6644.

Roberts, P. and Hallett, J., 1968. A laboratory study of ice nucleating properties of some mineral particulates. Quarterly Journal of the Royal Meteorological Society, **94**(399): 25-34.

Robinson, A., Donahue, N., Shrivastava, M., Weitkamp, E., Sage, A., Grieshop, A., Lane, T., Pierce, J. and Pandis, S., 2007. Rethinking organic aerosols: Semivolatile emissions and photochemical aging. Science, **315**: 1259-1262.

Robock, A., Oman, L. and Stenchikov, G., 2008. Regional climate responses to geoengineering with tropical and Arctic SO_2 injections. Journal of Geophysical Research, **113**: D16101.

Rodriguez, S., Querol, X., Alastuey, A. and Plana, F., 2002. Sources and processes affecting levels and composition of atmospheric aerosol in the western Mediterranean. Journal of Geophysical Research, **107**(D24): 4777.

Rodrıguez, S., Querol, X., Alastuey, A., Viana, M.M., Alarcon, M., Mantilla, E. and Ruiz, C.R., 2004. Comparative PM10-PM2.5 source contribution study at rural, urban and industrial sites during PM episodes in Eastern Spain. Sci. Total Environ., **328**: 95-113.

Rohs, S., Spang, R., Rohrer, F., Schiller, C. and Vos, H., 2010. A correlation study of high-altitude and midaltitude clouds and galactic cosmic rays by MIPAS-Envisat. Journal of Geophysical Research, **115**(D14212).

Romps, D.M., 2011. Response of tropical precipitation to global warming. Journal of the Atmospheric Sciences, **68**(1): 123-138.

Rondanelli, R. and Lindzen, R.S., 2010. Can thin cirrus clouds in the tropics provide a solution to the faint young Sun paradox? Journal of Geophysical Research, **115**: D02108.

Roosli, M., Theis, G., nzli, N.K., Staehelin, J., Mathys, P., Oglesby, L., Camenzind, M. and Braun-FahrlaKnder, C., 2001. Temporal and spatial variation of the chemical composition of PM10 at urban and rural sites in the Basel area, Switzerland. Atmospheric Environment, **35**: 3701-3713.

Rose, D., Gunthe, S.S., Su, H., Garland, R.M., Yang, H., Berghof, M., Cheng, Y.F., Wehner, B., Achtert, P., Nowak, A., Wiedensohler, A., Takegawa, N., Kondo, Y., Hu, M., Zhang, Y., Andreae, M.O. and Poschl, U., 2011. Cloud condensation nuclei in polluted air and biomass burning smoke near the mega-city Guangzhou, China -Part 2: Size-resolved aerosol chemical composition, diurnal cycles, and externally mixed weakly CCN-active soot particles. Atmospheric Chemistry and Physics, **11**(6): 2817-2836.

Rosenfeld, D. and Gutman, G., 1994. Retrieving microphysical properties near the tops of potential rain clouds by multi spectral analysis of AVHRR data. Atmospheric Research, **34**: 259-283.

Rosenfeld, D., Lohmann, U., Raga, G.B., O'Dowd, C.D., Kulmala, M., Fuzzi, S., Reissell, A. and Andreae, M.O., 2008. Flood or drought: How do aerosols affect precipitation? Science, **321**(5894): 1309-1313.

Rosenfeld, D. and Woodley, W.L., 2001. Pollution and clouds. Physics World, **14**(2): 33-37.

Rossow, W.B. and Schiffer, R.A., 1991. ISCCP Cloud Data Products. Bulletin of the American Meteorological Society, **72**: 2–20.

Rotstayn, L.D., 1999. Indirect forcing by anthropogenic aerosols: A global climate model calculation of the effective-radius and cloud-lifetime effects. Journal of Geophysical Research, **104**(D8): 9369-9380.

Rotstayn, L.D., Cai, W.J., Dix, M.R., Farquhar, G.D., Feng, Y., Ginoux, P., Herzog, M., Ito, A., Penner, J.E., Roderick, M.L. and Wang, M.H., 2007. Have Australian rainfall and cloudiness increased due to the remote effects of Asian anthropogenic aerosols? Journal of Geophysical Research, **112**: D09202.

Rotstayn, L.D. and Liu, Y.G., 2003. Sensitivity of the first indirect aerosol effect to an increase of cloud droplet spectral dispersion with droplet number concentration. Journal of Climate, **16**(21): 3476-3481.

Rotstayn, L.D. and Liu, Y.G., 2005. A smaller global estimate of the second indirect aerosol effect. Geophysical Research Letters, **32**(5): L05708.

Rotstayn, L.D. and Liu, Y.G., 2009. Cloud droplet spectral dispersion and the indirect aerosol effect: Comparison of two treatments in a GCM. Geophysical Research Letters, **36**: L10801.

Rotstayn, L.D. and Penner, J.E., 2001. Indirect aerosol forcing, quasi forcing, and climate response. Journal of Climate, **14**(13): 2960-2975.

Royal Society, 2009. Geoengineering the climate, Science, governance and uncertainty Royal Society, London.

Russell, M. and Allen, D.T., 2005. Predicting secondary organic aerosol formation rates in southeast Texas. Journal of Geophysical Research, **110**: D07S17.

Rypdal, K., Rive, N., Berntsen, T.K., Klimont, Z., Mideksa, T.K., Myhre, G. and Skeie, R.B., 2009. Costs and global impacts of black carbon abatement strategies. Tellus, **61B**(4): 625-641.

Sacks, W.J., Cook, B.I., Buenning, N., Levis, S. and Helkowski, J.H., 2009. Effects of global irrigation on the near-surface climate. Climate Dynamics, **33**: 159–175.

Safai, P.D., Budhavant, K.B., Rao, P.S.P., Ali, K. and Sinha, A., 2010. Source characterization for aerosol constituents and changing roles of calcium and ammonium aerosols in the neutralization of aerosol acidity at a semi-urban site in SW India. Atmospheric Research, **98**: 78-88.

Sakaeda, N., Wood, R. and Rasch, P.J., 2011. Direct and semidirect aerosol effects of southern African biomass burning aerosol. Journal of Geophysical Research, **116**: D12205.

Salam, A., Lohmann, U., Crenna, B., Lesins, G., Klages, P., Rogers, D., Irani, R., MacGillivray, A. and Coffin, M., 2006. Ice nucleation studies of mineral dust particles with a new continuous flow diffusion chamber. Aerosol Science and Technology, **40**(2): 134-143.

Salvador, P., Artınano, B., Querol, X., Alastuey, A. and Costoya, M., 2007. Characterisation of local and external contributions of atmospheric particulate matter at a background coastal site. Atmospheric Environment, **41**: 1-17.

Salzmann, M., Ming, Y., Golaz, J., Ginoux, P., Morrison, H., Gettelman, A., Kramer, M. and Donner, L., 2010. Two-moment bulk stratiform cloud microphysics in the GFDL AM3 GCM: description, evaluation, and sensitivity tests. Atmospheric Chemistry and Physics, **10**: 8037-8064.

Samset, B.H., Myhre, G., Skeie, R.B., Berntsen, T.K., Kirkevåg, A., Ghan, S.J., Easter, R.C., Bauer, S., Tsigaridis, K., Diehl, T., Chin, M., Lin, G., Penner, J., Balkanski, Y., Schulz, M., Bellouin, N., Zhang, K., Stier, P., Lamarque, J.-F. and Takemura, T., 2012. Understanding black carbon radiative forcing uncertainty due to vertical distributions. Nature Geoscience: submitted.

Sanderson, M.G., Jones, C.D., Collins, W.J., Johnson, C.E. and Derwent, R.G., 2003. Effect of climate change on isoprene emissions and surface ozone levels. Geophysical Research Letters, **30**(18): 1936.

Sandu, I., Brenguier, J.-L., Geoffroy, O., Thouron, O. and Masson, V., 2008. Aerosol impacts on the diurnal cycle of marine stratocumulus. Journal of the Atmospheric Sciences, **65**(8): 2705-2718.

Sassen, K., DeMott, P.J., Prospero, J.M. and Poellot, M.R., 2003. Saharan dust storms and indirect aerosol effects on clouds: CRYSTAL-FACE results. Geophysical Research Letters, **30**(12): 1633.

Sassen, K. and Dodd, G.C., 1988. Homogeneous nucleation rate for highly supercooled cirrus cloud droplets. Journal of the Atmospheric Sciences, **45**(8): 1357-1369.

Satheesh, S.K. and Moorthy, K.K., 2005. Radiative effects of natural aerosols: A review. Atmospheric Environment, **39**(11): 2089-2110.

Sato, T., Miura, H., Satoh, M., Takayabu, Y. and Wang, Y., 2009. Diurnal cycle of precipitation in the Tropics simulated in a global cloud-resolving model. Journal of Climate, **22**: 4809-4826.

Sausen, R., Isaksen, I., Grewe, V., Hauglustaine, D., Lee, D.S., Myhre, G., Köhlers, M.O., Pitari, G., Schumann, U., Stordal, F. and Zerefos, C., 2005. Aviation radiative forcing in 2000: An update on IPCC (1999). Meteorologische Zeitschrift, **14**: 555-561.

Savic-Jovcic, V. and Stevens, B., 2008. The structure and mesoscale organization of precipitating stratocumulus. Journal of the Atmospheric Sciences, **65**(5): 1587-1605.

Sawant, A.A., Na, K., Zhu, X. and Cocker III, D.R., 2004. Chemical characterization of outdoor PM2.5 and gas-phase compounds in Mira Loma, California. Atmospheric Environment, **38**: 5517-5528.

Schaller, R.C. and Fukuta, N., 1979. Ice nucleation by aerosol particles - Experimental studies using a wedge-shaped ice thermal-diffusion chamber. Journal of the Atmospheric Sciences, **36**(9): 1788-1802.

Schmidt, A., Carslaw, K.S., Mann, G.W., Rap, A., Pringle, K.J., Spracklen, D.V., Wilson, M. and Forster, P.M., 2012a. Importance of tropospheric volcanic aerosol for indirect radiative forcing of climate. Atmospheric Chemistry and Physics Discussions, **12**: 8009-8051.

Schmidt, H., Alterskjær, K., Bou Karam, D., Boucher, O., Jones, A., Kristjansson, J.E., Niemeier, U., Schulz, M., Aaheim, A., Benduhn, F., Lawrence, M. and Timmreck, C., 2012b. Solar irradiance reduction to counteract radiative forcing from a quadrupling of CO_2: climate responses simulated by four earth system models. Earth System Dynamics, **3**: 63-78.

Schmidt, K.S., Feingold, G., Pilewskie, P., Jiang, H., Coddington, O. and Wendisch, M., 2009. Irradiance in polluted cumulus fields: Measured and modeled cloud-aerosol effects. Geophysical Research Letters, **36**.

Schreier, M., Mannstein, H., Eyring, V. and Bovensmann, H., 2007. Global ship track distribution and radiative forcing from 1 year of AATSR data. Geophysical Research Letters, **34**(17): L17814.

Schulz, M., Textor, C., Kinne, S., Balkanski, Y., Bauer, S., Berntsen, T., Berglen, T., Boucher, O., Dentener, F., Guibert, S., Isaksen, I.S.A., Iversen, T., Koch, D., Kirkevåg, A., Liu, X., Montanaro, V., Myhre, G., Penner, J.E., Pitari, G., Reddy, S., Seland, Ø., Stier, P. and Takemura, T., 2006. Radiative forcing by aerosols as derived from the AeroCom present-day and pre-industrial simulations. Atmospheric Chemistry and Physics, **6**(12): 5225-5246.

Schumann, U. and Graf, K., 2012. Aviation-induced cirrus and radiation changes at diurnal timescales. Journal of Geophysical Research, **submitted**.

Schwartz, S.E. and Freiberg, J.E., 1981. Mass-transport limitation to the rate of reaction of gases in liquid droplets - Application to oxidation of SO_2 in aqueous solutions. Atmospheric Environment, **15**(7): 1129-1144.

Schwarz, J., Gao, R., Spackman, J., Watts, L., Thomson, D., Fahey, D., Ryerson, T., Peischl, J., Holloway, J., Trainer, M., Frost, G., Baynard, T., Lack, D., de Gouw, J., Warneke, C. and Del Negro, L., 2008a. Measurement of the mixing state, mass, and optical size of individual black carbon particles in urban and biomass burning emissions. Geophysical Research Letters, **35**: L13810.

Schwarz, J.P., Gao, R.S., Fahey, D.W., Thomson, D.S., Watts, L.A., Wilson, J.C., Reeves, J.M., Darbeheshti, M., Baumgardner, D.G., Kok, G.L., Chung, S.H., Schulz, M., Hendricks, J., Lauer, A., Karcher, B., Slowik, J.G., Rosenlof, K.H., Thompson, T.L., Langford, A.O., Loewenstein, M. and Aikin, K.C., 2006. Single-particle measurements of midlatitude black carbon and light-scattering aerosols from the boundary layer to the lower stratosphere. Journal of Geophysical Research, **111**: D16207.

Schwarz, J.P., Spackman, J.R., Fahey, D.W., Gao, R.S., Lohmann, U., Stier, P., Watts, L.A., Thomson, D.S., Lack, D.A., Pfister, L., Mahoney, M.J., Baumgardner, D., Wilson, J.C. and Reeves, J.M., 2008b. Coatings and their enhancement of black carbon light absorption in the tropical atmosphere. Journal of Geophysical Research, **113**: D03203.

Schwarz, J.P., Spackman, J.R., Gao, R.S., Watts, L.A., Stier, P., Schulz, M., Davis, S.M., Wofsy, S.C. and Fahey, D.W., 2010. Global-scale black carbon profiles observed in the remote atmosphere and compared to models. Geophysical Research Letters, **37**: L18812.

Sciare, J., Favez, O., Oikonomou, K., Sarda-Estève, R., Cachier, H. and Kazan, V., 2009. Long-term observation of carbonaceous aerosols in the Austral Ocean: Evidence of a marine biogenic origin. Journal of Geophysical Research, **114**: D15302.

Seager, R., Naik, N. and Vecchi, G., 2010. Thermodynamic and dynamic mechanisms for large-scale changes in the hydrological cycle in response to global warming. Journal of Climate, **23**(17): 4651-4668.

Seifert, A. and Beheng, K., 2006. A two-moment cloud microphysics parameterization for mixed-phase clouds, Part II: maritime versus continental deep convective storms. Meteorology and Atmospheric Physics, **92**: 67-88.

Seifert, A., Köhler, C. and Beheng, K.D., 2012. Aerosol-cloud-precipitation effects over Germany as simulated by a convective-scale numerical weather prediction model. Atmospheric Chemistry and Physics, **12**(2): 709-725.

Seifert, A. and Stevens, B., 2010. Microphysical scaling relations in a kinematic model of isolated shallow cumulus clouds. Journal of the Atmospheric Sciences, **67**(5): 1575-1590.
Seifert, A. and Zängl, G., 2010. Scaling relations in warm-rain orographic precipitation. Meteorological Zeitschrift, **19**: 417-426.
Seifert, P., Ansmann, A., Mattis, I., Wandinger, U., Tesche, M., Engelmann, R., Muller, D., Perez, C. and Haustein, K., 2010. Saharan dust and heterogeneous ice formation: Eleven years of cloud observations at a central European EARLINET site. Journal of Geophysical Research, **115**: D20201.
Seitz, R., 2011. Bright water: hydrosols, water conservation and climate change. Climatic Change, **105**(3-4): 365-381.
Sekiguchi, M., Nakajima, T., Suzuki, K., Kawamoto, K., Higurashi, A., Rosenfeld, D., Sano, I. and Mukai, S., 2003. A study of the direct and indirect effects of aerosols using global satellite data sets of aerosol and cloud parameters. Journal of Geophysical Research, **108**(D22): 4699.
Senior, C.A. and Mitchell, J.F.B., 1993. Carbon dioxide and climate: The impact of cloud parameterization. Journal of Climate, **6**: 393-418.
Senior, C.A. and Mitchell, J.F.B., 2000. The time-dependence of climate sensitivity. Geophysical Research Letters, **27**(17): 2685-2688.
Sesartic, A., Lohmann, U. and Storelvmo, T., 2011. Bacteria in the ECHAM5-HAM global climate model. Atmospheric Chemistry Physics Discussion, **11**: 1457-1488.
Sharon, T.M., Albrecht, B.A., Jonsson, H.H., Minnis, P., Khaiyer, M.M., van Reken, T.M., Seinfeld, J. and Flagan, R., 2006. Aerosol and cloud microphysical characteristics of rifts and gradients in maritime stratocumulus clouds. Journal of the Atmospheric Sciences, **63**(3): 983-997.
Sherwood, S.C., Ingram, W., Tsushima, Y., Satoh, M., Roberts, M., Vidale, P.L. and O'Gorman, P.A., 2010a. Relative humidity changes in a warmer climate. Journal of Geophysical Research, **115**: D09104.
Sherwood, S.C. and Meyer, C.L., 2006. The general circulation and robust relative humidity. Journal of Climate, **19**(24): 6278-6290.
Sherwood, S.C., Roca, R., Weckwerth, T.M. and Andronova, N.G., 2010b. Tropospheric water vapor, convection, and climate. Reviews of Geophysics, **48**: RG2001.
Shilling, J.E., Fortin, T.J. and Tolbert, M.A., 2006. Depositional ice nucleation on crystalline organic and inorganic solids. Journal of Geophysical Research, **111**: D12204.
Shindell, D. and Faluvegi, G., 2009. Climate response to regional radiative forcing during the twentieth century. Nature Geoscience, **2**(4): 294-300.
Shindell, D.T., Lamarque, J.-F., Schulz, M., Flanner, M., Jiao, C., Chin, M., Young, P., Lee, Y., Rotstayn, L., Milly, G., Faluvegi, G., Balkanski, Y., Collins, B., Conley, A.J., Dalsoren, S., Easter, R., Ghan, S., Horowitz, L., Liu, X., Myhre, G., Nagashima, T., Naik, V., Rumbold, S., Skeie, R., Sudo, K., Szopa, S., Takemura, T. and Yoon, J.-H., 2012a. Radiative forcing in the ACCMIP historical and future climate simulations. **submitted**.
Shindell, D.T., Voulgarakis, A., Faluvegi, G. and Milly, G., 2012b. Precipitation response to regional radiative forcing. Atmospheric Chemistry and Physics, **12**: 6969-6982.
Shresth, A.B., Wake, C.P., Dibb, J.E., Mayewski, P.A., Whitlow, S.I., Carmichael, G.R. and Ferm, M., 2000. Seasonal variations in aerosol concentrations and compositions in the Nepal Himalaya. Atmospheric Environment, **34**(20): 3349-3363.
Shupe, M.D., Daniel, J.S., de Boer, G., Eloranta, E.W., Kollias, P., Long, C.N., Luke, E.P., Turner, D.D. and Verlinde, J., 2008. A focus on mixed-phase clouds. The status of ground-based observational methods. Bulletin of the American Meteorological Society, **89**(10): 1549-1562.
Siebesma, A.P., Brenguier, J.-L., Bretherton, C.S., Grabowski, W.W., Heintzenberg, J., Kärcher, B., Lehmann, K., Petch, J.C., Spichtinger, P., Stevens, B. and Stratmann, F., 2009. Cloud-controlling factors. In: J. Heintzenberg and R.J. Charlson (Editors), Clouds in the Perturbed Climate System: Their Relationship to Energy Balance, Atmospheric Dynamics, and Precipitation. MIT Press, Cambridge, pp. 269-290.
Siebesma, A.P., Bretherton, C.S., Brown, A., Chlond, A., Cuxart, J., Duynkerke, P.G., Jiang, H.L., Khairoutdinov, M., Lewellen, D., Moeng, C.H., Sanchez, E., Stevens, B. and Stevens, D.E., 2003. A large eddy simulation intercomparison study of shallow cumulus convection. Journal of the Atmospheric Sciences, **60**(10): 1201-1219.
Siebesma, A.P., Soares, P.M.M. and Teixeira, J., 2007. A combined eddy-diffusivity mass-flux approach for the convective boundary layer. Journal of the Atmospheric Sciences, **64**: 1230-1248.
Sipila, M., Berndt, T., Petaja, T., Brus, D., Vanhanen, J., Stratmann, F., Patokoski, J., Mauldin, R., Hyvarinen, A., Lihavainen, H. and Kulmala, M., 2010. The role of sulfuric acid in atmospheric nucleation. Science, **327**(5970): 1243-1246.
Skeie, R., Berntsen, T., Myhre, G., Pedersen, C., Strom, J., Gerland, S. and Ogren, J., 2011. Black carbon in the atmosphere and snow, from pre-industrial times until present. Atmospheric Chemistry and Physics, **11**(14): 6809-6836.
Slingo, A., 1990. Sensitivity of the Earth's radiation budget to changes in low clouds. Nature, **343**: 49-51.
Small, J.D., Chuang, P.Y., Feingold, G. and Jiang, H., 2009. Can aerosol decrease cloud lifetime? Geophysical Research Letters, **36**: L16806.
Smirnov, A., Holben, B., Giles, D., Slutsker, I., O'Neill, N., Eck, T., Macke, A., Croot, P., Courcoux, Y., Sakerin, S., Smyth, T., Zielinski, T., Zibordi, G., Goes, J., Harvey, M., Quinn, P., Nelson, N., Radionov, V., Duarte, C., Losno, R., Sciare, J., Voss, K., Kinne, S., Nalli, N., Joseph, E., Moorthy, K., Covert, D., Gulev, S., Milinevsky,

G., Larouche, P., Belanger, S., Horne, E., Chin, M., Remer, L., Kahn, R., Reid, J., Schulz, M., Heald, C., Zhang, J., Lapina, K., Kleidman, R., Griesfeller, J., Gaitley, B., Tan, Q. and Diehl, T., 2011. Maritime aerosol network as a component of AERONET - first results and comparison with global aerosol models and satellite retrievals. Atmospheric Measurement Techniques, **4**(3): 583-597.

Smith, J., Barsanti, K., Friedli, H., Ehn, M., Kulmala, M., Collins, D., Scheckman, J., Williams, B. and McMurry, P., 2010. Observations of aminium salts in atmospheric nanoparticles and possible climatic implications. Proceedings of the National Academy of Sciences of the United States of America, **107**(15): 6634-6639.

Smith, S.J. and Rasch, P.J., 2012. The long-term policy context for solar radiation management. Climatic Change, **Submitted**.

Snow-Kropla, E., Pierce, J., Westervelt, D. and Trivitayanurak, W., 2011. Cosmic rays, aerosol formation and cloud-condensation nuclei: sensitivities to model uncertainties. Atmospheric Chemistry and Physics, **11**(8): 4001-4013.

Soden, B.J. and Held, I.M., 2006. An assessment of climate feedbacks in coupled ocean-atmosphere models. Journal of Climate, **19**: 3354-3360.

Soden, B.J., Held, I.M., Colman, R., Shell, K.M., Kiehl, J.T. and Shields, C.A., 2008. Quantifying climate feedbacks using radiative kernels. Journal of Climate, **21**(14): 3504-3520.

Soden, B.J. and Vecchi, G.A., 2011. The vertical distribution of cloud feedback in coupled ocean-atmosphere models. Geophysical Research Letters, **38**: L12704.

Solomon, S., Rosenlof, K.H., Portmann, R.W., Daniel, J.S., Davis, S.M., Sanford, T.J. and Plattner, G.-K., 2010. Contributions of stratospheric water vapor to decadal changes in the rate of global warming. Science, ***327***: 1219-1223.

Somerville, R.C.J. and Remer, L.A., 1984. Cloud optical-thickness feedbacks in the CO_2 climate problem. Journal of Geophysical Research, **89**(D6): 9668-9672.

Song, X. and Zhang, G.J., 2011. Microphysics parameterization for convective clouds in a global climate model: Description and single-column model tests. Journal of Geophysical Research, **116**: D02201.

Song, X.L. and Zhang, G.J., 2009. Convection parameterization, tropical Pacific double ITCZ, and upper-ocean biases in the NCAR CCSM3. Part I: Climatology and atmospheric feedback. Journal of Climate, **22**(16): 4299-4315.

Souza, P.A.d., Mello, W.Z.d., MarianiRauda, L. and SellaSilvia, M., 2010. Caracterization of fine and coarse particulate matter and composition of the water-soluble inorganic fraction in São José dos Campos (SP). Quím. Nova, **33**(6).

Spencer, R.W. and Braswell, W.D., 2008. Potential biases in feedback diagnosis from observational data: A simple model demonstration. Journal of Climate, **21**(21): 5624-5628.

Spencer, R.W. and Braswell, W.D., 2010. On the diagnosis of radiative feedback in the presence of unknown radiative forcing. Journal of Geophysical Research, **115**: D16109.

Spracklen, D., Jimenez, J., Carslaw, K., Worsnop, D., Evans, M., Mann, G., Zhang, Q., Canagaratna, M., Allan, J., Coe, H., McFiggans, G., Rap, A. and Forster, P., 2011. Aerosol mass spectrometer constraint on the global secondary organic aerosol budget. Atmospheric Chemistry and Physics, **11**(23): 12109-12136.

Spracklen, D.V., Carslaw, K.S., Kulmala, M., Kerminen, V.M., Sihto, S.L., Riipinen, I., Merikanto, J., Mann, G.W., Chipperfield, M.P., Wiedensohler, A., Birmili, W. and Lihavainen, H., 2008. Contribution of particle formation to global cloud condensation nuclei concentrations. Geophysical Research Letters, **35**: L06808.

Spracklen, D.V., Carslaw, K.S., Merikanto, J., Mann, G.W., Reddington, C.L., Pickering, S., Ogren, J.A., Andrews, E., Baltensperger, U., Weingartner, E., Boy, M., Kulmala, M., Laakso, L., Lihavainen, H., Kivekas, N., Komppula, M., Mihalopoulos, N., Kouvarakis, G., Jennings, S.G., O'Dowd, C., Birmili, W., Wiedensohler, A., Weller, R., Gras, J., Laj, P., Sellegri, K., Bonn, B., Krejci, R., Laaksonen, A., Hamed, A., Minikin, A., Harrison, R.M., Talbot, R. and Sun, J., 2010. Explaining global surface aerosol number concentrations in terms of primary emissions and particle formation. Atmospheric Chemistry and Physics, **10**: 4775-4793.

Stan, C., Khairoutdinov, M., DeMott, C.A., Krishnamurthy, V., Straus, D.M., Randall, D.A., Kinter, J.L. and Shukla, J., 2010. An ocean-atmosphere climate simulation with an embedded cloud resolving model. Geophysical Research Letters, **37**: L01702.

Stephens, G. and Hu, Y., 2010. Are climate-related changes to the character of global-mean precipitation predictable? Environmental Research Letters, **5**(2): 025209.

Stephens, G.L., L'Ecuyer, T., Forbes, R., Gettlemen, A., Golaz, J.-C., Bodas-Salcedo, A., Suzuki, K., Gabriel, P. and Haynes, J., 2010. Dreary state of precipitation in global models. Journal of Geophysical Research, **115**: D24211.

Stephens, G.L., Vane, D.G., Boain, R.J., Mace, G.G., Sassen, K., Wang, Z.E., Illingworth, A.J., O'Connor, E.J., Rossow, W.B., Durden, S.L., Miller, S.D., Austin, R.T., Benedetti, A., Mitrescu, C. and CloudSat Sci, T., 2002. The Cloudsat mission and the A-train - A new dimension of space-based observations of clouds and precipitation. Bulletin of the American Meteorological Society, **83**(12): 1771-1790.

Stephens, G.L., Vane, D.G., Tanelli, S., Im, E., Durden, S., Rokey, M., Reinke, D., Partain, P., Mace, G.G., Austin, R., L'Ecuyer, T., Haynes, J., Lebsock, M., Suzuki, K., Waliser, D., Wu, D., Kay, J., Gettelman, A., Wang, Z. and Marchand, R., 2008. CloudSat mission: Performance and early science after the first year of operation. Journal of Geophysical Research, **113**(D23): D00A18.

Stephens, G.L., Wild, M., Stackhouse, P.W., L'Ecuyer, T., Kato, S. and Henderson, D.S., 2012. The global character of the flux of downward longwave radiation. Journal of Climate, **25**(7): 2329-2340.

Stevens, B. and Brenguier, J.-L., 2009. Cloud-controlling factors: Low clouds. In: J. Heintzenberg and R.J. Charlson (Editors), Clouds in the Perturbed Climate System: Their Relationship to Energy Balance, Atmospheric Dynamics, and Precipitation. MIT Press, Cambridge, pp. 173-196.
Stevens, B., Cotton, W.R., Feingold, G. and Moeng, C.-H., 1998. Large-eddy simulations of strongly precipitating, shallow, stratocumulus-topped boundary layers. Journal of the Atmospheric Sciences, **55**(24): 3616-3638.
Stevens, B. and Feingold, G., 2009. Untangling aerosol effects on clouds and precipitation in a buffered system. Nature, **461**(7264): 607-613.
Stevens, B., Moeng, C.H., Ackerman, A.S., Bretherton, C.S., Chlond, A., De Roode, S., Edwards, J., Golaz, J.C., Jiang, H.L., Khairoutdinov, M., Kirkpatrick, M.P., Lewellen, D.C., Lock, A., Muller, F., Stevens, D.E., Whelan, E. and Zhu, P., 2005a. Evaluation of large-eddy simulations via observations of nocturnal marine stratocumulus. Monthly Weather Review, **133**(6): 1443-1462.
Stevens, B. and Schwartz, S.E., 2012. Observing and modeling Earth's energy flows. Surveys in Geophysics, **in press**.
Stevens, B. and Seifert, A., 2008. Understanding macrophysical outcomes of microphysical choices in simulations of shallow cumulus convection. Journal of the Meteorological Society of Japan, **86**: 143-162.
Stevens, B., Vali, G., Comstock, K., Wood, R., van Zanten, M.C., Austin, P.H., Bretherton, C.S. and Lenschow, D.H., 2005b. Pockets of open cells and drizzle in marine stratocumulus. Bulletin of the American Meteorological Society, **86**(1): 51-57.
Stier, P., Schutgens, N.A.J., Bian, H., Boucher, O., Chin, M., Ghan, S., Huneeus, N., Kinne, S., Lin, G., Myhre, G., Penner, J.E., Randles, C., Samset, B., Schulz, M., Yu, H. and Zhou, C., 2012. Host model uncertainties in aerosol forcing estimates: Results from the AeroCom prescribed intercomparison study. Atmospheric Chemistry and Physics, **submitted**.
Stier, P., Seinfeld, J., Kinne, S. and Boucher, O., 2007. Aerosol absorption and radiative forcing. Atmospheric Chemistry and Physics, **7**: 5237-5261.
Stier, P., Seinfeld, J.H., Kinne, S., Feichter, J. and Boucher, O., 2006. Impact of nonabsorbing anthropogenic aerosols on clear-sky atmospheric absorption. Journal of Geophysical Research, **111**: D18201.
Stjern, C.W., 2011. Weekly cycles in precipitation and other meteorological variables in a polluted region of Europe. Atmospheric Chemistry and Physics, **11**: 4095-4104.
Stone, E., Schauer, J., Quraishi, T.A. and Mahmood, A., 2010. Chemical characterization and source apportionment of fine and coarse particulate matter in Lahore, Pakistan. Atmospheric Environment, **44**: 1062-1070.
Stone, R.S., Anderson, G.P., Shettle, E.P., Andrews, E., Loukachine, K., Dutton, E.G., Schaaf, C. and Roman, M.O., III, 2008. Radiative impact of boreal smoke in the Arctic: Observed and modeled. Journal of Geophysical Research, **113**: D14S16.
Storelvmo, T., 2011. Uncertainties in aerosol direct and indirect effects attributed to uncertainties in convective transport parametrizations. Atmospheric Research, **in press**.
Storelvmo, T., Hoose, C. and Eriksson, P., 2011. Global modeling of mixed-phase clouds: The albedo and lifetime effects of aerosols. Journal of Geophysical Research, **116**: D05207.
Storelvmo, T., Kristjansson, J.E., Ghan, S.J., Kirkevag, A., Seland, O. and Iversen, T., 2006. Predicting cloud droplet number concentration in Community Atmosphere Model (CAM)-Oslo. Journal of Geophysical Research, **111**(D24): D24208.
Storelvmo, T., Kristjansson, J.E. and Lohmann, U., 2008a. Aerosol influence on mixed-phase clouds in CAM-Oslo. Journal of the Atmospheric Sciences, **65**(10): 3214-3230.
Storelvmo, T., Kristjansson, J.E., Lohmann, U., Iversen, T., Kirkevag, A. and Seland, O., 2008b. Modeling of the Wegener-Bergeron-Findeisen process-implications for aerosol indirect effects. Environmental Research Letters, **3**(4): 045001.
Storelvmo, T., Lohmann, U. and Bennartz, R., 2009. What governs the spread in shortwave forcings in the transient IPCC AR4 models? Geophysical Research Letters, **36**: L01806.
Stott, P.A., Mitchell, J.F.B., Allen, M.R., Delworth, T.L., Gregory, J.M., Meehl, G.A. and Santer, B.D., 2006. Observational constraints on past attributable warming and predictions of future global warming. Journal of Climate, **19**(13): 3055-3069.
Stramler, K., Del Genio, A.D. and Rossow, W.B., 2011. Synoptically driven Arctic winter states. Journal of Climate, **24**(6): 1747-1762.
Stratmann, F., Moehler, O., Shaw, R. and Heike, W., 2009. Laboratory cloud simulation: Capabilities and future directions. In: J. Heintzenberg and R.J. Charlson (Editors), Clouds in the Perturbed Climate System: Their Relationship to Energy Balance, Atmospheric Dynamics, and Precipitation. MIT Press, Cambridge, pp. 149-172.
Struthers, H., Ekman, A.M.L., Glantz, P., Iversen, T., Kirkevåg, A., Mårtensson, E.M., Seland, Ø. and Nilsson, E.D., 2011. The effect of sea ice loss on sea salt aerosol concentrations and the radiative balance in the Arctic. Atmospheric Chemistry and Physics, **11**: 3459-3477.
Stubenrauch, C.J., Rossow, W.B., Kinne, S., Ackerman, S., Cesana, G., Chepfer, H., Di Girolamo, L., Getzewich, B., Guignard, A., Heidinger, A., Maddux, B., Menzel, P., Minnis, P., Pearl, C., Platnick, S., Poulsen, C., Riedi, J., Sun-Mack, S., Walther, A., Winker, D., Zeng, S. and Zhao, G., 2012. Assessment of global cloud datasets from satellites: Project and database initiated by the GEWEX Radiation Panel. Bulletin of the American Meteorological Society: submitted.

Stuber, N. and Forster, P., 2007. The impact of diurnal variations of air traffic on contrail radiative forcing. Atmospheric Chemistry and Physics, **7**: 3153-3162.
Su, W., Loeb, N.G., Schuster, G.L., Chin, M. and Rose, F.G., 2012. Global all-sky shortwave direct radiative forcing of anthropogenic aerosols from combined satellite observations and GOCART simulations. Journal of Geophysical Research, **submitted**.
Su, W.Y., Schuster, G.L., Loeb, N.G., Rogers, R.R., Ferrare, R.A., Hostetler, C.A., Hair, J.W. and Obland, M.D., 2008. Aerosol and cloud interaction observed from high spectral resolution lidar data. Journal of Geophysical Research, **113**: D24202.
Sugiyama, M., Shiogama, H. and Emori, S., 2010. Precipitation extreme changes exceeding moisture content increases in MIROC and IPCC climate models. Proceedings of the National Academy of Sciences of the United States of America, **107**(2): 571-575.
Sun, J.M., Ariya, P.A., Leighton, H.G. and Yau, M.K., 2010. Mystery of ice multiplication in warm-based precipitating shallow cumulus clouds. Geophysical Research Letters, **37**: L10802.
Suzuki, K., Nakajima, T., Numaguti, A., Takemura, T., Kawamoto, K. and Higurashi, A., 2004. A study of the aerosol effect on a cloud field with simultaneous use of GCM modeling and satellite observation. Journal of the Atmospheric Sciences, **61**(2): 179-194.
Suzuki, K., Nakajima, T., Satoh, M., Tomita, H., Takemura, T., Nakajima, T.Y. and Stephens, G.L., 2008. Global cloud-system-resolving simulation of aerosol effect on warm clouds. Geophysical Research Letters, **35**(19): L19817.
Suzuki, K., Stephens, G.L., van den Heever, S.C. and Nakajima, T.Y., 2011. Diagnosis of the warm rain process in cloud-resolving models using joint CloudSat and MODIS observations. Journal of the Atmospheric Sciences, **68**(11): 2655-2670.
Svensmark, H., Bondo, T. and Svensmark, J., 2009. Cosmic ray decreases affect atmospheric aerosols and clouds. Geophysical Research Letters, **36**: L15101.
Tackett, J.L. and Di Girolamo, L., 2009. Enhanced aerosol backscatter adjacent to tropical trade wind clouds revealed by satellite-based lidar. Geophysical Research Letters, **36**: L14804.
Takahashi, K., 2009. The global hydrological cycle and atmospheric shortwave absorption in climate models under CO_2 forcing. Journal of Climate, **22**(21): 5667-5675.
Takemura, T., Nozawa, T., Emori, S., Nakajima, T.Y. and Nakajima, T., 2005. Simulation of climate response to aerosol direct and indirect effects with aerosol transport-radiation model. Journal of Geophysical Research, **110**(D2): D02202.
Takemura, T. and Uchida, T., 2011. Global climate modeling of regional changes in cloud, precipitation, and radiation budget due to the aerosol semi-direct effect of black carbon. Sola, **7**: 181-184.
Tanré, D., Bréon, F.-M., Deuzé, J.-L., Dubovik, O., Ducos, F., François, P., Goloub, P., Herman, M., Lifermann, A. and Waquet, F., 2011. Remote sensing of aerosols by using polarized, directional and spectral measurements within the A-Train: the PARASOL mission. Atmospheric Measurement Techniques, **4**(7): 1383-1395.
Tanré, D., Herman, M. and Kaufman, Y.J., 1996. Information on aerosol size distribution contained in solar reflected spectral radiances. Journal of Geophysical Research, **101**(D14): 19043-19060.
Tanré, D., Kaufman, Y.J., Herman, M. and Mattoo, S., 1997. Remote sensing of aerosol properties over oceans using the MODIS/EOS spectral radiances. Journal of Geophysical Research, **102**: 16971-16988.
Tao, W.-K., Chen, J.-P., Li, Z., Wang, C. and Zhang, C., 2012. Impact of aerosols on convective clouds and precipitation. Reviews of Geophysics, **50**: RG2001.
Tao, W.-K., Chern, J.-D., Atlas, R., Randall, D., Khairoutdinov, M., Li, J.-L., Waliser, D.E., Hou, A., Lin, X., Peters-Lidard, C., Lau, W., Jiang, J. and Simpson, J., 2009. A Multiscale Modeling System: Developments, applications, and critical issues. Bull Amer. Meteor. Soc., **90**: 515-534.
Targino, A.C., Coe, H., Cozic, J., Crosier, J., Crawford, I., Bower, K., Flynn, M., Gallagher, M., Allan, J., Verheggen, B., Weingartner, E., Baltensperger, U. and Choularton, T., 2009. Influence of particle chemical composition on the phase of cold clouds at a high-alpine site in Switzerland. Journal of Geophysical Research, **114**: D18206.
Tegen, I., Werner, M., Harrison, S.P. and Kohfeld, K.E., 2004. Relative importance of climate and land use in determining present and future global soil dust emission. Geophysical Research Letters, **31**: L05105.
Theodosi, C., Im, U., Bougiatioti, A., Zarmpas, P., Yenigun, O. and Mihalopoulos, N., 2010. Aerosol chemical composition over Istanbul. Science of the Total Environment, **408**: 2482-2491.
Tilmes, S., Garcia, R.R., Kinnison, E.D., Gettelman, A. and Rasch, P.J., 2009. Impact of geo-engineered aerosols on troposphere and stratosphere. Journal of Geophysical Research, **114**: D12305.
Tilmes, S., Müller, R. and Salawitch, R., 2008. The sensitivity of polar ozone depletion to proposed geoengineering schemes. Science, **320**(5880): 1201-1204.
Tinsley, B.A., 2000. Influence of solar wind on the global electric circuit, and inferred effects on cloud microphysics, temperature, and dynamics in the troposphere. Space Science Reviews, **94**: 231– 258.
Tomita, H., Miura, H., Iga, S., Nasuno, T. and Satoh, M., 2005. A global cloud-resolving simulation: Preliminary results from an aqua planet experiment. Geophysical Research Letters, **32**: L08805.
Tompkins, A.M. and Craig, G.C., 1998. Radiative–convective equilibrium in a three-dimensional cloud-ensemble model. Quarterly Journal of the Royal Meteorological Society, **124**(550): 2073–2097.

Tompkins, A.M., Gierens, K. and Radel, G., 2007. Ice supersaturation in the ECMWF integrated forecast system. Quarterly Journal of the Royal Meteorological Society, **133**: 53-63.
Torres, O., Bhartia, P.K., Herman, J.R., Ahmad, Z. and Gleason, J., 1998. Derivation of aerosol properties from satellite measurements of backscattered ultraviolet radiation: Theoretical basis. Journal of Geophysical Research, **103**: 17099-17110.
Torres, O., Bhartia, P.K., Herman, J.R., Sinyuk, A., Ginoux, P. and Holben, B., 2002. A long-term record of aerosol optical depth from TOMS observations and comparison to AERONET measurements. Journal of the Atmospheric Sciences, **59**: 398-413.
Torres, O., Tanskanen, A., Veihelmann, B., Ahn, C., Braak, R., Bhartia, P., Veefkind, P. and Levelt, P., 2007. Aerosols and surface UV products from Ozone Monitoring Instrument observations: An overview. Journal of Geophysical Research, **112**(D24).
Trenberth, K., Fasullo, J. and Kiehl, J., 2009. Earth's global energy budget. Bulletin of the American Meteorological Society, **90**(3): 311-323.
Trenberth, K.E. and Dai, A., 2007. Effects of Mount Pinatubo volcanic eruption on the hydrological cycle as an analog of geoengineering. Geophysical Research Letters, **34**: L15702.
Trenberth, K.E. and Fasullo, J.T., 2009. Global warming due to increasing absorbed solar radiation. Geophysical Research Letters, **36**: L07706.
Trenberth, K.E. and Fasullo, J.T., 2010. Simulation of present-day and twenty-first-century energy budgets of the Southern Oceans. Journal of Climate, **23**(2): 440-454.
Trenberth, K.E., Jones, P.D., Ambenje, P., Bojariu, R., Easterling, D., Klein Tank, A., Parker, D., Rahimzadeh, F., Renwick, J.A., Rusticucci, M., Soden, B. and Zhai, P., 2007. Observations: Surface and Atmospheric Climate Change. In: S. Solomon, D. Qin, M. Manning, Z. Chen, M. Marquis, K.B. Averyt, M. Tignor and H.L. Miller (Editors), Climate Change 2007: The Physical Science Basis. Contribution of Working Group I to the Fourth Assessment Report of the Intergovernmental Panel on Climate Change. Cambridge University Press, Cambridge, United Kingdom and New York, NY, USA.
Tselioudis, G. and Rossow, W.B., 2006. Climate feedback implied by observed radiation and precipitation changes with midlatitude storm strength and frequency. Geophysical Research Letters, **33**(2): L02704.
Tsigaridis, K. and Kanakidou, M., 2003. Global modelling of secondary organic aerosol in the troposphere: a sensitivity analysis. Atmospheric Chemistry and Physics, **3**: 1849-1869.
Tsigaridis, K. and Kanakidou, M., 2007. Secondary organic aerosol importance in the future atmosphere. Atmospheric Environment, **41**(22): 4682-4692.
Tsushima, Y., Emori, S., Ogura, T., Kimoto, M., Webb, M.J., Williams, K.D., Ringer, M.A., Soden, B.J., Li, B. and Andronova, N., 2006. Importance of the mixed-phase cloud distribution in the control climatefor assessing the response of clouds to carbon dioxide increase:a multi-model study. Climate Dynamics, **27**: 113–126.
Tuttle, J.D. and Carbone, R.E., 2011. Inferences of weekly cycles in summertime rainfall. Journal of Geophysical Research, **116**: D20213.
Twohy, C. and Anderson, J., 2008. Droplet nuclei in non-precipitating clouds: composition and size matter. Environmental Research Letters, **3**(4): 045002.
Twohy, C.H., Coakley, J.A., Jr. and Tahnk, W.R., 2009. Effect of changes in relative humidity on aerosol scattering near clouds. Journal of Geophysical Research, **114**: D05205.
Twohy, C.H., DeMott, P.J., Pratt, K.A., Subramanian, R., Kok, G.L., Murphy, S.M., Lersch, T., Heymsfield, A.J., Wang, Z.E., Prather, K.A. and Seinfeld, J.H., 2010. Relationships of biomass-burning aerosols to ice in orographic wave clouds. Journal of the Atmospheric Sciences, **67**(8): 2437-2450.
Twohy, C.H., Petters, M.D., Snider, J.R., Stevens, B., Tahnk, W., Wetzel, M., Russell, L. and Burnet, F., 2005. Evaluation of the aerosol indirect effect in marine stratocumulus clouds: Droplet number, size, liquid water path, and radiative impact. Journal of Geophysical Research, **110**: D08203.
Twomey, S., 1974. Pollution and the planetary albedo. Atmospheric Environment, **8**: 1251-1256.
Twomey, S., 1977. Influence of pollution on shortwave albedo of clouds. Journal of the Atmospheric Sciences, **34**(7): 1149-1152.
Udelhofen, P. and Cess, R., 2001. Cloud cover variations over the United States: An influence of cosmic rays or solar variability? Geophysical Research Letters, **28**(13): 2617-2620.
Ulbrich, I.M., Canagaratna, M.R., Zhang, Q., Worsnop, D.R. and Jimenez, J.L., 2009. Interpretation of organic components from Positive Matrix Factorization of aerosol mass spectrometric data. Atmospheric Chemistry and Physics, **9**: 2891-2918.
Unger, N., Menon, S., Koch, D.M. and Shindell, D.T., 2009. Impacts of aerosol-cloud interactions on past and future changes in tropospheric composition. Atmospheric Chemistry and Physics, **9**(12): 4115-4129.
Unger, N., Shindell, D.T., Koch, D.M., Amann, M., Cofala, J. and Streets, D.G., 2006. Influences of man-made emissions and climate changes on tropospheric ozone, methane, and sulfate at 2030 from a broad range of possible futures. Journal of Geophysical Research, **111**(D12): D12313.
Usoskin, I. and Kovaltsov, G., 2008. Cosmic rays and climate of the Earth: Possible connection. Comptes Rendus Geoscience, **340**(7): 441-450.
Uttal, T., Curry, J.A., McPhee, M.G., Perovich, D.K., Moritz, R.E., Maslanik, J.A., Guest, P.S., Stern, H.L., Moore, J.A., Turenne, R., Heiberg, A., Serreze, M.C., Wylie, D.P., Persson, O.G., Paulson, C.A., Halle, C., Morison,

J.H., Wheeler, P.A., Makshtas, A., Welch, H., Shupe, M.D., Intrieri, J.M., Stamnes, K., Lindsey, R.W., Pinkel, R., Pegau, W.S., Stanton, T.P. and Grenfeld, T.C., 2002. Surface heat budget of the Arctic Ocean. Bulletin of the American Meteorological Society, **83**(2): 255-+.

van den Heever, S.C., Stephens, G.L. and Wood, N.B., 2011. Aerosol indirect effects on tropical convection characteristics under conditions of radiative-convective equilibrium. Journal of the Atmospheric Sciences, **68**(4): 699-718.

vanZanten, M.C., Stevens, B., Vali, G. and Lenschow, D.H., 2005. Observations of drizzle in nocturnal marine stratocumulus. Journal of the Atmospheric Sciences, **62**(1): 88-106.

vanZanten, M.C., Stevens, B.B., Nuijens, L., Siebesma, A.P., Ackerman, A., Burnet, F., Cheng, A., Couvreux, F., Jiang, H., Khairoutdinov, M., Kogan, Y., Lewellen, D.C., Mechem, D., Nakamura, K., Noda, A., Shipway, B.J., Slawinska, J., Wang, S. and Wyszogrodzki, A., 2011. Controls on precipitation and cloudiness in simulations of trade-wind cumulus as observed during RICO. Journal of Advances in Modeling Earth Systems, **3**: M06001.

Várnai, T. and Marshak, A., 2009. MODIS observations of enhanced clear sky reflectance near clouds. Geophysical Research Letters, **36**: L06807.

Vavrus, S., Holland, M.M. and Bailey, D.A., 2011. Changes in Arctic clouds during intervals of rapid sea ice loss. Climate Dynamics, **36**(7-8): 1475-1489.

Vavrus, S., Waliser, D., Schweiger, A. and Francis, J., 2009. Simulations of 20th and 21st century Arctic cloud amount in the global climate models assessed in the IPCC AR4. Climate Dynamics, **33**(7-8): 1099-1115.

Verheggen, B., Cozic, J., Weingartner, E., Bower, K., Mertes, S., Connolly, P., Gallagher, M., Flynn, M., Choularton, T. and Baltensperger, U., 2007. Aerosol partitioning between the interstitial and the condensed phase in mixed-phase clouds. Journal of Geophysical Research, **112**(D23): D23202.

Verlinde, J., Harrington, J.Y., McFarquhar, G.M., Yannuzzi, V.T., Avramov, A., Greenberg, S., Johnson, N., Zhang, G., Poellot, M.R., Mather, J.H., Turner, D.D., Eloranta, E.W., Zak, B.D., Prenni, A.J., Daniel, J.S., Kok, G.L., Tobin, D.C., Holz, R., Sassen, K., Spangenberg, D., Minnis, P., Tooman, T.P., Ivey, M.D., Richardson, S.J., Bahrmann, C.P., Shupe, M., DeMott, P.J., Heymsfield, A.J. and Schofield, R., 2007. The mixed-phase Arctic cloud experiment. Bulletin of the American Meteorological Society, **88**(2): 205-221.

Vial, J., Dufresne, J.-L. and Bony, S., 2012. On the interpretation of inter-model spread in CMIP5 climate sensitivity estimates. Climate Dynamics: submitted.

Viana, M., Chi, X., Maenhaut, W., Querol, X., Alastuey, A., Mikuska, P. and Vecera, Z., 2006. Organic and elemental carbon concentrations during summer and winter sampling campaigns in Barcelona, Spain. Atmospheric Environment, **40**: 2180-2193.

Viana, M., Maenhaut, W., Chi, X., Querol, X. and lastuey, A., 2007. Comparative chemical mass closure of fine and coarse aerosols at two sites in South and West Europe: implications for EU air pollution policies. Atmospheric Environment, **41**: 315-326.

Viana, M., Querol, X., Ballester, F., Llop, S., Esplugues, A., Patier, R.F., Dos Santos, S.G. and Herce, M.D., 2008. Characterising exposure to PM aerosols for an epidemiological study. Atmospheric Environment, **42**: 1552-1568.

Vignati, E., Karl, M., Krol, M., Wilson, J., Stier, P. and Cavalli, F., 2010. Sources of uncertainties in modelling black carbon at the global scale. Atmospheric Chemistry and Physics, **10**: 2595-2611.

Vogelmann, A.M., Ackerman, T.P. and Turco, R.P., 1992. Enhancements in biologically effective ultraviolet radiation following volcanic eruptions. Nature, **359**: 47-49.

Vogelmann, A.M., McFarquhar, G.M., Ogren, J.A., Turner, D.D., Comstock, J.M., Feingold, G., Long, C.N., Jonsson, H.H., Bucholtz, A., Collins, D.R., Diskin, G.S., Gerber, H., Lawson, R.P., Woods, R.K., Andrews, E., Yang, H.-J., Chiu, J.C., Hartsock, D., Hubbe, J.M., Lo, C., Marshak, A., Monroe, J.W., McFarlane, S.A., Schmid, B., Tomlinson, J.M. and Toto, T., 2012. Racoro Extended-Term Aircraft Observations of Boundary Layer Clouds. Bulletin of the American Meteorological Society, **93**(6): 861-878.

Volkamer, R., Jimenez, J.L., San Martini, F., Dzepina, K., Zhang, Q., Salcedo, D., Molina, L.T., Worsnop, D.R. and Molina, M.J., 2006. Secondary organic aerosol formation from anthropogenic air pollution: Rapid and higher than expected. Geophysical Research Letters, **33**: L17811.

Volodin, E.M., 2008. Relation between temperature sensitivity to doubled carbon dioxide and the distribution of clouds in current climate models. Izvestiya Atmospheric and Oceanic Physics, **44**(3): 288-299.

von Blohn, N., Mitra, S.K., Diehl, K. and Borrmann, S., 2005. The ice nucleating ability of pollen: Part III: New laboratory studies in immersion and contact freezing modes including more pollen types. Atmospheric Research, **78**(3-4): 182-189.

Wagner, R., Mohler, O., Saathoff, H., Schnaiter, M. and Leisner, T., 2010. High variability of the heterogeneous ice nucleation potential of oxalic acid dihydrate and sodium oxalate. Atmospheric Chemistry and Physics, **10**(16): 7617-7641.

Wagner, R., Mohler, O., Saathoff, H., Schnaiter, M. and Leisner, T., 2011. New cloud chamber experiments on the heterogeneous ice nucleation ability of oxalic acid in the immersion mode. Atmospheric Chemistry and Physics, **11**(5): 2083-2110.

Waliser, D.E., Li, J.L.F., L'Ecuyer, T.S. and Chen, W.T., 2011. The impact of precipitating ice and snow on the radiation balance in global climate models. Geophysical Research Letters, **38**: L06802.

Wang, B.B. and Knopf, D.A., 2011. Heterogeneous ice nucleation on particles composed of humic-like substances impacted by O_3. Journal of Geophysical Research, **116**: D03205.

Wang, G., Wang, H., Yu, Y., Gao, S., Feng, J., Gao, S. and Wang, L., 2003. Chemical characterization of water-soluble components of PM10 and PM2.5 atmospheric aerosols in five locations of Nanjing, China. Atmospheric Environment, **37**: 2893-2902.

Wang, H. and Feingold, G., 2009a. Modeling mesoscale cellular structures and drizzle in marine stratocumulus. Part I: Impact of drizzle on the formation and evolution of open cells. Journal of the Atmospheric Sciences, **66**(11): 3237-3256.

Wang, H. and Feingold, G., 2009b. Modeling mesoscale cellular structures and drizzle in marine stratocumulus. Part II: The microphysics and dynamics of the boundary region between open and closed cells. Journal of the Atmospheric Sciences, **66**(11): 3257-3275.

Wang, H., Kawamuraa, K. and Shooter, D., 2005a. Carbonaceous and ionic components in wintertime atmospheric aerosols from two New Zealand cities: Implications for solid fuel combustion. Atmospheric Environment, **39**: 5865–5875.

Wang, H., Rasch, P. and Feingold, G., 2011a. Manipulating marine stratocumulus cloud amount and albedo: a process-modelling study of aerosol-cloud-precipitation interactions in response to injection of cloud condensation nuclei. Atmospheric Chemistry and Physics, **11**(9): 4237-4249.

Wang, H. and Shooter, D., 2001. Water soluble ions of atmospheric aerosols in three NewZealand cities: seasonal changes and sources. Atmospheric Environment, **35**: 6031–6040.

Wang, L., Khalizov, A., Zheng, J., Xu, W., Ma, Y., Lal, V. and Zhang, R., 2010a. Atmospheric nanoparticles formed from heterogeneous reactions of organics. Nature Geoscience, **3**(4): 238-242.

Wang, M., Ghan, S., Ovchinnikov, M., Liu, X., Easter, R., Kassianov, E., Qian, Y. and Morrison, H., 2011b. Aerosol indirect effects in a multi-scale aerosol-climate model PNNL-MMF. Atmospheric Chemistry and Physics, **11**(11): 5431-5455.

Wang, M. and Penner, J., 2009. Aerosol indirect forcing in a global model with particle nucleation. Atmospheric Chemistry and Physics, **9**: 239-260.

Wang, T., Li, S., Shen, Y., Deng, J. and Xie, M., 2010b. Investigations on direct and indirect effect of nitrate on temperature and precipitation in China using a regional climate chemistry modeling system. Journal of Geophysical Research, **115**: D00K26.

Wang, Y., Zhuang, G., Tang, A., Yuan, H., Sun, Y., Chen, S. and Zheng, A., 2005b. The ion chemistry and the source of PM 2.5 aerosol in Beijing. Atmospheric Environment, **39**: 3771-3784.

Wang, Y., Zhuang, G., Zhang, X., Huang, K., Xu, C., Tang, A., Chen, J. and An, Z., 2006. The ion chemistry, seasonal cycle, and sources of PM2.5 and TSP aerosol in Shanghai. Atmospheric Environment, **40**: 2935-2952.

Wang, Z., Zhang, H. and Shen, X., 2011c. Radiative forcing and climate response due to black carbon in snow and ice. Advances in Atmospheric Sciences, **28**(6): 1336-1344.

Waquet, F., Riedi, J., Labonnote, L., Goloub, P., Cairns, B., Deuzé, J. and Tanré, D., 2009. Aerosol remote sensing over clouds using A-Train observations. Journal of the Atmospheric Sciences, **66**(8): 2468-2480.

Warneke, C., Froyd, K.D., Brioude, J., Bahreini, R., Brock, C.A., Cozic, J., de Gouw, J.A., Fahey, D.W., Ferrare, R., Holloway, J.S., Middlebrook, A.M., Miller, L., Montzka, S., Schwarz, J.P., Sodemann, H., Spackman, J.R. and Stohl, A., 2010. An important contribution to springtime Arctic aerosol from biomass burning in Russia. Geophysical Research Letters, **37**: L01801.

Watanabe, M., Emori, S., Satoh, M. and Miura, H., 2009. A PDF-based hybrid prognostic cloud scheme for general circulation models. Climate Dynamics, **33**: 795-816.

Webb, M., Lambert, F.H. and Gregory, J., 2012. Origins of differences in climate sensitivity, forcing and feedback in climate models. Climate Dynamics, **Online first**.

Webb, M.J. and Lock, A., 2012. Coupling between subtropical cloud feedback and the local hydrological cycle in a climate model. Climate Dynamics: in press.

Weinstein, J.P., Hedges, S.R. and Kimbrough, S., 2010. Characterization and aerosol mass balance of PM2.5 and PM10 collected in Conakry, Guinea during the 2004 Harmattan period. Chemosphere, **78**: 980–988.

Welti, A., Lüönd, F., Stetzer, O. and Lohmann, U., 2009. Influence of particle size on the ice nucleating ability of mineral dusts. Atmospheric Chemistry and Physics, **9**(18): 6705-6715.

Wen, G., Marshak, A., Cahalan, R.F., Remer, L.A. and Kleidman, R.G., 2007. 3-D aerosol-cloud radiative interaction observed in collocated MODIS and ASTER images of cumulus cloud fields. Journal of Geophysical Research, **112**(D13): D13204.

Wetherald, R.T. and Manabe, S., 1980. Cloud cover and climate sensitivity. Journal of the Atmospheric Sciences, **37**(7): 1485-1510.

Wex, H., McFiggans, G., Henning, S. and Stratmann, F., 2010. Influence of the external mixing state of atmospheric aerosol on derived CCN number concentrations. Geophysical Research Letters, **37**: L10805.

Whitlock, C., Bartlett, D. and Gurganus, E., 1982. Sea foam reflectance and influence on optimum wavelength for remote-sensing of ocean aerosols. Geophysical Research Letters, **9**(6): 719-722.

Wigley, T.M.L., 2006. A combined mitigation/geoengineering approach to climate stabilization. Science, **314**: 452-454.

Wilcox, E.M., 2010. Stratocumulus cloud thickening beneath layers of absorbing smoke aerosol. Atmospheric Chemistry and Physics, **10**(23): 11769-11777.

Williams, K.D., Jones, A., Roberts, D.L., Senior, C.A. and Woodage, M.J., 2001. The response of the climate system to the indirect effects of anthropogenic sulfate aerosol. Climate Dynamics, **17**(11): 845-856.

Williams, K.D., Ringer, M.A., Senior, C.A., Webb, M.J., McAvaney, B.J., Andronova, N., Bony, S., Dufresne, J.-L., Emori, S., Gudgel, R., Knutson, T., Li, B., Lo, K., Musat, I., Wegner, J., Slingo, A. and Mitchell, J.F.B., 2006. Evaluation of a component of the cloud response to climate change in an intercomparison of climate models. Climate Dynamics, **26**: 145-165.

Williams, K.D. and Tselioudis, G., 2007. GCM intercomparison of global cloud regimes: present-day evaluation and climate change response. Climate Dynamics, **29**(2-3): 231-250.

Williams, K.D. and Webb, M.J., 2009. A quantitative performance assessment of cloud regimes in climate models. Climate Dynamics, **33**(1): 141-157.

Winker, D.M., Vaughan, M.A., Omar, A., Hu, Y.X., Powell, K.A., Liu, Z.Y., Hunt, W.H. and Young, S.A., 2009. Overview of the CALIPSO mission and CALIOP data processing algorithms. Journal of Atmospheric and Oceanic Technology, **26**: 2310-2323.

Wise, M.E., Baustian, K.J. and Tolbert, M.A., 2009. Laboratory studies of ice formation pathways from ammonium sulfate particles. Atmospheric Chemistry and Physics, **9**(5): 1639-1646.

Wise, M.E., Baustian, K.J. and Tolbert, M.A., 2010. Internally mixed sulfate and organic particles as potential ice nuclei in the tropical tropopause region. Proceedings of the National Academy of Sciences of the United States of America, **107**(15): 6693-6698.

Wood, R., 2005. Drizzle in stratiform boundary layer clouds. Part II: Microphysical aspects. Journal of the Atmospheric Sciences, **62**(9): 3034-3050.

Wood, R., 2007. Cancellation of aerosol indirect effects in marine stratocumulus through cloud thinning. Journal of the Atmospheric Sciences, **64**(7): 2657-2669.

Wood, R. and Bretherton, C.S., 2006. On the relationship between stratiform low cloud cover and lower-tropospheric stability. Journal of Climate, **19**(24): 6425-6432.

Wood, R., Bretherton, C.S., Leon, D., Clarke, A.D., Zuidema, P., Allen, G. and Coe, H., 2011a. An aircraft case study of the spatial transition from closed to open mesoscale cellular convection over the Southeast Pacific. Atmospheric Chemistry and Physics, **11**(5): 2341-2370.

Wood, R., Mechoso, C.R., Bretherton, C.S., Weller, R.A., Huebert, B., Straneo, F., Albrecht, B.A., Coe, H., Allen, G., Vaughan, G., Daum, P., Fairall, C., Chand, D., Gallardo Klenner, L., Garreaud, R., Grados, C., Covert, D.S., Bates, T.S., Krejci, R., Russell, L.M., de Szoeke, S., Brewer, A., Yuter, S.E., Springston, S.R., Chaigneau, A., Toniazzo, T., Minnis, P., Palikonda, R., Abel, S.J., Brown, W.O.J., Williams, S., Fochesatto, J., Brioude, J. and Bower, K.N., 2011b. The VAMOS Ocean-Cloud-Atmosphere-Land Study Regional Experiment (VOCALS-REx): goals, platforms, and field operations. Atmospheric Chemistry and Physics, **11**(2): 627-654.

Woodhouse, M.T., Carslaw, K.S., Mann, G.W., Vallina, S.M., Vogt, M., Halloran, P.R. and Boucher, O., 2010. Low sensitivity of cloud condensation nuclei to changes in the sea-air flux of dimethyl-sulphide. Atmospheric Chemistry and Physics, **10**: 7545-7559.

Woodward, S., Roberts, D.L. and Betts, R.A., 2005. A simulation of the effect of climate change-induced desertification on mineral dust aerosol. Geophysical Research Letters, **32**: L18810.

Wyant, M., Bretherton, C., Blossey, P. and Khairoutdinov, M., 2012. Fast cloud adjustment to increasing CO_2 in a superparameterized climate model. Journal of Advances in Modeling Earth Systems, **4**: M05001.

Wyant, M.C., Bretherton, C.S., Bacmeister, J.T., Kiehl, J.T., Held, I.M., Zhao, M., Klein, S.A. and Soden, B.J., 2006. A comparison of low-latitude cloud properties and their response to climate change in three AGCMs sorted into regimes using mid-tropospheric vertical velocity. Climate Dynamics, **27**(2-3): 261-279.

Wyant, M.C., Bretherton, C.S. and Blossey, P.N., 2009. Subtropical low cloud response to a warmer climate in a superparameterized climate model. Part I: Regime sorting and physical mechanisms. J. Adv. Modeling Earth Syst., **1**: Art. #7.

Xiao, H.-Y. and Liu, C.-Q., 2004. Chemical characteristics of water-soluble components in TSP over Guiyang, SW China, 2003. Atmospheric Environment, **38**: 6297–6306.

Xu, B., Cao, J., Hansen, J., Yao, T., Joswia, D., Wang, N., Wu, G., Wang, M., Zhao, H., Yang, W., Liu, X. and He, J., 2009. Black soot and the survival of Tibetan glaciers. Proceedings of the National Academy of Sciences of the United States of America, **106**(52): 22114-22118.

Xu, B., Cao, J., Joswiak, D.R., Liu, X., Zhao, H. and He, J., 2012. Post-depositional enrichment of black soot in snow-pack and accelerated melting of Tibetan glaciers. Environmental Research Letters, **7**: 014022.

Xu, K.M., Cederwall, R.T., Donner, L.J., Grabowski, W.W., Guichard, F., Johnson, D.E., Khairoutdinov, M., Krueger, S.K., Petch, J.C., Randall, D.A., Seman, C.J., Tao, W.K., Wang, D.H., Xie, S.C., Yio, J.J. and Zhang, M.H., 2002. An intercomparison of cloud-resolving models with the atmospheric radiation measurement summer 1997 intensive observation period data. Quarterly Journal of the Royal Meteorological Society, **128**(580): 593-624.

Xu, K.M., Cheng, A.N. and Zhang, M.H., 2010. Cloud-resolving simulation of low-cloud feedback to an increase in sea surface temperature. Journal of the Atmospheric Sciences, **67**(3): 730-748.

Xu, K.M., Wong, T., Wielicki, B.A., Parker, L., Lin, B., Eitzen, Z.A. and Branson, M., 2007. Statistical analyses of satellite cloud object data from CERES. Part II: Tropical convective cloud objects during 1998 El Nino and evidence for supporting the fixed anvil temperature hypothesis. Journal of Climate, **20**(5): 819-842.

Xue, H., Feingold, G. and Stevens, B., 2008. Aerosol effects on clouds, precipitation, and the organization of shallow cumulus convection. Journal of the Atmospheric Sciences, **65**(2): 392-406.

Yang, Q., Gustafson, W.I., Jr., Fast, J.D., Wang, H., Easter, R.C., Morrison, H., Lee, Y.N., Chapman, E.G., Spak, S.N. and Mena-Carrasco, M.A., 2011. Assessing regional scale predictions of aerosols, marine stratocumulus, and their interactions during VOCALS-REx using WRF-Chem. Atmospheric Chemistry and Physics, **11**(23): 11951-11975.

Yankofsky, S.A., Levin, Z., Bertold, T. and Sandlerman, N., 1981. Some basic characteristics of bacterial freezing nuclei. Journal of Applied Meteorology, **20**(9): 1013-1019.

Yao, X., Chan, C.K., Fang, M., Cadle, S., Chan, T., Mulawa, P., He, K. and Ye, B., 2002. The water-soluble ionic composition of PM2.5 in Shanghai and Beijing, China. Atmospheric Environment, **36**: 4223-4234.

Ye, B., Ji, X., Yang, H., Yao, X., Chan, C.K., Cadle, S.H., Chan, T. and Mulawa, P.A., 2003. Concentration and chemical composition of PM2.5 in Shanghai for a 1-year period. Atmospheric Environment, **37**(4): 499-510.

Yin, J. and Harrison, R.M., 2008. Pragmatic mass closure study for PM1.0, PM2.5 and PM10 at roadside, urban background and rural sites. Atmospheric Environment, **42**: 980-988.

Yin, J.H., 2005. A consistent poleward shift of the storm tracks in simulations of 21st century climate. Geophysical Research Letters, **32**(18): L18701.

Yokohata, T., Emori, S., Nozawa, T., Ogura, T., Kawamiya, M., Tsushima, Y., Suzuki, T., Yukimoto, S., Abe-Ouchi, A., Hasumi, H., Sumi, A. and Kimoto, M., 2008. Comparison of equilibrium and transient responses to CO_2 increase in eight state-of-the-art climate models. Tellus, **60A**(5): 946-961.

Yokohata, T., Webb, M.J., Collins, M., Williams, K.D., Yoshimori, M., Hargreaves, J.C. and Annan, J.D., 2010. Structural similarities and differences in climate responses to CO_2 increase between two perturbed physics ensembles. Journal of Climate, **23**(6): 1392-1410.

Yoshimori, M. and Broccoli, A.J., 2008. Equilibrium response of an atmosphere-mixed layer ocean model to different radiative forcing agents: Global and zonal mean response. Journal of Climate, **21**(17): 4399-4423.

Yoshimori, M., Yokohata, T. and Abe-Ouchi, A., 2009. A comparison of climate feedback strength between CO_2 doubling and LGM experiments. Journal of Climate, **22**(12): 3374-3395.

Young, I.R., Zieger, S. and Babanin, A.V., 2011. Global trends in wind speed and wave height. Science, **332**(6028): 451-455.

Yttri, K.E., 2007. Concentrations of particulate matter (PM10, PM2.5) in Norway. Annual and seasonal trends and spatial variability. Annex A, EMEP Particulate Matter Assessment Report, Part B, report EMEP/CCC-Report 8/2007, 292-307, ref. O-7726.

Yu, F. and Luo, G., 2009. Simulation of particle size distribution with a global aerosol model: contribution of nucleation to aerosol and CCN number concentrations. Atmospheric Chemistry and Physics, **9**: 7691-7710.

Yu, H., Kaufman, Y.J., Chin, M., Feingold, G., Remer, L.A., Anderson, T.L., Balkanski, Y., Bellouin, N., Boucher, O., Christopher, S., DeCola, P., Kahn, R., Koch, D., Loeb, N., Reddy, M.S., Schulz, M., Takemura, T. and Zhou, M., 2006. A review of measurement-based assessments of the aerosol direct radiative effect and forcing. Atmospheric Chemistry and Physics, **6**: 613-666.

Yu, H., McGraw, R. and Lee, S., 2012. Effects of amines on formation of sub-3 nm particles and their subsequent growth. Geophysical Research Letters, **39**: L02807.

Yu, H.B., Chin, M., Winker, D.M., Omar, A.H., Liu, Z.Y., Kittaka, C. and Diehl, T., 2010. Global view of aerosol vertical distributions from CALIPSO lidar measurements and GOCART simulations: Regional and seasonal variations. Journal of Geophysical Research, **115**: D00H30.

Yuan, T., Remer, L.A. and Yu, H., 2011. Microphysical, macrophysical and radiative signatures of volcanic aerosols in trade wind cumulus observed by the A-Train. Atmospheric Chemistry and Physics, **11**(14): 7119-7132.

Yun, Y., Penner, J.E. and Popovicheva, O., 2012. The effects of hygroscopicity of fossil fuel combustion aerosols on mixed-phase clouds. Atmospheric Chemistry and Physics Discussions, **12**: 19987–20006.

Yuter, S.E., Miller, M.A., Parker, M.D., Markowski, P.M., Richardson, Y., Brooks, H. and Straka, J.M., 2012. Comment on “Why do tornados and hailstorms rest on weekends?” by D. Rosenfeld and T. Bell. . Journal of Geophysical Research, **submitted**.

Zarzycki, C.M. and Bond, T.C., 2010. How much can the vertical distribution of black carbon affect its global direct radiative forcing? Geophysical Research Letters, **37**: L20807.

Zelinka, M.D. and Hartmann, D.L., 2010. Why is longwave cloud feedback positive? Journal of Geophysical Research, **115**: D16117.

Zelinka, M.D., Klein, S.A. and Hartmann, D.L., 2012a. Computing and partitioning cloud feedbacks using cloud property histograms. Part I: Cloud radiative kernels. Journal of Climate, **25**: 3715–3735.

Zelinka, M.D., Klein, S.A. and Hartmann, D.L., 2012b. Computing and partitioning cloud feedbacks using cloud property histograms. Part II: Attribution to changes in cloud amount, altitude, and optical depth. Journal of Climate, **25**: 3736–3754.

Zhang, G.J., Vogelmann, A.M., Jensen, M.P., Collins, W.D. and Luke, E.P., 2010. Relating satellite-observed cloud properties from MODIS to meteorological conditions for marine boundary layer clouds. Journal of Climate, **23**(6): 1374-1391.

Zhang, M., Bretherton, C., Blossey, P., Austin, P., Bacmeister, J., Bony, S., Brient, F., Cheng, A., de Roode, S., Endo, S., Del Genio, A., Franklin, C., Golaz, C., Hanny, C., Heus, T., Isotta, F., Dufresne, J.-L., Kang, I.-S., Kawai, H., Koehler, M., Kumar, S., Larson, V., Liu, Y., Lock, A., Lohman, U., Khairoutdinov, M., Molod, A., Neggers, R., Rasch, P., Sandu, I., Senkbeil, R., Siebesma, P., Siegenthaler-Le Drian, C., Stevens, B., Suarez, M., Xu, K.-M.,

von Salzen, K., Webb, M., Wolfe, A. and Zhao, M., 2012a. CGILS: First results from an international project to understand the physical mechanisms of low cloud feedbacks in general circulation models. Bulletin of the American Meteorological Society: submitted.

Zhang, M.H. and Bretherton, C., 2008. Mechanisms of low cloud-climate feedback in idealized single-column simulations with the Community Atmospheric Model, version 3 (CAM3). Journal of Climate, **21**(18): 4859-4878.

Zhang, Q., Alfarra, M.R., Worsnop, D.R., Allan, J.D., Coe, H., Canagaratna, M.R. and Jimenez, J.L., 2005a. Deconvolution and quantification of hydrocarbon-like and oxygenated organic aerosols based on aerosol mass spectrometry. Environmental Science and Technology, **39**(13): 4938-4952.

Zhang, Q., Jimenez, J.L., Canagaratna, M.R., Allan, J.D., Coe, H., Ulbrich, I., Alfarra, M.R., Takami, A., Middlebrook, A.M., Sun, Y.L., Dzepina, K., Dunlea, E., Docherty, K., DeCarlo, P.F., Salcedo, D., Onasch, T., Jayne, J.T., Miyoshi, T., Shimono, A., Hatakeyama, S., Takegawa, N., Kondo, Y., Schneider, J., Drewnick, F., Borrmann, S., Weimer, S., Demerjian, K., Williams, P., Bower, K., Bahreini, R., Cottrell, L., Griffin, R.J., Rautiainen, J., Sun, J.Y., Zhang, Y.M. and Worsnop, D.R., 2007a. Ubiquity and dominance of oxygenated species in organic aerosols in anthropogenically-influenced Northern Hemisphere midlatitudes. Geophysical Research Letters, **34**: L13801.

Zhang, Q., Worsnop, D.R., Canagaratna, M.R. and Jimenez, J.L., 2005b. Hydrocarbon-like and oxygenated organic aerosols in Pittsburgh: insights into sources and processes of organic aerosols. Atmospheric Chemistry and Physics, **5**(12): 3289-3311.

Zhang, R., Khalizov, A., Wang, L., Hu, M. and Xu, W., 2012b. Nucleation and growth of nanoparticles in the atmosphere. Chemical Reviews, **112**(3): 1957-2011.

Zhang, X., Zwiers, F., Hegerl, G., Lambert, F., Gillett, N., Solomon, S., Stott, P. and Nozawa, T., 2007b. Detection of human influence on twentieth-century precipitation trends. Nature, **448**(7152): 461-465.

Zhang, X.Y., Arimoto, R., An, Z.S., Cao, J.J. and Wang, D., 2001. Atmospheric dust aerosol over the Tibetian Plateau. Journal of Geophysical Research, **106**: 18471-18476.

Zhang, X.Y., Cao, J.J., Li, L.M., Arimoto, R., Cheng, Y., Huebert, B. and Wang, D., 2002. Characterization of atmospheric aerosol over Xian in the south margin of the loess plateau, China. Atmospheric Environment, **36**: 4189-4199.

Zhang, X.Y., Wang, Y.Q., Niu, T., Zhang, X.C., Gong, S.L., Zhang, Y.M. and Sun, J.Y., 2012c. Atmospheric aerosol compositions in China: spatial/temporal variability, chemical signature, regional haze distribution and comparisons with global aerosols. Atmospheric Chemistry and Physics, **12**: 779–799.

Zhang, X.Y., Wang, Y.Q., Zhang, X.C., Guo, W. and Gong, S.L., 2008. Carbonaceous aerosol composition over various regions of China during 2006. Journal of Geophysical Research, **113**: D14111.

Zhang, Y., 2008. Online-coupled meteorology and chemistry models: history, current status, and outlook. Atmospheric Chemistry and Physics, **8**(11): 2895-2932.

Zhang, Y.M., Zhang, X.Y., Sun, J.Y., Lin, W.L., Gong, S.L., Shen, X.J. and Yang, S., 2011. Characterization of new particle and secondary aerosol formation during summertime in Beijing, China. Tellus, **63B**: 382-394.

Zhao, T.L., Gong, S.L., Zhang, X.Y., Mawgoud, A.A. and Shao, Y.P., 2006. An assessment of dust emission schemes in modeling east Asian dust storms. Journal of Geophysical Research, **111**: D05S90.

Zhao, T.X.P., Yu, H.B., Laszlo, I., Chin, M. and Conant, W.C., 2008. Derivation of component aerosol direct radiative forcing at the top of atmosphere for clear-sky oceans. Journal of Quantitative Spectroscopy & Radiative Transfer, **109**(7): 1162-1186.

Zhou, C., Penner, J.E., Ming, Y. and Huang, X.L., 2012. Aerosol forcing based on CAM5 and AM3 meteorological fields. Atmospheric Chemistry and Physics Discussions, **12**: 10679-10727.

Zhu, P., Albrecht, B.A., Ghate, V.P. and Zhu, Z.D., 2010. Multiple-scale simulations of stratocumulus clouds. Journal of Geophysical Research, **115**: D23201.

Zhu, P., Dudhia, J., Field, P.R., Wapler, K., Fridlind, A., Varble, A., Zipser, E., Petch, J., Chen, M. and Zhu, Z.D., 2012. A limited area model (LAM) intercomparison study of a TWP-ICE active monsoon mesoscale convective event. Journal of Geophysical Research, **117**: D11208.

Zhuang, B.L., Liu, L., Shen, F.H., Wang, T.J. and Han, Y., 2010. Semidirect radiative forcing of internal mixed black carbon cloud droplet and its regional climatic effect over China. Journal of Geophysical Research, **115**: D00K19.

Zimmermann, F., Weinbruch, S., Schutz, L., Hofmann, H., Ebert, M., Kandler, K. and Worringen, A., 2008. Ice nucleation properties of the most abundant mineral dust phases. Journal of Geophysical Research, **113**: D23204.

Zobrist, B., Koop, T., Luo, B.P., Marcolli, C. and Peter, T., 2007. Heterogeneous ice nucleation rate coefficient of water droplets coated by a nonadecanol monolayer. Journal of Physical Chemistry C, **111**(5): 2149-2155.

Zubler, E.M., Lohmann, U., Lüthi, D., Schär, C. and Muhlbauer, A., 2011. Statistical analysis of aerosol effects on simulated mixed-phase clouds and precipitation in the Alps. Journal of the Atmospheric Sciences, **68**: 1474-1492.

Zuidema, P., Baker, B., Han, Y., Intrieri, J., Key, J., Lawson, P., Matrosov, S., Shupe, M., Stone, R. and Uttal, T., 2005. An arctic springtime mixed-phase cloudy boundary layer observed during SHEBA. Journal of the Atmospheric Sciences, **62**(1): 160-176.

Zuidema, P., Li, Z., Hill, R.J., Bariteau, L., Rilling, B., Fairall, C., Brewer, W.A., Albrecht, B. and Hare, J., 2012. On Trade Wind Cumulus Cold Pools. Journal of the Atmospheric Sciences, **69**(1): 258-280.

Zuidema, P., Xue, H. and Feingold, G., 2008. Shortwave radiative impacts from aerosol effects on marine shallow cumuli. Journal of the Atmospheric Sciences, **65**(6): 1979-1990.

Tables

Table 7.2: Global and regional anthropogenic and natural emissions important for atmospheric aerosols. For the anthropogenic components the maximum and minimum values from available inventories are presented according to Granier et al. (2011). Units are Tg yr^{-1} except for BVOCs in TgC yr^{-1} and DMS in TgS yr^{-1}. Dust and sea-spray estimates span the range in the historical CMIP5 simulations. SOA range is taken from Spracklen et al. (2011). BVOC range from Arneth et al. (2008).

Year 2000 Emissions	Dust		Anthropogenic NMVOCs		Anthropogenic BC		Anthropogenic OA		Anthropogenic SO_2		Anthropogenic NH_3			Natural	Global
Tg yr^{-1}	MIN	MAX	MIN	MAX	MIN	MAX	MIN	MAX	MIN	MAX	MIN	MAX	Source	MIN	MAX
Total	744	8061	121.00	139.50	4.60	5.60	6.40	12.70	102.00	145.00	37.50	38.90	Sea Spray	1441	6786
Western Europe	0.1	71	9.20	14.30	0.32	0.38	0.32	0.40	6.10	14.10	3.40	4.50	PBAP Including spores 28	50	1000
Central Europe	All Europe		2.30	3.50	0.11	0.21	0.25	0.39	4.60	10.00	1.10	1.20	Dimethylsulphide	10	40
USA	0.2	372	13.00	17.50	0.27	0.40	0.36	0.51	13.50	17.80	3.30	4.40	Monoterpenes	32	121
Canada	All N. America		1.50	3.40	0.04	0.04	0.03	0.06	2.20	2.90	0.51	0.60	Isoprene	412	601
Central America			2.90	4.10	0.11	0.11	0.17	0.35	3.70	4.10	1.10	1.10	SOA	50	380
South America	4	380	8.40	12.90	0.20	0.33	0.32	0.83	3.80	8.80	3.40	3.50			
Africa	519	3807	10.80	14.50	0.46	0.62	1.05	1.91	5.30	8.80	2.30	2.40			
China	23	386	11.50	24.50	0.71	1.41	1.10	3.80	19.20	21.10	8.90	13.60			
India	20	347	7.30	10.80	0.45	0.84	1.00	3.27	4.00	7.90	3.70	8.50			
Oceania	0	7.6	0.00	1.50	0.03	0.04	0.04	0.08	2.40	2.70	0.72	0.72			

Table 7.3: Key aerosol properties of the main aerosol species in the troposphere. Brown carbon is a particular type of OA but is treated here as an additional component because it is light absorbing. The estimate of aerosol burdens and lifetimes in the troposphere are based on the AeroCom models, except for primary biological aerosol particles (PBAP), which are treated by analogy to other coarse mode aerosol types.

Aerosol Species	Global Burden	Mass Size Distribution	Sources	Sinks	Lifetime	Key Climate Relevant Properties
Black carbon		Freshly emitted: 0–80 nm Aged: accumulation mode	Combustion of fossil fuels, biofuels and biomass	Wet deposition Dry deposition	1 week to 10 days	Large mass absorption efficiency in the visible
Brown carbon		Freshly emitted: 100–400 nm Aged: accumulation mode	Combustion of biofuels and biomass	Wet deposition Dry deposition	1 week	Medium mass absorption efficiency in the visible. Light scattering.
Organic aerosol		POA: Aitken mode SOA: nuclei mode Aged OA : accumulation mode Biogenic POA : coarse mode	Combustion of fossil fuel, biofuel and biomass. Continental and marine ecosystems. Some anthropogenic non-combustion activities.	Wet deposition Dry deposition	1 week	Light scattering. Lens effect when deposited on black or brown carbon. CCN active (depending on aging time and mechanism). IN active (biogenic POA)
Sulphate		Secondary: Nuclei, Aitken, and accumulation mode Primary: coarse mode	Primary: marine and volcanic emissions. Secondary: oxidation of SO_2 from natural and anthropogenic sources	Wet deposition Dry deposition	1 week	Light scattering. Very hygroscopic. Lens effect when deposited on black or brown carbon. CCN active.
Nitrate		Accumulation and coarse modes	Oxidation of NOx	Wet deposition Dry deposition	1 week	Light scattering. CCN active.
Dust	(sensitive to size cutoff)	Coarse and super-coarse modes, with a small accumulation mode	Wind erosion, soil resuspension. Some agricultural practices and industrial activities (cement)	Sedimentation Dry deposition Wet deposition	1 day to 1 week depending on size	IN active, light scattering and absorption, greenhouse effect.
Sea-salt	(sensitive to size cutoff)	Coarse mode and accumulation mode	Wave breaking. Wind erosion.	Sedimentation Wet deposition Dry deposition	1 day to 1 week depending on size	Light scattering. Very hygroscopic. CCN active.
PBAP		Mostly coarse mode	Terrestrial and oceanic ecosystems	Sedimentation Wet deposition Dry deposition	1 day to 1 week depending on size	IN active.

Table 7.4: List of references for each category of estimates displayed in Figure 7.19.

Estimate	Acronym	References
RFari from CMIP5/ACCMIP models	CMIP5/ ACCMIP	[PLACEHOLDER FOR FINAL DRAFT]
RFaci published prior to TAR	TAR	(Boucher and Lohmann, 1995; Chuang et al., 1997; Feichter et al., 1997; Jones et al., 1994; Kaufman and Chou, 1993; Kiehl et al., 2000; Lohmann and Feichter, 1997; Lohmann et al., 2000; Rotstayn, 1999),
RFaci published between TAR and AR4	AR4	(Chen and Penner, 2005; Chuang et al., 2002; Ghan et al., 2001; Hansen et al., 2005; Jones et al., 2001; Kristjansson, 2002; Ming et al., 2005; Penner et al., 2006; Quaas and Boucher, 2005; Quaas et al., 2004; Rotstayn and Liu, 2003; Rotstayn and Penner, 2001; Suzuki et al., 2004; Takemura et al., 2005; Williams et al., 2001)
RFaci published since AR4	AR5	(Barahona et al., 2011; Bellouin et al., 2011; Haerter et al., 2009; Kvalevåg and Myhre, 2007; Lohmann et al., 2010; Lohmann et al., 2007; Penner et al., 2011; Rotstayn and Liu, 2009; Schmidt et al., 2012a; Storelvmo, 2011; Storelvmo et al., 2009; Wang and Penner, 2009; Zhou et al., 2012)
RFaci using or constrained by satellite observations	SAT	(Bellouin et al., 2012; Dufresne et al., 2005; Lebsock et al., 2008; Quaas and Boucher, 2005; Quaas et al., 2008; Quaas et al., 2009; Storelvmo et al., 2009)
RFaci from inverse studies	INV	(Knutti et al., 2002)
AFaci published prior to AR4	AR4	(Easter et al., 2004; Ghan et al., 2001; Johns et al., 2006; Jones et al., 2001; Kristjansson, 2002; Kristjansson et al., 2005; Lohmann, 2002b; Lohmann and Feichter, 1997; Lohmann et al., 2000; Menon et al., 2002; Ming et al., 2005; Peng and Lohmann, 2003; Penner et al., 2006; Penner et al., 2003; Quaas et al., 2006; Rotstayn, 1999; Rotstayn and Liu, 2005; Rotstayn and Penner, 2001; Storelvmo et al., 2006; Takemura et al., 2005; Williams et al., 2001)
AFaci published since AR4	AR5	(Chen et al., 2010; Ghan et al., 2011; Hoose et al., 2009; Kirkevåg et al., 2008; Makkonen et al., 2012; Menon and DelGenio, 2007; Ming et al., 2007b; Penner et al., 2011; Quaas et al., 2009; Rotstayn and Liu, 2009; Storelvmo et al., 2008a)
AFari+aci in liquid stratiform clouds published prior to AR4	AR4	(Ghan et al., 2012; Lohmann and Feichter, 2001; Lohmann et al., 2007; Posselt and Lohmann, 2008; Posselt and Lohmann, 2009; Quaas et al., 2004; Quaas et al., 2006; Quaas et al., 2009; Rotstayn et al., 2007; Salzmann et al., 2010)
AFari+aci in liquid stratiform clouds published since AR4	AR5	(Ghan et al., 2012; Lohmann et al., 2007; Makkonen et al., 2012; Posselt and Lohmann, 2008; Posselt and Lohmann, 2009; Quaas et al., 2009; Rotstayn et al., 2007; Salzmann et al., 2010)
AFari+aci in liquid and mixed-phase stratiform clouds	+MPC	(Hoose et al., 2010b; Hoose et al., 2008; Jacobson, 2006; Lohmann, 2004; Lohmann and Diehl, 2006; Lohmann and Ferrachat, 2010; Lohmann and Hoose, 2009; Salzmann et al., 2010; Storelvmo et al., 2008a; Storelvmo et al., 2008b; Yun et al., 2012),
AFari+aci in stratiform and convective clouds	+CNV	(Koch et al., 2009a; Lohmann, 2008; Menon and DelGenio, 2007; Menon and Rotstayn, 2006; Unger et al., 2009; Wang et al., 2011b)
AFari+aci from CMIP5/ACCMIP models	CMIP5/ ACCMIP	[PLACEHOLDER FOR FINAL DRAFT]
AFari+aci including satellite observations	SAT	(Bellouin et al., 2012; Lohmann and Lesins, 2002; Quaas et al., 2006; Quaas et al., 2009; Sekiguchi et al., 2003)
AFari+aci from inverse studies	INV	(Anderson et al., 2003; Andronova and Schlesinger, 2001; Church et al., 2011; Forest et al., 2006; Forest et al., 2002; Gregory et al., 2002; Hansen et al., 2011; Harvey and Kaufmann, 2002; Huber and Knutti, 2011; Libardoni and Forest, 2011; Murphy et al., 2009; Shindell and Faluvegi, 2009; Stott et al., 2006)

Table 7.5: Estimates of aerosol AF (in W m^{-2}) in some of the CMIP5 models. The AF are estimated from fixed-SST experiments using atmosphere-only version of the models listed. Different models include different aerosol effects.

Modelling Group	Model Name	AFari+aci from All Anthropogenic Aerosols	AFari+aci from Sulphate Aerosols Only
CCCma	CanESM2	–0.87	–0.90
CSIRO-QCCCE	CSIRO-Mk3-6-0	–1.41	–1.10
GFDL	GFDL-AM3	–1.44[a]	
GISS	GISS-E2-R[b]	–1.10[a]	
GISS	GISS-E2-R-TOMAS[b]	–0.76[a]	
IPSL	IPSL-CM5A-LR	–0.72	–0.71
LASG-IAP	FGOALS-s2	–0.38	
MIROC	MIROC-CHEM[b]	–1.24[a]	
MIROC	MIROC5	–1.28	–1.05
MOHC	HadGEM2-A	–1.22	–1.16
MPI	MPI-M		
MRI	MRI-CGM3	–1.10	–0.48
NCAR	NCAR-CAM5.1[b]	–1.09[a]	
NCC	NorESM1-M	–1.00	
Ensemble mean		–1.05	
Standard deviation		0.29	

Notes:
(a) From ACCMIP (Shindell et al., 2012a).
(b) These models include the BC on snow effect.

Chapter 7: Clouds and Aerosols

Coordinating Lead Authors: Olivier Boucher (France), David Randall (USA)

Lead Authors: Paulo Artaxo (Brazil), Christopher Bretherton (USA), Graham Feingold (USA), Piers Forster (UK), Veli-Matti Kerminen (Finland), Yutaka Kondo (Japan), Hong Liao (China), Ulrike Lohmann (Switzerland), Philip Rasch (USA), S. K. Satheesh (India), Steven Sherwood (Australia), Bjorn Stevens (Germany), Xiao-Ye Zhang (China)

Contributing Authors: Govindswamy Bala (India), Nicolas Bellouin (UK), Angela Benedetti (UK), Sandrine Bony (France), Ken Caldeira (USA), Antony Del Genio (USA), Maria Cristina Facchini (Italy), Mark Flanner (USA), Steven Ghan (USA), Claire Granier (France), Corinna Hoose (Germany), Andy Jones (UK), Makoto Koike (Japan), Ben Kravitz (USA), Ben Laken (Spain), Matthew Lebsock (USA), Natalie Mahowald (USA), Gunnar Myhre (Norway), Colin O'Dowd (Ireland), Alan Robock (USA), Bjørn Samset (Norway), Hauke Schmidt (Germany), Michael Schulz (Norway), Graeme Stephens (USA), Trude Storelvmo (USA), Dave Winker (USA), Matthew Wyant (USA)

Review Editors: Sandro Fuzzi (Italy), Joyce Penner (USA), Venkatachalam Ramaswamy (USA), Claudia Stubenrauch (France)

Date of Draft: 5 October 2012

Notes: TSU Compiled Version

Figures

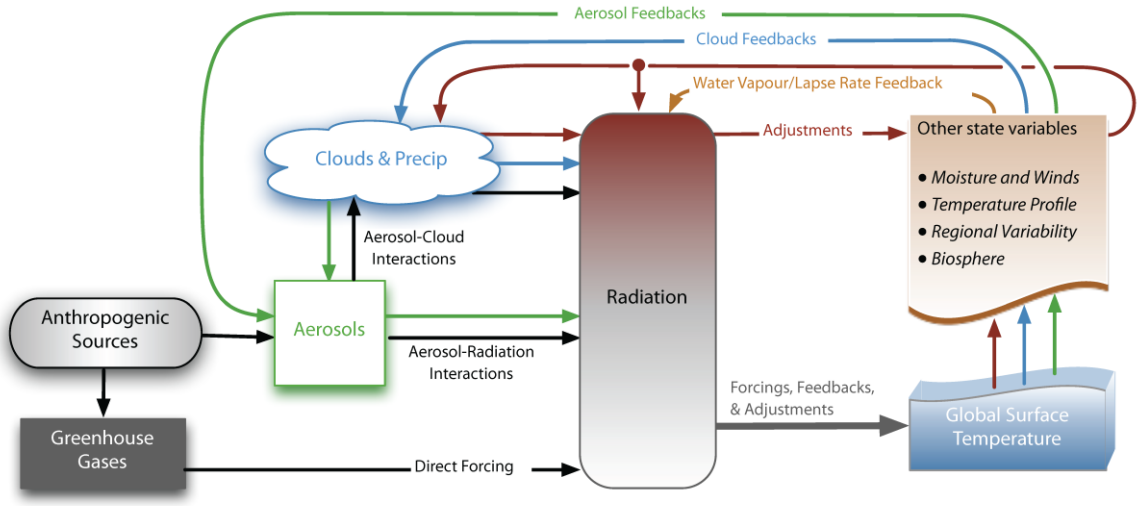

Figure 7.1: Overview of feedback and forcing pathways involving clouds and aerosols. Forcing mechanisms are represented by black arrows; forcing agents are boxes with grey shadows, rapid forcing adjustments (also called rapid responses) are shown with brown arrows and feedbacks are other-coloured arrows. See text for further discussion.

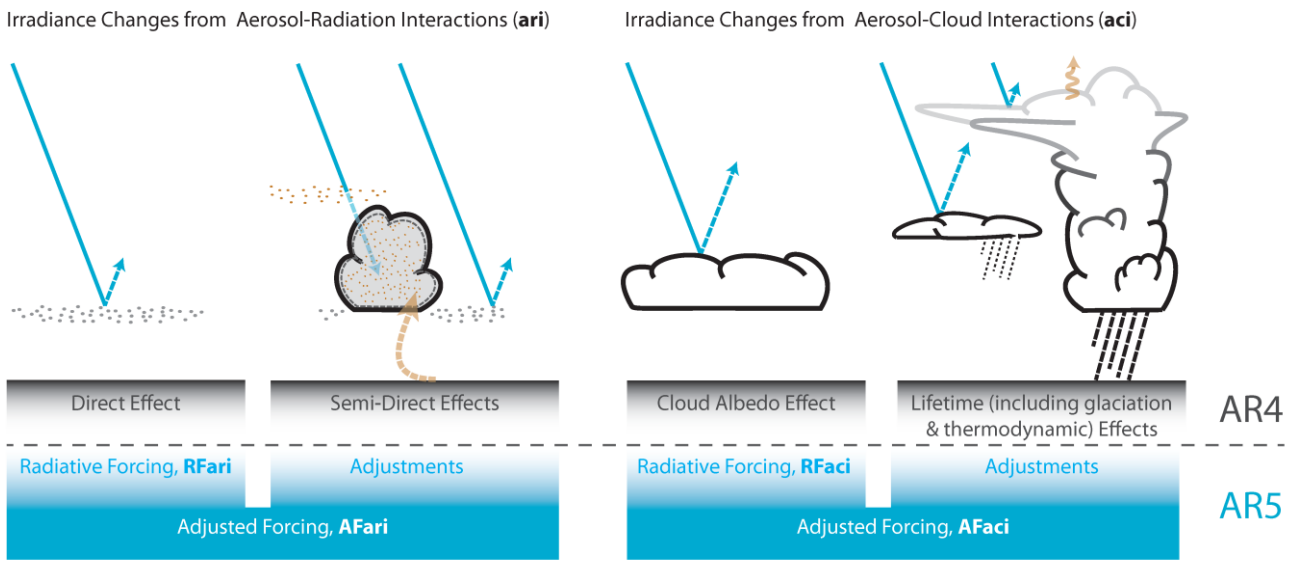

Figure 7.2: Schematic of the new terminology used in this assessment report for aerosol-radiation and aerosol-cloud interactions and how they relate to the terminology used in AR4. The radiative forcing from aerosol-radiation interactions (abbreviated RFari) encompasses radiative effects from anthropogenic aerosols before any adjustment takes place, and corresponds to what is usually referred to as the aerosol direct effect. Rapid adjustments induced by aerosol radiative effects on the surface energy budget, the atmospheric profile and cloudiness contribute to the adjusted forcing from aerosol-radiation interactions (abbreviated AFari). They include what has earlier been referred to as the semi-direct effect. The radiative forcing from aerosol-cloud interactions (abbreviated RFaci) refers to the instantaneous effect on cloud albedo due to changing concentrations of cloud condensation and ice nuclei. All subsequent changes to the cloud lifetime and thermodynamics are rapid adjustments, which contribute to the adjusted forcing from aerosol-cloud interactions (abbreviated AFaci).

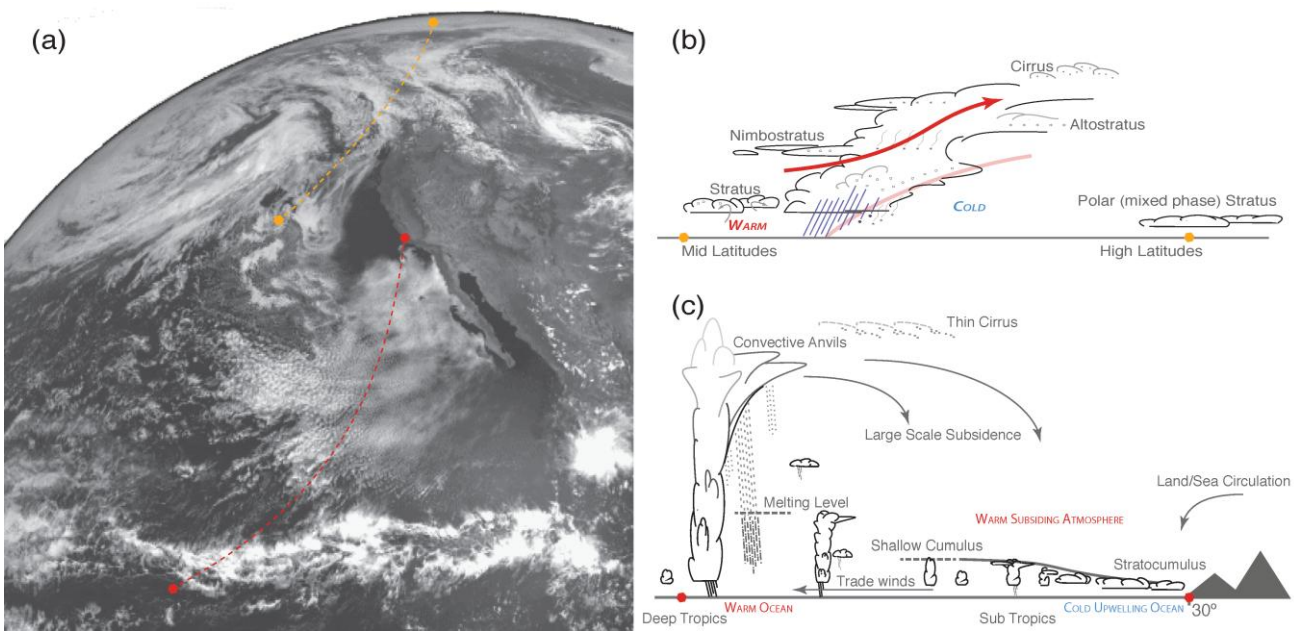

Figure 7.3: Diverse cloud regimes reflect diverse meteorology. (a) A visible-wavelength geostationary satellite image shows (from top to bottom) expanses and long arcs of cloud associated with extratropical cyclones, subtropical coastal stratocumulus near Baja California breaking up into shallow cumulus clouds in the central Pacific, and mesoscale convective systems outlining the Pacific intertropical convergence zone or ITCZ. (b) A schematic section through a typical warm front of an extratropical cyclone (see orange dots in panel (a)) showing multiple layers of upper-tropospheric ice (cirrus) and mid-tropospheric water (altostratus) cloud upwind of the frontal zone, an extensive region of nimbostratus associated with frontal uplift and turbulence-driven boundary layer cloud in the warm sector. (c) A schematic section along the low-level trade wind flow from a subtropical west coast of a continent to the ITCZ (see red dots in panel (a)), showing typical low-latitude cloud types, shallow stratocumulus above the cool waters of the oceanic upwelling zone near the coast and trapped under a strong subsidence inversion, and shallow cumulus over warmer waters further offshore transitioning to precipitating cumulonimbus cloud systems with extensive cirrus anvils associated with rising air motions in the ITCZ.

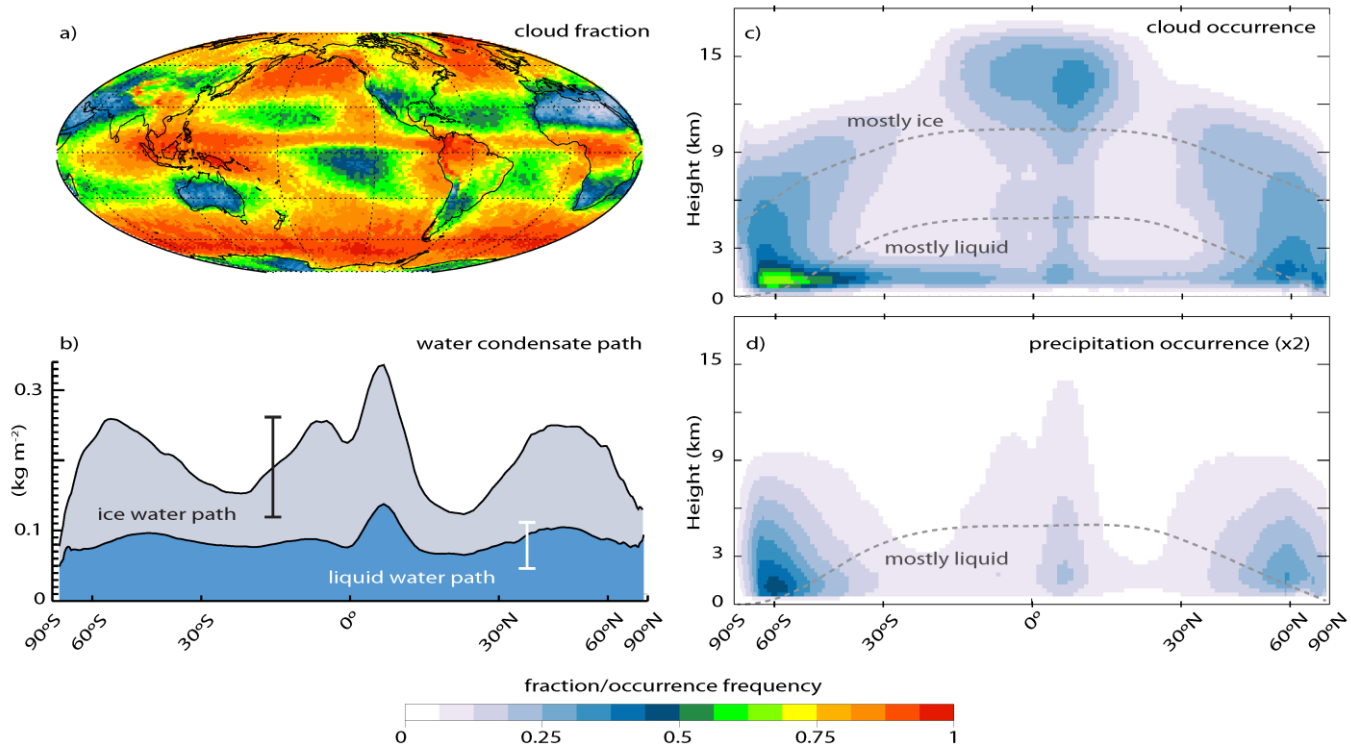

Figure 7.4: (a) Annual mean cloud fractional occurrence (CloudSat/CALIPSO 2B-GEOPROF-LIDAR dataset for 2006–2011); (b) annual zonal mean liquid water path (blue shading, ocean only, O'Dell et al. (2008) microwave radiometer dataset for 1988–2005; the 90% uncertainty range, assessed to be 70–150% of the plotted value, is schematically indicated by the white error bar) and ice water path (grey shading, from CloudSat 2C-ICE dataset for 2006–2011; the 90% uncertainty range, assessed to be 50–200% of the plotted value, is schematically indicated by the black error bar). (c-d) latitude-height sections of annual zonal mean cloud (including precipitation falling from cloud) occurrence and precipitation (attenuation-corrected radar reflectivity >0 dBZ) occurrence; the latter has been doubled to make use of a common colour scale (2B-GEOPROF-LIDAR dataset). The dashed curves show the annual-mean 0°C and −38°C isotherms.

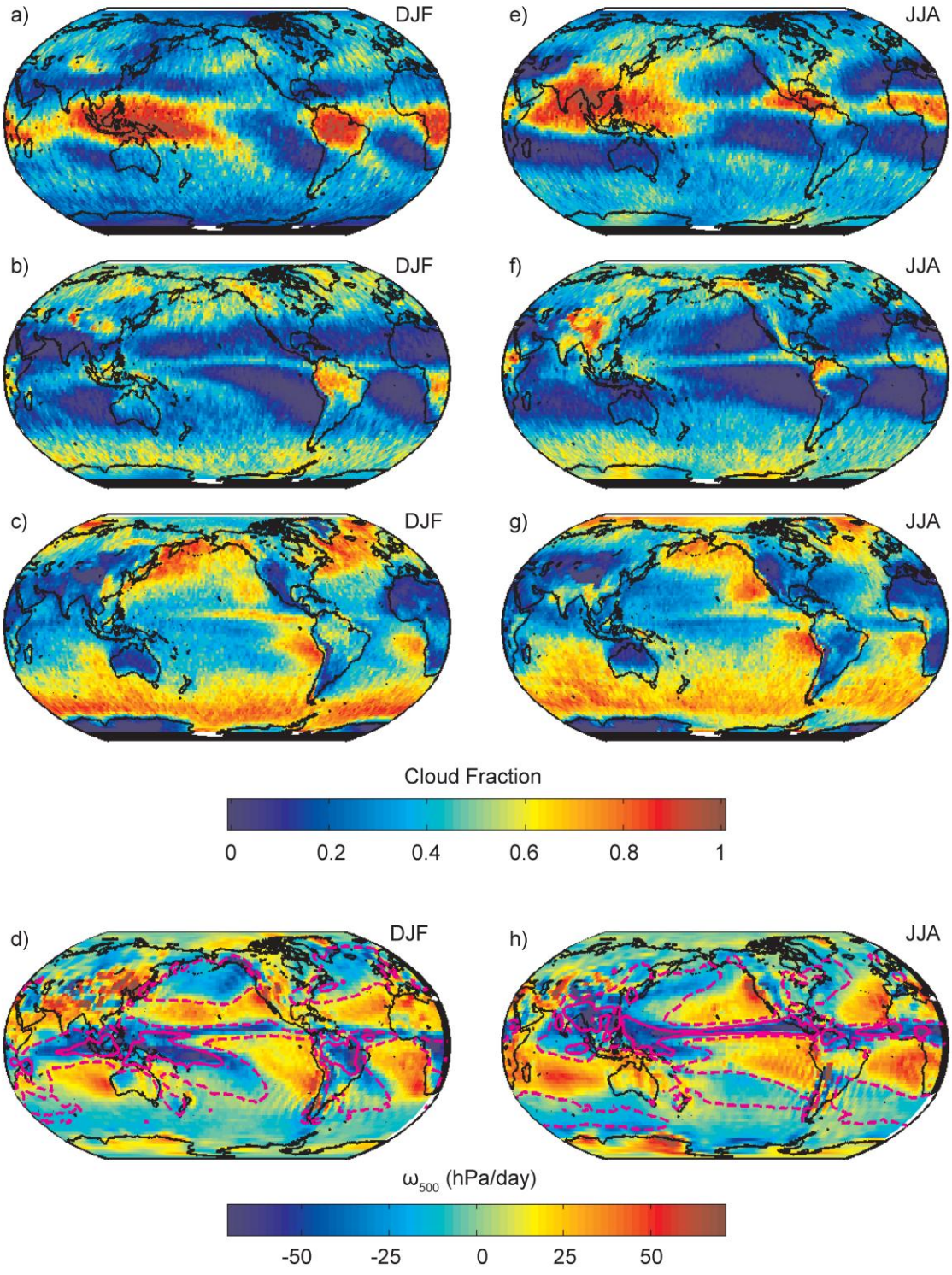

Figure 7.5: (a-d) DJF mean high, middle and low cloud cover from CloudSat/CALIPSO GEOPROF dataset (2006–2011), and 500 hPa vertical pressure velocity (colours) and GPCP precipitation (magenta contours at 3 mm day^{-1} in dash and 7 mm day^{-1} in solid); (e-h) same as (a-d), except for JJA. For low clouds, the CALIPSO-only GOCCP dataset is used at locations where it indicates as larger fractional cloud cover, because the GEOPROF dataset removes some clouds with tops at altitudes below 750 m. Low cloud amounts are likely underrepresented in regions of high cloud (Chepfer et al., 2008), although not as severely as with earlier satellite technologies.

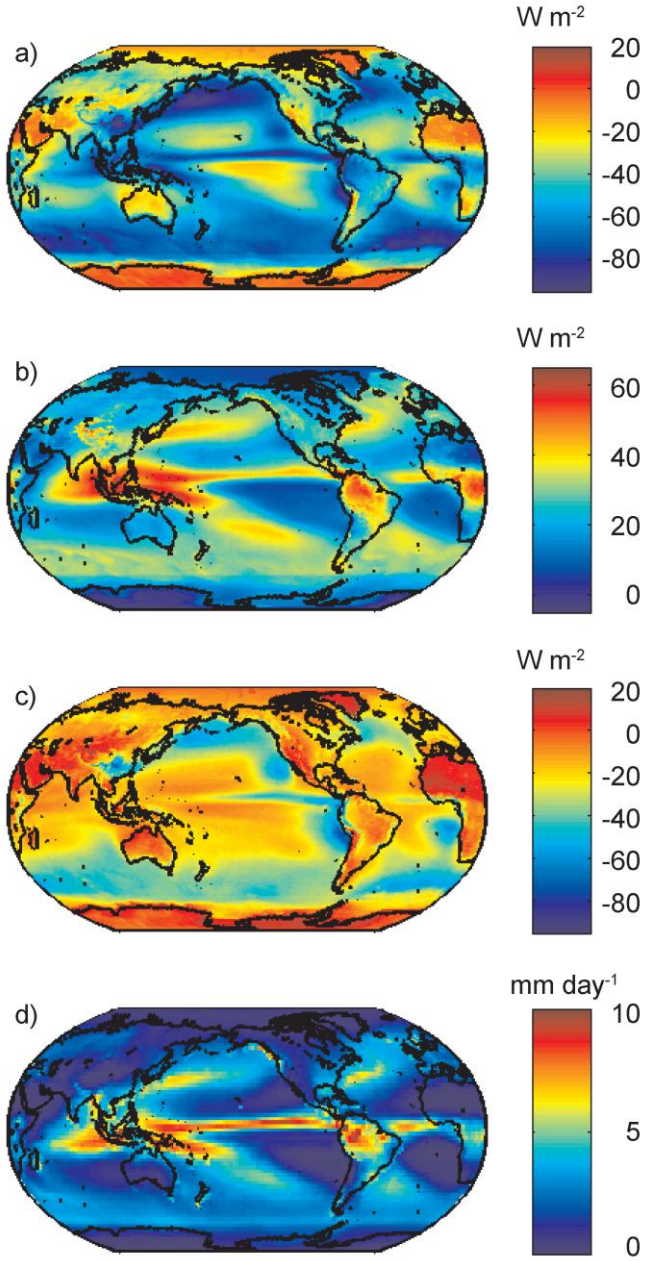

Figure 7.6: Distribution of annual-mean top of atmosphere (a) SWCRE, (b) LWCRE, (c) net CRE (2001–2010 average from CERES-EBAF) and (d) precipitation (1981–2000 average from GPCP).

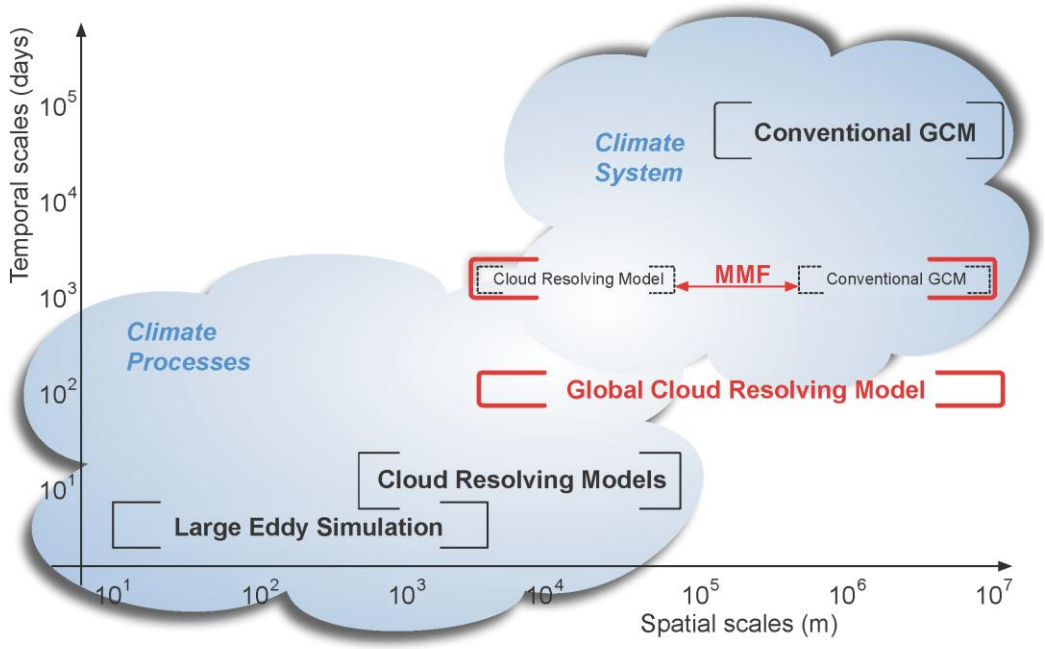

Figure 7.7: Model and simulation strategy for representing the climate system and climate processes at different space and time scales. Models are usually defined based on the range of spatial scales they represent, shown by square brackets. The temporal scales that can be represented for a given model class can vary; for instance climate models can be run for a few time steps, or can simulate millennia. The figure indicates the typical timescales for which a given model is used. Computational power prevents one model from covering all time and space scales. Since the AR4 the development of global cloud resolving models, and hybrid approaches such as the multi-scale modelling framework, have helped fill the gap between climate system and climate process models.

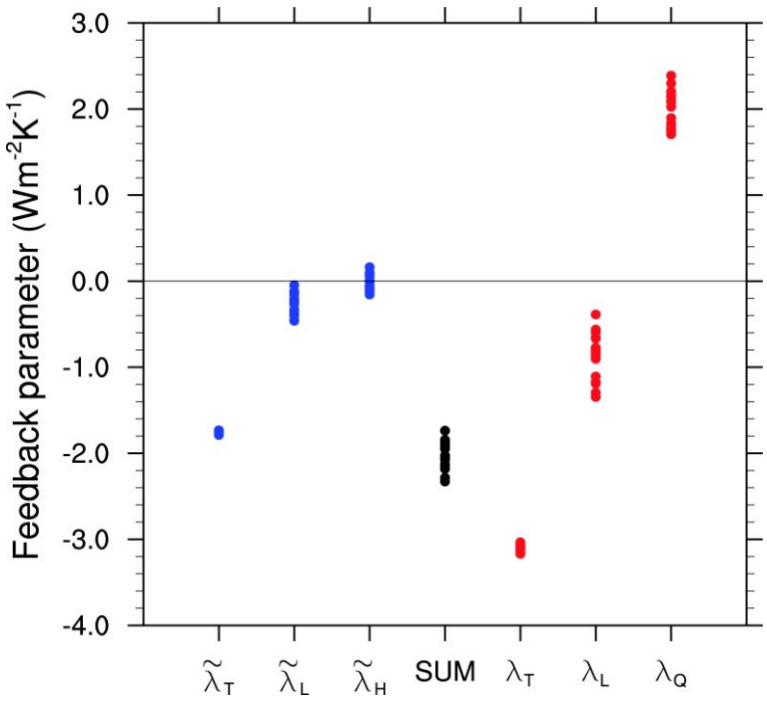

Figure 7.8: Clear-sky feedback parameters as predicted by [CMIP3] GCMs. Black points in the centre show the total radiative response including the Planck response, with the Planck response and individual feedbacks from water vapour and lapse rate shown to the right in red. On the left are the equivalent three parameters calculated in an alternative, relative humidity-based framework. In this framework the Planck stabilization and each of the two feedbacks are all weaker and more consistent among the models. [PLACEHOLDER FOR FINAL DRAFT: Current working draft of figure taken from Held and Shell (2012); additional data from CMIP5 TBA].

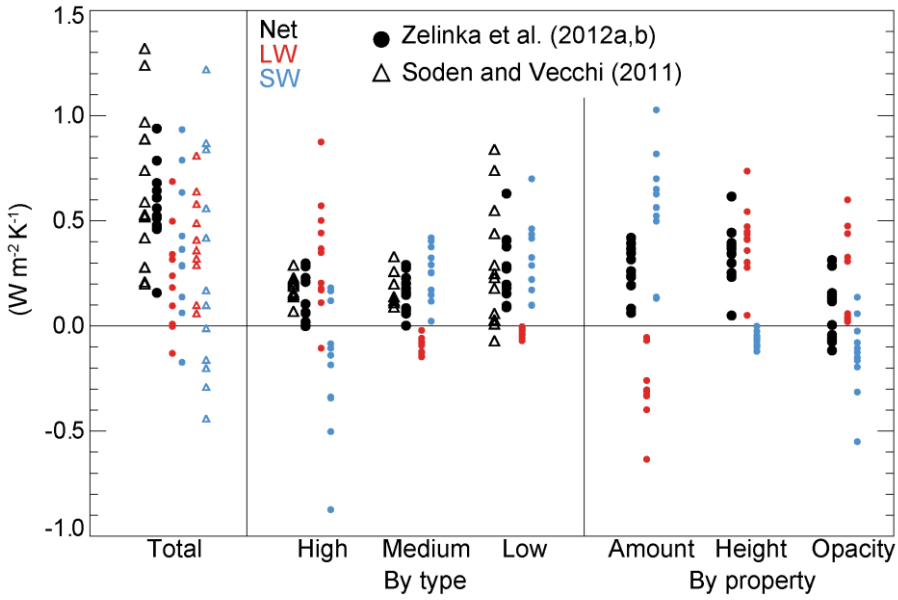

Figure 7.9: Cloud feedback parameters as predicted by GCMs. Total feedback shown at left by black symbols, broken out into infrared and visible components in red and blue, respectively (Zelinka et al., 2012a; Zelinka et al., 2012b). Centre panel shows components attributable to clouds in different height ranges (see text); values reported by Soden and Vecchi (2011) do not conform exactly to this definition but are shown for comparison, with their "mixed" category assigned "medium". Right panel shows components attributable to different cloud property changes (not available from all studies).

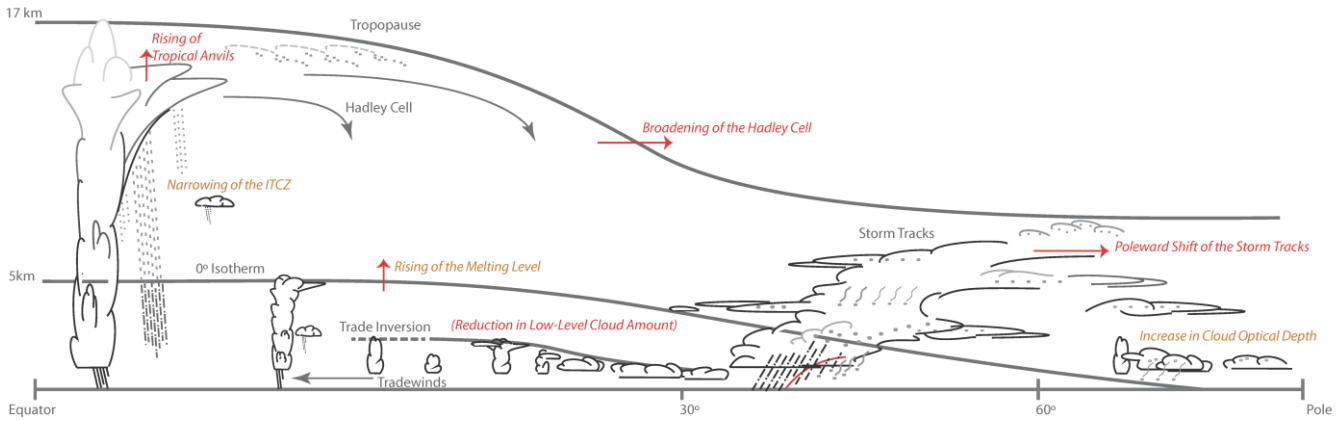

Figure 7.10: Robust cloud responses to greenhouse warming (those simulated by most models and possessing some kind of independent support or understanding). Key climatological features (tropopause, freezing level, circulations) are shown in grey. Changes anticipated in a warmer climate are shown in red (if contributing positive feedback) or brown (if contributing little or ambiguously to feedback); no robust mechanisms contribute negative feedback. Changes include rising high cloud tops and melting level, and increased polar cloud cover and/or optical thickness (high confidence); broadening of the Hadley Cell and/or poleward migration of storm tracks, and narrowing of the ITCZ (medium confidence); and reduced low-cloud amount and/or optical thickness (low confidence). Confidence assessments are based on degree of GCM consensus, strength of independent lines of evidence from observations or process models, and degree of basic understanding.

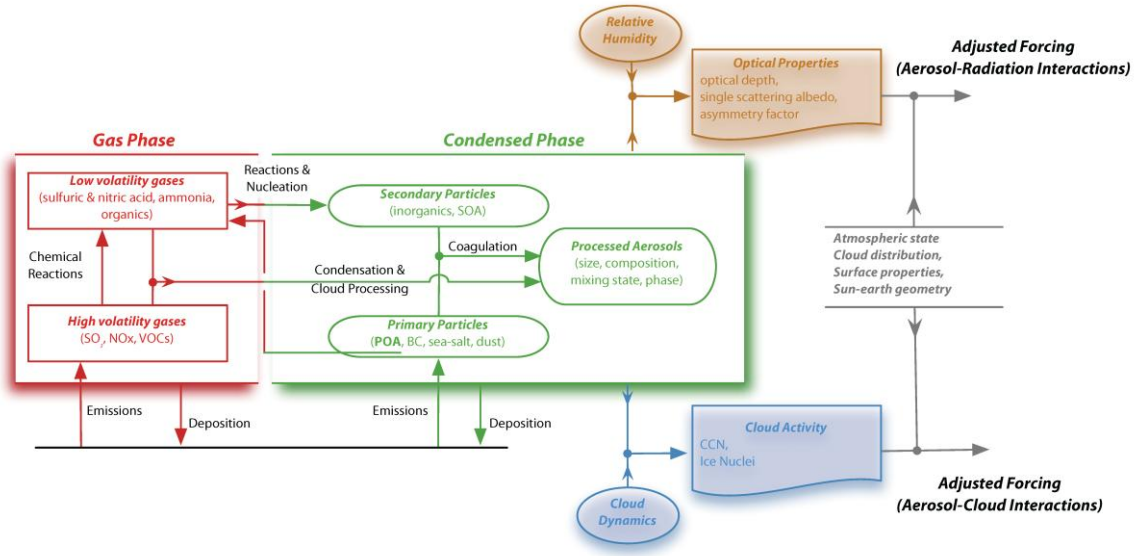

Figure 7.11: Overview of atmospheric aerosol processes and environmental variables influencing aerosol-radiation and aerosol-cloud interactions. Gas-phase processes and variables are highlighted in red while particulate-phase processes and variables appear in green. Although this figure shows a linear chain of processes from aerosols to forcings, it is increasingly recognized that aerosols and clouds form a coupled system with two-way interactions.

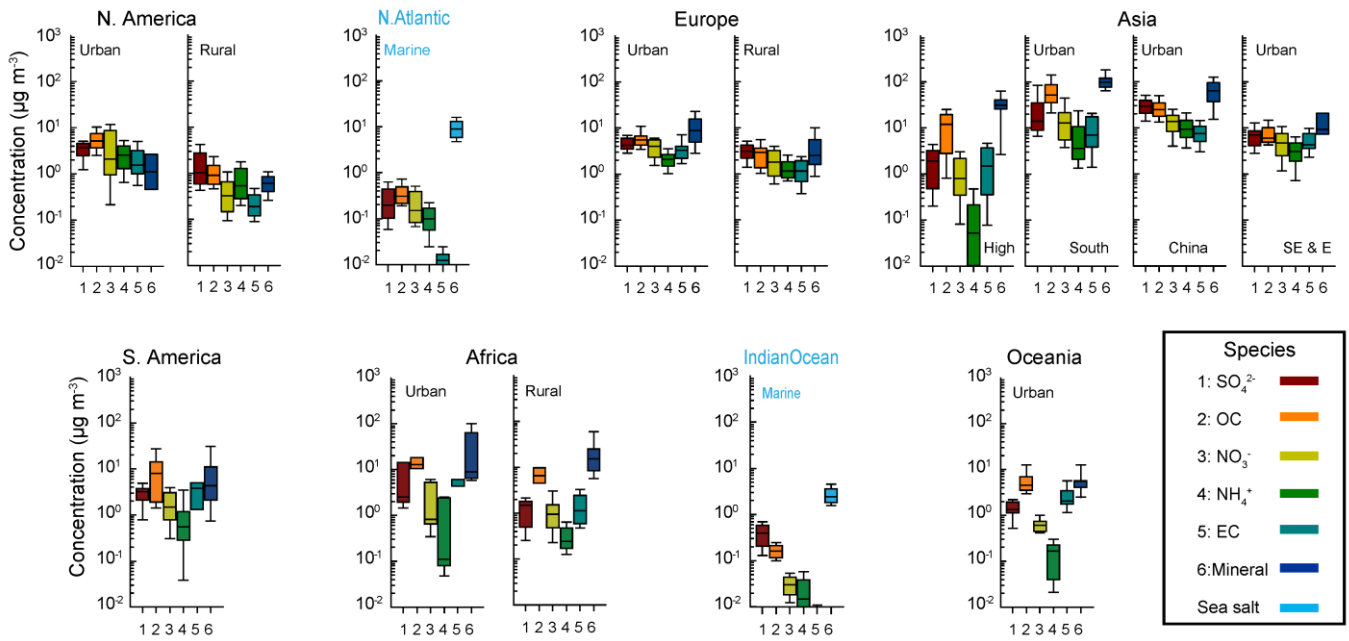

Figure 7.12: Bar chart plots summarizing the annual, seasonal or monthly mean mass surface concentration (µg m^{-3}) of seven major aerosol components for particles with diameter smaller than 10 µm, from various rural and urban sites in six continental areas of the world with at least an entire year of data, and two marine sites. For each location, the panels represent the median, the 25–75 percentiles (box), and the 10–90 percentiles (whiskers) for each aerosol component. These include: 1) urban North America. (Chow et al., 1993; Ito et al., 2004; Kim et al., 2000; Liu et al., 2005; Malm and Schichtel, 2004; Sawant et al., 2004); rural North America (Chow et al., 1993; Liu et al., 2005; Malm and Schichtel, 2004; Malm et al., 1994); 2) marine northern hemisphere Atlantic Ocean (Ovadnevaite et al., 2011; Rinaldi et al., 2009); 3) urban Europe (Hueglin et al., 2005; Lenschow et al., 2001; Lodhi et al., 2009; Lonati et al., 2005; Perez et al., 2008; Putaud et al., 2004; Querol et al., 2006; Querol et al., 2008; Querol et al., 2001; Querol et al., 2004; Rodriguez et al., 2002; Rodrıguez et al., 2004; Roosli et al., 2001; Viana et al., 2006; Viana et al., 2007; Yin and Harrison, 2008); rural Europe (Gullu et al., 2000; Hueglin et al., 2005; Kocak et al., 2007; Putaud et al., 2004; Puxbaum et al., 2004; Querol et al., 2009; Querol et al., 2001; Querol et al., 2004; Rodriguez et al., 2002; Rodrıguez et al., 2004; Salvador et al., 2007; Theodosi et al., 2010; Viana et al., 2008; Yin and Harrison, 2008; Yttri, 2007); 4) high Asia, with altitude larger than 1680 m. (Carrico et al., 2003; Decesari et al., 2010; Ming et al., 2007; Qu et al., 2008; Ram et al., 2010; Rastogi and Sarin, 2005; Rengarajan et al., 2007; Shresth et al., 2000; Zhang et al., 2001; Zhang et al., 2012; Zhang et al., 2008); urban South Asia (Chakraborty and Gupta, 2010; Khare and Baruah, 2010; Kumar et al., 2007; Lodhi et al., 2009; Raman et al., 2010; Rastogi and Sarin, 2005; Safai et al., 2010; Stone et al., 2010); urban China (Cheng et al., 2000; Hagler et al., 2006; Oanh et al., 2006; Wang et al., 2003; Wang et al., 2005b; Wang et al., 2006; Xiao and Liu, 2004; Yao et al., 2002; Ye et al., 2003; Zhang et al., 2002; Zhang et al., 2012; Zhang et al., 2011); rural China (Hagler et al., 2006; Hu et al., 2002; Zhang et al., 2012) [PANEL MISSING]; urban China (Cheng et al., 2000; Hagler et al., 2006; Oanh et al., 2006; Wang et al., 2003; Wang et al., 2005b; Wang et al., 2006; Xiao and Liu, 2004; Yao et al., 2002; Ye et al., 2003; Zhang et al., 2002; Zhang et al., 2012; Zhang et al., 2011); South-East and East Asia (Han et al., 2008; Khan et al., 2010; Kim et al., 2007; Lee and Kang, 2001; Oanh et al., 2006); 5) South America (Artaxo et al., 1998; Artaxo et al., 2002; Bourotte et al., 2007; Celis et al., 2004; Fuzzi et al., 2007; Gioda et al., 2011; Mariani and Mello, 2007; Martin et al., 2010; Morales et al., 1998; Souza et al., 2010); 6) urban Africa (Favez et al., 2008; Mkoma, 2008; Mkoma et al., 2009b); rural Africa (Maenhaut et al., 1996; Mkoma, 2008; Mkoma et al., 2009a; Mkoma et al., 2009b; Nyanganyura et al., 2007; Weinstein et al., 2010); 7) marine southern hemisphere Indian Ocean (Rinaldi et al., 2011; Sciare et al., 2009); 8) urban Oceania (Chan et al., 1997; Maenhaut et al., 2000; Radhi et al., 2010; Wang et al., 2005a; Wang and Shooter, 2001).

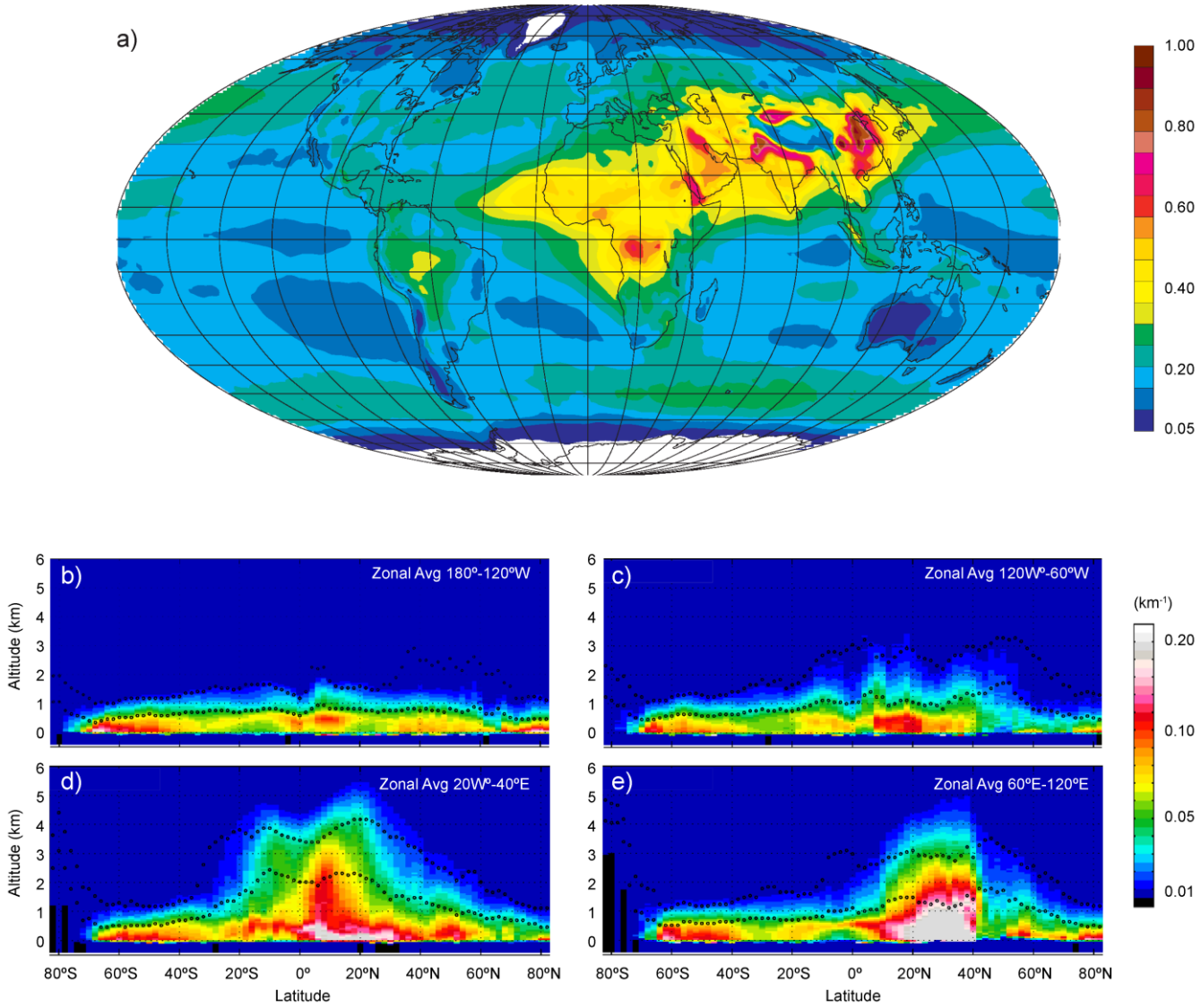

Figure 7.13: a) spatial distribution of the AOD (unitless) from the MACC model with assimilation of MODIS AOD (Benedetti et al., 2009; Morcrette et al., 2009) for the year 2010; b) to e) latitudinal vertical cross-sections of the aerosol extinction coefficient (km^{-1}) for four longitudinal bands (180°W to 120°W, 120°W to 60°W, 20°W to 40°E, and 60°E to 120°E) from the CALIOP instrument (Winker et al., 2009). The black circles show the extinction scale height for 90% (top) and 63% (bottom) of the average AOD.

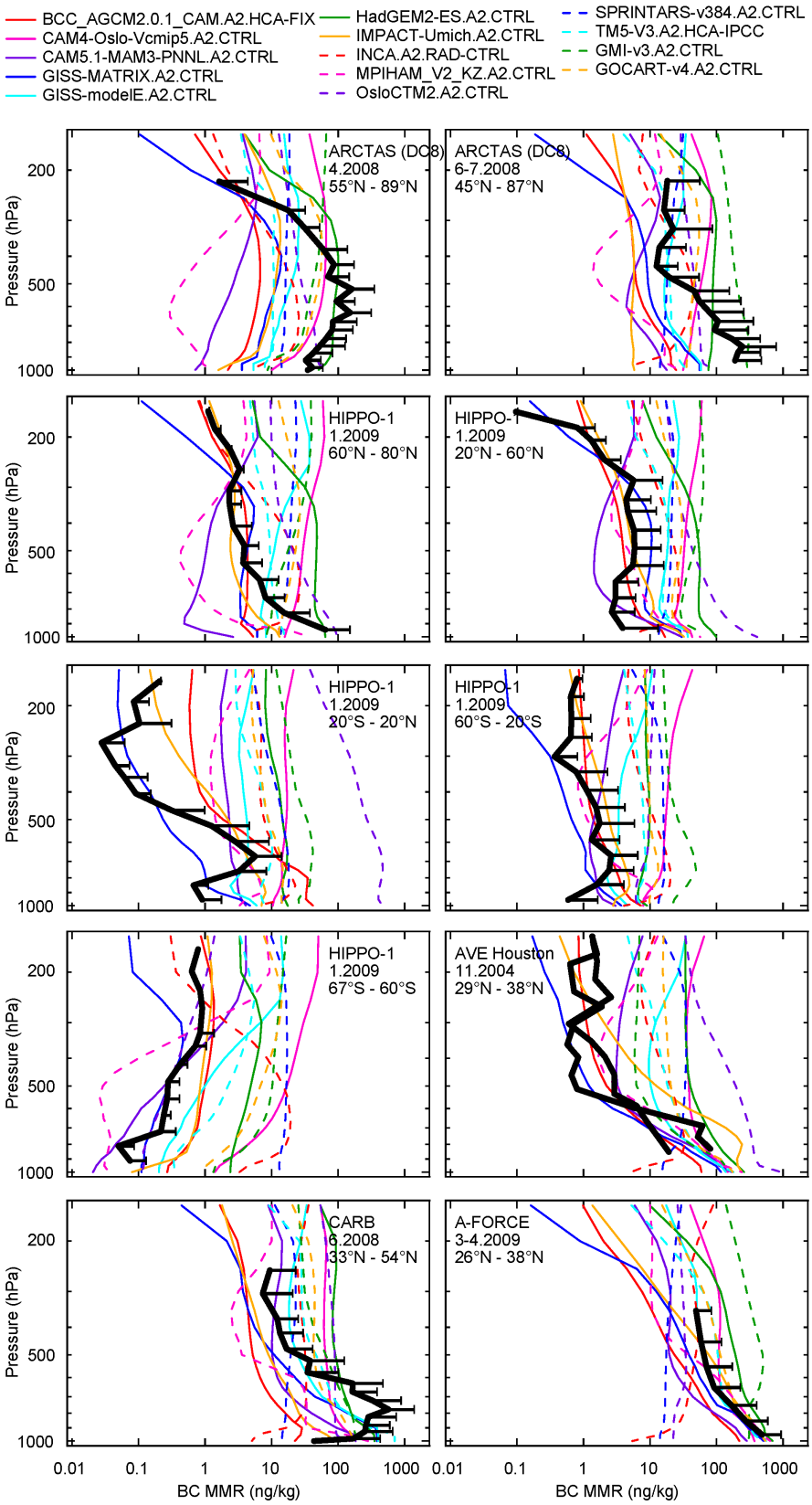

Figure 7.14: Comparison of profiles of BC mass mixing ratios (ng kg^{-1}) as measured by airborne SP2 instruments during the ARCTAS (Jacob et al., 2010), HIPPO1 (Schwarz et al., 2006; Schwarz et al., 2010) and A-FORCE (Oshima et al., 2012) campaigns and as simulated by a range of AeroCom models. The model values are averages for the month corresponding to each field campaign.

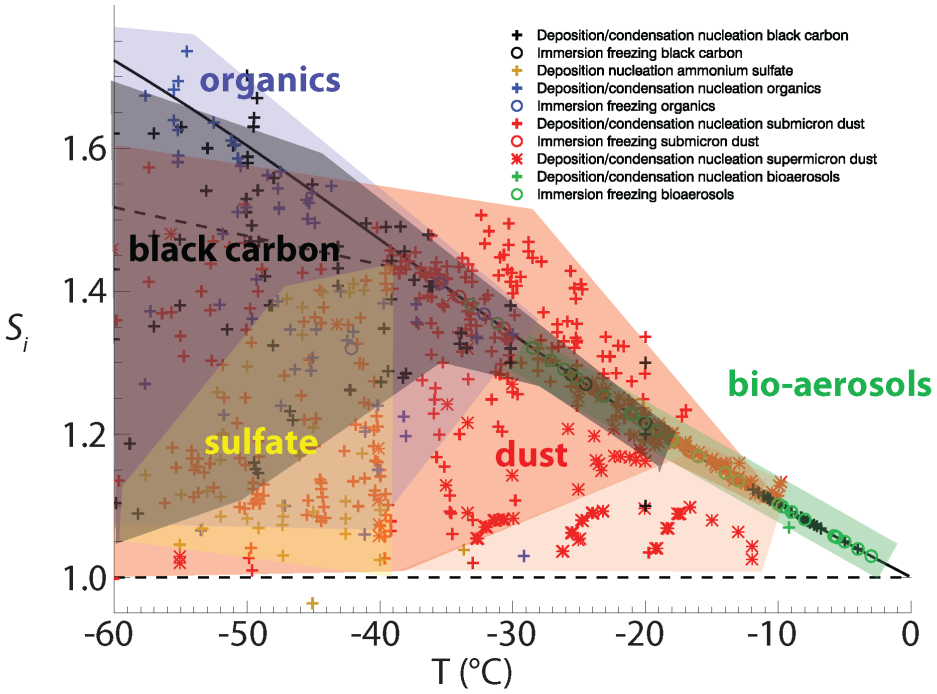

Figure 7.15: The onset temperatures and relative humidities for deposition/condensation freezing and immersion freezing for **bioaerosols** (Ahern et al., 2007; Diehl et al., 2001; Iannone et al., 2011; Kanji et al., 2011; Mohler et al., 2008; Mortazavi et al., 2008; von Blohn et al., 2005; Yankofsky et al., 1981), **mineral dusts** (Archuleta et al., 2005; Bundke et al., 2008; Connolly et al., 2009; Cziczo et al., 2009; Field et al., 2006; Kanji and Abbatt, 2006; Kanji et al., 2011; Knopf and Koop, 2006; Koehler et al., 2010; Kulkarni and Dobbie, 2010; Lüönd et al., 2010; Mohler et al., 2006; Murray et al., 2011; Niedermeier et al., 2010; Niemand et al., 2012; Roberts and Hallett, 1968; Salam et al., 2006; Schaller and Fukuta, 1979; Welti et al., 2009; Zimmermann et al., 2008), **organics** (Baustian et al., 2010; Kanji et al., 2008; Petters et al., 2009; Prenni et al., 2007; Shilling et al., 2006; Wagner et al., 2010; 2011; Wang and Knopf, 2011; Zobrist et al., 2007), **solid ammonium sulphate** (Abbatt et al., 2006; Baustian et al., 2010; Mangold et al., 2005; Shilling et al., 2006; Wise et al., 2009; 2010) and **BC (soot)** (Crawford et al., 2011; DeMott, 1990; DeMott et al., 1999; Diehl and Mitra, 1998; Dymarska et al., 2006; Fornea et al., 2009; Gorbunov et al., 2001; Kanji et al., 2011; Mohler et al., 2005), from a compilation of experimental data of sub- and super-micron aerosol particles in the literature (for references see supplementary material). The large range of observed ice nucleation onset conditions is due to different experimental setups, particle sizes, activated fractions and chemical composition. Only those IN species for which at least three papers exists are shown. The solid line refers to saturation with respect to liquid water and the dashed line refers to the homogeneous freezing of solution droplets after Koop et al. (2000). Adapted from Hoose and Möhler (2012).

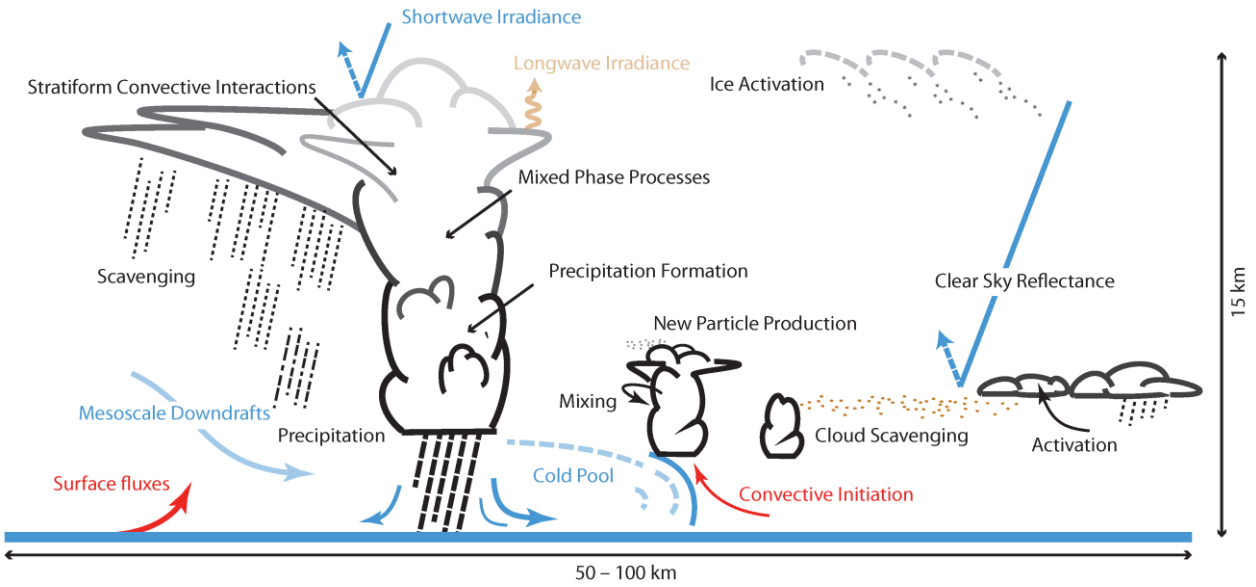

Figure 7.16: Schematic depicting the myriad aerosol-cloud-precipitation related processes occurring within a typical GCM grid box. The schematic conveys the importance of considering aerosol-cloud-precipitation processes as part of an interactive system encompassing a large range of spatiotemporal scales. Cloud types include low-level stratocumulus and cumulus where research focuses on droplet activation, mixing, cloud scavenging, and new particle formation; ice-phase cirrus clouds where a key issue is homogeneous freezing; and deep convective clouds where some of the key questions relate to aerosol influences on liquid, ice, and liquid-ice pathways for precipitation formation, cold pool formation, and scavenging. These processes influence the short- and longwave forcing of the system and hence climate.

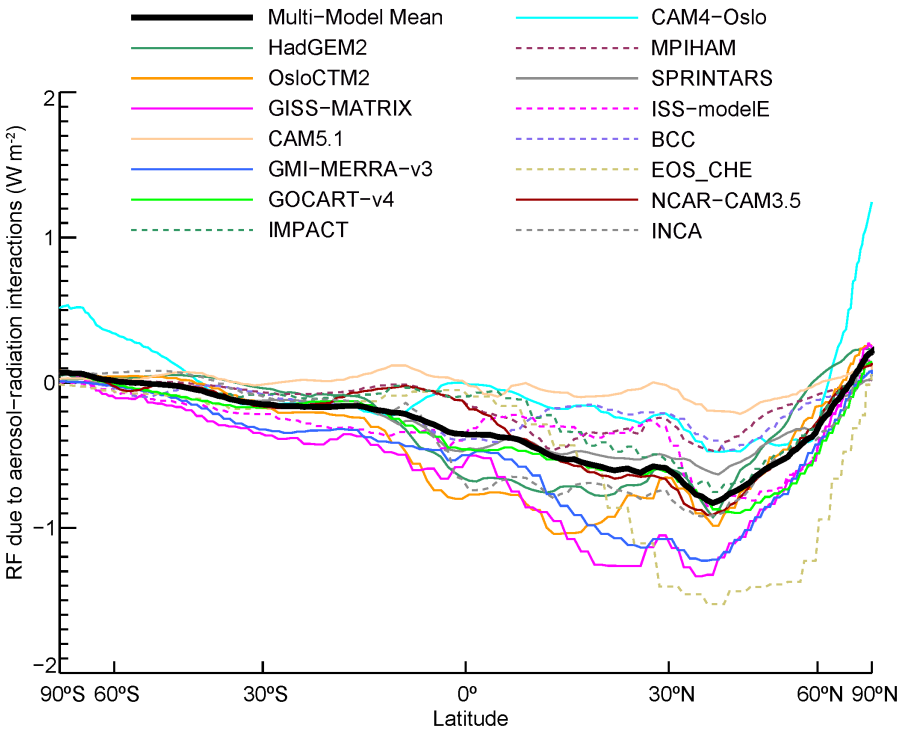

Figure 7.17: Annual zonal mean RFari (in W m^{-2}) due to all anthropogenic aerosols from the different AeroCom II models. No adjustment for missing species in certain models has been applied. The multi-model mean is shown with a black solid line. Adapted from Myhre et al. (2012).

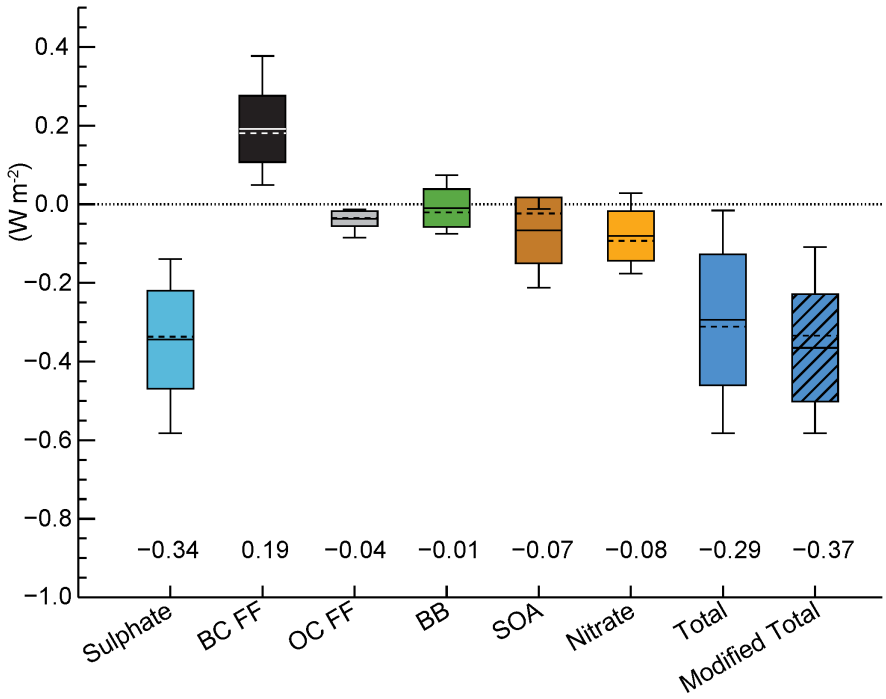

Figure 7.18: Mean (solid line), median (dashed line), one standard deviation (box) and full (min-max) range (whiskers) for RFari (in W m^{-2}) from different aerosol types from AeroCom II models. The forcings are for the 1850 to 2000 period. Adapted from Myhre et al. (2012).

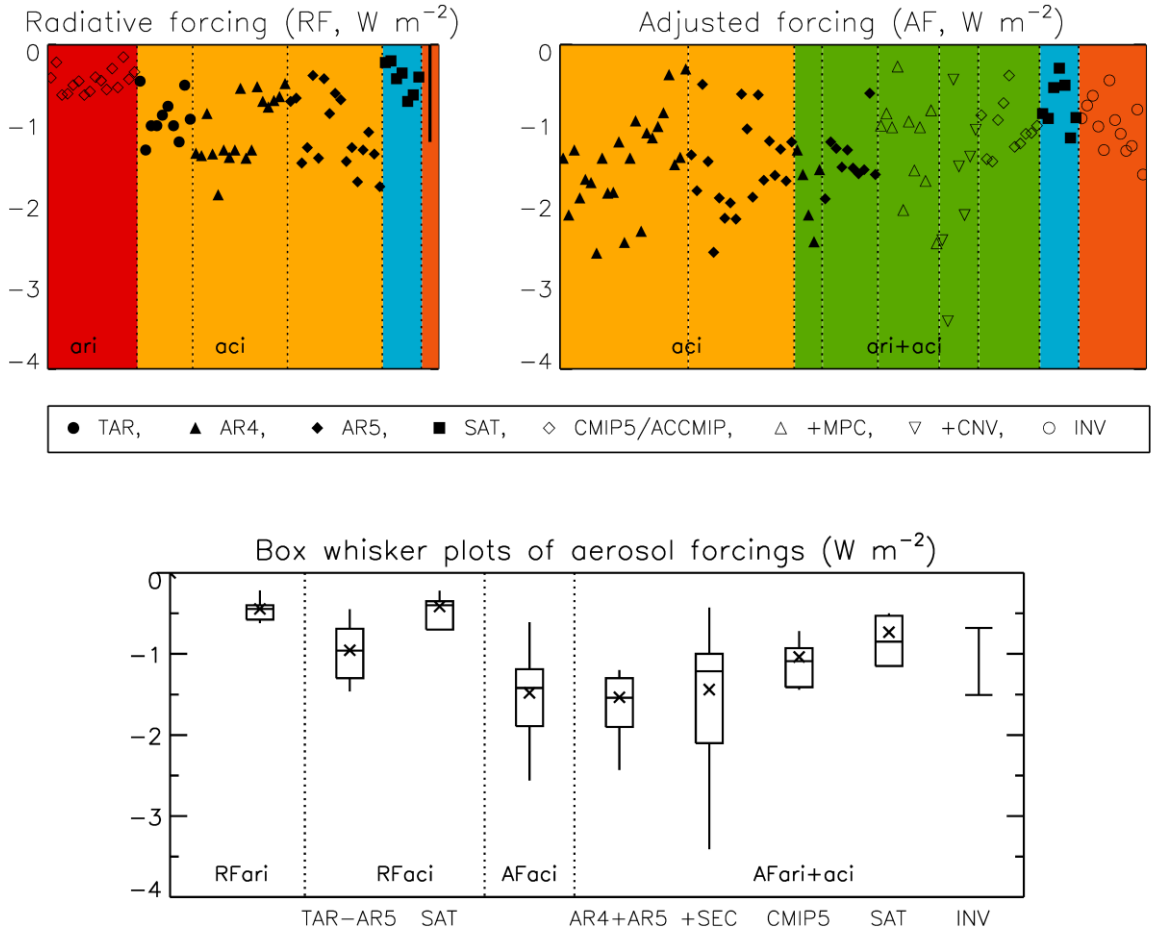

Figure 7.19: Upper panel: GCM, satellite and inverse estimates of RFari, RFaci, AFaci and AFari+aci. Each symbol represents the best estimate per model and paper as detailed in Table 7.4. The RFaci studies are divided into those from GCMs published prior to TAR, AR4 and AR5, those including satellite data (SAT) and the inverse estimate (INV). AFaci and AFari+aci studies from GCMs on liquid stratiform clouds are also divided into those published prior to AR4 and AR5 and from the CMIP5/ACCMIP models. GCM estimates that include adjustments beyond aci in liquid stratifrom clouds are marked +MPC when including aci in mixed-phase clouds and are marked +CNV when including aci in convective clouds. For RFaci from inverse estimates the range instead of the best estimate is given because it is only one study.

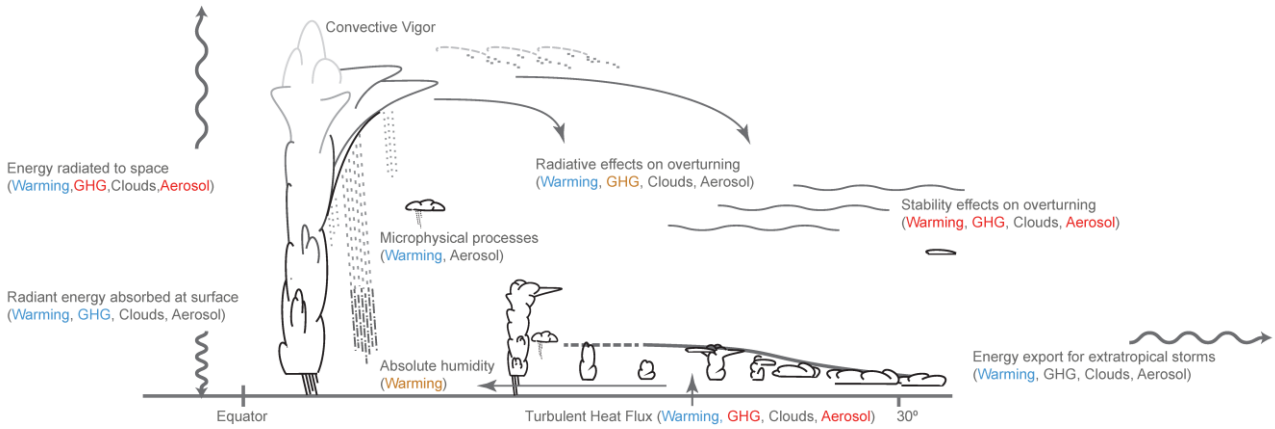

Figure 7.20: Illustration of major drivers affecting precipitation. Radiative drivers cool the atmosphere, warm the surface, and thereby provide the energy for evaporation and condensation/precipitation. Circulations organize and distribute precipitation. The ability of changes in the position or strength of circulation features to change the distribution of precipitation is referred to as a dynamic effect, the ability of warmer circulations to transport more water vapour and thereby change the amount of precipitation is referred to as a thermodynamic effect. The immediate effect of warming, greenhouse gases, clouds and aerosols on precipitation is indicated by blue or red if their change over the 20th century is thought to have changed a precipitation driver in a way that will increase, respectively decrease, precipitation. Grey indicates that changes are unknown or have multiple effects of different sign.

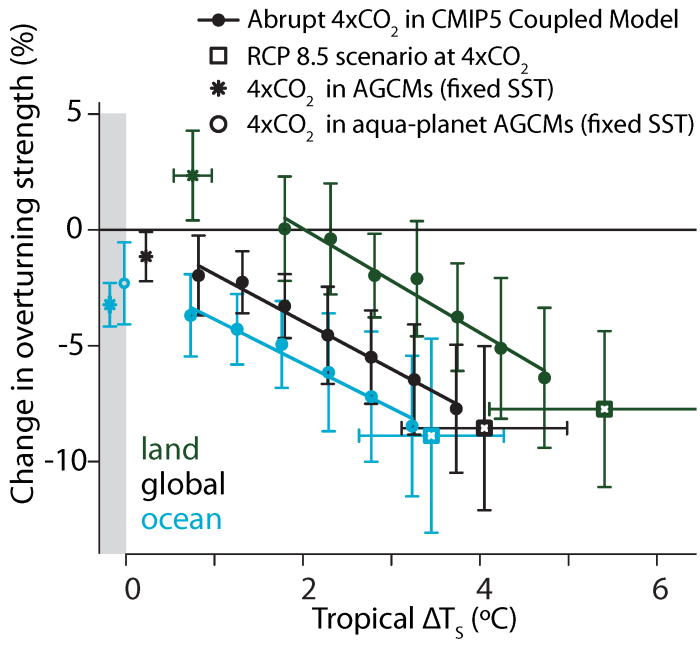

Figure 7.21: Illustration of the response of the large-scale overturning to increasing CO_2 concentrations (adapted from Bony et al., 2012). Approximately half of the response is evident before any warming is felt, but additional warming continues to slow down the circulation and adds linearly to the rapid adjustment. The rapid adjustment is different over land and ocean, with the increase in CO_2 initially causing an intensification of the circulation over land. The robustness of the result is illustrated by the common behaviour of 15 CMIP5 models, irrespective of the details of their configuration.

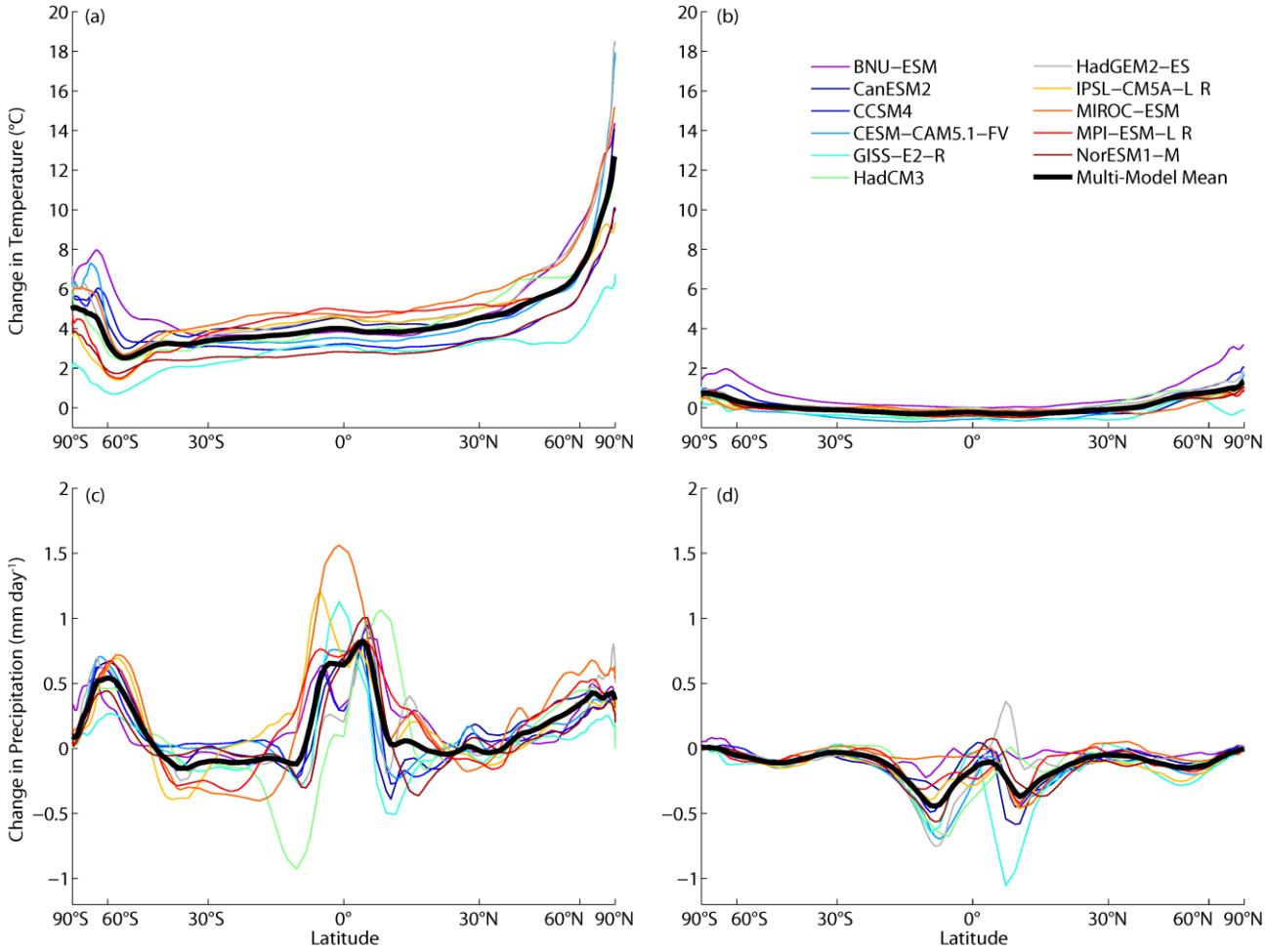

Figure 7.22: Zonally- and annually-averaged change in surface air temperature (°C) for (a) an abrupt 4 × CO_2 experiment and (b) the GeoMIP G1 experiment for 11 coupled atmosphere-ocean general circulation models. (c) and (d) Same as (a) and (b) but for the change in precipitation (mm day^{-1}). In the GeoMIP G1 experiment (Kravitz et al., 2011) an abrupt fourfold increase in CO_2 concentration is balanced by a reduction in total solar irradiance to produce a top of atmosphere flux imbalance of less than ±0.1 W m^{-2} during the first 10 years of the simulation. All changes are relative to the pre-industrial control experiment and averaged over years 21–50.

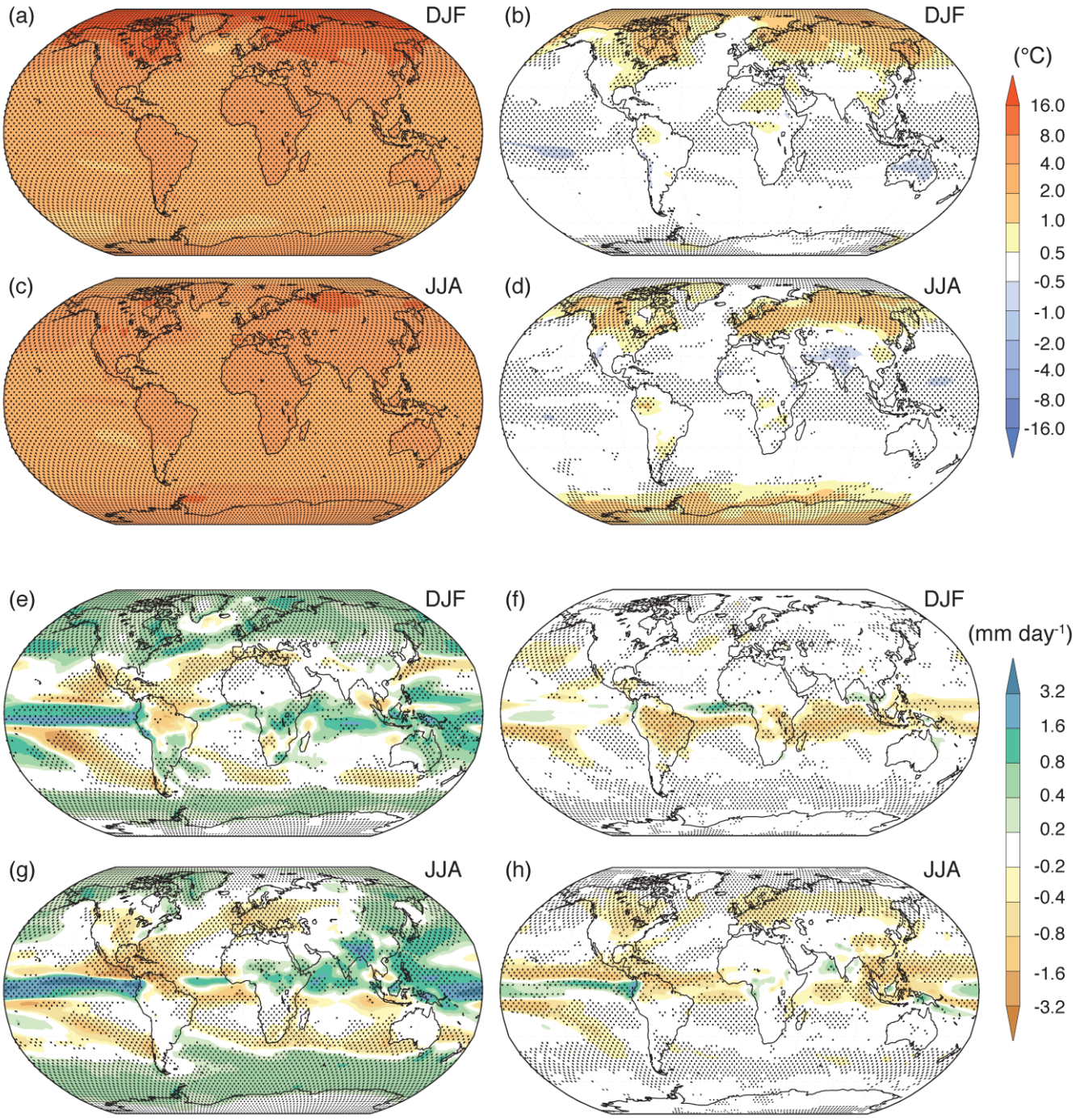

Figure 7.23: Multi-model mean of the change in surface air temperature (°C) averaged over December, January and February months for (a) the abrupt 4 × CO_2 simulation and (b) the GeoMIP G1 experiment. (c-d) same as (a-b) but for the June, July and August months. (e-h) same as (a-d) but for the change in precipitation (mm day^{-1}). All changes are relative to the pre-industrial control experiment and averaged over years 21-50. Stippling denotes agreement on the sign of the temperature anomaly in at least 75% of the models in panels.

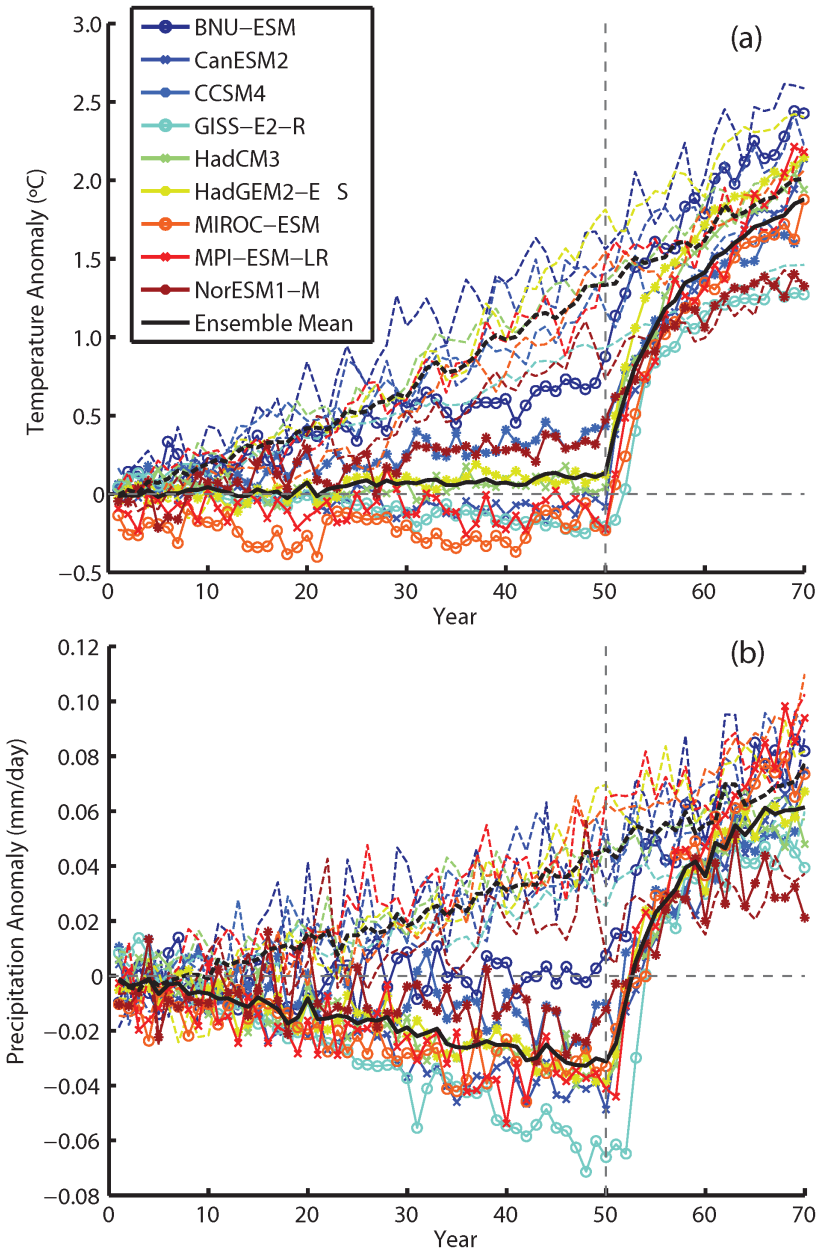

Figure 7.24: Timeseries of surface temperature (°C, left) and precipitation change (mm day^{-1}, right) for GeoMIP experiment G2, relative to each model's 1 × CO_2 reference simulation. Solid lines are simulations using SRM to balance a 1% yr^{-1} increase in CO_2 concentration until year 50 after which SRM is stopped. Dashed lines are for 1% CO_2 increase simulations with no SRM.

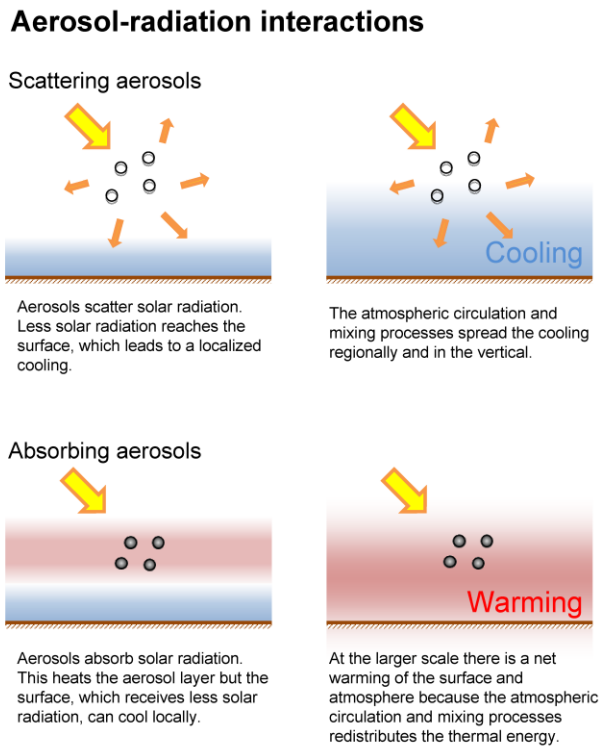

FAQ 7.2, Figure 1: Overview of aerosol-radiation interactions and their impact on climate. The left panels show the instantaneous radiative effects of aerosols, while the right panels show their overall impact after the climate system has responded to their radiative effects.

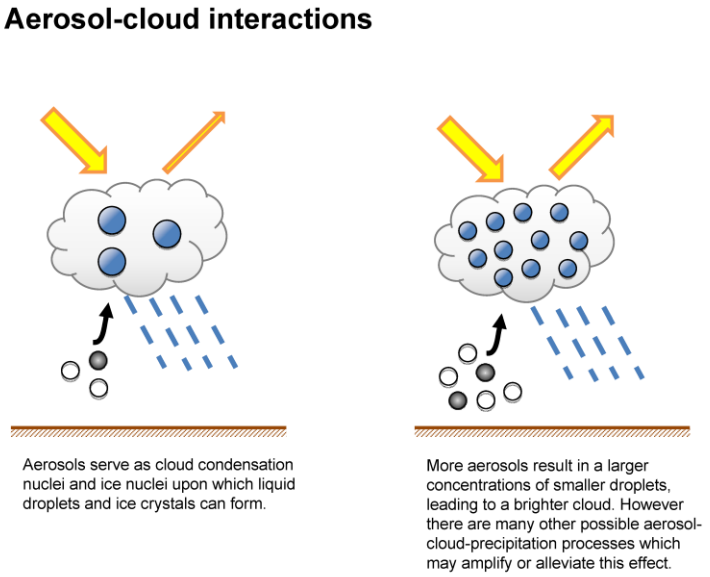

FAQ 7.2, Figure 2: Overview of aerosol-cloud interactions and their impact on climate. The left and right panels represent a clean and a polluted low-level cloud, respectively.

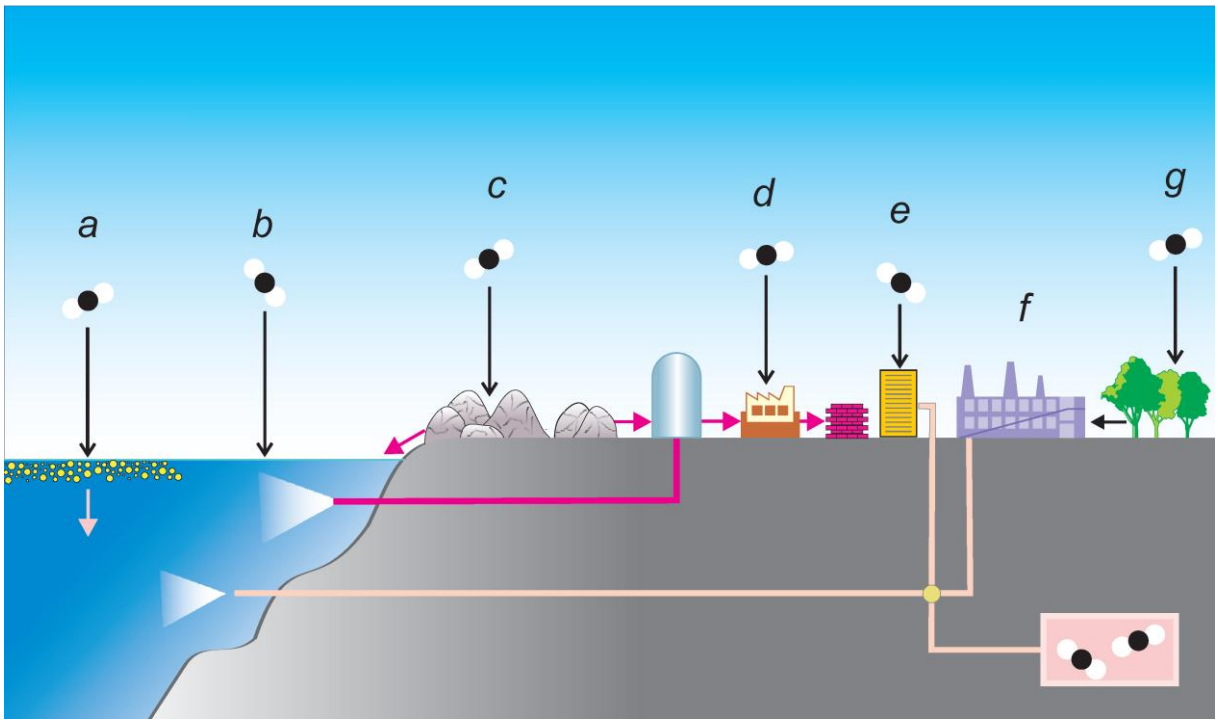

FAQ 7.3, Figure 1: Overview of some carbon dioxide removal methods. (a) nutrients are added to the ocean, which increases oceanic productivity in the surface ocean and transports a fraction of the resulting biogenic carbon downward, (b) alkalinity from solid minerals is added to the ocean, which causes more atmospheric CO_2 to dissolve in the ocean, (c) the weathering rate of silicate rocks is increased, and the dissolved carbonate minerals are transported to the ocean, (d) alkalinity from mined silicate rocks is extracted, then combined with atmospheric CO_2 to produce solid carbonate minerals, (e) atmospheric CO_2 is captured chemically, and stored either underground or in the ocean, (f) biomass is burned at an electric power plant with carbon capture, and the captured CO_2 is stored either underground or in the ocean and (g) CO_2 is captured through afforestation and reforestation to be stored in land ecosystems.

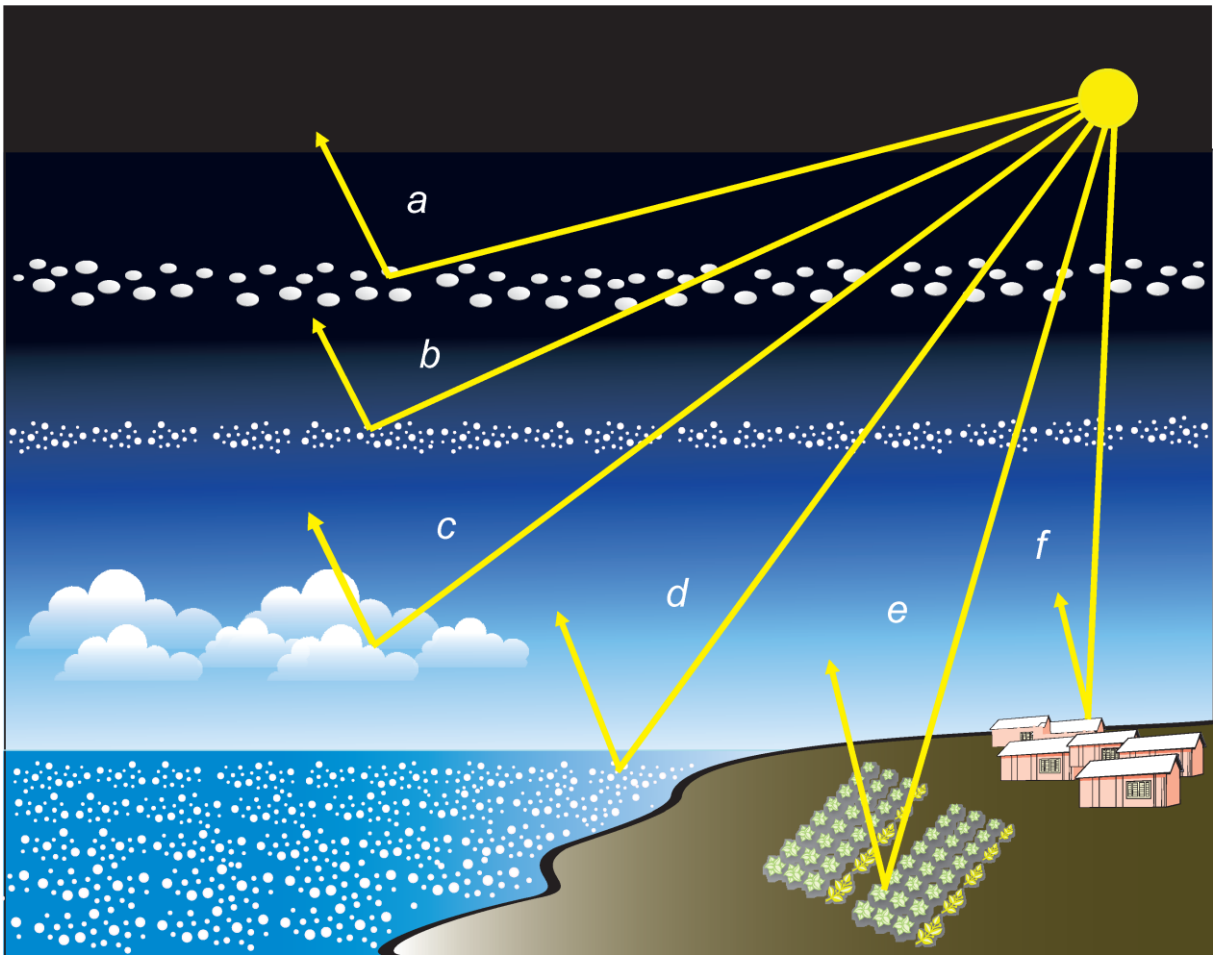

FAQ 7.3, Figure 2: Overview of some proposed solar radiation management (SRM) schemes to reflect sunlight to space that would otherwise be absorbed. Illustrated methods, counter-clockwise from upper left, are (a) reflectors in space, (b) aerosols in the stratosphere, (c) enhanced reflectivity of marine clouds, (d) making the ocean surface more reflective, (e) growing more reflective crops, and (f) whitening of roofs and other built structures.